ВЕСТНИК ТРАНСПЛАНТОЛОГИИ И ИСКУССТВЕННЫХ ОРГАНОВ

VESTNIK TRANSPLANTOLOGII I ISKUSSTVENNYKH ORGANOV

RUSSIAN JOURNAL OF TRANSPLANTOLOGY AND ARTIFICIAL ORGANS

УЧРЕДИТЕЛИ: ОБЩЕРОССИЙСКАЯ ОБЩЕСТВЕННАЯ ОРГАНИЗАЦИЯ ТРАНСПЛАНТОЛОГОВ «РОССИЙСКОЕ ТРАНСПЛАНТОЛОГИЧЕСКОЕ ОБЩЕСТВО»

ФГБУ «НМИЦ ТИО ИМЕНИ АКАДЕМИКА В.И. ШУМАКОВА» МИНЗДРАВА РОССИИ

ФГАОУ ВО ПЕРВЫЙ МГМУ ИМЕНИ И.М. СЕЧЕНОВА МИНЗДРАВА РОССИИ (СЕЧЕНОВСКИЙ УНИВЕРСИТЕТ)

THE OFFICIAL JOURNAL OF ALL-RUSSIAN PUBLIC ORGANIZATION OF TRANSPLANTOLOGISTS "RUSSIAN TRANSPLANT SOCIETY"

SHUMAKOV NATIONAL MEDICAL RESEARCH CENTER OF TRANSPLANTOLOGY AND ARTIFICIAL ORGANS

I.M. SECHENOV FIRST MOSCOW STATE MEDICAL UNIVERSITY (SECHENOV UNIVERSITY)

2021. Том XXIII. № 2

2021. Vol. XXIII. № 2

Научно-практический журнал основан в 1999 г.
Регистр. № 018616

Scientific and Practical Journal was founded in 1999
Reg. № 018616

Журнал «Вестник трансплантологии и искусственных органов» включен ВАК РФ в перечень российских рецензируемых научных изданий, в которых должны быть опубликованы результаты диссертационных работ

"Russian Journal of Transplantology and Artificial Organs" is included in the list of leading peer-reviewed scientific publication editions, produced in the Russian Federation and is recommended for publication of primary results of dissertation research

Журнал «Вестник трансплантологии и искусственных органов» индексируется в Scopus и размещен на платформе Web of Science Core Collection: Emerging Science Citation Index

"Russian Journal of Transplantology and Artificial Organs" is indexed in Scopus and in the Emerging Science Citation Index of the Web of Science Core Collection

ISSN 1995-1191

Адрес для корреспонденции:

Россия, 123182, Москва, ул. Щукинская, 1
Тел./факс +7 (499) 193 87 62
E-mail: vestniktranspl@gmail.com
Интернет-сайт журнала: http://journal.transpl.ru
Научная электронная библиотека: http://elibrary.ru

Address for correspondence:

1, Shchukinskaya st., Moscow 123182, Russia
Tel./Fax +7 (499) 193 87 62
E-mail: vestniktranspl@gmail.com
Journal's web site: http://journal.transpl.ru
Scientific eLibrary: http://elibrary.ru

Подписной индекс в каталоге ООО «Прессинформ» «Газеты и журналы» – 80248

СОДЕРЖАНИЕ

CONTENTS

ТРАНСПЛАНТОЛОГИЯ И ИСКУССТВЕННЫЕ ОРГАНЫ В НОВОЙ НОМЕНКЛАТУРЕ НАУЧНЫХ СПЕЦИАЛЬНОСТЕЙ: ГАРМОНИЧНОЕ СОЧЕТАНИЕ СТАБИЛЬНОСТИ И ОБНОВЛЕНИЯ

TRANSPLANTOLOGY AND ARTIFICIAL ORGANS IN THE NEW NOMENCLATURE OF SCIENTIFIC SPECIALTIES: A HARMONIOUS COMBINATION OF STABILITY AND RENEWAL

В 2021 году в нашей стране утверждена новая номенклатура научных специальностей, по которым присуждаются ученые степени (приказ Минобрнауки России № 118 от 24 февраля 2021 года). Изменения предприняты с целью развития перспективных научных направлений и междисциплинарных исследований, а также актуализации наименований научных специальностей.

Номенклатура научных специальностей, по которым присуждаются ученые степени, – это важный инструмент реализации государственной политики в сфере подготовки и аттестации научных и научно-педагогических кадров, создающий предпосылки для концентрации усилий научного сообщества на развитии перспективных научных направлений. Новая номенклатура направлена также на интеграцию современной российской науки в международное научное пространство.

В новой номенклатуре научная специальность «трансплантология и искусственные органы» (3.1.14, медицинские и биологические науки) сохранила свое самостоятельное место, интегрировала в себя смежные направления науки и входит в группу научных специальностей «Клиническая медицина».

Трансплантология, опираясь на новейшие достижения науки и биомедицинских технологий, продолжает свое развитие в тесной связи с ин-

A new nomenclature of scientific specialties under which academic degrees are awarded was approved in Russia in 2021 by Order No. 118 of the Russian Ministry of Education and Science, dated February 24, 2021. The changes were undertaken with the aim of developing emerging research areas and interdisciplinary research, as well as updating the names of scientific specialties.

The nomenclature of scientific specialties under which academic degrees are awarded is an important tool for implementing state policy on training and certification of scientific and pedagogical personnel, creating preconditions for concentrating the efforts of the scientific community on development of up-and-coming research areas. The new nomenclature is also targeted at integrating modern Russian science into the international scientific space.

In the new nomenclature, scientific specialty "Transplantology and artificial organs" (3.1.14, medical and biological sciences) has retained its free-standing position, integrated into itself allied areas of science and is included in group of scientific specialties "Clinical medicine".

Relying on the latest achievements in science and biomedical technology, transplantology continues to evolve in close connection with innovative, cellular and bioengineering technologies, regenerative

новационными, клеточными и биоинженерными технологиями, регенеративной медициной, созданием и применением биоискусственных органов и систем.

В проекте обновленной редакции паспорта специальности «трансплантология и искусственные органы» сохранены основные характеристики, заложенные еще 35 лет назад при открытии специальности, но существенно расширен раздел «области исследования», отражающий современный уровень развития последних.

Можно констатировать, что современная трансплантология – яркий пример стабильного развития и возможностей современной медицины – прочно завоевала свои позиции и как многопрофильная научная дисциплина, и как область клинической медицины, связанная с инновационными технологиями, использующая новейшие достижения естественных и точных наук. По сути, трансплантология является интегральной областью научных исследований, аккумулирующих и активно использующих достижения иммунологии, молекулярной биологии и биохимии, биотехнологии, точных наук (биомеханика, биоинженерия и др.), тесно связанной с обоснованной инновационной политикой.

С уважением,
академик РАН С.В. Готье

medicine, creation and use of bioartificial organs and systems.

The draft of the updated version of the passport of specialty "Transplantology and artificial organs" retains the basic characteristics laid down 35 years ago when the specialty was created. However, the section "fields of research" was significantly expanded, reflecting its current level of development.

It can be said that modern transplantology is a vivid example of the stable development and potentials of modern medicine; it has solidly gained its positions both as a multidisciplinary research discipline and as a field of clinical medicine that is associated with innovative technology, using the latest achievements in natural and exact sciences. Transplantology is arguably an integral area in scientific research, accumulating and actively using achievements in immunology, molecular biology, biochemistry, biotechnology, exact sciences (biomechanics, bioengineering, etc.), and closely connected to a sound innovation policy.

Sincerely,
S.V. Gautier
Member, Russian Academy of Sciences

DOI: 10.15825/1995-1191-2021-2-8-12

ROTATIONAL CORONARY ANGIOGRAPHY IN HEART TRANSPLANT RECIPIENTS

S.A. Sakhovsky, E.A. Kalchenko, B.L. Mironkov

Shumakov National Medical Research Center of Transplantology and Artificial Organs, Moscow, Russian Federation

As a screening method for detecting coronary lesions, coronary angiography (CAG) is becoming increasingly important in the activities of transplant centers. Angiography examination of coronary arteries is performed in potential recipients of various organs, related donors, and annually in heart recipients. Given the grave condition of recipients in the early post-transplant period and annual angiographic studies, it is necessary to strive for reduction of radiation load on the body and reduction of dose of X-ray contrast agents used. **Objective:** to assess the possibilities of using rotational CAG in the activities of transplant centers. **Materials and methods.** We observed 254 patients who underwent CAG. Their ages ranged from 21 to 79 years (mean 46.92 ± 1), and 90% were men. All patients were divided into two groups: group 1 included 142 patients who underwent rotational CAG, while group 2 was the control group (where classical polyprojection CAG was performed) and included 112 patients. Group 1 was divided into 2 subgroups – the subgroup of patients after heart transplantation who underwent endomyocardial biopsy along with CAG (n = 51), and the subgroup of patients who underwent only rotational CAG. **Results.** In 91% of patients, CAG was performed by radial access. In group 1, stenotic lesions were detected in 33 patients: 19 had single-vessel lesions, 9 had two-vessel lesions, and 5 had three-vessel lesions. A total of 56 hemodynamically significant stenoses were detected, 9 of which were chronic total occlusions. In 83 patients (60%), performing only 2 series of rotational scans (one left and one right coronary artery) was sufficient. In 32 (23%) patients, one more clarifying projection was required, in 17 patients two and in 9 – 3–5 additional projections. In 3 cases, we switched to polyprojection CAG. The average amount of contrast agent used was 24.4 ± 0.9 ml, the average X-ray dose was 34561.3 ± 1695.2 mGycm^2. The need for a contrast agent was significantly higher in the comparison group – 24.4 ± 0.9 mL and 103.5 ± 1.7 mL, respectively. The average X-ray dose in the main group was 34561.3 ± 1695.2 mGycm^2, in the comparison group 41430.9 ± 4141.7 mGycm^2. However, there was no significant difference between the groups. Subgroup analysis showed that patients who underwent only rotational CAG had lower radiation exposure compared to patients who underwent CAG combined with endomyocardial biopsy biopsy (EMB), as well as significantly lower load compared to the control group. **Conclusion.** Rotational CAG can be considered as the method of choice at transplant centers, where screening diagnostics of the state of the coronary bed is required, which is equivalent in terms of information content and safety. Rotational CAG allows to reduce the amount of injected contrast agent by more than three times, which in turn reduces the number of associated complications, as well as the radiation exposure of patients and medical personnel.

Keywords: rotational coronary angiography, heart transplantation, transplantology.

INTRODUCTION

Coronary angiography is becoming increasingly important in transplantation centers as a screening tool for detecting coronary lesions [1, 2]. Rejuvenation of atherosclerosis in modern civilization, and its increasing spread in the population, reduces the pool of potential donors and becomes a contraindication for recipients [3]. Cardiac recipients are a special category of patients in whom coronary angiography is considered the gold standard for evaluating the condition of the coronary arteries. These patients undergo CAG immediately after heart transplantation to detect donor-associated atherosclerotic lesions in the graft coronary arteries. And subsequently, a CAG screening is performed annually to detect and control the progression of heart transplant vasculopathy. Every related organ donor over 30 years of age, as well as all recipients of other organs, with the exception of pediatric patients, undergo a CAG prior to the removal and transplant surgery [4].

Rotational CAG (rCAG) is a relatively modern method, which allows to optimize the CAG procedure as much as possible, by reducing the procedure time and reducing the use of contrast agent. The latter is especially relevant for patients with end-stage renal failure, potential recipients with severe concomitant conditions, as well as potential related donors, who are exposed to contrast-induced nephropathy after CAG, which in turn requires correction and rescheduling of transplantation.

Corresponding author: Stepan Sakhovsky. Address: 1, Shchukinskaya str., Moscow, 123182, Russian Federation. Phone: (926) 636-00-31. E-mail: milifolium@gmail.com

Consideration of the advantages of rCAG, in comparison with classical polyprojection CAG, is a hot issue in transplantation practice.

Objective: to compare rCAG with conventional coronary angiography in patients admitted at Shumakov National Medical Research Center of Transplantology and Artificial Organs.

MATERIALS AND METHODS

We present results on observation of 254 patients who were admitted at Shumakov National Medical Research Center of Transplantology and Artificial Organs from 2018 to 2020 for CAG. The age of study subjects ranged from 21 to 79 years (mean 46.92 ± 1); 90% were men. All patients were divided into two groups: group 1 included 142 patients for whom rCAG was performed; group 2 was the control group (where conventional polyprojection CAG was performed), which included 112 people. Group 1 was divided into 2 subgroups: a subgroup of patients after orthotopic heart transplantation (OHTx), in whom endomyocardial biopsy (EMB) was performed together with CAG (n = 51), and a subgroup of patients in whom only rCAG was performed. All patients underwent standard examination, which included ECG and EchoCG. ECG included 12-channel recording of heart potentials using a Megacart device (Siemens, Germany). EchoCG was performed on a VIVID 9 apparatus (GE, USA). Conventional poly-projection CAG was performed according to M. Judkins technique by femoral or radial access using ALLURA XPER apparatus (Phillips, The Netherlands). The standard protocol included 5 projections for the left coronary artery and 2 projections for the right one. Rotational CAG was performed on ALLURA XPER (Phillips, The Netherlands) using the XperSwing software.

The study data were processed by parametric statistics using Microsoft Excel and IBM SPSS Statistics version 22. The arithmetic mean of the indices and standard errors of the mean were given in the study. The significance of differences was assessed by criteria for nonparametric variables: Wilcoxon signed-rank test for pairwise comparisons of dependent variables and Mann–Whitney U test for comparisons of independent variables.

RESULTS

The procedure recorded a 100% success. CAG was performed by radial access in 91% of patients, and by femoral access in the rest of the patients. Radial access had technical difficulties in 10 patients: 2 vascular loops of the brachial or radial artery, 1 radial artery occlusion, and 7 severe radial artery spasms. Two cases required conversion of the access to femoral access. A single bilateral diagnostic catheter was required to perform 90% of CAG. None of the studied patients showed signs of contrast-induced nephropathy.

CAG in the first group revealed stenotic lesions in 33 patients: 19 patients had single-vessel lesions, 9 patients had two-vessel lesions, and 5 patients had three-vessel lesions. A total of 56 hemodynamically significant stenoses were detected, 9 of which were chronic total occlusions. In 83 patients (60%), only 2 series of rotational imaging (one of the left coronary arteries and one of the right one) were enough. Due to the severity and prevalence of stenotic lesions, 32 (23%) patients required one more clarifying projection, 17 patients required two, and 9 patients required 3–5 additional projections. In 3 cases, there was a transition to polyprojection CAG. The average amount of contrast agent used was 24.4 ± 0.9 mL, the mean X-ray exposure dose was 34561.3 ± 1695.2 mGycm^2.

When comparing the groups of patients who underwent rotational and conventional polyprojection CAG, there was a significantly greater need for a contrast agent – 24.4 ± 0.9 mL and 103.5 ± 1.7 ml, respectively. The mean X-ray dose in the main group was 34561.3 ± 1695.2 mGycm^2, in the comparison group 41430.9 ± 4141.7 mGycm^2. However, there was no reliable difference between the groups. Radiation exposure indicators are presented in Table.

This can be explained by the fact that in 51 patients, EMB was performed along with CAG, which increased fluoroscopy time and consequently radiation exposure. This was confirmed by a subgroup analysis, which showed that patients who underwent rCAG alone had a lower radiation exposure compared with patients who underwent CAG in combination with EMB, as well as a significantly lower exposure compared with the comparison group.

Table

Comparison of groups (subgroup groups) by the amount of contrast agent used and X-ray dose

Group	Main group		Comparison group	p
Subgroup	CAG subgroup	CAG + EMB subgroup		
Quantity of contrast agent used, mL	24.4 ± 0.9		103.5 ± 1.7	**0.001**
Dose, mGycm	34561.3 ± 1695.2		41430.9 ± 4141.7	0.678
	28390.9 ± 1679.8			**0.001**

DISCUSSION

Transplant coronary artery disease is a major cause of graft death in heart recipients, which in turn reduces quality of life and increases mortality in this patient population. CAG remains the screening method of choice for detecting donor-transmitted coronary artery atherosclerosis in the early postoperative period. Recent guidelines on the management of heart transplant recipients consider CAG as the gold standard for detecting coronary lesions in the graft bed, both in the early postoperative period and cardiac allograft vasculopathy (CAV) in the long-term period. The nature of coronary bed lesions is determined according to S.Z. Gao classification, which was modified at Shumakov National Medical Research Center of Transplantology and Artificial Organs [5, 6]. The Stanford classification is used to describe the morphology of coronary lesions from discrete atherosclerosis to concentric arterial obliteration [5, 7].

However, analysis of polyprojection angiograms may underestimate both the prevalence and the extent of CAV due to vascular remodeling involving the entire coronary bed, which does not always reduce the lumen diameter at an early stage [8, 9]. Therefore, angiograms should be interpreted serially, as new, concentric lesions may not be visualized on single-plane angiograms. Because of these limitations, additional imaging techniques, such as intravascular ultrasound (IVUS), and optical coherence tomography (OCT) and the like have been proposed to increase CAV detection sensitivity.

Technological advances in angiographic equipment and software have made it possible to perform rCAG. Rotational CAG is a relatively new imaging technique that involves a predefined algorithm for rotating the X-ray tube around the patient in all required axes. The obtained angiograms provide significantly more information and allow to reconstruct a three-dimensional image of the vascular bed and visualize each coronary artery in different projections using a single injection of a radiopaque contrast agent into the left or right coronary artery system [10–12].

Numerous studies have demonstrated the advantages of rotational angiography, including reduced volume of radiopaque contrast agent, reduced procedure time, and less radiation exposure compared to standard coronary angiography [13, 14–16]. Adult studies have shown that rCAG provides comparable, and in some cases superior, image quality to static angiography for the evaluation of coronary heart disease. There is evidence on the use of rCAG in children. The International Society for Heart and Lung Transplantation (ISHLT) recommends coronary angiography even once a year in patients after heart transplantation [17, 18].

Since OHTx patients generally do not suffer from angina, due to donor heart denervation, coronary artery stenosis is an incidental finding, which is a prognostic sign of graft rejection process. Along with heart recipients, there are additional categories of patients (potential recipients of kidneys, livers, lungs, etc., related organ donors) in transplant centers that require CAG screening. For these groups of patients, rotational CAG is preferred as a highly informative diagnostic method with minimal risks of complications (e.g. contrast-induced nephropathy, etc.).

CONCLUSION

Rotational coronary angiography represents a relatively new angiographic method, which is equivalent in terms of image quality and information content, requires less use of contrast agent, is characterized by less radiation exposure and less CAG procedure time, as compared to the conventional polyprojection CAG. This approach can be preferable in the activities of transplantation centers, where screening diagnostics of coronary bed condition is required, because it is informative, and allows to reduce by more than threefold the amount of contrast agent introduced in the patient and the associated risks of complications, as well as reduce radiation exposure on patients and medical staff.

The authors declare no conflict of interest.

REFERENCES

1. *Natsional'nye* klinicheskie rekomendatsii: transplantatsiya serdtsa / Pod red. S.V. Got'e i dr. M.: Rossiyskoe transplantologicheskoe obshchestvo, 2013: 93.
2. *Kal'chenko EA, Goncharova AYu, Sakhovskiy SA.* Problema diagnostiki i lecheniya bolezni koronarnykh arteriy peresazhennogo serdtsa (obzor literatury). *Diagnosticheskaya i interventsionnaya radiologiya*. 2019; 13 (3): 58–67.
3. *Sakhovskiy SA, Abugov SA, Vartanyan EL, Puretskiy MV, Polyakov RS, Mardanyan GV, Mironkov BL.* Endovaskulyarnaya korrektsiya strukturnoy patologii klapanov i aorty u retsipientov serdtsa. *Endovaskulyarnaya khirurgiya*. 2021; 8 (1): 53–59.
4. *Natsional'nye* klinicheskie rekomendatsii: transplantatsiya pecheni / Professional'naya assotsiatsiya: Obshcherossiyskaya obshchestvennaya organizatsiya transplantologov "Rossiyskoe transplantologicheskoe obshchestvo". 2016: 13. URL: http://transpl.ru/files/rto/transpl_pecheni.pdf (10.03.2021).
5. *Gao SZ, Alderman EL, Schroeder JS, Silverman JF, Hunt SA.* Accelerated coronary vascular disease in the heart transplant patient: coronary arteriographic findings. *J Am Coll Cardiol.* 1988; 12: 334–340.
6. *Kazakov EN, Kormer AYa, Chestukhin VV, Golubitskiy VV.* Patologiya koronarnykh arteriy peresazhennogo serdtsa po dannym koronarografii. *Transplantologiya i iskusstvennye organy*. 1996; 4: 74–77.
7. *Johnson DE, Gao SZ, Schroeder JS, DeCampli WM, Billingham ME.* The spectrum of coronary artery pathologic findings in human cardiac allografts. *J Heart Transplant*. 1989; 8: 349–359.

8. *Nissen S.* Coronary angiography and intravascular ultrasound. *Am J Cardiol*. 2001; 87: 15A–20A.
9. *Rickenbacher PR, Pinto FJ, Chenzbraun A, Botas J, Lewis NP, Alderman EL et al.* Incidence and severity of transplant coronary artery disease early and up to 15 years after transplantation as detected by intravascular ultrasound. *J Am Coll Cardiol*. 1995; 25: 171–177.
10. *Garcia JA, Movassaghi B, Casserly IP, Klein AJ, Chen SY, Messenger JC et al.* Determination of optimal viewing regions for X-ray coronary angiography based on a quantitative analysis of 3D reconstructed models. *Int J Cardiovasc Imaging*. 2009; 25: 455–462.
11. *Hudson PA, Klein AJ, Kim MS, Wink O, Hansgen A, Casserly IP et al.* A novel dual-axis rotational coronary angiography evaluation of coronary artery disease – case presentation and review. *Clin Cardiol*. 2010; 33: E16–E19.
12. *Klein AJ, Garcia JA, Hudson PA, Kim MS, Messenger JC, Casserly IP et al.* Safety and efficacy of dual-axis rotational coronary angiography vs. standard coronary angiography. *Catheter Cardiovasc Interv*. 2011; 77: 820–827.
13. *Empen K, Kuon E, Hummel A, Gebauer C, Dorr M, Konemann R et al.* Comparison of rotational with conventional coronary angiography. *Am Heart J*. 2010; 160: 552–563.
14. *Liu HL, Jin ZG, Yang SL, Luo JP, Ma DX, Liu Y, Han W.* Randomized study on the safety and efficacy of dual-axis rotational versus standard coronary angiography in. *Chin Med J*. 2012; 125: 1016–1022.
15. *Liu H, Jin Z, Deng Y, Jing L.* Dual-axis rotational coronary angiography can reduce peak skin dose and scattered dose: a phantom study. *J Appl Clin Med Phys*. 2014; 15: 4805.
16. *Loomba RS, Rios R, Buelow M, Eagam M, Aggarwal S, Arora RR.* Comparison of contrast volume, radiation dose, fluoroscopy time, and procedure time in previously published studies of rotational versus conventional coronary angiography. *Am J Cardiol*. 2015; 116: 43–49.
17. *Ponikowski P, Voors AA, Anker SD et al.* 2016 ESC Guidelines for the diagnosis and treatment of acute and chronic heart failure: The task Force for the diagnosis and treatment of acute and chronic heart failure of the European Society of Cardiology (ESC) Developed with the special contribution of the Heart Failure Association (HFA) of the ESC. *Eur Heart J*. 2016; 37: 2129–2200.
18. *Herre JM.* Heart transplant medicine: beyond the guidelines. *J Heart Lung Transplant*. 2013; 32: 1170–1171.

The article was submitted to the journal on 21.04.2021

DOI: 10.15825/1995-1191-2021-2-13-20

CORRELATION BETWEEN INSULIN-LIKE GROWTH FACTOR 1 LEVELS AND TACROLIMUS DOSE IN PEDIATRIC LIVER RECIPIENTS

R.M. Kurabekova[1], O.M. Tsirulnikova[1, 2], O.E. Gichkun[1, 2], G.A. Olefirenko[1], I.E. Pashkova[1], A.A. Belchenkov[1], O.P. Shevchenko[1, 2]

[1] Shumakov National Medical Research Center of Transplantology and Artificial Organs, Moscow, Russian Federation

[2] Sechenov University, Moscow, Russian Federation

Introduction. To prevent post-transplant complications associated with unbalanced immunosuppression, objective indicators reflecting the state of the immune system and associated with the immunosuppressant dose are required. In pediatric liver transplantation, an important indicator of hepatocellular function and restoration of anthropometric characteristics is insulin-like growth factor 1 (IGF-1), which exhibits both nonspecific and selective immunomodulator properties. **Objective:** to assess the correlation between growth hormone and IGF-1 levels and tacrolimus dose and blood concentrations in pediatric liver recipients and to determine the possibility of using the IGF-1 level in selecting the drug dose required to achieve its target concentration in the blood. **Materials and methods.** We examined 156 children aged from 2 to 105 (median – 8) months with liver cirrhosis of various etiology, who received liver from a living related donor. The concentration of growth hormone and IGF-1 was determined in blood plasma before, one month, and one year after transplantation using the enzyme-linked immunosorbent assay. Tacrolimus residual concentration was measured in the patient's whole blood by immunochemical method. **Results.** Growth hormone levels in the blood of pediatric liver recipients did not correlate with the dose or concentration of immunosuppressant tacrolimus one month or one year after transplantation, whereas the IGF-1 content was directly related to tacrolimus dose one year later ($r = 0.41$, $p = 0.001$), but not a month after surgery. The correlation coefficient was higher in uncomplicated post-transplant recipients ($r = 0.51$, $p = 0.002$) than in those with complications ($r = 0.26$, $p = 0.17$). The diagnostic efficiency of the IGF-1 level as an objective criterion for selecting the tacrolimus dose required to achieve its target blood concentration was 0.80 ± 0.11; 95% CI [0.58–1.00] ($p = 0.007$). In recipients with blood IGF-1 levels ≥115.7 ng/mL, the probability of prescribing a tacrolimus dose ≥0.25 mg/kg/day was 14 times higher than in children with lower blood IGF-1 levels. The estimated accuracy of the test was 83%, positive predictive value was 71%, and negative predictive value was 85%. **Conclusion.** The IGF-1 level was found to correlate with tacrolimus dose in liver transplant recipients one year after transplantation. The diagnostic efficiency of IGF-1 as a potential indicator for choosing the tacrolimus dose required to achieve its target blood concentration is 80%, which suggests further study of the test to assess the effectiveness of immunosuppression and selection of an individual immunosuppressant dose.

Keywords: living-donor liver transplantation, congenital biliary tract diseases, biomarker, effectiveness of immunosuppression.

INTRODUCTION

After organ transplantation, all patients are prescribed immunosuppressive drugs to prevent rejection, which in turn may have side effects [1, 2]. A 2–3-component immunosuppressive therapy in pediatric liver recipients includes tacrolimus (TAC), a calcineurin inhibitor. The difficulty in selecting the optimal dose of calcineurin inhibitors is associated with the narrow therapeutic index and significant variability of individual pharmacokinetics of drugs. If the drug dose is insufficient, graft rejection is possible, an excessive dose may lead to infectious complications.

The initial dose of immunosuppressants is prescribed taking into account clinical parameters like age, race, donor/recipient leukocyte antigen (HLA) compatibility, presence of HLA antibodies, etc. The effective TAC dose is selected based on the results of monitoring its residual concentration in the blood [3].

To reduce the incidence of complications, objective indicators reflecting the state of the immune system and associated with TAC dose or serum levels are needed [4, 5]. Methods currently being developed to assess the immunosuppression efficacy are based primarily on measurement of parameters characterizing the T cell respon-

Corresponding author: Olga Shevchenko. Address: 1, Shchukinskaya str., Moscow, 123182, Russian Federation. Phone: (499) 190-38-77. E-mail: transplant2009@mail.ru

se: quantitative determination of T cell proliferation, T cell cytokine secretion, adenosine triphosphate (ATP) release in T cells, phenotyping of T cell determinants, etc. [6, 7]. Despite a significant number of studies, immunosuppression efficacy indicators have not found their application in clinical practice for a number of reasons, such as duration and complexity of analysis or its lack of accuracy and reproducibility [8, 9].

In pediatric liver transplant (LT) recipients, the growth hormone/insulin-like growth factor 1 (IGF-1) system related to hepatocellular function, growth and body weight regulation are important indicators. elevated levels of growth hormone are combined with stunted growth and body weight due to reduced IGF-1 levels in the blood. Liver transplantation in children is accompanied by improved anthropometric parameters during restoration of growth hormone/IGF-1 system [10, 11].

IGF-1, synthesized mainly in the liver, mediates the peripheral effects of growth hormone, exerting a proliferative, regenerative, and antiapoptotic effect on various tissues [12]. The effect of IGF-1 on the immune system is associated with regulation of proliferation, differentiation, and metabolism of various cells. IGF-1 exhibits both nonspecific immunomodulator properties (it stimulates lymphopoiesis, immunoglobulin synthesis, T cell differentiation [13, 14], and demonstrates a selective inhibitory effect on IL-2-dependent lymphocyte growth [15].

Experimental studies have identified various mechanisms of interaction between IGF-1 and TAC. Particularly, it has been shown that both factors realize some of their effects through calcineurin-dependent cellular pathways [16–18]. In addition, it was found that intravenous and oral administration of TAC in rats increases the IGF-1 levels in the blood [19, 20]. The relationship between IGF-1 and TAC levels in the blood in paediatric liver recipients has not yet been studied.

The purpose of this study was to assess the correlation of growth hormone and IGF-1 levels with TAC dose and blood levels in pediatric liver recipients and to determine the possibility of using IGF-1 levels in selecting the drug dose required to achieve its target blood concentration.

MATERIALS AND METHODS

The study included 156 children with end-stage liver failure due to congenital and hereditary liver diseases, 65 boys and 91 girls aged from 2 to 105 (median 8) months. The etiology of liver failure included the following diseases: biliary atresia, Caroli syndrome, biliary hypoplasia, Alagille syndrome, Byler disease, and other rare liver diseases, including Crigler–Najjar syndrome, Von Gierke disease, alpha-1 antitrypsin deficiency, tyrosinemia, fulminant and autoimmune hepatitis, cryptogenic cirrhosis, and others (Table 1).

The patients included in the study underwent living-donor liver transplantation. The recipients received 2- or 3-component immunosuppressive therapy, which included tacrolimus, corticosteroids, and mycophenolates. The starting TAC dose at its first use was 0.1 mg/kg/day, in the early postoperative period – 0.2–0.3 mg/kg/day. The dose was further adjusted to achieve the target concentration of the drug in the blood – 4–8 ng/mL during the first month after transplantation and 3–6 ng/ml in the subsequent period.

Table 1

Patients included in the study

Number of patients		156
Age, months		8 (2–105)
Sex (M/F), number (%)		65 (42) / 91 (58)
Diseases, number of cases; %	Biliary atresia	86; 55%
	Caroli disease	15; 10%
	Biliary hypoplasia	14; 9%
	Alagille syndrome	12; 8%
	Byler's disease	7; 4%
	Others	22; 14%

TAC serum levels were measured in the patient's whole blood by immunochemical method on an ARCHITECT i2000 analyzer (Abbott, USA) using the ARCHITECT Tacrolimus Kit (Abbott, USA). Growth hormone levels were measured in blood plasma by ELISA using a specific reagent kit (DBC, Canada). IGF-1 levels were measured in blood plasma by sandwich enzyme-linked immunosorbent assay using the OCTEIA IGF-1 kit (IDS Ltd., UK). Optical density was measured using a Zenyth 340r automatic microplate reader (Biochrom Anthos, UK).

Data are presented as arithmetic mean (M) and standard deviation (SD) – M ± SD, upper and lower bounds of the 95% confidence interval (CI) with normal distribution of the indicator. Data from nonparametric samples are presented as median and interquartile range (2nd–3rd quartile or 25–75th percentile). Comparative statistical analysis was performed using nonparametric statistics methods: Mann–Whitney U-test, paired Wilcoxon test, Spearman correlation analysis. Differences were considered statistically significant when the probability of error was less than 0.05 ($p < 0.05$).

ROC (receiver operating characteristic) analysis was performed to evaluate the informativeness of the test. The area under the ROC curve reflects the likelihood that the test is able to separate one group of patients from another. The null hypothesis was that the area under the ROC curve does not differ from 0.5. Diagnostic sensitivity and specificity of the test, as well as optimal threshold value of the biomarker were determined at the point of maximum sum of sensitivity and specificity. Relative risk was determined using a four-field contingency table for the threshold IGF-1 concentration and estimated 95% CI. The RR value was considered statistically significant ($p < 0.05$) if the lower limit of CI was greater than 1. We

also calculated test accuracy (Ac), positive predictive value (PPV) and negative predictive value (NPV).

Data were calculated using statistical programs: MS Office Excel (MS, USA), SPSS Statistics 20 (IBM, USA), and Statistica 7.0 (StatSoft, Inc., USA).

RESULTS AND DISCUSSION

The median and interquartile range of plasma levels of growth hormone and IGF-1 in children with liver failure were 4.3 (1.6 to 7.2) and 8.7 (0 to 24.8) ng/mL, respectively. After liver transplantation, growth hormone levels significantly decreased to 1.4 (1.1 to 2.5) ng/mL one month later ($p = 0.003$) and 2.5 (1.6 to 5.6) ng/mL one year after surgery ($p = 0.015$). Blood IGF-1 levels increased to 74.2 (52.1 to 126.6) ng/mL one month later ($p = 0.0001$) and 79.6 (42.9 to 111.7) ng/mL one year after surgery ($p = 0.0002$). Data obtained confirm previous reports and show that liver transplantation in children with end-stage liver disease is accompanied by increased IGF-1 levels and decreased concentrations of growth hormone in the blood, which is obviously a consequence of graft functioning [10, 21].

Table 2

Correlation between growth hormone (GH) levels and TAC levels and its dose at various periods after liver transplantation (LT)

TAC administration time after LT	TAC	Coefficient of correlation with growth hormone levels		
		before LT	month after LT	year after LT
Month	Concentration, ng/mL	0.16	0.05	0.01
	Dose, mg/kg/day	0.00	–0.05	–0.03
Year	Concentration, ng/mL	0.31	–0.17	0.24
	Dose, mg/kg/day	–0.13	0.07	–0.07

Table 3

Correlation between IGF-1 blood levels and serum TAC levels and its dose at different periods after liver transplantation (LT)

TAC administration time after LT	TAC	Coefficient of correlation with IGF-1 levels		
		before LT	month after LT	year after LT
Month	Concentration, ng/mL	0.10	0.20	0.17
	Dose, mg/kg/day	–0.05	0.05	0.19
Year	Concentration, ng/mL	0.07	0.09	0.26
	Dose, mg/kg/day	0.24	0.19	0.41*

* $p = 0.001$.

After transplantation, recipients received TAC at an average dose of 0.22 ± 0.12 mg/kg/day one month and 0.16 ± 0.07 mg/kg/day one year after LT. Patients' TAC serum levels averaged 5.9 ± 3.4 ng/mL one month and 7.2 ± 3.0 ng/mL one year after transplantation.

Correlation analysis of growth hormone content before and after transplantation with TAC levels and dose administered one month and one year after transplantation showed no statistically significant relationships between growth hormone levels and concentration or dose of the immunosuppressant (Table 2).

Analysis of the association of IGF-1 levels with the dose and blood concentration of the drug showed a significant direct correlation between the moderate strength ($r = 0.41$, $p = 0.001$) and TAC dose one year after liver transplantation (Table 3). No statistically significant associations with either dose or concentration were found before and one month after surgery.

Thus, the results obtained show that the level of growth hormone, unlike IGF-1, does not correlate with TAC dose or levels, although the content of these hormones in pediatric liver recipients one year after transplantation, as well as in healthy children, is related [11]. The absence of such a correlation may particularly be due to significant changes in the level of growth hormone in blood as a result of circadian rhythms of its secretion.

IGF-1 levels one year after transplantation correlates with the administered dose, but not with serum TAC levels. Absence of such a relationship may be due to the significant variability of immunosuppressant concentrations in the blood and the low values of residual drug concentrations.

It should be noted that the revealed correlation does not explain the causal relationship between IGF-1 levels and the immunosuppressant dose required/sufficient to achieve the target plasma concentration of the drug. The relationship between IGF-1 levels and TAC dose and the mechanisms underlying this interaction in pediatric liver recipients has not been studied and may be the subject of a separate study.

Experimental studies have shown an increase in IGF-1 blood levels in rats in response to TAC administration [19, 20], which agrees with the direct correlation between IGF-1 levels and TAC dose (obtained in our study) one year after transplantation, but does not explain the absence of such correlation one month after surgery. At the same time, considering the effect of IGF-1 on lymphocyte proliferation [14, 22] and the inhibitory effect of TAC on T-cell division [23, 24], we can assume that higher IGF-1 levels in the body leads to more active lymphocyte proliferation, which requires a higher TAC dose to inhibit.

The absence of correlation between IGF-1 levels and TAC dose one month after transplantation may be due to the fact that the optimal dose of the immunosuppressant in the majority of recipients during this period has not

yet been selected. The presence of correlation one year after transplantation may be due to the fact that by this period, the optimal TAC dose can be chosen in a part of recipients, at least with a favorable postoperative period. This is confirmed by the results of analysis of correlation between IGF-1 levels and TAC dose depending on complications: the correlation coefficient in recipients with uneventful post-transplantation period (r = 0.51, p = 002) is higher than in recipients with complications (r = 0.26, p = 0.17).

Moreover, the direct correlation between IGF levels and TAC dose revealed in our work is consistent with the experimental data on the common mechanisms of realization of some effects of IGF and TAC through calcineurin cellular pathways [16, 17, 20], which probably suggests competition for common binding sites and, consequently, direct correlation between the content of these factors in the blood mediated through them.

However, despite the lack of study of the mechanisms underlying the identified relationship, the obtained result allows us to consider the IGF-1 blood levels as a potential indicator for selection of a drug dose in pediatric liver recipients.

Based on regression analysis between IGF-1 levels and TAC dose in recipients without complications one year after transplantation (Fig. 1), we obtained a linear dependence equation: $y = 0.091 + 0.0007 \times x$, which allows the calculation of TAC dose (y) by IGF-1 levels (x). The coefficient of determination of linear regression (r^2) is 0.34, r = 0.58, p = 0.0002.

To assess the informative characteristics of IGF-1 levels as an objective criterion for TAC dose selection, the recipients were divided into 2 groups: those receiving low (0.03–0.24 mg/kg/day) and higher TAC dose (0.25–0.36 mg/kg/day). IGF-1 levels in these groups were 7.1 (0.1 to 25.5) and 13.2 (11.0 to 24.4) ng/mL before transplantation, respectively. One month later, they were 86.3 (56.5–161.3) and 115.0 (82.4–168.4) ng/ml, respectively. There were no significant differences in IGF-1 levels in children who received high and low doses of TAC both before (p = 0.212) and one month after transplantation (p = 0.302). One year after surgery, however, recipients who received a higher TAC dose had significantly higher IGF-1 levels: 138.6 (110.2 to 189.7) ng/mL than those who received a lower dose: 64.3 (43.5 to 100.0) ng/mL (p = 0.005) (Fig. 2).

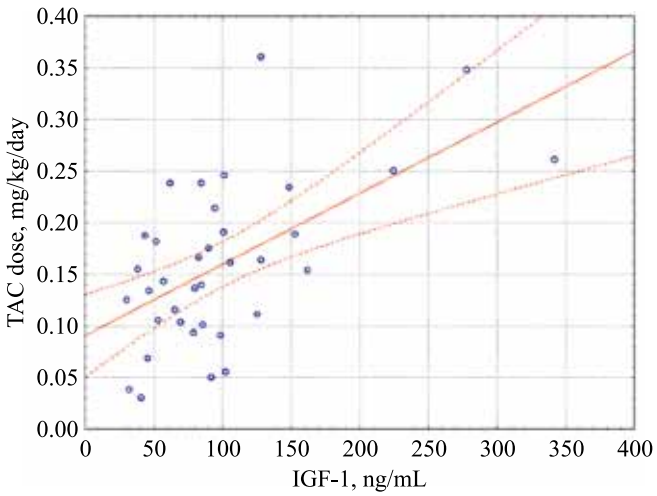

Fig. 1. Linear regression analysis of IGF-1 blood levels with TAC dose in pediatric recipients without complications one year after liver transplantation ($y = 0.091 + 0.0007 \times x$), $r^2 = 0.34$, r = 0.58, p = 0.0002

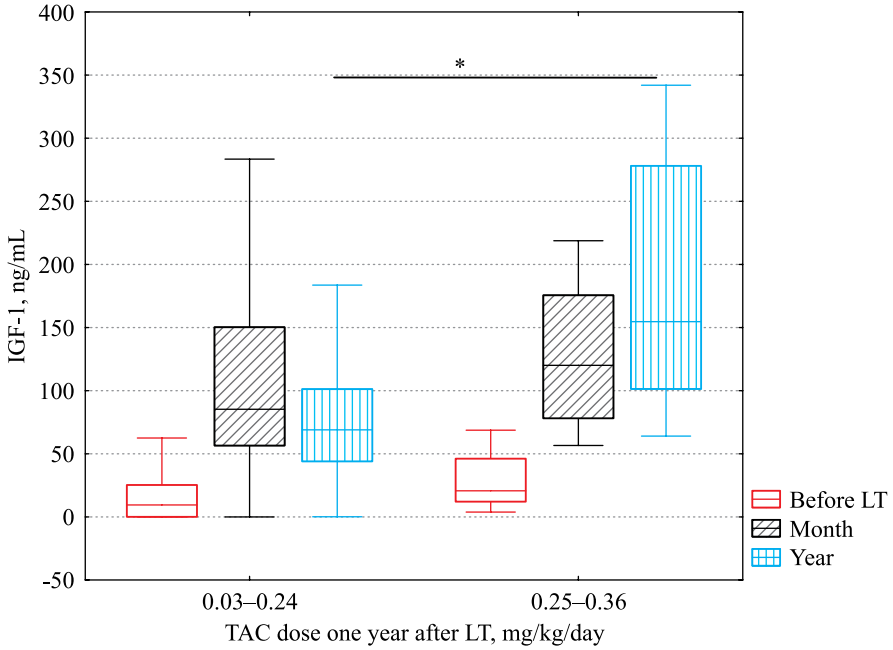

Fig. 2. Dynamics of IGF-1 blood levels in pediatric recipients who received different TAC doses one year after liver transplantation (a/LT), * p = 0.001

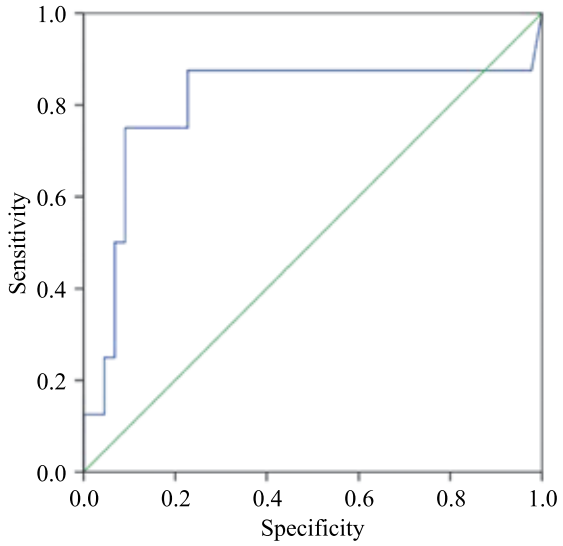

Fig. 3. ROC analysis of IGF-1 blood levels in pediatric recipients one year after liver transplantation (LT), as an indicator for choosing a TAC dose one year after LT: AUC = 0.80 ± 0.11; 95% CI 0.58–1.00, p = 0.007

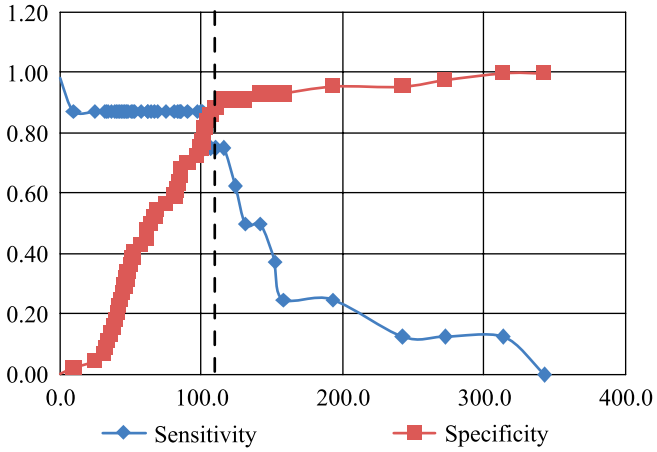

Fig. 4. Sensitivity and specificity of IGF-1 blood levels in pediatric recipients one year after liver transplantation (LT) as an indicator for TAC dose adjustment a year after LT

Table 4

Characteristics of a TAC dose requirement test based on IGF-1 levels one year after liver transplantation

Characteristics	Values
TAC dose requirement test	≥0.25 mg/kg/day
AUROC, 95% CI	0.80 ± 0.11; [0.58–1.00]
Sensitivity	0.75
Specificity	0.91
IGF-1 threshold	115.7 ng/mL
Relative risk, 95% CI	14.3 ± 1.0; [2.0–106.1]*
Test accuracy (Ac)	83%
Positive predictive value (PPV)	71%
Negative predictive value (NPV)	85%

* p < 0.05.

ROC analysis showed that the area under the curve (AUC) was 0.80 ± 0.11; 95% CI [0.58–1.00], p = 0.007 (Fig. 3). Based on an analysis of the dependence of test sensitivity and specificity on IGF levels, the threshold level of the biomarker was determined (Fig. 4) and relative risk values were calculated. The test accuracy, the positive predictive value and negative predictive value were also measured (Table 4).

According to results obtained, the IGF-1 levels in recipients makes it possible to determine the TAC dose with an 80% probability. Recipients with IGF-1 levels ≥115.7 ng/mL had a 14-fold higher risk of TAC dosing ≥0.25 mg/kg/day than children with lower IGF-1 levels. The estimated test accuracy was 83%, and the probabilities of positive and negative predictions were 71% and 85%, respectively, which are considered "good test" indicators.

Current methods for assessing the efficacy of immunosuppression based on the T cell response are complex and time-consuming [8, 9]. Determination of IGF-1 levels by immunoassay takes about 6 hours and is an acceptable method in terms of complexity and duration for clinical transplantology. Besides, IGF-1 has important properties that allow it to be considered as a potential biomarker for TAC dose selection, at least in liver recipients, because more than 90% of IGF-1 circulating in the systemic bloodstream is synthesized in the liver [25, 26]. IGF-1 levels are significantly higher than that of other peptide hormones, and IGF-1 half-life is 2–4 hours, which is 6–10 times longer than that of other similar hormones. IGF-1 levels in the blood plasma of healthy children, unlike growth hormone, whose secretion varies throughout the day, is quite stable, it gradually increases with age and reaches its maximum values at puberty.

The present study is observational, retrospective and hypothesis-driven, which requires a prospective study to confirm or refute. In addition, the study did not examine the possible influence of other factors on serum IGF levels, such as the recipients' age, concentrations of various hormones, doses of corticosteroids and mycophenolates administered during immunosuppressive therapy, etc., since the authors assumed that these factors do not differ significantly in patients of the same age group.

The authors declare no conflict of interest.

REFERENCES

1. *Miloh T, Barton A, Wheeler J, Pham Y, Hewitt W, Keegan T et al.* Immunosuppression in pediatric liver transplant recipients: Unique aspects. *Liver Transpl.* 2017; 23 (2): 244–256.
2. *Catic-Dordevic A, Cvetkovic T, Stefanovic N, Velickovic-Radovanovic R.* Current Biochemical Monitoring and Risk Management of Immunosuppressive Therapy after Transplantation. *J Med Biochem.* 2017; 36 (1): 1–7.

3. *Venkataramanan R, Shaw LM, Sarkozi L, Mullins R, Pirsch J, MacFarlane G et al*. Clinical utility of monitoring tacrolimus blood concentrations in liver transplant patients. *J Clin Pharmacol.* 2001; 41 (5): 542–551.
4. *Sood S, Haifer C, Yu L, Pavlovic J, Churilov L, Gow PJ et al*. A novel immune function biomarker identifies patients at risk of clinical events early following liver transplantation. *Liver Transpl.* 2017; 23 (4): 487–497.
5. *Sharon E, Shi H, Kharbanda S, Koh W, Martin LR, Khush KK et al*. Quantification of transplant-derived circulating cell-free DNA in absence of a donor genotype. *PLoS Comput Biol.* 2017; 13 (8).
6. *Shipkova M, Wieland E*. Editorial: Immune monitoring in solid organ transplantation. *Clin Biochem.* 2016; 49 (4–5): 317–319.
7. *Crespo E, Bestard O*. Biomarkers to assess donor-reactive T-cell responses in kidney transplant patients. *Clin Biochem.* 2016; 49 (4–5): 329–337.
8. *Schlickeiser S, Boes D, Streitz M, Sawitzki B*. The use of novel diagnostics to individualize immunosuppression following transplantation. *Transpl Int.* 2015; 28 (8): 911–920.
9. *Mannon RB, Morris RE, Abecassis M, Axelrod D, Bala S, Friedman GS et al*. Use of biomarkers to improve immunosuppressive drug development and outcomes in renal organ transplantation: A meeting report. *Am J Transplant.* 2020; 20 (6): 1495–1502.
10. *Shevchenko OP, Tsirulnikova OM, Tsirulnikova IE, Kurabekova RM, Olefirenko GA, Stepanova OI et al*. Dynamics of insulin-like growth factor-1 (IGF-1) in children after AB0-incompatible liver transplantation. *Vestnik transplantologii i iskusstvennykh organov*. 2014; XVI (2): 46–51.
11. *Kurabekova RM, Tsiroulnikova OM, Pashkova IE, Makarova LV, Mozheyko NP, Monakhov AR, Shevchenko OP*. Association between Growth Hormone and Insulin-like Growth Factor-1 (IGF-1) Levels, Liver Function and Short-Term Survival of Paediatric Liver Recipients. *Gastroenterology, Hepatology, Coloproctology*. 2020; 30 (4): 44–51.
12. *Weigent DA*. Lymphocyte GH-axis hormones in immunity. *Cell Immunol.* 2013; 285 (1–2): 118–132.
13. *Van Buul-Offers SC, Kooijman R*. The role of growth hormone and insulin-like growth factors in the immune system. *Cell Mol Life Sci.* 1998; 54 (10): 1083–1094.
14. *Robbins K, McCabe S, Scheiner T, Strasser J, Clark R, Jardieu P*. Immunological effects of insulin-like growth factor-I – enhancement of immunoglobulin synthesis. *Clin Exp Immunol.* 1994; 95 (2): 337–342.
15. *Walsh PT, Smith LM, O'Connor R*. Insulin-like growth factor-1 activates Akt and Jun N-terminal kinases (JNKs) in promoting the survival of T lymphocytes. *Immunology.* 2002; 107 (4): 461–471.
16. *Li SY, Fang CX, Aberle NS, 2nd, Ren BH, Ceylan-Isik AF, Ren J*. Inhibition of PI-3 kinase/Akt/mTOR, but not calcineurin signaling, reverses insulin-like growth factor I-induced protection against glucose toxicity in cardiomyocyte contractile function. *J Endocrinol.* 2005; 186 (3): 491–503.
17. *González-Juanatey JR, Piñeiro R, Iglesias MJ, Gualillo O, Kelly PA, Diéguez C et al*. GH prevents apoptosis in cardiomyocytes cultured in vitro through a calcineurin-dependent mechanism. *J Endocrinol.* 2004; 180 (2): 325–335.
18. *Maestri M, Dionigi P, Pettenazza P, Visconti F, Rademacher J, Gaspari A et al*. Treatment of the nephrotoxicity of immunosuppressive drugs with insulin-like growth factor-I. *Minerva Chir.* 1998; 53 (5): 391–396.
19. *Mabuchi M, Kawamura I, Takeshita S, Fushimi M, Takakura S, Hirosumi J et al*. Insulin-like growth factor-I enhances choleretic action of FK506 in rats. *Transplant Proc.* 2003; 35 (4): 1596–1598.
20. *Kawamura I, Takeshita S, Fushimi M, Mabuchi M, Seki J, Goto T*. Induction of choleresis by immunosuppressant FK506 through stimulation of insulin-like growth factor-I production in the liver of rats. *Eur J Pharmacol.* 2001; 419 (1): 99–105.
21. *Maes M, Sokal E, Otte JB*. Growth factors in children with end-stage liver disease before and after liver transplantation: a review. *Pediatr Transplant.* 1997; 1 (2): 171–175.
22. *Clark R, Strasser J, McCabe S, Robbins K, Jardieu P*. Insulin-like growth factor-1 stimulation of lymphopoiesis. *J Clin Invest.* 1993; 92 (2): 540–548.
23. *Naesens M, Kuypers DR, Sarwal M*. Calcineurin inhibitor nephrotoxicity. *Clin J Am Soc Nephrol.* 2009; 4 (2): 481–508.
24. *Kershner RP, Fitzsimmons WE*. Relationship of FK506 whole blood concentrations and efficacy and toxicity after liver and kidney transplantation. *Transplantation.* 1996; 62 (7): 920–926.
25. *De Palo EF, Bassanello M, Lancerin F, Spinella P, Gatti R, D'Amico D et al*. GH/IGF system, cirrhosis and liver transplantation. *Clin Chim Acta.* 2001; 310 (1): 31–37.
26. *Leung KC, Ho KK*. Measurement of growth hormone, insulin-like growth factor I and their binding proteins: the clinical aspects. *Clin Chim Acta.* 2001; 313 (1–2): 119–123.

The article was submitted to the journal on 1.03.2021

DOI: 10.15825/1995-1191-2021-2-21-29

ANALYSIS OF RECIPIENT AND GRAFT SURVIVAL AFTER PRIMARY AND SECOND KIDNEY TRANSPLANTATION

A.V. Pinchuk[1–3], N.V. Shmarina[1], I.V. Dmitriev[1], V.E. Vinogradov[3, 4], A.I. Kazantsev[1]

[1] Sklifosovsky Research Institute of Emergency Care, Moscow, Russian Federation
[2] A.I. Evdokimov Moscow State University of Medicine and Dentistry, Moscow, Russian Federation
[3] Research Institute for Healthcare Organization and Medical Management, Moscow, Russian Federation
[4] City Clinical Hospital No.52, Moscow, Russian Federation

Objective: to evaluate the 1- and 5-year graft and recipient survival after primary and second kidney transplantation, to compare the outcomes depending on the age of recipients. **Material and methods.** The treatment outcomes for 364 patients who underwent kidney transplantation at Sklifosovsky Research Institute of Emergency Care, Moscow over the period from 2007 to 2019. Of these, 213 patients underwent kidney transplantation for the first time, while 151 patients were having a second transplantation. We analyzed the effect of previous transplants, as well as the age of the recipients on long-term survival rates. **Results.** No significant difference in 1- and 5-year survival of kidney recipients after primary and second transplantations was found. In contrast, the long-term graft survival significantly depended on this criterion and turned out to be significantly higher after primary transplantations. The 1- and 5-year survival of older recipients was lower than the survival of younger recipients after primary and second kidney transplantation. The 1-year graft survival after primary kidney transplantation was higher in young recipients than in older recipients of the same group, however, but there were no significant differences in the 5-year graft survival. After second transplantations, there were no significant differences in the 1- and 5-year graft survival depending on the age of recipients. **Conclusion.** A history of previous transplantation is an important factor in kidney transplantation outcome, which must be taken into account in clinical practice.

Keywords: primary kidney transplantation, second kidney transplantation, outcomes, recipient survival, kidney graft survival.

INTRODUCTION

Most experts believe that a second kidney transplant significantly affects the survival rate of renal allografts (RA). However, reports on studies carried out in this direction are often contradictory. According to the Collaborative Transplant Study (CTS) of the University of Heidelberg, carried out from 1990 to 2018, the 1-year survival rate of RA after primary and second kidney transplants was 90% and 85%, respectively; the 5-year survival was 76% and 70%, respectively [1]. Pour-Reza-Gholi et al. analyzed the results of 2,150 kidney transplants, 103 of which were second transplant surgeries. The 1-, 2-, 3-, and 5-year graft survival rates in patients who underwent primary transplantation were significantly higher than in patients who did second transplantations (92.9%, 91.5%, 89.8%, 85.3% and 81.4%, 78.9% , 78.9%, 73.7%, respectively (P = 0.0037). No significant differences in recipient survival were noted by the researchers (P = 0.63) [2].

Conflicting data has been published in the Australian and New Zealand registry ANZDATA for the period of 2011 to 2018. For primary and second kidney transplants, 1-year recipient survival was 96% and 99%, while 5-year recipient survival was 88% and 93%. The 1-year survival rate of RA also did not differ significantly (94% and 97%, respectively), while the 5-year survival rate was 75% and 85%, respectively [3]. Jędrzejko et al. analyzed the treatment outcomes of 406 patients who underwent kidney transplantation from 2013 to 2015, and obtained similar results. First transplantation had no significant effect on RA and recipient survival [4]. Ingsathit and colleagues analyzed data from Thailand's transplant registry, looking at the outcomes of 3,337 transplants performed between 1993 and 2011. There were no statistically significant differences in 1-, 5-, and 10-year RA and recipient survival rates in the primary and repeat kidney transplant groups (P = 0.63 and P = 0.42, respectively) [5]. Similar results were published by Korean scientists (Sang Hyup Han et al.). They analyzed the outcomes of 3,000 patients who underwent kidney transplantation from 1969 to 2018, of which 201 cases were repeat kidney transplants. Patient and death-censored graft survival for primary and repeat transplantation did not differ (P = 0.684 and P = 0.564, respectively) [6]. Heldal et al. analyzed the outco-

Corresponding author: Nonna Shmarina. Address: 3, Bolshaya Sukcharevsraya sq., Moscow, 129090, Russian Federation. Phone/fax: (495) 625-28-80. E-mail: nonna_shm@mail.ru

mes of 733 kidney transplants in recipients over 65 years of age. In 687 cases, the transplants were primary, and in 46, they were repeats. The 5-year death-censored and death-uncensored graft survival did not differ between the groups (P = 0.789 and P = 0.475, respectively) [7].

In Eurotransplant, a large multicenter retrospective study, it was observed that primary non-function had a higher incidence after a second kidney transplantation than after a primary transplantation (12.7% and 7.1%, respectively, P < 0.001) [8]. There were no statistically significant differences in recipient survival after primary and second kidney transplant surgeries (P = 0.532). However, the 5-year death-censored graft survival was significantly higher after primary transplantation (89% and 85%, P < 0.001) [9].

A study published by Puneet Sood et al. found no significant effect of prior transplantation on 1- and 5-year censored and uncensored graft survival (P = 0.70) [10]. In contrast, the group of recipients who underwent primary kidney transplantation had better 1- and 5-year survival compared with the group of patients who had a second kidney transplantation (P = 0.013) [11].

Objective: to evaluate the 1- and 5-year graft and recipient survival after primary and second kidney transplantation, and to compare the outcomes depending on the age of recipients.

MATERIAL AND METHODS

The study was based on a retrospective analysis of the results of 364 kidney transplants performed at Sklifosovsky Research Institute of Emergency Care in Moscow, from 2007 to 2019. The inclusion criterion was primary and repeated (second) kidney transplantation from a deceased donor. The exclusion criterion was combined kidney transplantation and transplantation of other organs from a living related donor. The patients were divided into groups – those that have had only primary transplantation and those with a second transplantation.

Follow-up period: from the time of kidney transplant surgery until loss of RA function or recipient death – completed follow-up; in case of loss of communication with the recipient – a censored follow-up.

Study: To assess the recipient and graft survival rate, we used data from the medical records of patients at the kidney transplantation department of Sklifosovsky Research Institute of Emergency Care, and out-patient medical records of RA recipients of the Moscow City Scientific and Practical Center for Nephrology and Transplant Kidney Pathology.

Study groups: The first comparison group, formed by stratified sampling by recipient gender and age, quality of donor organ (standard donor or expanded criteria donor), consisted of 213 RA recipients out of 1316 recipients with primary kidney transplantation. The second study group consisted of 151 recipients who underwent a second kidney transplantation.

Table 1

Main characteristics of patients after the first and second kidney transplantation

Recipients, n	All (n = 364)	Group 1 (n = 213)	Group 2 (n = 151)	P
Age, m (25–75%), years	45 (35; 54)	46 (36; 54)	44 (34; 54)	0.45
Age range, years	18–72	18–72	20–71	
Male, % (n)	57.4 (209)	60.6 (129)	53 (80)	0.25
Female, % (n)	42.6 (155)	39.4 (84)	47 (71)	
BMI, m (25–75%), kg/m^2	24.1 (21.2; 27.7)	24.6 (21.6; 28.2)	23.9 (21.1; 27.1)	0.12
Sensitized, % (n)	45.1 (134)	21.3 (35)*	74.4 (99)*	0.000
No data, % (n)	18.4 (67)	23.0 (49)	11.9 (18)	

* patients with no data were excluded from the estimation.

Recipients of both groups did not differ significantly in gender, age, and body mass index (Table 1). A significant difference between the groups was found in the number of patients sensitized to the major histocompatibility complex (HLA) (P = 0.000). Thus, HLA antibodies were found in a greater number of patients with repeated kidney transplantation in comparison with patients who had not had any previous transplantation.

Among the diseases leading to end-stage kidney disease, chronic glomerulonephritis (44.8%, n = 163) and chronic pyelonephritis (16.8%, n = 61) were most common in RA recipients in both groups. The latter – both as an independent disease, and as a complication of congenital anomalies of the urinary system and kidney stone. However, a comparative assessment of the disease pattern between the groups revealed differences (P = 0.00028). Specifically, there were significantly fewer patients with polycystic kidney disease, diabetes mellitus, and hypertension among the repeat transplant recipients (Fig. 1).

In the study groups, there were no significant differences in the characteristics of donor organs (Table 2).

To assess recipient and kidney graft survival rates, depending on age, groups 1 and 2 patients were considered in subgroups. The subgroups were divided by age as follows: from 18 to 49 years old (young recipients) and from 50 to 72 years old (older recipients) (Table 3).

Immunosuppressive therapy: patients in both groups received a three-component immunosuppressive therapy (calcineurin inhibitors + inosine monophosphate dehydrogenase/proliferative signal inhibitors + corticosteroids (100% of recipients in both groups). In order to prevent acute rejection, 84.1% of recipients received induction

with chimeric monoclonal antibodies – antagonists of CD-25 antigen or lymphocyte-depleting antibodies (antithymocyte immunoglobulin) (Table 4).

There were statistically significant differences in the used induction component and the basic immunosuppressive agent in the recipients of the study groups. Specifically, group 2 recipients with a high immunological risk received a more aggressive immunosuppressive therapy: 92.7% of patients received tacrolimus, and 62.9% received induction with lymphocyte-depleting antibodies. These drugs were used reliably less often in group 1 patients with a low immunological risk.

The data obtained was *statistically analyzed* using the Statistica for Windows v.12.0 software package, StatSoft Inc. (USA). Normality of distribution was assessed by the Shapiro–Wilk test. Mann–Whitney U test, Fisher's exact test (two-sided), chi-squared test for four-field and arbitrary tables were used to compare groups. The value $P < 0.05$ was considered statistically significant. The Kaplan–Meier estimator was used to analyze the survival rate. Survival across groups was compared using a log-rank test. Confidence intervals for survival were considered according to Weibull. Survival curves were calculated from the date of surgical treatment.

RESULTS AND DISCUSSION

Analysis of recipient survival after primary and second transplantations revealed no significant differences. Specifically, the 1-year recipient survival rate in group 1 and group 2 was 98% (95% CI 97–99) and 97% (95%

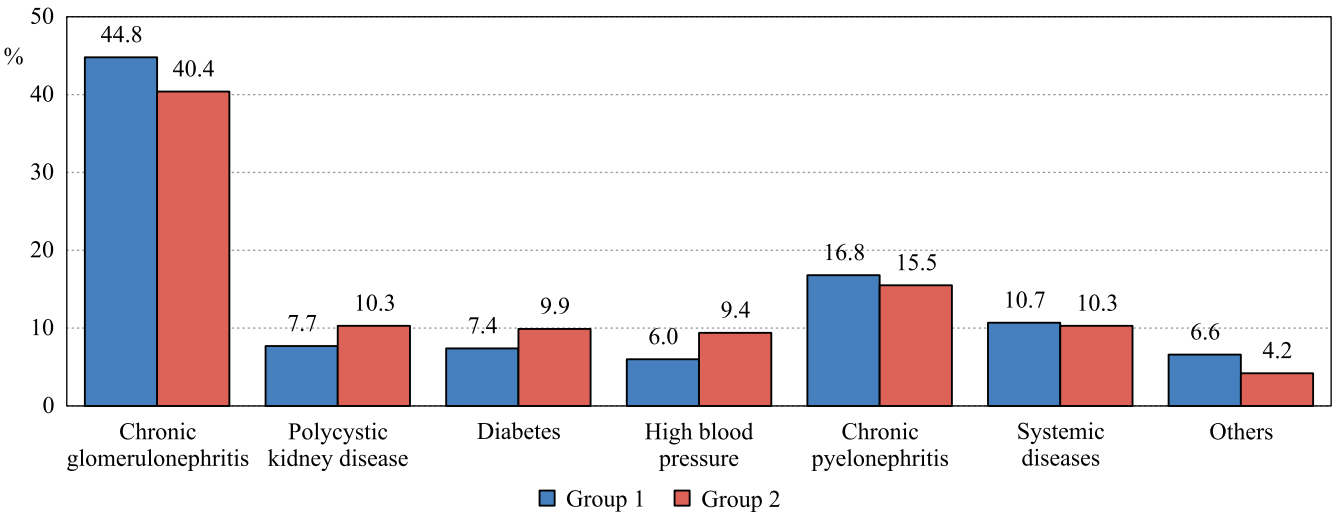

Fig. 1. Diseases that led to end-stage chronic renal failure in kidney graft recipients

Table 2

Donor characteristics

Renal allograft, n	All (n = 364)	Group 1 (n = 213)	Group 2 (n = 151)	P
Donor gender: Make, % (n) Female, % (n) No data, % (n)	 63.7 (232) 28.6 (104) 7.7 (28)	 62.0 (132) 29.1 (62) 8.9 (19)	 66.2 (100) 27.8 (42) 6 (9)	0.11
Donor's age, years: m, (25–75%) Age range No data, % (n)	 47 (38; 54) 18–69 (26)	 47 (39; 53) 18–69 (18)	 46 (34; 55) 20–67 (8)	0.38
Donor criteria: Standard, % (n) Extended, % (n) No data, % (n)	 64.8 (236) 28.3 (103) 6.9 (25)	 62.9 (134) 29.1 (62) 8 (17)	 67.5 (102) 27.2 (41) 5.3 (8)	0.06
Renal allograft preservation, hours: m, (25–75%) No data, % (n)	 13 (11; 16) (5)	 13 (11; 16) (2)	 14 (11.3; 16) (3)	0.36
HLA incompatibility: m, (25–75%) No data, % (n)	 4 (3; 4) 2.2 (8)	 4 (3; 5) 2.8 (6)	 4 (3; 4) 1.3 (2)	0.55

CI 94–98), respectively, (P = 0.06). Their 5-year survival rate was 98% (95% CI 95–99) and 93% (95% CI 89–96), respectively (P = 0.23) (Fig. 2).

Thus, our results confirm that there are no statistically significant differences in the 1- and 5-year survival rates of recipients after primary and repeated kidney transplantation, and are consistent with similar survival rates of RA recipients in the world.

Analysis of the renal graft survival in recipients of the study groups found statistically significant differences. Specifically, the 1-year graft survival in group 1 and group 2 was 97% (95% CI 95–99) and 88% (95% CI 84–92), respectively (P = 0.0027). The 5-year RA survival in the study groups was 90% (95% CI 86–93) and 75% (95% CI 68–80), respectively (P = 0.0048) (Fig. 3).

It should be noted that only 1.4% (n = 3) of group 1 recipients had a primary nonfunction, whereas in group 2 recipients, such an outcome was observed in 7.9% (n = 12) of cases (P = 0.002).

Our study comparing 1- and 5-year renal graft survival after primary and second transplantation, showed a significant difference in long-term survival and confirmed previously published data from the University of Heidelberg and Pour-Reza-Gholi et al. The high incidence of primary non-function after a second kidney transplantation was also confirmed, although according to our observations, it turned out to be lower than in the Eurotransplant study.

Table 3

Distribution of renal allograft recipients of the studied groups into subgroups

Groups	1		2	
Subgroups	1.1	1.2	2.1	2.2
Age, years	18–49	50–72	18–49	50–71
Recipients %, n	60.6 (129)	39.4 (84)	60.9 (92)	39.1 (59)

Table 4

Immunosuppressive therapy in groups 1 and 2

Number of recipients, n	All (n = 364)	Group 1 (n = 213)	Group 2 (n = 151)	P
Induction:				
Basiliximab, % (n)	47.6 (173)	62 (132)	27.2 (41)	0.000
Lymphocyte-depleting antibodies, % (n)	36.5 (133)	17.8 (38)	62.9 (95)	
No induction, % (n)	15.9 (58)	20.2 (43)	9.9 (15)	
Calcineurin inhibitors:				
Cyclosporine, % (n)	21.4 (78)	31.5 (67)	7.3 (11)	0.000
Tacrolimus, % (n)	78.6 (286)	68.5 (146)	92.7 (140)	
Mycophenolates, % (n)	98.9 (360)	99.5 (212)	98 (148)	0.17
Everolimus, % (n)	1.1 (4)	0.5 (1)	2 (3)	

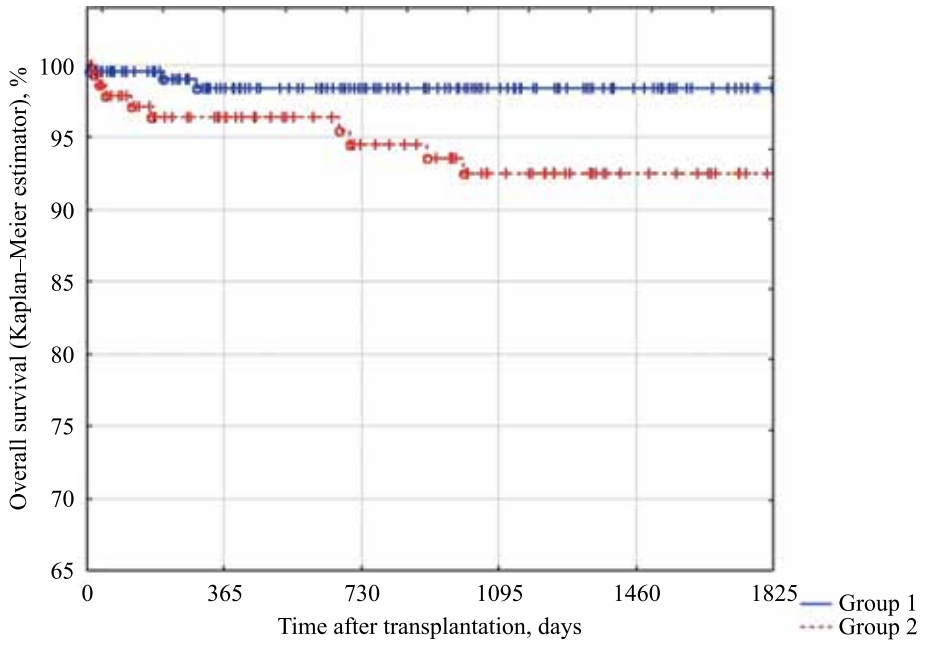

Fig. 2. Kidney recipient survival after primary and second transplantation

The 1- and 5-year survival rates of relatively young recipients in group 1 (subgroup 1.1) were 100%. The 1- and 5-year survival rate of older recipients in this group (subgroup 1.2) was 95% (95% CI 91–98) (Fig. 4).

A comparison of the 1-year 1- and 5-year recipient survival in subgroups 1.1 and 1.2 revealed statistically significant differences (P = 0.024 and P = 0.017). Thus, higher survival rates were found in the subgroup of young recipients after primary transplantation.

The 1-year survival rate for young recipients of group 2 (subgroup 2.1) was 100%, and their 5-year survival rate was 98% (95% CI 96–99). For older recipients (subgroup 2.2), it was 91% (95% CI 84–96) and 82% (95% CI 74–90), respectively (Fig. 5).

A comparison of the 1-year and 5-year recipient survival in subgroups 2.1 and 2.2 of group 2 found statistically significant differences (P = 0.009 and P = 0.001). In both group 1 and group 2 recipients, higher survival rates were observed among younger recipients.

Thus, the survival rate of young recipients in groups 1 and 2 was, as expected, statistically higher than in older

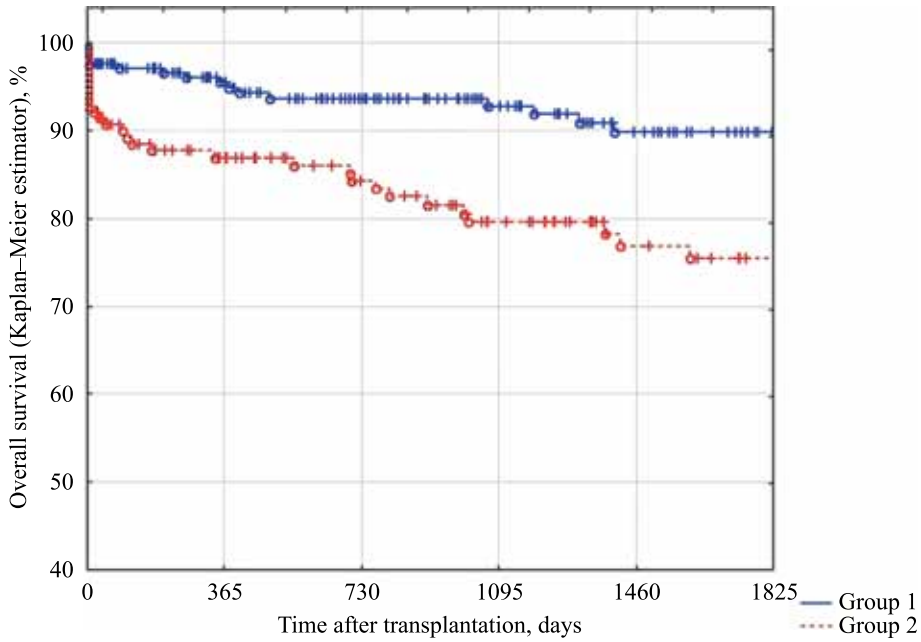

Fig. 3. Graft survival in recipients after primary and second kidney transplantation

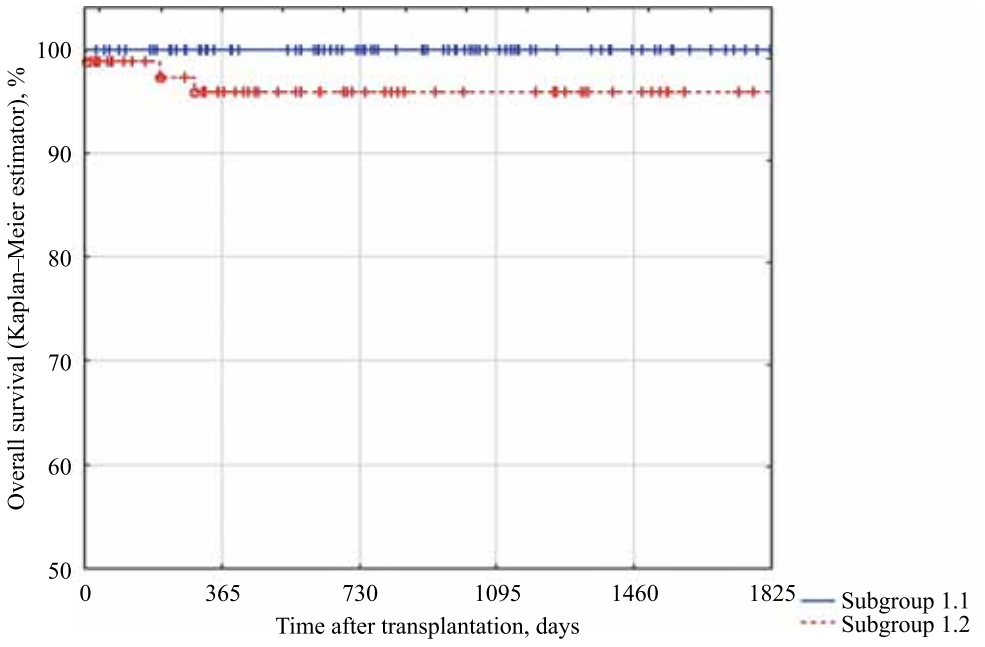

Fig. 4. Recipient survival in group 1 according to patient age

recipients. This distribution is also characteristic of the general population.

The 1-year and 5-year kidney graft survival in young recipients of group 1 was 98% (95% CI 97–99) and 91% (95% CI 87–95), respectively. In older patients in group 1, the RA survival rate was 91% (95% CI 86–96) and 82% (95% CI 75–88), respectively (Fig. 6).

A comparison of the 1-year kidney graft survival in young and older recipients of group 1 (subgroups 1.1 and 2.1) revealed a statistically significant difference (P = 0.006); however, when comparing 5-year survival in these subgroups, no significant differences were observed (P = 0.14), although the RA survival rate remained higher in young recipients.

Perhaps this loss of RA survival advantage in younger recipients is due to the tendency to develop more frequent humoral rejection observed in the early years after transplantation, whereas in elderly recipients, the significance of immunological factors of graft loss is no longer as high.

The 1- and 5-year RA survival in young recipients of group 2 was 91% (95% CI 86–95) and 80% (95%

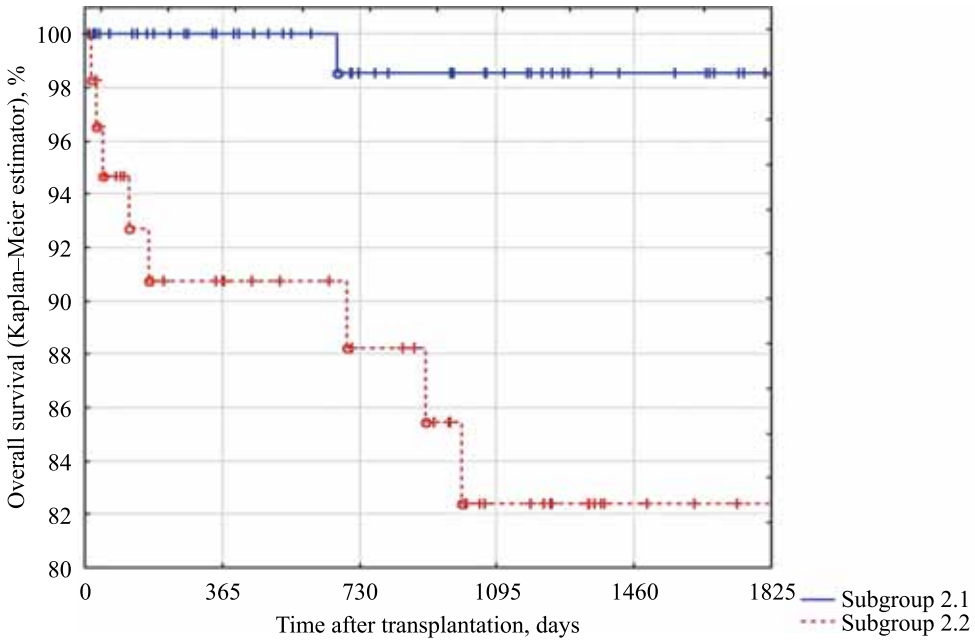

Fig. 5. Recipient survival in group 2 according to patient age

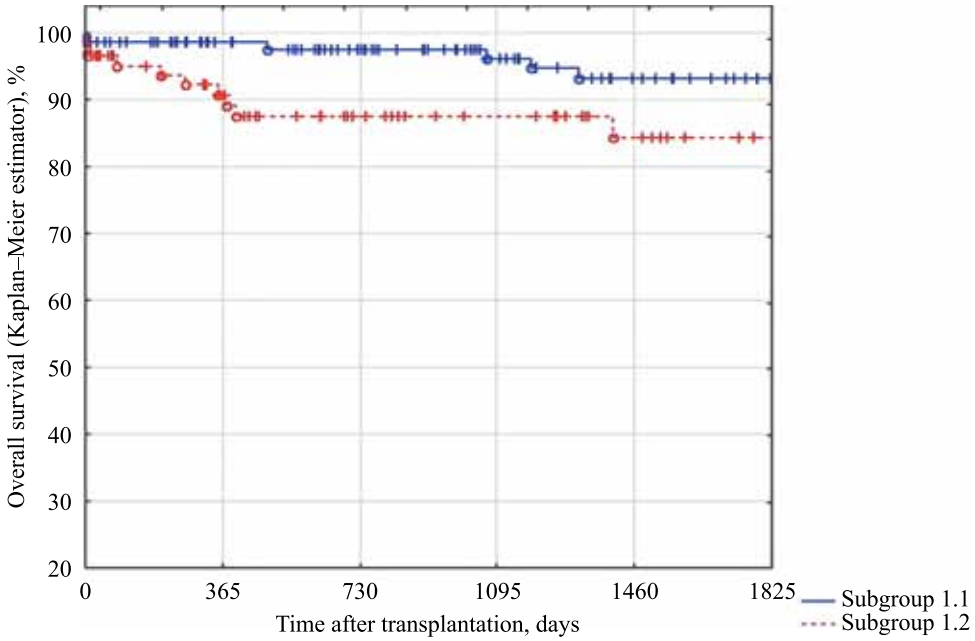

Fig. 6. Graft survival in group 1 recipients depending on age

CI 73–86), respectively. In older recipients, it is 80% (95% CI 72–88) and 70% (95% CI 61–80), respectively (Fig. 7).

A comparison of 1- and 5-year graft survival in recipients of different ages in group 2 (subgroups 2.1 and 2.2) found no statistically significant differences (P = 0.078 and P = 0.17).

The absence of the expected statistical difference in the 5-year RA survival rate in recipients of different age groups is probably due to the influence of factors that are different in nature, but similar in direction. Specifically, the RA loss in young recipients may be predominantly associated with immunological causes leading to graft loss as a result of rejection. Whereas RA loss is more often in older recipients due to primary non-functioning graft or death. This seems logical, taking into account the age-related characteristics of comorbidity and the current clinical practice of organ allocation from age-related and suboptimal donors.

Thus,

1. The 1-year recipient survival after primary and second kidney transplantation in our observations was 98% and 97% (P = 0.06); the 5-year survival was 98% and 93% (P = 0.23), respectively.
2. The 1-year RA survival after primary and second transplantation was 97% and 88% (P = 0.0027), the 5-year survival was 90% and 75% (P = 0.0048), respectively.
3. After primary transplants, the 1-year RA survival rates in subgroups 1.1 and 1.2 were 98% and 91% (P = 0.006), respectively. The 5-year RA survival in these subgroups was not statistically different – 91% and 82% (P = 0.14).
4. The 1-year RA survival in subgroups 2.1 and 2.2 was 91% and 80%, respectively (P = 0.078), 5-year survival rates were 80% and 70% (P = 0.17). After repeated transplantations, there were no significant differences in 1- and 5-year RA survival depending on recipient age.
5. The incidence of primary non-function after primary transplantation and after repeated transplantation was 1.4% and 7.9%, respectively (P = 0.002).

CONCLUSION

The generally accepted opinion that primary transplantation has a negative effect on the outcome of a second one is still being debated among specialists and needs to be confirmed, since data from various transplant centers published in the medical literature are contradictory. Our paper presents a 12-year experience of one Russian transplant center in relation to the outcomes of repeated kidney transplants. We did not find any statistically significant difference in the 1- and 5-year recipient survival rates after primary and repeated kidney transplants. On the other hand, graft survival after primary transplant was significantly higher than after the second transplant. In addition, primary non-function was significantly more frequent after repeated transplantations. At the same time, recipient survival in the older age group was naturally significantly lower than with younger recipients, both after primary and after repeated transplantation. A comparison of the 1-year survival of primary renal transplants showed it to be significantly higher in the subgroup of young recipients. However, a comparison of the 5-year survival of primary kidney transplants no longer revealed any statistically significant difference,

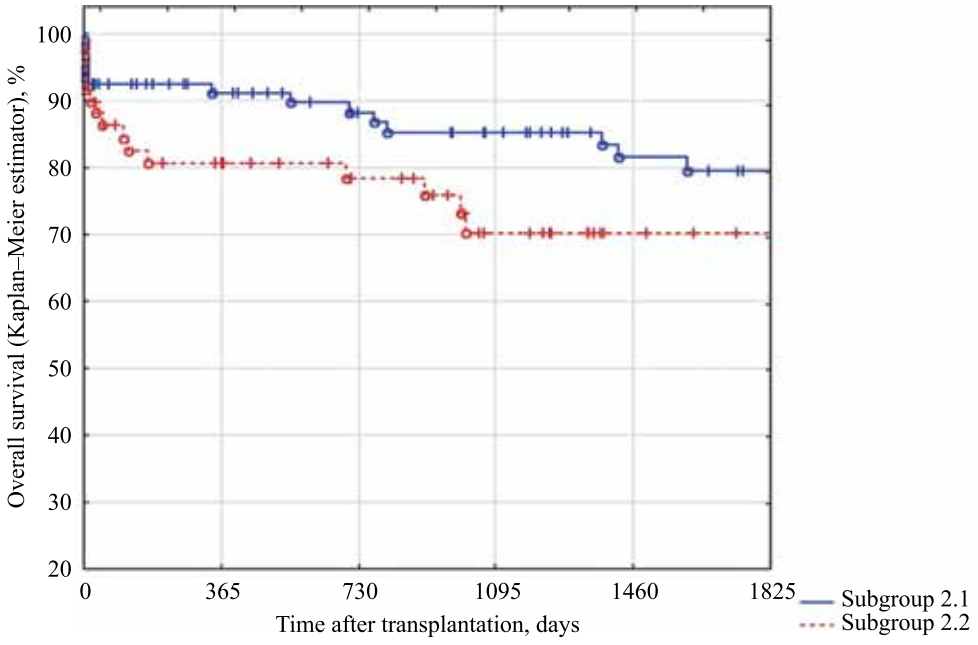

Fig. 7. Graft survival in group 2 recipients depending on age

apparently due to the activity of immunological factors of graft loss in young recipients. When comparing 1- and 5-year survival rates for repeated grafts depending on recipient age, significant and clinically significant differences were evident, which is clearly shown in Fig. 7, but their reliability has not been statistically confirmed.

The authors declare no conflict of interest.

REFERENCES

1. https://www.ctstransplant.org/public/graphics/sample.shtml.
2. *Pour-Reza-Gholi F*, *Nafar M*, *Saeedinia A*, *Farrokhi F*, *Firouzan A*, *Simforoosh N et al.* Kidney retransplantation in comparison with first kidney transplantation *Transplant Proc*. 2005; 37 (7): 2962–2964. PMID: 16213274. doi: 10.1016/j.transproceed.2005.08.034.
3. https://www.anzdata.org.au/wp-content/uploads/2019/09/c07_transplant_2018_ar_2019_v1.0_20200525.pdf.
4. *Jędrzejko K*, *Kieszek R*, *Kwapisz M*, *Nita M*, *Durlik M*, *Kwiatkowski A*. The comparison of kidney transplantation results from the same deceased donor between patients with the first transplantation and retransplanted patients. *Transplantation Proceedings*. 2018; 50 (6): 1726–1729. PMID: 30056889. doi: 10.1016/j.transproceed.2017.12.058.
5. *Ingsathit A, Kantachuvesiri S, Rattanasiri S, Avihingsanon Y, Premasathian N, Pongskul C et al.* Long-term outcome of kidney retransplantation in comparison with first kidney transplantation: a report from the Thai Transplantation Registry. *Transplant Proc*. 2013; 45 (4): 1427–1430. PMID: 23726588. doi: 10.1016/j.transproceed.2012.08.029.
6. *Sang Hyup Han*, *Jin Go*, *Sun Cheol Park*, *Sang Seob Yun.* Long-Term Outcome of Kidney Retransplantation in Comparison With First Transplantation: A Propensity Score Matching Analysis. *Transplant Proc*. 2019; 51 (8): 2582–2586. PMID: 31474448. doi: 10.1016/j.transproceed.2019.03.070.
7. *Heldal K, Hartmann A, Lønning K, Leivestad T, Reisæter AV, Line PD et al.* Should patients older than 65 years be offered a second kidney transplant? *BMC Nephrol*. 2017; 18 (1): 13. PMID: 28077080. doi: 10.1186/s12882-016-0426-0.
8. *Assfalg V, Selig K, Tolksdorf J, van Meel M, de Vries E, Ramsoebhag A-M et al.* Repeated Kidney Re-Transplantation – The Eurotransplant experience: a retrospective multicenter outcome analysis. *Transplant International*. 2020; 33 (6): 617–631. PMID: 31903658. doi: 10.1111/tri.13569.
9. *Dabare D, Kassimatis T, Hodson J, Arslan Khurram M, Papadakis G, Rompianesi 1 G et al.* Outcomes in Third and Fourth Kidney Transplants Based on the Type of Donor. *Transplantation*. 2019 Jul; 103 (7): 1494–1503. PMID: 30130325. doi: 10.1097/TP.0000000000002428.
10. *Sood P, Xiaotian G, Mehta R, Landsittel D, Wu C, Nusrat R et al.* Kidney Transplant Outcomes After Primary, Repeat and Kidney After Nonrenal Solid Organ Transplantation A Single-Center Experience. *Transplant Direct*. 2016; 2 (6): e75.4. PMID: 27500265. doi: 10.1097/TXD.0000000000000586.
11. *Trébern-Launay K, Foucher Y, Giral M, Legendre C, Kreis H, Kessler M et al.* Poor long-term outcome in second kidney transplantation: a delayed event. *PLoS One*. 2012; 7 (10): e47915. PMID: 23110130. doi: 10.1371/journal.pone.0047915.

The article was submitted to the journal on 2.09.2020

DOI: 10.15825/1995-1191-2021-2-30-35

INVASIVE PULMONARY ASPERGILLOSIS AFTER HEART TRANSPLANTATION

M.A. Simonenko[1], M.Yu. Sitnikova[1], P.A. Fedotov[1], Yu.V. Sazonova[1], M.A. Bortsova[1], K.I. Monosova[1], L.A. Vasilieva[2], L.B. Mitrofanova[1], G.V. Nikolaev[1], M.L. Gordeev[1], M.A. Karpenko[1]

[1] Almazov National Medical Research Centre, St. Petersburg, Russian Federation
[2] Pavlov First St. Petersburg State Medical University, St. Petersburg, Russian Federation

Objective: to assess the incidence, determine the peculiarities of the course of invasive pulmonary aspergillosis (IPA) and identify risk factors for IPA in heart transplant recipients. **Materials and methods.** From January 2010 to December 2019, 137 heart transplantations (HT) were performed: mean age 46 ± 14 years; male 102 (74%) and female 35 (26%). All patients received a three-component immunosuppressive therapy: calcineurin inhibitors, mycophenolate mofetil (MMF) and Glucocorticoid (GCs). Induction therapy consisted of Basiliximab (81%, n = 111) and antithymocyte immunoglobulin (15%, n = 20). A retrospective analysis of patients with identified post-HT invasive IPA was performed; risk factors for IPA were assessed. In patients with early IPA, the length of stay in the intensive care unit (ICU), the duration of mechanical ventilation, and the initial severity of the condition were studied. All patients with suspected pneumonia underwent bronchoscopy with examination of bronchoalveolar lavage (BAL) and chest computed tomography (chest CT scan). **Results.** During the follow-up, there were 58 episodes of pneumonia, of which 16 (28%) were IPA (age 33 to 64 years). All patients had a target level of immunosuppressive drugs concentration in blood; basiliximab was used as induction therapy in 15 of 16 patients. Half of the recipients developed IPA in the early post-HT period (less than 3 months after HT), in the rest (n = 8) – at a later date (3 months to 1 year after HT). The diagnosis was verified: 14 out of 16 patients showed an increase in the Aspergillus antigen positivity in the BAL to 7.2 (2.8 ± 1.6); chest CT scan revealed specific changes. In two patients, there were no diagnostic criteria for IPA, but the diagnosis was made based on the results of histological examination after resection of the left lower lobe of the lung. All patients received voriconazole therapy for 2 to 6 months, their immunosuppressive therapy was adjusted (tacrolimus and MMF dose adjustment) and their white blood cell count was monitored. Complete cure of the disease was achieved in 13 (81%) patients. Two patients died within 30 days after HT in the intensive care unit, one died from urogenital diseases caused by bacterial flora and leading to urosepsis, 4 months after IPA treatment was initiated. All patients had risk factors for IPA: taking immunosuppression, including GCs (n = 16), prolonged ICU stay (n = 14), inotropic support exceeding 2 days in the early post-transplant period (n = 10), cachexia during HT (n = 6), leukopenia (n = 9) and neutropenia (n = 14). **Conclusion.** In heart transplantat recipients, the incidence of IPA among respiratory tract infections is 28%. The risk of developing IPA was highest during the first year following HT. In the majority of recipients, the disease was detected at the early stages; diagnosis required surgical intervention in 12% of cases. A decrease in the risk of developing IPA was associated with correction of the following risk factors for this disease in all patients: volume of immunosuppressive therapy during the first year after transplantation and prevention of the development of neutropenia as a marker of infectious complications or immunosuppression overdose. Early diagnosis of IPA allowed for initiation of timely specific therapy in most recipients and achievement of a positive effect in 80% of them.

Keywords: heart transplantation, infectious complications, invasive pulmonary aspergillosis.

INTRODUCTION

The number of heart transplant (HT) recipients is increasing every year. Infectious diseases are the most frequent complications and the leading cause of mortality in the post-transplant period. The number of heart recipients is increasing every year. Infectious diseases are the most frequent complications and the leading cause of post-transplant mortality [1, 2].

Invasive pulmonary aspergillosis (IPA) is an opportunistic fungal infection that can develop within the first year after HT (most commonly within <1 to 3 months after surgery) and can be fatal [3, 4]. When pneumonia develops in patients regardless of the timing after heart transplantation, it is shown to exclude its fungal genesis. Currently, there are no data on the incidence of IPA in the post-transplant population [4, 5]. Some studies

Corresponding author: Maria Symonenko. Address: 2, Akkuratova str., St. Petersburg, 197341, Russian Federation. Phone: (921) 952-43-55. E-mail: dr.maria.simonenko@gmail.com, simonenko_ma@almazovcentre.ru

have reported that this complication predominates in men (84%), whose average age is 43 years, one third of which has ischemic congestive heart failure (CHF) [4, 6]. Patients usually complain of fever and cough, but clinical manifestations may be absent in the initial stages of the disease [4, 6]. Laboratory findings may include leukopenia and neutropenia up to agranulocytosis [4, 6, 7]. Radiological findings include infiltrative changes, and chest CT scan may show "frosted-glass" changes, which is typical for various respiratory diseases of viral or fungal origin [4, 6, 7]. Absence of clinical symptoms at the initial stages of the disease and the risk of developing infectious complications caused by mixed flora (bacterial + fungal, viral + fungal) often lead to untimely diagnosis and increases the mortality rate.

Objective: to assess the incidence, features of the course and identify risk factors for the development of pulmonary aspergillosis in HT recipients.

MATERIALS AND METHODS

From January 2010 to December 2019, 137 orthotopic HTs were performed using the bicaval technique at Almazov National Medical Research Centre, St. Petersburg, Russia. This included 102 men (74%) and 6 children (5 of them were female) 10–16 years old (median 15 years). The mean age of the recipients was 46 ± 14 years.

During the first year after HT, all patients received three-component immunosuppressive therapy: calcineurin inhibitors (FK-506), mycophenolate mofetil (MMF)/everolimus, and glucocorticoids (GCS). During the first year after HT, the volume of glucocorticoids was gradually reduced to complete cancellation. In the case of development of leukopenia and/or neutropenia against the background of GCS reduction, the volume of MMF therapy also decreased. Induction therapy was represented by Basiliximab (81%, n = 111) and antithymocyte immunoglobulin (15%, n = 20). Along with immunosuppressive therapy, pneumocystis pneumonia prophylaxis was carried out for 6 months (sulfamethoxazole + trimethoprim together with folic acid), antifungal (nystatin for 1 month) antiviral (valganciclovir for 1 year) therapy was used. Prophylactic therapy in all patients included statins (atorvastatin at a dose of up to 20 mg/day), calcium preparations together with cholecalciferol, proton pump inhibitors, and antihypertensive, antiarrhythmic, etc. therapy was prescribed as indicated.

This study was carried out in accordance with the principles of the Declaration of Helsinki. For the period from January 2010 to December 2019, a retrospective analysis of clinical and laboratory characteristics in patients with post-HT IPA was carried out, its risk factors were evaluated. In patients with early IPA, the initial severity of the condition, length of stay in the intensive care unit (ICU), and duration of mechanical ventilation were studied. All patients with suspected pneumonia underwent chest CT scan and bronchoscopy, followed by bronchoalveolar lavage (BAL): culture, cytology, Aspergillus antigen, cytomegalovirus infection, and pneumocystis. Laboratory diagnostics included evaluation of inflammation markers (clinical blood count with WBC count and C-reactive protein (quantitative) over time, polymerase chain reaction to cytomegalovirus and Epstein–Barr virus, blood culture, general analysis and sputum culture, general analysis, and urine culture, and if fungal infection was suspected (development of leukopenia and/or neutropenia), a blood test for galactomannan was performed. Immunosuppressive therapy was adjusted: in patients with confirmed IPA, mycophenolate mofetil therapy was reduced or, in the case of bacterial infection, it was temporarily canceled, and serum tacrolimus levels corresponded to the target values, according to the timing after HT (8–12 ng/mL).

The data were statistically processed using SPSS 21.ORU. Mean values and standard deviation (M ± SD) were calculated. In the case of a small sample ($n < 20$), the data were presented as medians (Me), [minimum and maximum values]. With a distribution other than normal, the nonparametric Mann–Whitney method was used to assess the differences; the data are presented as medians (Me), [25th and 75th percentiles]. Fisher's exact test was used to assess differences in qualitative parameters. The criterion for statistical significance of the obtained differences was $p < 0.05$.

RESULTS

During the follow-up, 58 episodes of pneumonia were recorded among all patients who underwent HT, of which 16 (28%) people were diagnosed with IPA.

General characteristics of patients. The age of these patients ranged from 33 to 64 years (Me 55 years). The patients who underwent IPA had characteristic risk factors for fungal infections: 6 had cardiac cachexia at the time of HT, all had ongoing immunosuppressive therapy, including GCS (n = 16), leukopenia (n = 9), and neutropenia (n = 14), inotropic support lasting more than 2 days in the early postoperative period (n = 10) and long stay in the ICU (n = 14).

Basiliximab was used as induction therapy in 15 out of 16 patients, and antithymocyte globulin was used in one patient. Half of the recipients developed IPA early after HT (less than 3 months after HT), while the rest (n = 8) developed IPA between 3 months and 1 year after HT. None of the patients developed IPA for more than 1 year after HT. In the early postoperative period, an extracorporeal membrane oxygenation (ECMO) system was installed in one patient due to right ventricular heart failure [8], against the background of which pneumonia of mixed (bacterial + fungal) origin was detected. In 14 out of 16 patients, there was increased Aspergillus antigen positivity in BAL (from 1.45 to 10.2) and chest CT scan showed "frosted-glass" changes. In two patients no

effect of antibiotic therapy, laboratory and instrumental criteria for IPA were absent, and transthoracic resection of the lung lobe was performed for differential diagnosis with oncopathology due to anatomical inaccessibility for transbronchial biopsy. The IPA diagnosis was verified by histological examination. Characteristic histological changes are shown in Fig.

After detection of IPA, all patients were treated with voriconazole for 2 to 6 months (initially by intravenous administration of 400 mg × 2 times a day, and then orally after normalization of the CRP level).

Features of immunosuppressive therapy. At the time of IPA development, all patients were receiving tacrolimus, MMF, and glucocorticoid therapy; immunosuppressive drugs concentrations in blood were targeted. When pneumonia was detected, MMF was temporarily canceled, then the timing of the resumption of such therapy was determined individually, taking into account the clinical symptoms (absence of fever), level of inflammation markers and under control of heart graft function. Taking into account drug interactions after antimycotic therapy, all patients required a reduction of the tacrolimus dose by at least 2–3 times, and after the end of voriconazole, the tacrolimus dose was increased again to achieve the target blood concentration values, followed by regular laboratory monitoring. In three patients, due to the development of agranulocytosis, the mycophenolate mofetil dose was temporarily canceled or reduced, and colony-stimulating factors were used until the transition through nadir.

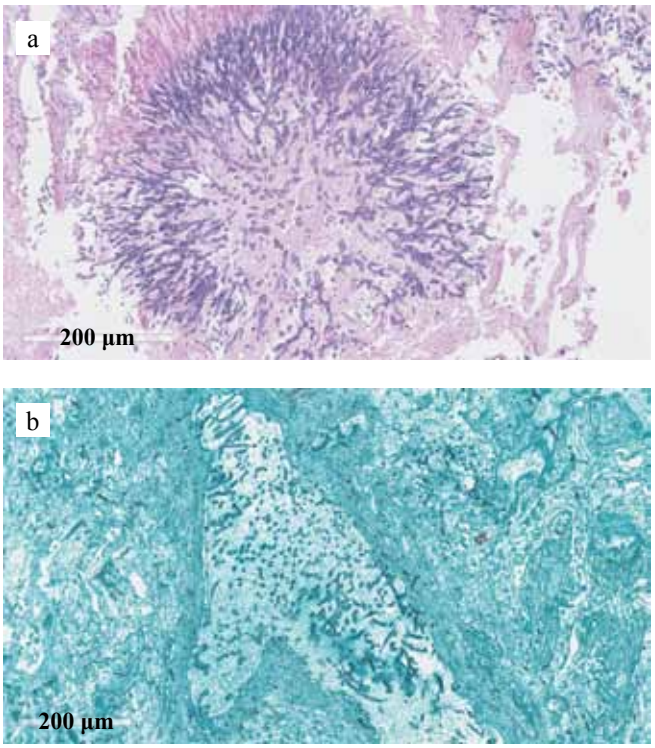

Fig. Aspergillosis with dichotomous branching of septate hyphae: A. H&E Stain, 200×. B. Grocott's stain, 200×

Every 1–2 weeks from the beginning of the infectious process, the heart graft function was assessed – ECG (every week), ECHO (at least once in 2 weeks). None of the patients had any cardiac graft function damage during IPA; therefore, the endomyocardial biopsy (EMB) was postponed until the acute infectious process was relieved and was performed after normalization of inflammatory markers in the absence of fever, no earlier than 2 months after IPA development.

The disease was completely cured in 13 (81%) patients within six months. Two patients died within 30 days after HT from infectious complications of bacterial genesis followed by development of sepsis. Another patient died 4 months after the start of IPA treatment from urosepsis. None of the convalescents had recurrent IPA in the long-term after heart transplantation.

DISCUSSION

When infectious complications develop in patients after heart transplantation, an examination should always be conducted to find the etiology, with mandatory exclusion of the presence of mixed flora. With persisting radiological changes, even if there is a positive effect (reduction or normalization of C-reactive protein (CRP) levels, absence of fever) against the background of standard antibiotic therapy for the treatment of pneumonia, continuation of the examination is always indicated in order to exclude non-bacterial genesis of the process, for example, cytomegalovirus or coronavirus infection, aspergillosis, pulmonary mycosis or toxic everolimus-associated alveolitis. Aspergillus is found in cultures of sputum (8–34%) and BAL (45–62%) [11], and its detection in the early stages of the lesion allows arresting the process without reducing lung function and increases patient post-HT survival.

Common risk factors for IPA are steroid-dependent asthma or chronic obstructive pulmonary disease [14], but none of the described cohort of patients had such comorbidities. P. Munoz et al. and T. Pelaez et al. distinguish another risk factor – diabetes mellitus [5, 14]. According to our results, 63% (n = 10 of 16) of patients diagnosed with IPA had type 2 diabetes mellitus or post-transplant diabetes. Other risk factors for IPA in solid organ recipients are cytomegalovirus infection, use of mechanical circulatory support and/or renal replacement therapy in the early postoperative period [5, 11].

Reducing the risk of IPA may be associated with adjusting the volume of immunosuppressive therapy during the first year after transplantation, preventing neutropenia and normalizing nutritional status, which are reversible risk factors for this disease. An overdose of immunosuppressive therapy increases the risk of post-transplant complications, especially infectious ones. None of the patients in the described group were at risk of developing IPA in the long term after surgery (more than 1 year), which can be associated with reduced

volume of immunosuppressive therapy over time: decrease in GCS up to complete cancellation, timing after introduced induction therapy and a decrease in calcineurin inhibitor concentrations. Given the drug interactions of antimycotic drugs, regular laboratory monitoring of the concentrations of immunosuppressive drugs (to maintain target values), clinical blood count with WBC count (as a marker of inflammation and to assess tolerance of optimal doses of antiproliferants) and CRP, as well as radiological monitoring of chest organs (X-rays, CT) help to reduce the risk of infectious complications and ensure detection of post-transplant diseases [4, 9, 10].

Given the immunocompromised status of patients, characterized by atypical symptoms of infectious processes (including absence of fever), laboratory and imaging examination results should be evaluated taking into account the anamnesis. For example, "normalization" of the WBC count at initial chronic leukopenia may reflect the accession of bacterial flora, and changes in WBC counts combined with increased CRP in the long-term after HT period may require the exclusion of oncopathology, etc. [9, 11–12]. Meanwhile, "frosted-glass" changes in the lung tissue, characteristic of fungal and viral pneumonia, can persist in the long-term period after the relief of a previous IPA or pneumonia caused by SARS-CoV-2, etc. Another peculiarity of radiological dynamics of the process is that the volume of pulmonary infiltrates may even increase during the first 7–10 days of antifungal therapy, but such dynamics are a predictor of granulocyte recovery [13].

The drugs of choice for the treatment of IPA are amphotericin B, caspofungin, and voriconazole [4, 11, 13]. Survival rates were higher in patients treated with voriconazole compared to those treated with amphotericin B (70.8% and 57.9%, respectively) [4, 11]. The standard regimen for prescribing voriconazole in patients after solid organ transplantation is 6 mg/kg, 2 doses intravenously, then 4 mg/kg intravenously every 12 hours, with the dynamic transition to oral administration of the drug, 200 mg/day every 12 hours. In patients taking calcineurin inhibitors (cyclosporin, tacrolimus), it is necessary to consider drug interactions when adding antimycotic agents to therapy, which lead to increased concentrations of immunosuppressive drugs in a short time. This requires a reduction in cyclosporine and tacrolimus doses from the very first day of administration of antimycotic drugs [11, 13]. The minimum duration of antimycotic therapy in immunocompromised patients is 6–12 weeks, but the duration of conservative therapy in each case is determined individually and depends on the time of resolution of the pulmonary lesion [10, 13, 15]. Surgical resection of tissues infected by Aspergillus can be considered as an adjunct to conservative treatment in patients with involvement of large vessel lesion, development of pericarditis and/or pleurisy [13, 15].

According to reports, mortality from IPA is 30–40% [4, 13]. In our present study, out of 16 recipients diagnosed with IPA, 3 died (19%), and IPA had not been cured at the time of death. However, those who died had other infectious complications in addition to IPA (mixed infection: bacterial and fungal.

CONCLUSION

In post-HT patients, the incidence of IPA among respiratory tract infections was 28%. The highest risk of IPA was in the first year after HT. In the majority of recipients, the disease was detected at the initial stages; in 12% of cases, surgical intervention was required for diagnosis. A decrease in IPA risk was associated with correction of the following risk factors for this disease in all patients: volume of immunosuppressive therapy during the first year after transplantation and prevention of the development of neutropenia as a marker of infectious complications or an immunosuppression overdose. Early diagnosis of IPA made it possible to initiate timely specific therapy in the majority of recipients and achieve a positive effect in 80% of them.

The authors declare no conflict of interest.

REFERENCES

1. ISHLT Registry – Heart Transplantation: overall. *JHLT*. 2019 Oct; 38 (10): 1015–1066.
2. *Fedotov P, Sazonova Y, Rubinchik V, Simonenko M, Sitnikova M*. Infectious episodes in early post-transplant period and in long-term follow-up of heart transplantation. *Journal of Transplantology*. 2015; 3: 47–55.
3. *Hummel M*. Early postoperative therapy after heart transplantation: prophylaxis, diagnosis and antibiotic, antimycotic and antiviral therapy of infections. *Transplantationsmedizin*. 2011; 23: 190–197.
4. *Montoya JG, Chaparro SV, Celis D, Cortes JA, Leung AN, Robbins RC, Stevens DA*. Invasive aspergillosis in the setting of cardiac transplantation. *Clinical Infectious Diseases*. 2003; 37 (Suppl. 3): S281–292.
5. *Munoz P, Rodriguez C, Bouza E, Palomo J, Yanez JF, Dominguez MJ, Desco M*. Risk factors of invasive aspergillosis after heart transplantation: protective role of oral Itraconazole prophylaxis. *American Journal of Transplantation*. 2004; 4: 636–643. doi: 10.1111/j.1600-6143.2004.00390.x.
6. *Denning DW, Cadranel J, Beigelman-Aubry C, Ader F, Chakrabarti A, Blot S et al*. Chronic pulmonary aspergillosis: rationale and clinical guidelines for diagnosis and management, ESCMID/ERS Guidelines: Task force report. *Eur Respir J*. 2016; 47: 45–68. doi: 10.1183/13993003.00583-2015.
7. *Al-Abdely HM, Alothman AF, Al Salman J, Al-Musawi T, Almaslamani M, Butt AA et al*. Clinical practice guidelines for the treatment of invasive *Aspergillus* infections in adults in the Middle East region: Expert panel recommendations. *Journal of Infection and Public Health by Elsevier*. 2014; 7: 20–31. doi: 10.1016/j.jiph.2013.08.003.

8. *Simonenko MA, Nikolaev GV, Malikov KN, Fedotov PA, Sazonova YuV, Bortsova MA et al*. Heart transplantation in recipients with initial pulmonary hypertension: 9 years of experience in Almazov National Medical Research Centre. *Russian Journal of Transplantology and Artificial Organs*. 2019; 21 (4): 7–13. doi: 10.15825/1995-1191-2019-4-7-13.
9. *Misch EA, Safdar N*. Updated guidelines for the diagnosis and management aspergillosis. *Journal of Thoracic Disease*. 2016; 8 (12): E1771–E1776.
10. *Ullmann AJ, Aguado JM, Arikan-Akdagli S, Denning DW, Groll AH, Lagrou K*. Dignosis and management of *Aspergillus* diseases: executive summary of the 2017 ESCMID-ECMM-ERS guideline. *Clinical Microbiology and Infection*. 2018; 24: e1–e38. doi: 10.1016/j.cmi.2018.01.002.
11. *Singh N, Paterson DL*. *Aspergillus* Infections in Transplant Recipients. *Clinical Microbiology Reviews*. 2005; 18 (1): 44–49. doi: 10.1128/CMR.18.1.44-69-2005.
12. *Montoya JG, Giraldo LF, Efron B, Stinson EB, Gamberg P, Hunt S et al.* Infectious complications among 620 consecutive heart transplant patients at Stanford University Medical Center. *Clin Infect Dis*. 2001; 33: 629–640.
13. *Walsh TJ, Anaissie EJ, Denning DW, Herbrecht R, Kontoyiannis DP, Marr KA et al*. Treatment of Aspergillosis: Clinical Practice Guidelines of the Infectious Diseases Society of America. *Clinical Infectious Diseases*. 2008; 46: 327–360. doi: 10.1086/525258.
14. *Pelaez T, Munoz P, Guinea J, Valerio M, Giannella M, Klaassen CHW, Bouza E*. Outbreak of Invasive Aspergillosis after major heart surgery caused by spores in the air of the intensive care unit. *Clin Infect Dis*. 2012; 54 (3): e24–e31. doi: 10.1093/cid/cir771.
15. *Patterson TF, Thompson GR III, Denning DW, Fishman JA, Hadley S, Herbrecht R et al.* Practice guidelines for the diagnosis and management of Aspergillosis: 2016 Update by the Infectious Diseases Society of America. *Clinical Infectious Diseases*. 2016; 63 (4): e1–60. doi: 10.1093/cid/ciw326.

The article was submitted to the journal on 11.03.2021

DOI: 10.15825/1995-1191-2021-2-36-40

KIDNEY TRANSPLANTATION IN KAZAKHSTAN: THE BURDEN OF ORGAN SHORTAGE

S.A. Abdugafarov, M.N. Asykbayev, D.J. Saparbay

National Research Oncology Center, Center for Urology, Nephrology and Kidney Transplantation, Nur-Sultan, Kazakhstan

Kidney transplantation has been the best replacement therapy for end-stage kidney disease for over 60 years. The Republican Coordination Center for Transplantation reports that as of January 29, 2020, there were 2675 people on the kidney transplant waiting list in the Republic of Kazakhstan. The issue of deceased donation in Kazakhstan is problematic for various reasons. Over the past couple of years, the already low rates of deceased donors have fallen by more than 2 times. **Objective:** to objectively assess the effectiveness of deceased-donor kidney transplant in order to indicate the need for development of cadaveric donation and reduce the number of patients in the transplant waitlist. **Materials and methods.** Fifty-two kidney transplants from a deceased donor were performed at the National Research Oncology Center (NROC) from 2010 to 2020. The age group of recipients ranged from 20 to 75 years old. In most cases, end-stage chronic renal failure resulted in chronic glomerulonephritis (76%), pyelonephritis (1.9%), polycystic kidney disease (9.6%) and diabetic nephropathy (11.5%). **Results.** The 1-year and 5-year survival rates were 96% and 86%, respectively. There was delayed graft function in 13 of cases. In one case (1.92%), there was intraoperative hyperacute rejection of the kidney transplant that could not be treated with high doses of glucocorticosteroids; the kidney graft was removed. Two patients (3.8%) in the early postoperative period, on days 2 and 7 after surgery, developed a clinic of acute renal transplant rejection; after the rejection crisis was stopped by drug therapy, graft function was restored. One patient (1.92%) died as a result of bilateral pneumonia, which led to sepsis and death. **Conclusion.** Graft and recipient survival rates after deceased-donor kidney are comparable to those after living-donor kidney transplantation. The solution to the problems of increasing the number of deceased organ transplants should not rest entirely on the shoulders of transplant doctors; this task must also be addressed at the government level with constant propaganda to explain to the citizens the need for a deceased organ donation program.

Keywords: kidney transplantation, posthumous donor, organ shortage.

BACKGROUND

Kidney transplantation remains the primary therapy for end-stage kidney disease. At present, over 90,000 kidney transplants are performed annually in the world [1]. However, organ shortage still remains extremely severe [2, 3]. According to statistics, there is a progressive increase in the number of patients in need of kidney transplantation. The Republican Coordination Center for Transplantation (RCCT) reports that as of January 29, 2020, there were 2,675 people in the Republic of Kazakhstan waitlisted for kidney transplant. Of these, 75 patients are children under 18 years of age. The issue of cadaveric donation in Kazakhstan is problematic for various reasons, both on the part of society and on the part of donor hospitals. Since the end of 2019, the government has been actively working in this direction. It is worth noting that over the past couple of years, the already low cadaveric donor indicators have decreased by more than twice [4].

According to the RCCT, from 2012 to the end of 2019, 1278 kidney transplants were performed at all transplant centers in Kazakhstan, including 161 deceased-donor kidney transplants [4]. Deceased donors accounted for 12.5% of the total number of operations performed and less than 1% per million population, which is a very low figure.

According to world statistics provided by the Global Observatory on Donation and Transplantation (GODT) on kidney transplantation for 2017 (Fig. 1), Kazakhstan occupies one of the last positions in terms of number of deceased-donor kidney transplants per million population [1].

Objective: to objectively assess the effectiveness of deceased-donor kidney transplant in order to indicate the need for development of cadaveric donation programs and reduce the number of patients in the transplant waitlist.

Corresponding author: Dzhamilya Saparbay. Address: 3, Kerey and Zhanibek khandar str., Nur-Sultan city, 01-0000, Republic of Kazakhstan.
Phone: (7172) 70-29-41. E-mail: dzhamilyasaparbay@gmail.com

MATERIALS AND METHODS

This work is based on a clinical review of 52 cases of deceased-donor kidney transplantations in the period from 2012 to 2019 at the National Research Oncology Center, Nur-Sultan, Kazakhstan (Fig. 2).

The age group of the recipients ranged from 20 to 75 years old. In most cases, end-stage chronic kidney disease resulted in chronic glomerulonephritis (76%), pyelonephritis (1.9%), polycystic kidney disease (9.6%) and diabetic nephropathy (11.5%), all of whom were on long-term hemodialysis at the time of kidney transplantation.

Priority was given to recipients who were to undergo a kidney transplant for the first time, since repeated kidney transplants had a high immunological risk and there was no tissue compatibility with a deceased donor. In one case, a repeated kidney transplantation from a cadaver was performed, while there was tissue compatibility

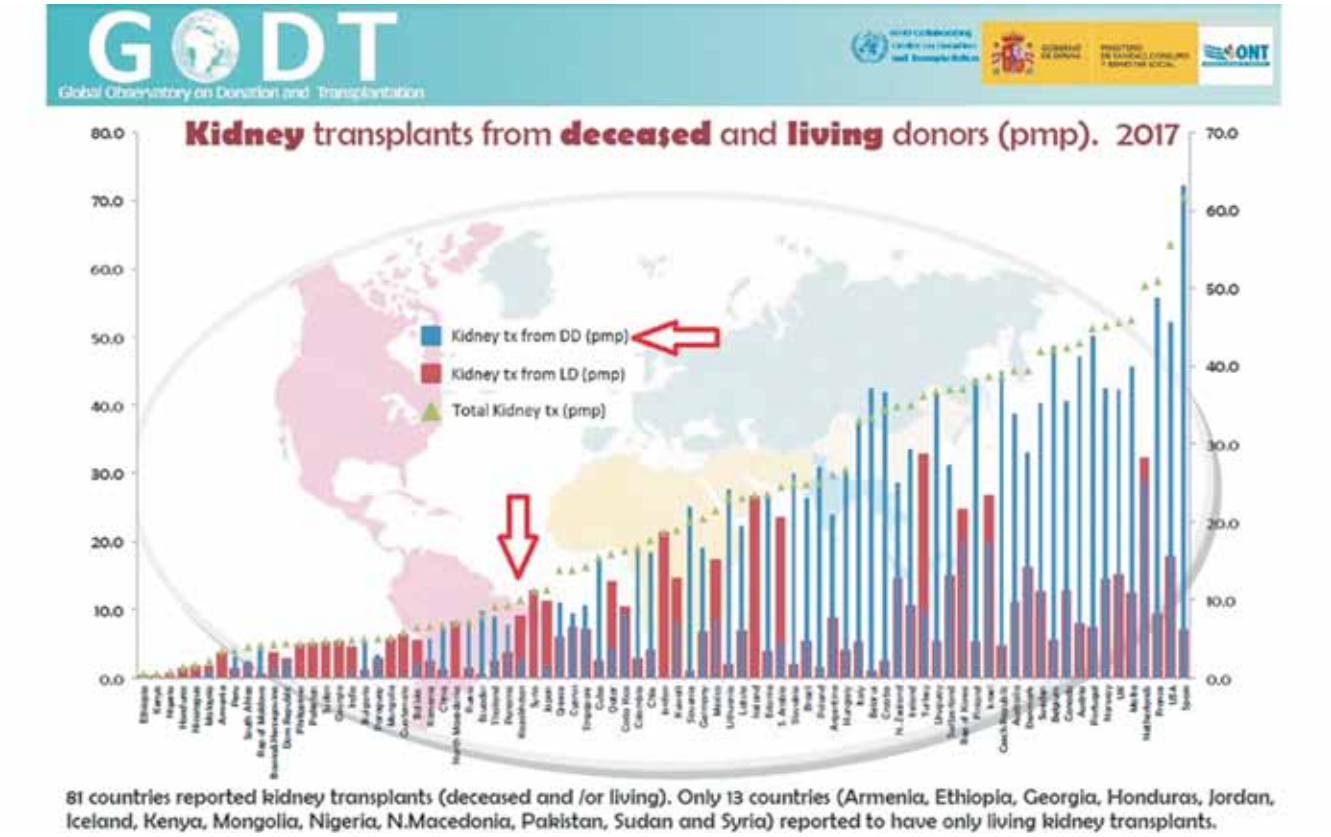

Fig. 1. Statistics on kidney transplants performed in the world per million population (Global Observatory on Donation and Transplantation data for 2017)

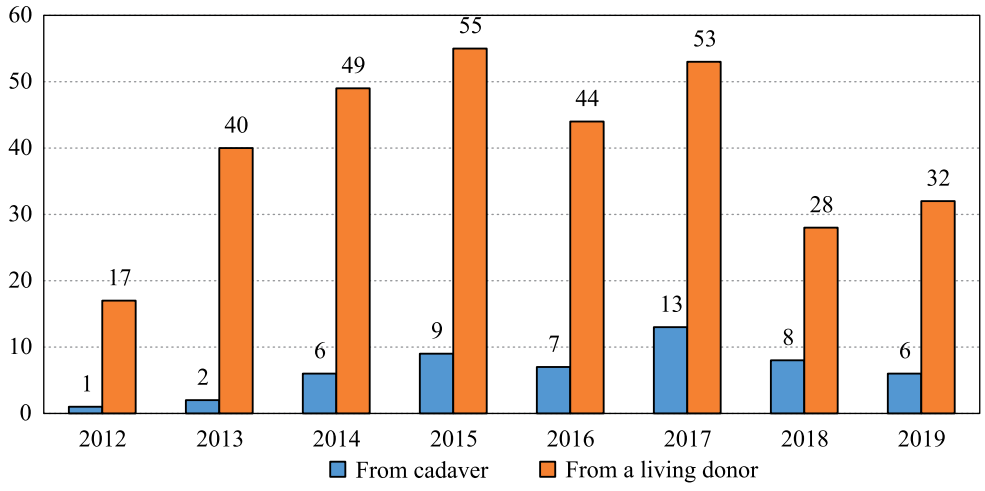

Fig. 2. The number of deceased-donor and living-donor kidney transplants performed in Kazakhstan from 2012 to 2019

between the donor and the recipient and there was a low immunological risk.

Cold ischemia time varied from 6 to 23 hours and depended on many reasons, including the location of the deceased donor, and the time it took to perform the necessary tissue compatibility tests and conduct a cross match test. In most cases, transplantation was performed according to the standard technique in the retroperitoneal space, in the right iliac region. In two cases, in the left iliac region. In one case, taking into account simultaneous kidney and pancreas transplantation, the transplantation was carried out through a laparotomic incision into the abdominal cavity. Secondary heat ischemia did not exceed 40 minutes. There were no technical difficulties during the operation, given the great length of the donor kidney vessels and the possibilities for various types of vessel modeling.

Immunosuppressive therapy during surgery and in the postoperative period as a whole, in comparison to that used after living-donor kidney transplantation, has slight differences and included the use of thymoglobulin at the rate of 1.25–1.5 mg/kg body weight (rabbit antithymocyte immunoglobulin), prograf (tacrolimus) with target plasma levels of 8–12 ng/mL or Sandimune Neoral (cyclosporine) 250–350 ng/mL, CellSept (mycophenolate mofetil) 2 grams per day or Mayfortic (mycophenolic acid) 1540 mg per day and high doses of glucocorticoids.

RESULTS

In 35 cases (67%) after renal transplant reperfusion, initial appearance was noted within the first 10 minutes. In 13% cases, there was delayed graft function due to prolonged cold ischemia and subsequent reperfusion injury, which required postoperative renal replacement therapy before the transplanted kidney began to function. In one case, there was an intraoperative ultra-acute graft rejection that could not be treated with high doses of glucocorticoids; the kidney transplant was removed. Two patients (3.8%) developed a clinic of acute renal graft rejection in the early postoperative period – on days 2 and 7 after surgery; after the rejection crisis was stopped by drug therapy, graft function was restored. In the early postoperative period, one patient after simultaneous kidney and pancreas transplantation developed acute rejection of the transplanted organs, which could not be treated conservatively and required subsequent removal. One (1.92%) patient died as a result of bilateral pneumonia, which led to sepsis and death.

DISCUSSION

Organ transplantation is the most rapidly developing branch of surgery. The first human kidney transplantation was performed more than 60 years ago [5]. This treatment remains the gold standard in the treatment of end-stage kidney disease [6]. Currently, transplantation as a science has become multidisciplinary, including not only surgery but also immunology, genetics, nephrology, and pharmacology [7]. Advances in immunology have improved graft and recipient survival [8]. The use of a cross-match test practically eliminated the possibility of developing acute rejection. Identification of donor-specific antibodies in recipients and the use of desensitizing therapy have reduced the frequency of antibody-mediated rejections [9]. Organ preservation methods, which include modern preservation solutions, as well as various mechanical devices to preserve organ viability, reduce the degree of ischemic injury to the organ [10]. Transplant science is continuously evolving and the main limitation is organ shortage. One of the important factors, of course, is the lack of public awareness and the general unpreparedness of the society for organ donation. This is a complex issue that requires ethical and religious debate. However, the society around the world should be convinced that it is currently the only way to save lives and improve the quality of life for this group of patients. The idea of creating artificial organs and using organs from animals, even at the stage of experiments and before application in practice, still requires decades of research. As an alternative to heart transplantation, ventricular assist devices and artificial heart are now being used as a specific therapeutic regimen and have been shown to prolong life compared to conservative therapy alone. However, no artificial organ, kidney or heart can match the life expectancy or quality of life of a successfully transplanted organ.

CONCLUSION

A kidney transplant from a posthumous donor has priority over kidney transplantation from a living donor for various reasons. The main advantage is the exclusion of organ removal from a living donor, and exclusion of all risks associated with surgical intervention (donor nephrectomy).

According to the WHO program, deceased-donor organ transplantation is the main direction in treating patients who have been waitlisted for organ transplantation. In developed European countries and the USA, the main emphasis is on development of cadaveric transplantation. In Kazakhstan, the number of patients on the waiting list for cadaveric kidney is growing, while the number of cadaveric donors is falling.

The task of increasing the number of cadaveric organ transplants should not rest entirely on the shoulders of transplantologists, it should also be addressed at the government level with constant propaganda to explain to the citizens the need for a cadaveric donation program.

The authors declare no conflict of interest.

REFERENCES

1. Global Observatory on donation and Transplantation. www.transplant-observatory.org.

2. *Abouna GM.* Organ shortage crisis: Problems and Possible Solutions. *Transplantation Proceedings*. 2008; 40: 34–38.
3. *Tuppin P, Savoye E.* Comparison of international data on organ procurement and transplantation: impact of donor policies on organ shortage. *Organ Tissues Cells*. 2006; 3: 159.
4. RGP na PKhV "Respublikanskiy tsentr po koordinatsii transplantatsii i vysokotekhnologichnykh meditsinskikh uslug" MZ RK. "Statistika. List ozhidaniya – Avgust 2020". Accessed September 4, 2020.
5. *Barker CF, Markmann JF.* Historical Overview of Transplantation Cold spring Harb. *Perspect Med*. 2013 Apr; 3 (4): a014977.
6. *Abecassis M, Bartlett ST, Allan J Collins, Davis CL, Delmonico FL et al*. Kidney transplantation as primary therapy for End-Stage Renal Disease: A National Kidney Foundation / Kidney Disease Outcomes Quality Initiative. *Clin J Am Soc Nephrol*. 2008 Mar; 3 (2): 471–480.
7. *Beyar R.* Challenges in organ transplantation: *Maimonides Med J*. 2011 Apr; 2 (2): e0049.
8. *Gautier SV, Moysyuk YaG.* Transplantologiya. Farmakoterapiya bez oshibok. Rukovodstvo dlya vrachey. M.: E-noto, 2014. 432 s.
9. *Johnson PW, Glennie MJ.* Rituximab: mechanisms and applications. *Br J Cancer*. 2001 Nov 30; 85 (11): 1619–1623.
10. *Kosieradzaki M, Rowinski W.* Ischemia/Reperfusion Injury in Kidney Transplantation: Mechanisms and Prevention. *Transpl Proceedings*. 2008; 40: 3279–3288.

The article was submitted to the journal on 10.11.2020

DOI: 10.15825/1995-1191-2021-2-41-51

CADAVERIC KIDNEY ALLOTRANSPLANTATION AT KRASNOYARSK REGIONAL CLINICAL HOSPITAL

V.S. Arutyunyan[1], A.V. Keosyan[1], M.A. Firsov[1, 2], D.P. Evdokimov[2], M.R. Tsokaev[2], O.S. Amelchugova[2], E.V. Lukicheva[2]

[1] Krasnoyarsk State Medical University, Krasnoyarsk, Russian Federation
[2] Krasnoyarsk Regional Clinical Hospital, Krasnoyarsk, Russian Federation

Objective: to evaluate the early and long-term outcomes of cadaveric kidney allotransplantation (CKAT) based on a retrospective analysis of 71 cases treated at Krasnoyarsk Regional Clinical Hospital (KRCH). **Materials and methods.** From March 2014 to June 2019, 71 kidney transplants were performed at KRCH – 42 (59.15%) men and 29 (40.85%) women. The age of the patients varied from 20 to 59 years (mean age 39.6 ± 8.14 years). The causes of end-stage chronic kidney disease which subsequently led to CKAT were chronic glomerulonephritis, chronic tubulointerstitial nephritis, hypertensive nephropathy (HN), diabetic nephropathy resulting from type I diabetes (DN), nephropathy of mixed genesis (HN + DN), vesicoureteral reflux, congenital angiodysplasia of the kidneys, and Alport syndrome. The mean number of HLA mismatches was 4.5 ± 0.9. **Results.** Hospitalization lasted for an average of 34.05 ± 9.56 days. Primary function was observed in 32 (45.08%) patients, while 39 (54.92%) cases had delayed function. Post-transplant complications were noted in 23 (32.39%) patients, of whom 12 (16.9%) had early post-transplant complications, while 15 (21.13%) encountered complications in the late post-transplant period. The most frequently diagnosed were immunological, infectious, and urological complications. Vascular, surgical, oncological, and other complications were less frequent. The annual graft survival rate was 87.3%. Patient survival rate was 95.77%. One (1.4%) and 2 (2.81%) patients died in the early and late post-transplant periods, respectively. Hospital mortality – 1 case (1.4%). **Conclusion.** Kidney transplantation is the most effective treatment for patients with irreversible chronic kidney disease. About 87.33% of transplants were found to be effective. However, 32.39% of patients had postoperative complications. The vast majority of complications were reversible and were corrected conservatively or surgically. Nevertheless, graft loss occurred in 12.67% of cases. The success of transplantation depends on a number of factors related to both the donor and the recipient, as well as the immunological status and surgical technique. A personalized approach to recipients helps to reduce postoperative complications, prevent nephrotoxicity and rejection reactions.

Keywords: kidney transplantation, chronic kidney disease.

INTRODUCTION

Intensification of transplantation activity and making of progress in the organization of organ donor processes are the most promising solution to the problem posed by a steady increase in the number of patients with end-stage chronic kidney disease (CKD) [1, 2].

Trends in modern medicine are such that kidney transplantation provides better long-term outcomes compared to other renal replacement therapy methods in end-stage CKD. Survival rates of kidney recipients are higher than those of patients on long-term hemo- or peritoneal dialysis [3].

Kidney transplantation is highly effective not only socially, but also economically. Over a three-year period, the cost of providing one CKD patient with hemodialysis is higher than that of a renal transplant patient [4].

Deceased-donor kidney transplant was performed for the first time in Krasnoyarsk Krai in March 2014 at the Krasnoyarsk Regional Clinical Hospital (KRCH) in Krasnoyarsk, Russia. From March 2014 to June 2019, 71 cadaveric kidney transplants were performed; the number of such surgeries is increasing annually.

Along with development of the donor service, the number of donor bases has increased from 1 in 2014 to 7 in 2019. The region had 23.8 donors per million population in 2018 [5]. Today, 8.8% of patients on hemo- and peritoneal dialysis are on the active waiting list for kidney transplantation at KRCH. The average waiting time for a donor kidney is 286 days.

So, it is obvious that there is not just a high demand for kidney transplantation in Krasnoyarsk Krai, but also a significant demand for transplantation and donor services.

OBJECTIVE

The aim of this study is to evaluate the early and long-term outcomes of cadaveric kidney allotransplantation

Corresponding author: Mikhail Firsov. Address: 3a, Partizana Zheleznyaka str., Krasnoyarsk, 660022, Russian Federation. Phone: (902) 941-89-09. E-mail: firsovma@mail.ru

(CKAT) based on a retrospective analysis of 71 cases treated at KRCH in Krasnoyarsk.

MATERIALS AND METHODS

We conducted a retrospective analysis of the treatment of 71 patients aged 20 and above, who underwent CKAT from March 2014 to June 2019 at the 2nd surgical ward of KRCH in Krasnoyarsk (Fig. 1).

The work of the KRCH transplant service is carried out in accordance with the standards and clinical guidelines for kidney donation and transplantation adopted by the Russian Transplant Society [6, 7].

The donor service at KRCH was assessed. Forty-eight patients were effective donors. The main reasons for exclusion from being a donor were identified infectious diseases, increasing phenomena of multiple organ failure syndrome, cardiac arrest during follow-up, and identified intraoperative focal organ tumors. The average age of effective donors was 44.17 ± 8.07 years. Azotemia values were as follows: creatinine 92.33 ± 20.27 mmol/L, urea 5.47 ± 1.74 mmol/L, potassium 3.7 ± 0.43 mmol/L.

The CKAT waiting list was analyzed. While being placed on the waiting list, 26 (36.62%) patients had anuria, 32 (45.08%) had oliguria, and 13 (18.3%) were diagnosed with preserved diuresis. Before transplantation, 67 (94.36%) patients underwent renal replacement therapy using hemodialysis. Dialysis time in recipients ranged from 0 (4 patients (5.66%) were operated on at the pre-dialysis stage) to 120 months, averaging 33.59 ± 23.87 months.

Among the recipients, men accounted for 59.15% (n = 42), while women were 40.85% (n = 29). The age of the patients varied from 20 to 59 years (mean age 39.6 ± 8.14 years). The main characteristics of the recipients are presented in Table.

Table

Demographics of kidney recipients

Indicator	Number of recipients	%
Donor age, years Range (average) 20–59 (39.6 ± 8.14)		
20–29	10	14.1
30–39	25	35.2
40–49	22	31.0
50–59	14	19.7
Donor gender (f/m)	29/42	

The causes of end-stage CKD and further CKAT were: chronic glomerulonephritis (CGN) (57, 80.28%), chronic tubulointerstitial nephritis (CTN) (5, 7.04%), hypertensive nephropathy (HN) (4, 5.63%), diabetic nephropathy (DN) (1, 1.4%), nephropathy of mixed genesis (HN + DN) (1, 1.4%), vesicoureteral reflux (VUR) (1, 1.4%), congenital renal angiodysplasia (CRAD) (1, 1.4%), Alport syndrome (1, 1.4%).

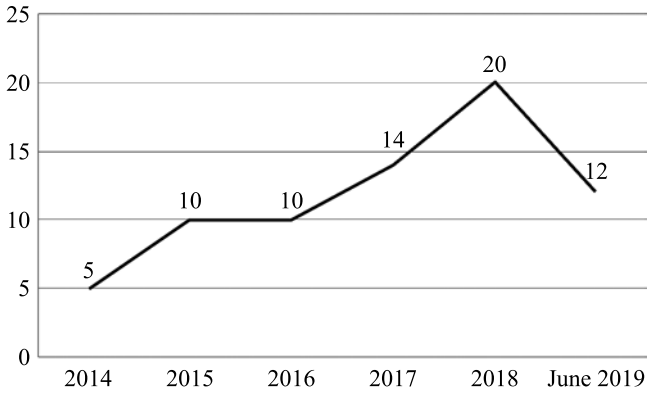

Fig. 1. Number of cadaveric kidney allotransplantations performed during the study period

The list of studies corresponded to the standard set of diagnostic measures approved by the Russian Transplant Society; all patients on the CKAT waiting list were subjected to HLA typing and HLA antibody titer determination [7]. The average number of HLA mismatches was 4.5 ± 0.9.

The laboratory values of the general blood analysis of recipients had no significant deviations: red blood cell – 3.78 ± 0.48 × 10^{12}/L, hemoglobin – 118.84 ± 13.47 g/L, white blood cells – 7.52 ± 1.67 × 10^{9}/L, platelets – 205.32 ± 45.4 × 10^{9}/L.

Azotemic indicators had a fairly high range of values: urea – 15.07 ± 6 mmol/L, creatinine – 663.77 ± 175.79 μmol/L. This was primarily due to the different periods of dialysis duration and technique, as well as the analysis time.

Standard cross-over heterotopic kidney transplantation was performed in 68 (95.77%) patients (right to left 23 (32.39%) kidneys, left to right 45 (63.38%) kidneys). In 3 (4.22%) cases, an organ-side transplant was performed (right to right 1 (1.4%) kidney, left to left 2 (2.82%) kidneys). Access in these cases was chosen due to the impossibility of performing cross-sectional transplantation for various reasons: early transplanted pancreas, inability to access the main vessels, etc.

An overwhelming number of kidneys (52 transplants (73.24%)) had standard anatomy. However, 13 kidneys had vascular features: 11 (15.5%) organs had 2 renal arteries (RAs); 1 (1.4%) – 2 RAs and 2 renal veins (RVs) and in 1 (1.4%) case – 3 RVs. In addition, 5 (7.04%) kidneys had cysts, which was subsequently confirmed histologically; in 1 (1.4%) case, an up to 7 mm bulk lesion was revealed, which was verified as a papillary adenoma during an urgent intraoperative pathomorphological examination in order to rule out malignant tumor of the kidney. One kidney (1.4%) had a complete doubling of the pelvicalyceal system with a complete doubling of the ureter.

The revealed features of angioarchitectonics in 6 (8.45%) cases required reconstructive surgery: 3 (4.22%)

cases – the accessory RA was anastomosed end-to-side with the main RA; 1 (1.4%) case – 2 RAs on the site were reconstructed into 1 RA on a common site of smaller size; 2 (2.81%) cases – short RV was lengthened using a portion of the inferior vena cava.

The detected tumors in donor organs also required additional surgical manipulations: kidney cysts were detected in 5 (7.04%) cases, walls of the cysts were excised, in 1 (1.4%) graft with an up to 7 mm bulk lesion, a wedge-shaped kidney resection was performed.

All patients underwent standard heterotopic renal transplantation to the iliac area. The average duration of the operation was 191.27 ± 28.4 minutes. Intraoperative blood loss averaged 222.53 ± 76.95 mL.

The vast majority of transplants were performed using the standard technique consisting of RA anastomosis with the external iliac artery (ELA) in an end-to-side manner in 62 (87.32%) cases, while in 9 (12.67%) cases, anastomosis was made with the internal iliac artery (ILA) by the end-to-end technique due to the impossibility of matching the ELA and RA diameters. The RVs were in all cases anastomosed with the external iliac vein end-to-side. Ureteroneocystoanastomosis in all cases was performed according to the Lich-Gregoir procedure with double-J stent. Average duration of conservation was 439.46 ± 128.35 minutes.

Immunosuppression was induced taking into account the immunological risk (PRA level, number of HLA mismatches, recipient age): in 64 (90.14%) cases, induction was performed according to the Basiliximab + Methylprednisolone scheme; in 5 (7.04%) cases, due to a high immunological risk and high PRA level, induction was performed with Thymoglobulin + Methylprednisolone; in 2 (2.81%) cases, induction with methylprednisolone was done.

Immunosuppressive therapy was initiated according to a standard 3-component scheme: calcineurin inhibitors (CIs), MMF and glucocorticosteroids. In 68 (97.18%) cases, Tacrolimus + Mycophenolic acid + Methylprednisolone; in 3 (2.8%) cases, Cyclosporin + Mycophenolic acid + Methylprednisolone; two patients had already received immunosuppressive therapy with Cyclosporin – due to previous transplantation, it was decided not to convert; one patient converted from tacrolimus to cyclosporine due to development of post-transplant diabetes mellitus.

RESULTS

The effectiveness of surgical interventions was evaluated based on the peculiarities of the course and development of post-transplant complications. It was divided into early (≤3 months after surgery) and late (>3 months after surgery).

Laboratory parameters were monitored daily in the early postoperative period. A fall in hemoglobin levels was observed, which reached its minimum values by day 3, then it was restored. Increased manifestations of anemia were observed in 15 (21.12%) patients, which required an average of 877.33 ± 369.46 mL in blood transfusion. This was probably due to the development of hemorrhagic complications like intraoperative bleeding, parenchymal and wound bleeding in the early postoperative period, and hemostasis defects during hemodialysis sessions.

In accordance with clinical guidelines, on day 1 after CKAT, all patients underwent standard determination of calcineurin inhibitor blood concentration at the rate of 0.1–0.2 mg/kg/day every other day until the end of hospitalization (Fig. 2). The average tacrolimus levels from day 1 to day 15 corresponded to the target levels after CKAT (8–15 ng/ml). An increase in concentration by day 3 was associated with initiation of immunosuppressive therapy and subsequent dose adjustment [8].

White blood cell (WBCs) and potassium levels decreased to minimum values by day 5, after which they increased.

In the first 2 days, patients showed increased WBC levels, with a subsequent decrease to minimum values by day 5, which may correspond to a period of high concentration of immunosuppressants in the blood [9]. After dosage adjustment, WBC levels reached normal values.

Creatinine content steadily decreased from 624.22 ± 196.85 μmol/L on day 1 to 222.01 ± 116.43 μmol/L on day 15 day after surgery. Urea concentration increased from 18.57 ± 5.38 mmol/L on day 1 to 19.67 ± 5.22 mmol/L on day 2, and for three days there was almost no change (19.51 ± 7.14 mmol/L on day 5), after which urea level gradually decreased to 14.44 ± 5.63 mmol/L on day 15 (Fig. 3).

An increase in urine output was noted in the first 5 days after surgery from 1481.37 ± 1189 mL to 2806.27 ± 1539.68 mL by day 5, then urine output decreased, reaching normal values by day 10 and day 15

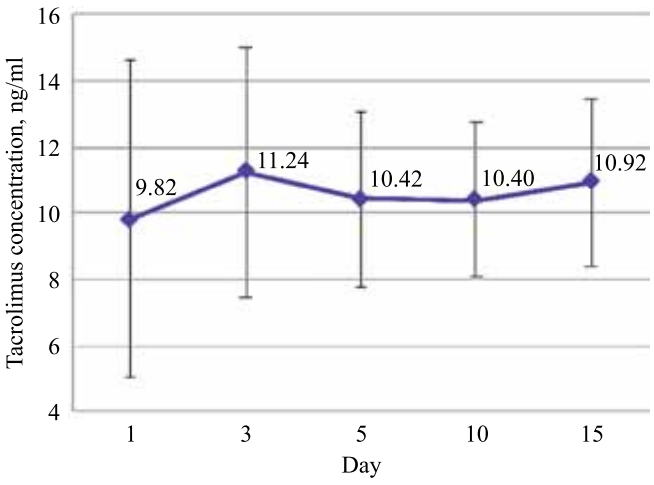

Fig. 2. Tacrolimus concentrations after surgery

(2484.26 ± 910.75 mL and 2463.28 ± 835.57 mL, respectively) (Fig. 4).

Ultrasound examination was carried out during week 1 every day, and then once every second day starting from week 2 till the end of hospitalization. Renal graft sonography in the early days showed a slowdown in RA blood flow up to day 5. Blood flow velocity in the RA increased in the following days. Blood flow velocity in the segmental artery (SA) and arcuate artery (AA) increased throughout the entire follow-up period (Fig. 5). Average renal speed indicators were within normal limits [10, 11].

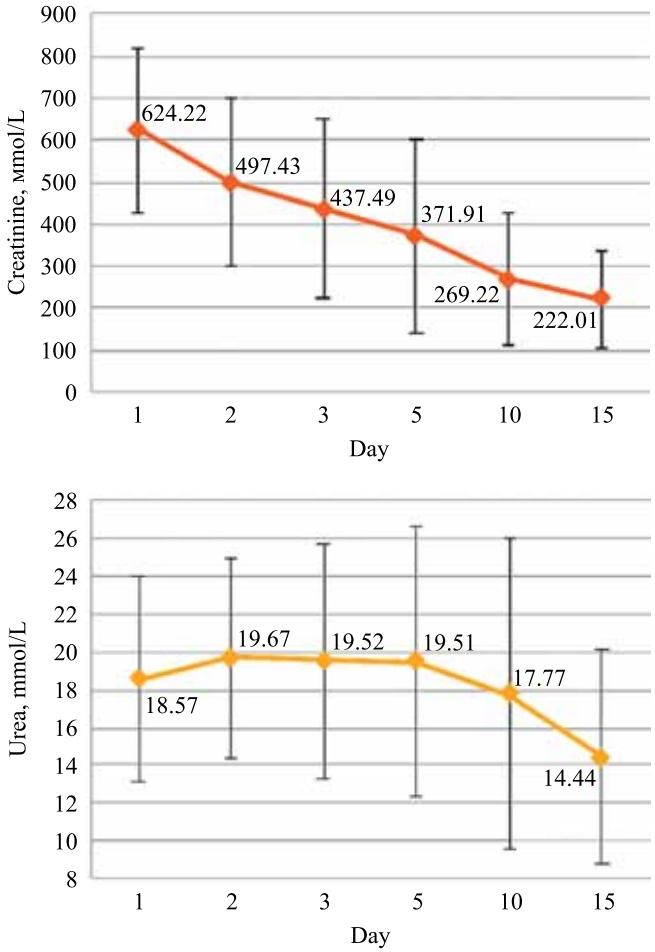

Fig. 3. Postoperative azotemic indicators

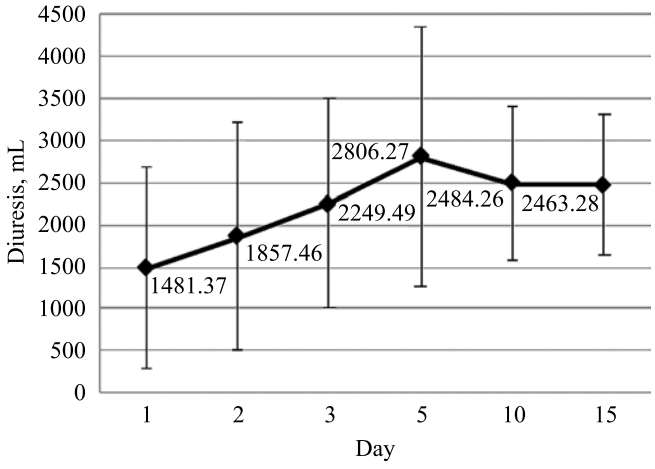

Fig. 4. Postoperative diuresis

Resistive indices RA and SA increased in the first 3 days, and then decreased in subsequent days. The AA resistive index decreased throughout the observation period (Fig. 6). The average values of the resistive indices were within the reference values [10, 11].

Drains were removed at postoperative day 4.22 ± 0.81, the urethral catheter at postoperative day 8.35 ± 1.52, and the ureteral stent at postoperative day 27.67 ± 6.27.

The average duration of hospitalization was 34.05 ± 9.56 days.

Primary function was observed in 32 (45.08%) patients, while delayed function was noted in 39 (54.92%) patients. The criterion for delayed function included one or more hemodialysis sessions in the first 7 days after surgery [12]. Hemodialysis sessions were performed in 39 patients in numbers ranging from 1 to 18, on average 3.34 ± 2.18.

Postoperative complications were divided into several types: immunological (9.85%), infectious (8.45%), urological (7.04%), vascular (5.63%), surgical (2.81%), oncological (2.81%) and others (4.22%).

Post-transplant complications were recorded in 23 (32.39%) patients, of which 11 (15.49%) had the complications **in the early post-transplant period**.

Among immunological complications, acute cellular rejection was most common (n = 3; 4.22%), which in all cases was stopped by a course of methylprednisolone pulse therapy in a total dose of 1.5–2.0 g. Acute humoral graft rejection in all cases (n = 2; 2.81%) resulted in graftectomy.

Vascular complications (n = 2; 2.81%) were associated with renal vein thrombosis of the graft and resulted in graftectomy. Surgical complications (n = 2; 2.81%): postoperative wound hematoma – revision, wound debridement was performed; subcapsular hematoma rupture with massive bleeding – graftectomy was performed.

Post-transplant tacrolimus-induced diabetes mellitus developed in 1 (1.4%) patient; according to recommendations, tacrolimus was converted to cyclosporine with a positive effect [13, 14]. Acute nephrotoxicity caused by CIs and confirmed histologically was recorded in one patient, which required a dose adjustment of the immunosuppressive drug with a positive effect.

Fifteen (21.13%) patients had a complicated **late post-transplant period**.

Immunological complications (n = 2; 2.81%): in 1 (1.4%) case, acute cellular rejection was diagnosed, arrested conservatively, in another 1 (1.4%) patient – chronic steroid-resistant graft rejection with loss of graft function. Vascular complications (n = 2; 2.81%): RA stenosis – graft artery was stented; renal artery thrombosis – graftectomy was performed.

Urological complications (n = 5; 7.04%): 2 (2.81%) patients had VUR, 1 (1.4%) patient underwent transurethral correction of the ureteral orifice. One (1.4%) patient developed purulent graft pyelonephritis, conservative measures had no effect, sepsis, graftectomy, death on day 187 after transplantation. Ureteral obliteration (n = 1; 1.4%) – laser ureterotomy was performed with a positive outcome. Ureterocystoanastomosis stricture (n = 1; 1.4%) required neoureterocystoanastomosis. A possible cause of complications associated with development of ureteral stricture is due to disruption in its blood supply against the background of acute cellular rejection previously suffered in these patients [15, 16 [15, 16].

Oncological complications (n = 2; 2.81%): one patient developed Kaposi's sarcoma; conservative therapy gave a positive trend – tumor regression. Prostate cancer T1M0N0 was diagnosed a year later in one patient after performing transurethral resection of the prostate against the background of increasing infravesical obstruction; small acinar adenocarcinoma was diagnosed on the basis of pathomorphological examination of the surgical material. In both cases, conversion from MMF to everolimus was performed.

Infectious complications (n = 6; 8.45%): in 5 (7.04%) cases, CMV viremia, in 1 (1.4%) case, hepatitis B reactivation – antiviral therapy was prescribed.

Acute nephrotoxicity caused by CIs developed in 1 (1.4%) patient. The immunosuppressive drug dose was adjusted with a positive effect.

Drug-induced ulcerative colitis (UC) in 1 patient required withdrawal of the immunosuppressive drug,

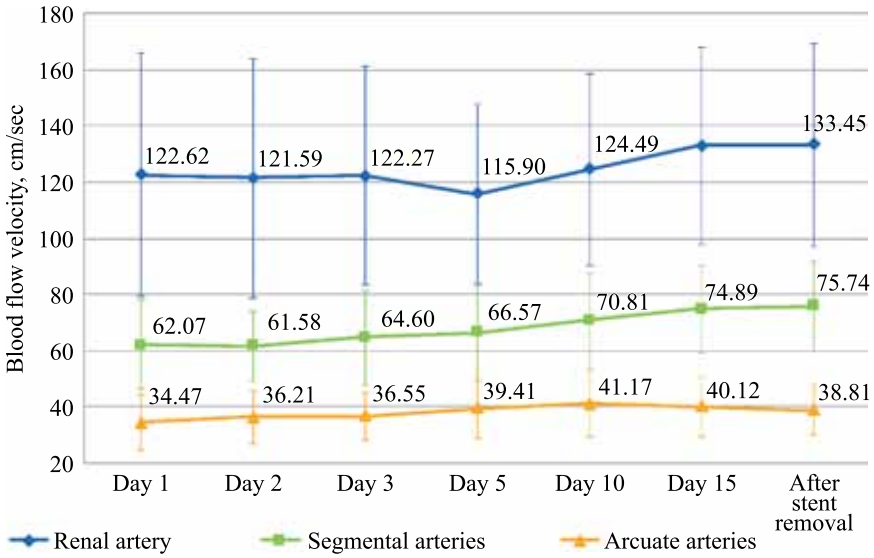

Fig. 5. Blood flow velocity indicators according to graft sonography

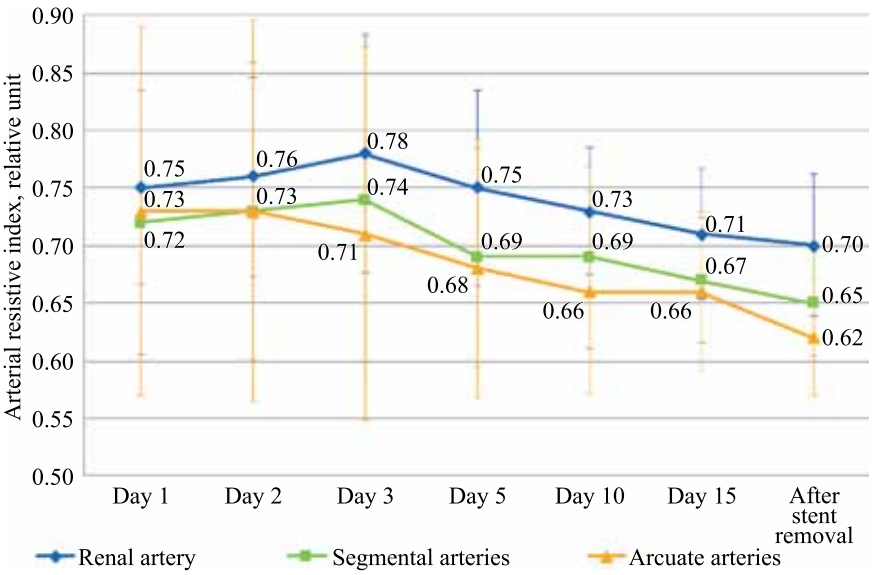

Fig. 6. Renal arterial resistive index according to sonography data

against which the UC phenomena subsided, but later there was loss of graft function.

Combinations of complications were conditionally divided into monospecific, when complications of one type developed, and polyspecific, combining complications of 2 or more types.

Monospecific complications were recorded in 19 (26.76%) patients, 3 (4.22%) patients had a combination of 2 types of complications, and 2 (2.8%) patients had polyspecificity, combining 3 or more types. At the same time, a combination of complications could develop both during either or both postoperative periods.

The 1-year and 5-year graft survival after CKAT were 87.3% and 73.51% respectively. Loss of graft function predominantly occurred in the 5th year after surgery (after 48 months) (Fig. 7).

The group of patients with 3 or more HLA matches (n = 12) had a higher percentage of primary function compared to the group of patients with 2 or less HLA matches (n = 59) (58.33% and 42.37% respectively), as well as the best 3-year survival rate (100% and 85.9%, respectively) (Fig. 8).

Graftectomies were performed in 9 (12.67%) patients. In the early post-transplant period (up to 3 months after surgery), grafts were removed in 4 (5.63%) patients, while in the late post-transplant period, 5 (7.04%) patients had graftectomy. The reasons for graftectomy were surgical, immunological, vascular, and urological complications.

Patient survival rate was 95.77% (68 patients) (Fig. 9).

One patient died at the early post-transplant period; 2 (2.81%) patients died at the late post-transplant stage. Hospital mortality was 1 case (1.4%), the cause of death was sepsis against the background of acute purulent graft pyelonephritis. In 2 (2.81%) cases, the cause was acute cardiovascular failure due to acute coronary syndrome (ACS).

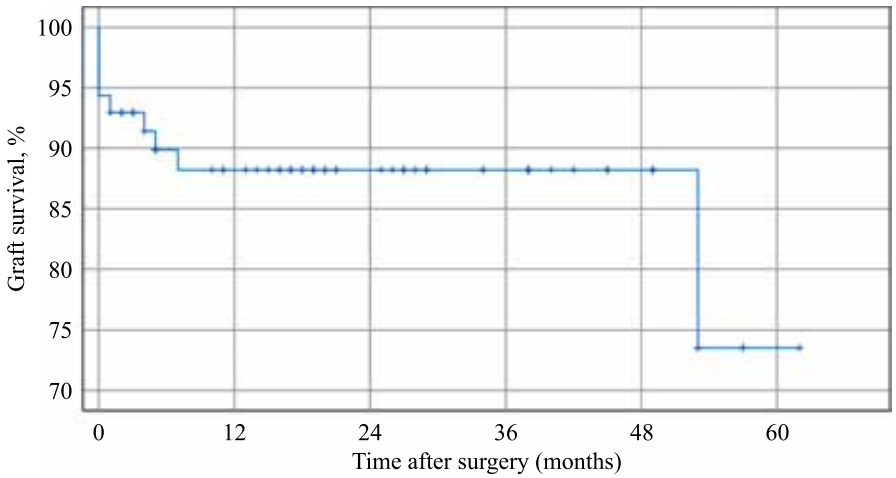

Fig. 7. Graft survival

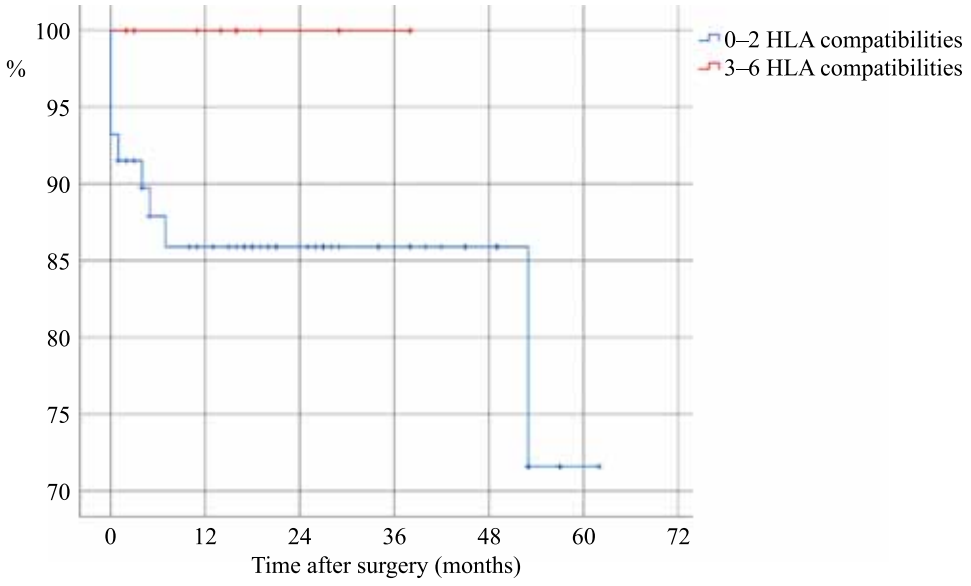

Fig. 8. Graft survival depending on the number of HLA matches

This is consistent with reports indicating that deaths after kidney transplantation are often due to cardiac pathology [17].

DISCUSSION

Analyzing the results obtained, we can identify a number of factors influencing the outcome, graft functionality and development of complications.

Post-transplant complications that developed in 23 (32.39%) patients had an adverse effect on graft function: of them, 11 (15.49%) in the early post-transplant period, and 15 (21.13%) in the late post-transplant period. Complications were divided into several types: immunological (9.85%), infectious (8.45%), urological (7.04%), vascular (5.63%), surgical (2.81%), oncological (2.81%) and others (4.22%).

Donor factor

When evaluating effective donors, it was noted that the mean age was 44.17 ± 8.07 years, and azotemia indicators were within reference values: creatinine 92.33 ± 20.27 μmol/L, urea 5.47 ± 1.74 mmol/L, potassium 3.7 ± 0.43 mmol/L.

An important factor influencing outcome is the duration of preservation. Prolonged cold ischemia time is a recognized risk factor for graft dysfunction. Maximum reduction in cold ischemia time is one of the clinically feasible options for prevention of graft dysfunction [18]. The graft preservation period in the analyzed patients was 439.46 ± 128.35 minutes.

In addition, it should be noted that 26.76% of the donor organs had vascular features, development of the pelvicalyceal system and the ureter, tumors that required reconstructive surgery. 18.3% of the kidneys had vascular features, but vascular reconstruction was required only in 8.45% of cases. Renal parenchymal tumors were detected both preoperatively and intraoperatively in 6 (8.45%) cases. When kidney cysts were detected (n = 5; 7.04%), the walls of the cysts were excised, followed by histological examination; in all cases, benign nature was confirmed. Intraoperatively, when processing 1 (1.4%) graft, a tissue formation up to 7 mm in size was detected, a wedge-shaped kidney resection was performed with urgent pathomorphological examination – papillary renal adenoma was verified.

The relationship of change in creatinine difference between recipients on day 15 and the donor was 94.14 ± 75.16 μmol/L, with a donor-recipient creatinine difference of 142.87 ± 102.50 μmol/L for donors 45 years old and above, and 58 ± 39.57 μmol/L for 44 years old and younger.

Recipient factor

Patient age, etiology of CKD, and comorbidity are important predictors of CKAT outcome. Recipients ranged in age from 20 to 59 years (mean age 39.6 ± 8.14 years). The main pathologies that caused CKD and further CKAT were: CGN (57 patients, 80.28%), CTN (5 patients, 7.04%), HN (4 patients, 5.63%), DN (1 patient, 1.4%), mixed nephropathy (1 patient, 1.4%), VUR (1 patient, 1.4%), CRAD (1 patient, 1.4%), and Alport syndrome (1 patient, 1.4%). The baseline azotemic values of the recipients before CKAT and the dialysis duration of recipients play a significant role in the postoperative period. The mean uremic values of those studied were: urea 15.07 ± 6 mmol/L, creatinine 663.77 ± 175.79 μmol/L; the fairly large range of values is primarily associated with the dialysis method and various dialysis durations, which ranged from 0 (4 patients were operated on at the pre-dialysis stage) up to 120 months (mean 33.59 ± 23.87 months). Postoperative hemodialysis sessions were required for 39 patients, ranging from 1 to 18, on average 3.34 ± 2.18.

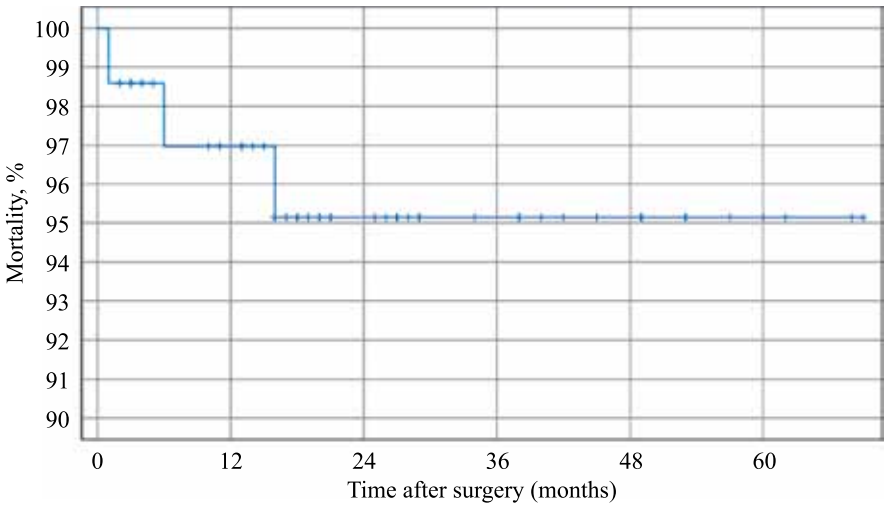

Fig. 9. Recipient survival

Immunological factor

An important factor influencing the development of complications, restoration of graft function and postoperative complications is the number of haplotype mismatches. There was an average of 4.5 ± 0.9 HLA mismatches.

The group of patients with 3 or more HLA matches (n = 12) had a higher percentage of primary function compared to the group with 2 or less HLA matches (n = 59) (58.33% and 42.37% respectively), as well as a better 3-year survival (100% and 85.9%, respectively).

There was a direct correlation between the number of HLA matches and graft survival. In patients with 3 or more HLA matches, graft survival was 100%, whereas in the group with 2 or less HLA matches, it was 85.9%.

Technological factor

Prior to March 2014, there were no kidney transplant surgeries performed in Krasnoyarsk Krai. We noted that the highest number of complications in the early postoperative period was observed in patients who underwent CKAT in 2014–2016. A decrease in the number of complications is associated with mastering and improving donor conditioning methods, organ explantation and CKAT technology, and accumulation of experience by medical and nursing personnel. At KRCH, CKAT is no longer a unique operation, but a routine one.

Twenty percent of patients had early postoperative complications after CKAT in 2014–2016, whereas in 2017–2019 it was only 13.04%. The need for early postoperative graftectomy was 8% in 2014–2016 and 4.34% in 2017–2019.

Graftectomies were performed in 9 (12.67%) patients. The main reasons leading to graftectomy in our observation were vascular thrombosis (4.22%).

So, primary function was observed in 32 (45.08%) patients, while delayed function in 39 (54.92%). One-year graft survival after CKAT was 87.3%. The main reasons leading to graftectomy in our observation were vascular thrombosis (4.22%), acute humoral (2.81%) and chronic steroid-resistant rejection (1.4%). The possibility of postponed acute cellular graft rejection having an influence on occurrence of strictures and ureteral obliteration in the late postoperative period cannot be ruled out. In 2 (2.81%) patients out of 4 (5.63%) who had cellular rejection, ureteral strictures of various lengths developed in the late post-transplantation period. Sepsis was the most formidable complication in the group of transplanted patients. It led to death in 1 (1.4%) patient from the group of patients. The overall patient survival was 95.77% (68 patients).

Timely prevention and elimination of early and late complications of kidney transplantation predetermines the further functionality and survival of the donor organ. In this regard, it is necessary to monitor the recipient's condition and organ function both at the inpatient and at the outpatient treatment stages.

CONCLUSION

In Krasnoyarsk Krai today, there is a high demand for donor services and kidney transplantation. The number of effective donors and kidney transplants in KRCH is increasing every year, and fewer complications are being recorded.

Kidney transplantation is the treatment of choice for end-stage chronic kidney disease. Our data shows that 87.33% of transplants were effective. However, 32.39% of patients had postoperative complications, including immunological (9.85%), infectious (8.45%), urological (7.04%), vascular (5.63%), surgical (2.81%), oncological (2.81%) and other (4.22%) complications. The vast majority of complications were reversible and were corrected conservatively or surgically. Nevertheless, 12.67% of patients had graft loss.

The factors described above play a significant role in the success of transplantation. A personalized approach to recipients helps to reduce postoperative complications and prevent nephrotoxicity and rejection reactions.

The authors declare no conflict of interest.

REFERENCES

1. *Lamb KE, Lodhi S, Meier-Kriesche HU.* Long-term renal allograft survival in the United States: a critical reappraisal. *Am J Transplant*. 2011 Mar; 11 (3): 450–462. doi: 10.1111/j.1600-6143.2010.03283.x. Epub 2010 Oct 25. PMID: 20973913.
2. *Tomilina NA, Andrusev AM, Peregudova NG, Shinkarev MB.* Renal replacement therapy for End Stage Renal Disease in Russian Federation, 2010–2015. Russian National Renal Replacement Therapy Registry Report of Russian Public Organization of Nephrologists "Russian Dialysis Society", Part 1. *Nefrologiya i dializ [Nephrology and dialysis]*. 2017; 19 (4, supplement): 1–95. doi: 10.28996/1680-4422-2017-4sup- pl-1-95. [In Russ, English abstract].
3. *Kramer A, Boenink R, Noordzij M, Bosdriesz JR, Stel VS, Beltrán P et al.* The ERA-EDTA Registry Annual Report 2017: a summary. *Clin Kidney J*. 2020 Jun 22; 13 (4): 693–709. doi: 10.1093/ckj/sfaa048. PMID: 32897277; PMCID: PMC7467580.
4. *Smirnov AV, Dobronravov VA, Kayukov IG, Bodur-Oorzhak AS, Essaian AM, Kucher AG*. Epidemiology and social-economical aspects of chronic kidney disease. *Nephrology*. 2006; 10 (1): 7–13. https://doi.org/10.24884/1561-6274-2006-10-1-7-13 [In Russ].
5. *Gautier SV, Khomyakov SM*. Organ donation and transplantation in the Russian Federation in 2018. 11th report of the Registry of the Russian Transplant Society. *Russian Journal of Transplantology and Artificial Organs*. 2019; 21 (3): 7–32. https://doi.org/10.15825/1995-1191-2019-3-7-32.

6. Rossiyskoe transplantologicheskoe obshchestvo. Natsional'nye klinicheskie rekomendatsii "Posmertnoe donorstvo organov". 2016.
7. Rossiyskoe transplantologicheskoe obshchestvo. Natsional'nye klinicheskie rekomendatsii "Transplantatsiya pochki". 2016.
8. *Gautier SV, Moysyuk YG*. Transplantologiya. Farmakoterapiya bez oshibok. Rukovodstvo dlya vrachey. Moscow: E-noto, 2014.
9. *Van Besouw NM, van der Mast BJ, Smak Gregoor PJ, Hesse CJ, IJzermans JN, van Gelder T et al.* Effect of mycophenolate mofetil on erythropoiesis in stable renal transplant patients is correlated with mycophenolic acid trough levels. *Nephrol Dial Transplant*. 1999 Nov; 14 (11): 2710–2713. doi: 10.1093/ndt/14.11.2710. PMID: 10534517.
10. *Carlo Gerardo B. Ramirez, Jerry McCauley.* Contemporary Kidney Transplantation. Basel, Switzerland: Springer International Publishing, 2018.
11. *Danovich GM.* Kidney transplantation. Moscow: GEOTAR-Media, 2014.
12. *Yarlagadda SG, Coca SG, Garg AX, Doshi M, Poggio E, Marcus RJ et al.* Marked variation in the definition and diagnosis of delayed graft function: a systematic review. *Nephrol Dial Transplant*. 2008 Sep; 23 (9): 2995–3003. doi: 10.1093/ndt/gfn158. Epub 2008 Apr 11. PMID: 18408075; PMCID: PMC2727302.
13. *Pirsch JD, Miller J, Deierhoi MH, Vincenti F, Filo RS.* A comparison of tacrolimus (FK506) and cyclosporine for immunosuppression after cadaveric renal transplantation. FK506 Kidney Transplant Study Group. *Transplantation*. 1997 Apr 15; 63 (7): 977–983. doi: 10.1097/00007890-199704150-00013. PMID: 9112351.
14. *Shivaswamy V, Boerner B, Larsen J.* Post-Transplant Diabetes Mellitus: Causes, Treatment, and Impact on Outcomes. *Endocr Rev*. 2016 Feb; 37 (1): 37–61. doi: 10.1210/er.2015-1084. Epub 2015 Dec 9. PMID: 26650437; PMCID: PMC4740345.
15. *Katz JP, Greenstein SM, Hakki A, Miller A, Katz SM, Simonian S.* Transitional epithelial lesions of the ureter in renal transplant rejection. *Transplantation*. 1988 Apr; 45 (4): 710–714. doi: 10.1097/00007890-198804000-00009. PMID: 3282352.
16. *Faenza A, Nardo B, Catena F, Scolari MP, d'Arcangelo GL, Buscaroli A, Rossi C, Zompatori M.* Ureteral stenosis after kidney transplantation. A study on 869 consecutive transplants. *Transpl Int*. 1999; 12 (5): 334–340. PMID: 10551998.
17. *Al-Khafaji A.* ICU Care of Abdominal Organ Transplant Patients. Oxford University Press, 2013.
18. *Moysyuk YG, Poptsov VN, Sushkov AI, Moysyuk LY, Malinovskaya YuO, Belskikh LV*. Early liver allograft dysfunction: risk factors, clinical course and outcomes. Transplantologiya. *The Russian Journal of Transplantation*. 2016; (2): 16–28. [In Russ, English abstract].

The article was submitted to the journal on 25.02.2021

DOI: 10.15825/1995-1191-2021-2-52-59

IMMEDIATE OUTCOMES OF TREATMENT OF SEVERE MITRAL ANNULAR CALCIFICATION

R.M. Muratov, M.N. Sorcomov, A.S. Sachkov, S.I. Babenko, A.M. Sleptsova, M.I. Terekhov
A.N. Bakulev National Medical Research Center of Cardiovascular Surgery, Moscow, Russian Federation

Mitral annular calcification (MAC) is a chronic degenerative process involving the fibrous part of the mitral complex, characterized by calcium deposition and loss of valve function. MAC prevalence is 8–10%, but despite this, the clinical significance of MAC is underestimated. Currently, there are reports that complete decalcification leads to improved long-term outcomes in patients with severe MAC. An analysis of the immediate outcomes of mitral valve surgery in patients with severely calcified mitral annulus with decalcification was performed. The calcified annulus fibrosus underwent complete decalcification in all cases. Calcium deposits were removed in a single block, in 6 cases it was reconstructed with a xeno-pericardial patch; in 2 cases the annulus fibrosus was sutured. There were 2 cases of in-hospital mortality, caused by acute heart failure on day 8 in 1 patient and pulmonary embolism on day 30 after operation in the second patient. There were no complications associated with coronary artery injury and left ventricular posterior wall rupture. Experience in the treatment of severe mitral valve calcification with extensive annulus fibrosus decalcification and subsequent reconstruction is possible and gives satisfactory results.

Keywords: heart base calcification, radiation therapy, decalcification.

INTRODUCTION

Calcification of the base of the heart is a progressive degenerative process characterized by calcification of the fibrous skeleton of the heart with involvement of the mitral annulus and the surrounding myocardium, which may eventually lead to loss of valve function. Multiple studies have shown that there is a high prevalence of this disease in clinical practice, ranging from 7% to 24%. In a series of 258 autopsies, the overall incidence in persons over 50 years of age reached 8.5%; a higher prevalence is found in older women, which reaches 43.5% by the age of 90 years [1].

Systematic retrospective, echocardiographic studies have shown that severe calcinosis is closely associated with age, atrioventricular valve regurgitation, and aortic valve stenosis. Mohammad et al. retrospectively reviewed 24,380 echocardiograms and found that severe mitral annulus calcification was present in 11.7% of patients with mitral regurgitation [2]. Improvement of highly sensitive diagnostic methods used in clinical practice made it possible to estimate the prevalence of this pathological condition. A study by Allison et al. based on CT scan in asymptomatic patients revealed that 8% were found to have mitral annular calcification and suggested that the calcification may be of atherosclerotic nature [3]. Severe mitral valve calcification can serve as a marker for structural changes in the heart, with increased risk of cardiovascular disease and sudden cardiac death [4].

Population aging, leading to an inevitable increase in risk factors (arterial hypertension, diabetes mellitus, kidney disease) [5], and use of radiation treatment for thoracic tumors will significantly increase the prevalence of severe mitral valve calcification in the future, and as a consequence, lead to complex changes in the patient population, creating additional problems in the treatment of this condition. Surgical treatment of patients with valve disease combined with annulus calcification is associated with high in-hospital mortality and postoperative complications. To prevent postoperative surgical complications, surgical treatment of severe calcification requires additional complex procedures. Techniques involving complete decalcification and reconstruction of the mitral valve annulus described in the mid-1990s have not lost their relevance at the present time and are the most preferred surgical techniques that would avoid severe postoperative surgical complications [6, 7].

Objective: to evaluate the immediate outcomes of surgical treatment of severe mitral valve calcification with complete decalcification in a single block and reconstruction of the annulus fibrosus.

MATERIAL AND METHODS

The study enrolled 8 patients operated on from 2016 to the present with severe mitral annular calcification. The mean age of the patients was 64.12 ± 10.57 (47–80 years), all patients were female and had NYHA heart failure functional class 3–4. Most of them had va-

Corresponding author: Maxim Sorcomov. Address: 135, Rublevskoye sh., Moscow, 121552, Russian Federation.
Phone: (495) 414-78-49. E-mail: sorcommn@gmail.com

rious comorbidities aggravating the course of the underlying disease. The mean logistic EuroScore II risk score was 9.73 ± 4.49% (ranged widely from 3.07 to 15.66%), the 30-day Society of Thoracic Surgeons Predicted Risk of Mortality (STS PROM) was 8.96 ± 6.93% (ranged from 3.99 to 21.26%). In 2 patients, the operation was repeated, 1 patient had undergone 2 years earlier mitral valve repair with Sorin 29 mechanical prosthesis, De Vega tricuspid valve plasty and Labyrinth operation for mitral valve prolapse and persistent atrial fibrillation, the present hospitalization was for paraprosthetic fistula. The second patient, 13 years earlier, underwent mitral valve repair with Carbomedics 29 mechanical prosthesis, Boyd tricuspid valve plasty for rheumatic lesion. Her return visit to the hospital was due to aortic stenosis and mitral prosthesis dysfunction – increase in pannus with formation of mitral stenosis.

Four patients had rhythm and conduction disorders: 2 had permanent atrial fibrillation, tachysystolic variant, 1 had third-degree atrioventricular (AV) block, for which a permanent pacemaker was implanted, 1 had an incoming AV block, Mobitz type I.

Transthoracic echocardiographic examination was performed on Phillips iE 33 (Philips Medical Systems, Andover, MA). In addition, visualization of cardiac structures, hemodynamic characteristics of the valves were calculated, and ventricular function was assessed. To visualize the mitral annulus and assess the extent of annulus fibrosus calcification, the study was performed from parasternal access along the short axis. Grade 3–4 mitral regurgitation was revealed in 4 patients (50%). Mitral stenosis in 6 patients (75%), mean values of peak and mean diastolic gradients on mitral valve were 19.33 ± 8.09 and 9.8 ± 7.19 mmHg. Aortic valve stenosis in 4 (50%) patients, mean peak and mean systolic gradients were 103.25 ± 12.57 and 74.75 ± 15.73 mmHg, and combination with aortic valve insufficiency in 2 (25%) patients. Relative tricuspid regurgitation requiring surgical correction was detected in 1 patient (12.5%). The functional state of the left ventricular myocardium was in satisfactory condition, the mean value of left ventricular ejection fraction was 67 ± 10.7%. Changes in left ventricular geometry in the form of eccentric hypertrophy were observed in 3 patients, with an EDV/BSA ratio of 70.3 ± 33.4 mL/m^2, (79 to 137.5 mL/m^2). The mean pulmonary artery pressure by measuring the tricuspid regurgitation rate in continuous-wave Doppler ultrasound was 55.25 ± 13.9 mmHg.

All patients underwent computed tomography (CT) scan. Calcification was defined as a particle with density of ≥200 Hounsfield units (HU). Calcium levels (3259.5 to 7383.18), calcium volume in the fibrous ring (1005.1 to 2222.82 mm^3), weight (2725.6 to 6014 mg), and extent of calcification expressed in degree of the arc involved (62 and –331 degrees) were calculated based on the slices. Calcium was quantified according to the method described by Agatston et al. [8].

All patients underwent coronarography. Right coronary artery (RCA) dominance was observed in 6 patients, left coronary artery (LCA) dominance was noted in 1 patient, and balanced circulation was observed in 1 patient. Coronary artery lesions were detected in 1 patient (right coronary artery of the proximal third 85%, posterior interventricular branch of the right coronary artery 80%, circumflex branch 75%). Additional clinical characteristics of the patients are presented in Table.

SURGICAL TECHNIQUE

In all cases, access was performed through median sternotomy with cardiopulmonary bypass (CPB) by cannulating the vena cava and ascending aorta with hypothermia 28 °C. Cardioplegia in isolated mitral correction was performed in an antegrade manner into the aortic root; with interventions on the aortic valve, it was performed selectively into the coronary artery orifices. The mitral valve was accessed through the vertical bicuspid access. Complete decalcification was performed by opening the fibrous tissue over the decalcification; calcium was removed in a single block throughout the acute route, between 2 fibrous triangles. After decalcification, a defect was usually formed completely separating the left atrial myocardium from the ventricle. In 2 cases,

Table

Clinical characteristics of patients (n = 8)

Body surface area (kg/m^2)	1.80 ± 0.18 (1.57–2.16)
Diabetes (n)	3
CKD-EPI creatinine clearance (mL/min/1.732 m^2)	72.25 (50–109)
Stage 3 CKD	3
Chronic obstructive pulmonary disease (n)	3
Hypothyroidism (n)	2
Arterial hypertension	6
Stroke	2
Etiology degenerative / endocarditis* / RILI / rheumatism	3/1/2/2

* – endocarditis was secondary to degenerative changes in the mitral valve.

the annulus fibrosus was repaired by suturing the formed defect, in one case with a mattress-twisted stitch with 4-0 monofilament, and in the other case with 6 vertical figure-of-8 sutures with 2-0 braided sutures. In 6 cases, the mitral annulus fibrosus defect was closed by closing the atrioventricular junction defect with a xenopericardial patch (manufactured by Bakulev Scientific Center for Cardiovascular Surgery, Moscow) of various sizes. Xenopericardium was implanted in 5 cases with 4-0 continuous monofilament prolene sutures in one row. In the first case, the lower edge of the patch was fixed to the left ventricular myocardium with 12 U-shaped sutures on Teflon spacers (this maneuver was performed due to the large size of the defect and the 8 × 1.5 cm patch for more reliable fixation of the latter). The upper row of the flap was fixed to the edge of the left atrial wall defect.

In all cases, the severed posterior mitral valve leaflet was captured in the prosthetic suture; in the patient with infective endocarditis, the anterior leaflet in the area of commissures. The prosthesis was implanted with

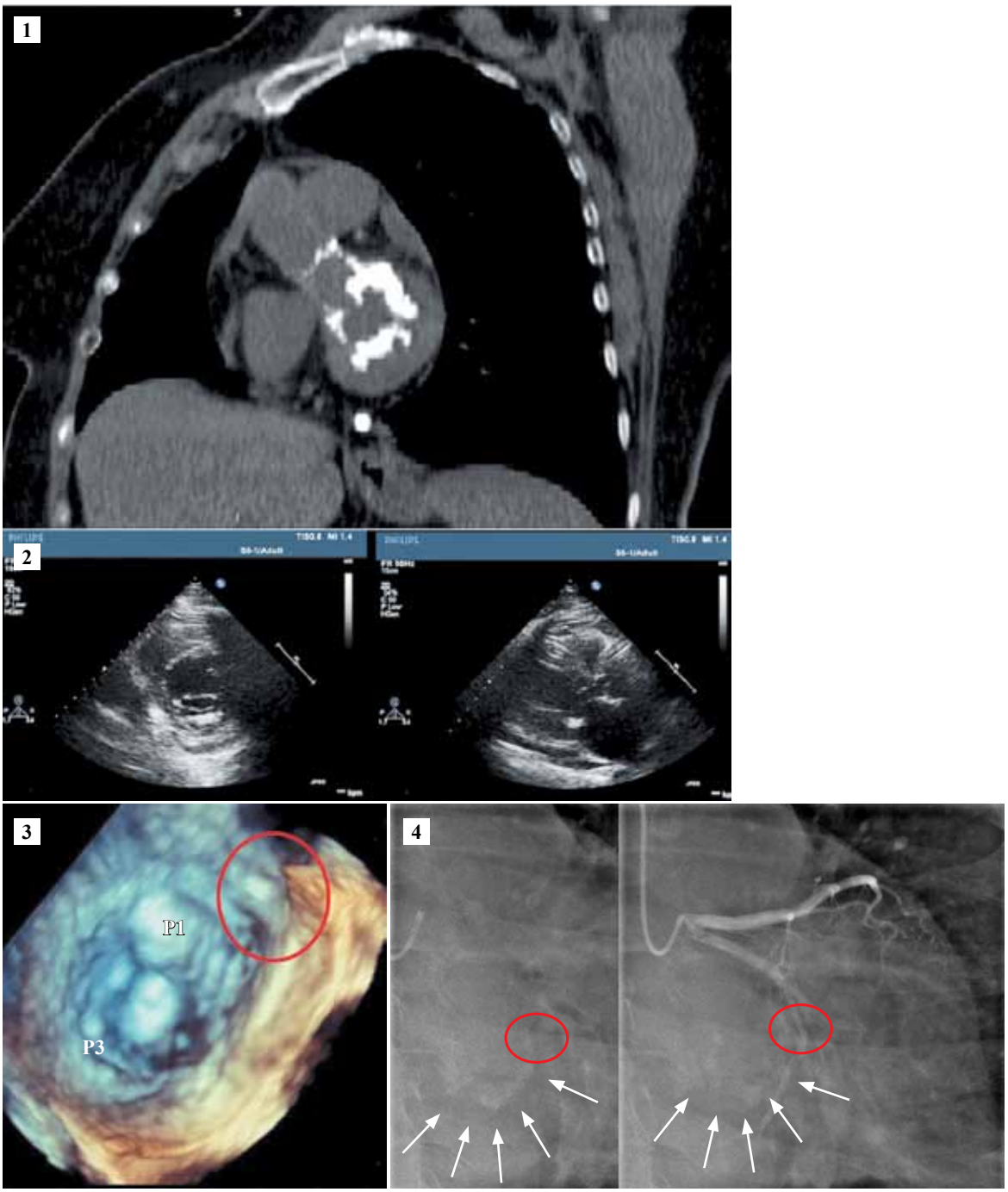

Fig. 1. Computed tomography: 1 – Chest MSCT; 2 – echocardiography, longitudinal and cross-sectional parasternal access; 3 – 3D reconstruction of the mitral valve; 4 – coronary angiography (arrows show mitral annulus calcification, the circle indicates the possible location of coronary artery lesion)

U-shaped sutures with spacers, so that in the projection of the native annulus fibrosus, the sutures were applied intraannularly, and in the area of annulus fibrosus reconstruction, the sutures were applied supraannularly behind the central part of the xenopericardial patch.

Additional surgical procedures were performed in the following volume: aortic valve prosthetics in 4 (50%) patients (mechanical n = 4), subcommissural suture annuloplasty of the aortic valve with suturing of the left atrial auricle from the inside in 1 patient, plastic surgery, Morrow myectomy in 1 patient.

RESULTS

The mean CPB time was 258 ± 58.89 minutes, the mean aortic clamping time was 152.25 ± 41.58 minutes. The mean reperfusion time was 105.7 ± 37 minutes.

Mechanical prostheses of different sizes were implanted in the mitral valve position: Carbonix MDM 26 in 1 case, MDM prostheses size 28 in 4 cases, Medtronic 27 prosthesis in 1 case, Medtronic 31 prosthesis in 1 case, biological prosthesis BiolAB 31 in 1 case.

Two (25%) patients died in the early period. One case was associated with the development of acute heart failure followed by multiple organ failure. The second case of in-hospital mortality was associated with pulmonary embolism on day 31 after surgery in an obese patient (BMI 43.28 kg/m^2) who underwent prolonged ventilation (619 hours of mechanical ventilation) for acute stroke, after being transferred to the general ward.

The mean time spent in the intensive care unit was 128 ± 204.81 hours (19 to 619 hours). In the early postoperative period, there were 3 cases of prolonged ventilation (more than 72 hours) associated in 1 case with acute heart failure; in 1 case, there was impaired cerebral circulation, in 1 case there was neurologic deficit.

There were no cases of coronary artery injury, hemorrhage and left ventricular posterior wall rupture. Among nonlethal complications, hydrothorax was the most common – in 4 patients. There was one case of third-degree AV block, for which a permanent pacemaker was implanted, as well as 1 case of pericarditis with the development of cardiac tamponade.

Mean hospital stay was 18.8 ± 12.6 days (7 to 42 days). At the time of discharge, the functional status of the patients had significantly improved (NYHA class 1–2). The mean diastolic gradient at the mitral valve was up to 5.6 ± 1.4 mmHg, peak 10.5 ± 3.4 mmHg. The indexed left ventricular end-diastolic volume was 62.7 ± 20.6 ml/m^2.

DISCUSSION

Currently, the strategy for surgical treatment of mitral valve defects complicated by severe mitral annular calcification can be divided into several types. A less aggressive approach to calcified annulus fibrosus involves intra-atrial fixation of the prosthesis behind the atrial myocardium. Nataf et al. used this technique in 21 patients, but the results were unsatisfactory, 1 case of hospital mortality. due to atrial wall rupture in a patient

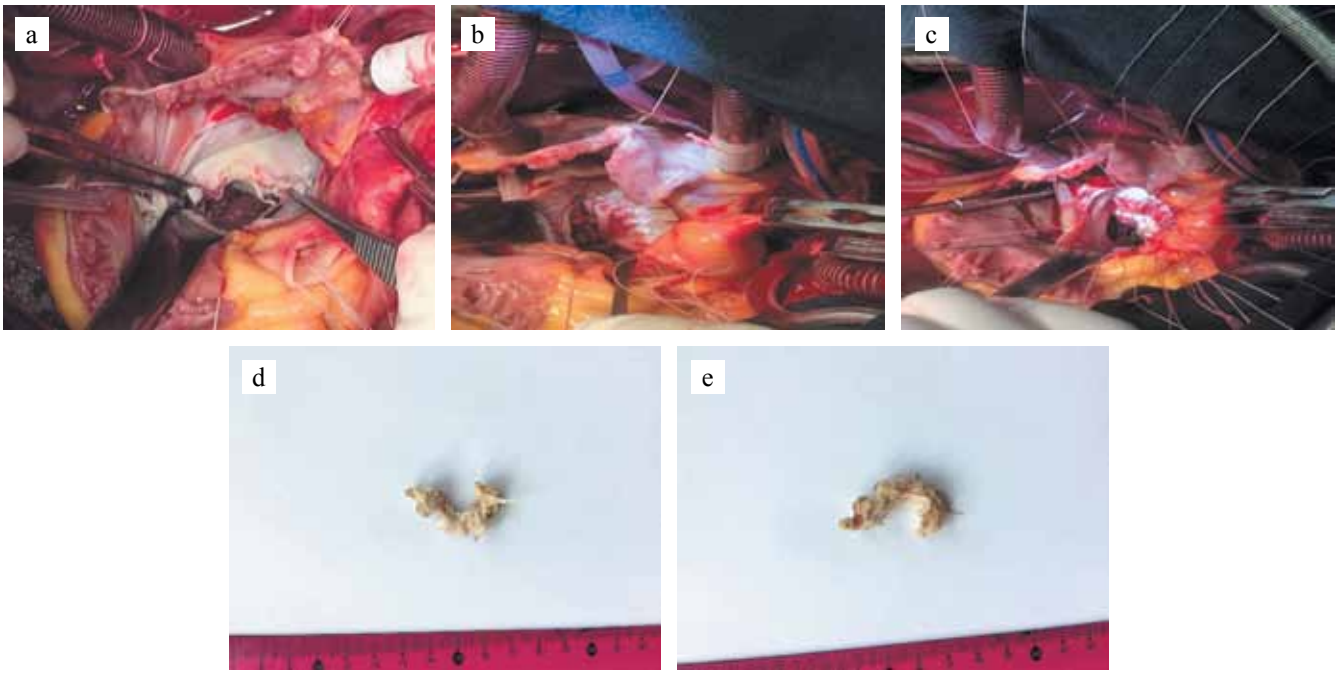

Fig. 2. a – Mitral valve exposure, base calcification in the posterior mitral leaflet projection. b – Pericardial patch plasty after complete decalcification. c – U-shaped prosthetic sutures on spacers. d, e – excised annulus fibrosus calcium from ventricular and atrial surfaces

with renal failure on hormonal therapy and 4 cases of paraprosthetic fistulas [9].

Hussain C.T. et al. suggested limited debridement of the calcified annulus with creation of a 1.5-cm wide polytetrafluoroethylene (PTFE) felt washer in between the annulus and sewing ring of the prosthesis from trigone to trigone posteriorly. The valve and the washer are tied down. The washer is then sutured to the atrial wall with a second suture line (n = 20). This "sparing" decalcification technique ensures prosthesis implantation with a low risk of ventricular rupture. One case of hospital mortality was associated with the initial severity of the patient. The authors noted the absence of paraprosthetic leaks and repeated interventions. The only serious limitation of this technique is its use in patients with wide annulus, as it results in significant reduction in the annulus fibrosus size [10].

Another method of surgical treatment of the pathology, avoiding direct manipulations with calcified fibrous rings, is creation of a bypass anastomosis between atrium and left ventricular apex with a valve-containing conduit. This concept is not new, it has been adopted from the arsenal of mitral valve atresia treatment [11]. The technique can be used as an independent option; severe mitral valve regurgitation is a limitation preventing wide application of this technique. Creation of bypass anastomosis may be safer than standard mitral valve replacement in severe patients with concomitant lesions of other valves and heart structures. However, due to small number of observations and absence of long-term results, careful study is required [12].

Within a little more than a quarter of a century since a solution to this problem was described, at least 3 different methods aimed at complete decalcification with subsequent restoration of the integrity of the annulus fibrosus of the mitral valve have been proposed. The methods described by Carpentier and David are the most widely used in clinical practice for annulus fibrosus reconstruction after complete decalcification. Both methods are aimed at restoring the integrity of the posterior hemisphere of the annulus fibrosus after complete decalcification; in the first case, reconstruction is performed by suturing the edges of the defect; in the second case, pericardial patch is used. Both methods have proven satisfactory and show comparable results. Depending on the depth of calcium deposition, this maneuver may result in injury to the obturator artery in the lateral commissure, and the AV node in the medial commissure projection. The fact of type-1 left ventricular rupture is also important. NG C.K. and colleagues demonstrated the experience of surgical treatment of severe annular calcification in 21 patients using both methods in isolated mitral valve surgery; freedom from reoperation by the 5th year of follow-up was 94.5% with 100% survival [13]. In contrast, Uchimuro T. and colleagues from the University of Tokyo reported 6.6% hospital mortality in 61 patients, including rupture from pseudoaneurysm in a 93-year-old patient on day 80 after surgery. It is worth noting the advanced age of the patients, whose average age was 70 years; almost half of the patients underwent aortic prosthetics in addition to mitral valve intervention. Sudden cardiac death dominated the structure of the cardiac mortality in the mid-term follow-up in 6 out of 12 cases. One patient underwent reoperation 6 years after operation due to paraprosthetic fistula.

Multiple comorbidities that reduce the functional reserve necessary for recovery after surgery classify this pathology as a systemic disease, which is expected to increase the risk of postoperative mortality and complications. A recent retrospective, multicenter study identified several key points. First, patients who underwent surgery with mitral valve ring calcification had a high mortality rate (5.8%); there was also a high rate of postoperative complications in the form of repeated reoperation for bleeding, acute kidney injury requiring dialysis, and prolonged stay on artificial ventilation. A correlation between in-hospital mortality and number of surgeries performed was revealed. Clinics with fewer than 50 operations a year had a higher hospital mortality rate [14]. The authors attribute these results to the high initial severity and complexity of surgery. Patients with calcification were much older, had high levels of diabetes mellitus and hypertension. In addition, the study confirmed the relationship of mitral annulus calcification with prior radiation therapy. A retrospective study of surviving patients who received radiotherapy and combined chemotherapy for childhood cancer showed a high cumulative incidence of cardiovascular complications, including abnormal calcium deposition in the annulus fibrosus [15].

Operative mortality in previous studies ranges from 6 to 20% [16–19]. However, most of these studies are single-center and performed on small groups of patients. Due to the lack of a unified classification and strategy regarding operative tactics, direct comparison of results is not reliable. Studies with high surgical mortality included patients with concomitant surgical procedures on other valves and coronary arteries. Another significant risk factor influencing early mortality and survival is mitral valve replacement. A recent study compared the outcomes of surgical treatment (prosthetic versus reconstructive) in octogenarian patients, which found mitral prosthetics to be an independent predictor of 90-day mortality (31.6% versus 18.9%; $p = 0.01$) and was associated with decreased survival at 1, 3, 5 years (71 ± 3%, 61 ± 4% and 59 ± 4% versus prosthetic outcomes with 56 ± 5%, 50 ± 6%, and 45 ± 6%) [20].

A team of authors from the Mayo Clinic (Rochester, Minnesota), systematized mitral valve calcification to determine treatment strategies. The authors identified

3 degrees of annulus fibrosus damage. The mild degree corresponds to localized areas of calcium deposition or an arc of circumference limited to 180 degrees. Such calcifications in our practice were quite common, including in patients who had undergone radiation therapy, as a rule, trivial methods were used for implantation of prosthesis. Medium calcification is defined as dense, continuous calcification occupying 4/3 of the circumference. And the most severe degree of calcification occupies almost the entire annulus fibrosus with transition to the left ventricular wall and subclavian structures. This category of patients belongs to the category of inoperable patients [21].

Over the past decades, endovascular methods of treatment have evolved tremendously; now the third generation of transcatheter prostheses has appeared, allowing them to be successfully used in clinical practice. If in the aortic position, these devices are firmly established as a surgical option and the results are close to the traditional method of treatment; in the mitral position, the results remain unsatisfactory. By 2019, just over 300 different transvalvular devices were implanted in the mitral position with a 30-day mortality of 13.6%. However, this study did not include patients with severe annulus fibrosus calcification [22]. On the contrary, the experience of treating patients with severe calcification in a series of 116 patients was associated with high mortality, 30-day mortality reached 25%. By the 1st year, the survival rate was 46.3% [23].

CONCLUSION

Despite the initial severity of patients, complete decalcification followed by restoration of the integrity of the annulus fibrosus is a relatively safe and technically reproducible method. Both reconstruction techniques showed satisfactory outcomes, without occurrence of left ventricular posterior wall rupture, fatal bleeding, or coronary artery injury. Further gathering of material with long-term assessment is required.

The authors declare no conflict of interest.

REFERENCES

1. *Pomerance XA.* Pathological and clinical study of calcification of the mitral valve ring. *J Clin Path*. 1970; 23: 354–361. doi.org/10.1136/jcp.23.4.354.
2. *Movahed MR, Saito Y, Ahmadi-Kashani M, Ebrahimi R.* Mitral Annulus Calcification is associated with valvular and cardiac structural abnormalities. *Cardiovasc Ultrasound*. 2007; 5: 14. Published online 2007 Mar 14. doi: 10.1186/1476-7120-5-14.
3. *Allison MA, Cheung P, Criqui MH et al.* Mitral and aortic annular calcification are highly associated with systemic calcified atherosclerosis. *Circulation*. 2006; 113: 861–866. doi.org/10.1161/CIRCULATIONAHA.105.552844.
4. *Hoffmann U, Massaro JM, D'Agostino RB Sr, Kathiresan S, Fox CS, O'Donnell CJ.* Cardiovascular Event Prediction and Risk Reclassification by Coronary, Aortic, and Valvular Calcification in the Framingham Heart Study. *J Am Heart Assoc*. 2016; 5 (2): e003144. Published 2016 Feb 22. doi: 10.1161/JAHA.115.003144.
5. *Abramowitz Y, Jilaihawi H, Chakravarty T, Mack MJ, Makkar RR.* Mitral Annulus Calcification. *J Am Coll Cardiol*. 2015; 66 (17): 1934–1941. doi: 10.1016/j.jacc.2015.08.872.
6. *Carpentier AF, Pellerin M, Fuzellier JF et al*. Extensive calcification of the mitral valve anulus: pathology and surgical management. *J Thorac Cardiovasc Surg*. 1996; 111: 718–729. doi.org/10.1016/S0022-5223(96)70332-X.
7. *David TE, Feindel CM, Armstrong S, Sun Z*. Reconstruction of the mitral anulus. A ten-year experience. *J Thorac Cardiovasc Surg*. 1995; 110: 1323–1332. doi: https://doi.org/10.1016/S0022-5223(95)70055-2.
8. *Agatston AS, Janowitz WR, Hildner FJ, Zusmer NR, Viamonte M Jr, Detrano R.* Quantification of coronary artery calcium using ultrafast computed tomography. *J Am Coll Cardiol*. 1990; 15 (4): 827–832. doi: 10.1016/0735-1097(90)90282-t.
9. *Nataf P, Pavie A, Jault F, Bors V, Cabrol C, Gandjbakhch I.* Intraatrial insertion of a mitral prosthesis in a destroyed or calcified mitral annulus. *Ann Thorac Surg*. 1994; 58: 163–167. https://doi.org/10.1016/0003-4975(94)91092-8.
10. *Hussain ST, Idrees J, Brozzi NA, Blackstone EH, Pettersson GB*. Use of annulus washer after debridement: a new mitral valve replacement technique for patients with severe mitral annular calcification. *J Thorac Cardiovasc Surg*. 2013; 145: 1672–1674. doi: https://doi.org/10.1016/j.jtcvs.2012.12.049.
11. *Lansing AM, Elbl F, Solinger RE, Rees AH*. Left atrial-left ventricular bypass for congenital mitral stenosis. *Ann Thorac Surg*. 1983; 35: 667–669. doi: https://doi.org/10.1016/S0003-4975(10)61081-8.
12. *Meghji Z, Nguyen A, Geske JB, Schaff HV.* Myectomy and Left Atrial-to-Left Ventricular Conduit for Severe Calcific Mitral Stenosis and Hypertrophic Cardiomyopathy. *Ann Thorac Surg*. 2018 Jul; 106 (1): e21–e23. doi: https://doi.org/10.1016/j.athoracsur.2018.01.060.
13. *Ng CK, Punzengruber C, Pachinger O, Nesser J, Auer H, Franke H et al*. Valve repair in mitral regurgitation complicated by severe annulus calcification. *Ann Thorac Surg*. 2000; 70: 53–58. doi: https://doi.org/10.1016/S0003-4975(00)01347-3.
14. *Kaneko T, Hirji S, Percy E, Aranki S, McGurk S, Body S et al.* Characterizing Risks Associated With Mitral Annular Calcification in Mitral Valve Replacement. *Ann Thorac Surg*. 2019; 108, 1761–1767. doi: https://doi.org/10.1016/j.athoracsur.2019.04.080.
15. *Mulrooney DA, Kawashima TF, Mitby PF et al.* Cardiac outcomes in a cohort of adult survivors of childhood and adolescent cancer: retrospective analysis of the Childhood Cancer Survivor Study cohort. *BMJ*. 2009; 339: b4606.

16. *Uchimuro T, Fukui T, Shimizu A, Takanashi S*. Mitral valve surgery in patients with severe mitral annular calcification. *Ann Thorac Surg*. 2016; 101: 889–895.
17. *Feindel CM, Tufail Z, David TE, Ivanov J, Armstrong S.* Mitral valve surgery in patients with extensive calcification of the mitral annulus. *J Thorac Cardiovasc Surg*. 2003; 126 (3): 777–782. doi: 10.1016/s0022-5223(03)00081-3.
18. *David TE, Feindel CM, Armstrong S, Sun Z.* Reconstruction of the mitral anulus. A ten-year experience. *J Thorac Cardiovasc Surg*. 1995; 110 (5): 1323–1332. doi: 10.1016/S0022-5223(95)70055-2.
19. *Mihaljevic T, Koprivanac M, Kelava M, Smedira NG, Lytle BW, Blackstone EH*. Mitral valve replacement in patients with severely calcified mitral valve annulus: surgical technique. *The Journal of thoracic and cardiovascular surgery*. 2013; 146 (1): 233–235.
20. *Chikwe J, Goldstone AB, Passage J et al.* A propensity score-adjusted retrospective comparison of early and mid-term results of mitral valve repair versus replacement in octogenarians. *Eur Heart J*. 2011; 32 (5): 618–626. doi: 10.1093/eurheartj/ehq331.
21. *Eleid MF, Foley TA, Said SM, Pislaru SV, Rihal CS*. Severe Mitral Annular Calcification. Multimodality Imaging for Therapeutic Strategies and Interventions. *JACC Cardiovascular imaging*. 2016; 9 (11): 1318–1337. doi.org/10.1016/j.Jcmg.2016.09.001.
22. *Del Val D, Ferreira-Neto AN, Wintzer-Wehekind J, Dagenais F, Paradis JM, Bernier M et al*. Early Experience With Transcatheter Mitral Valve Replacement: A Systematic Review. *J Am Heart Assoc*. 2019 Sep 3; 8 (17): e013332. https://doi.org/10.1161/JAHA.119.013332.
23. *Guerrero M, Urena M, Himbert D, Wang DD, Eleid M, Kodali S et al*. 1-Year Outcomes of Transcatheter Mitral Valve Replacement in Patients With Severe Mitral Annular Calcification. *J Am Coll Cardiol*. 2018; 71 (17): 1841–1853. https://doi.org/10.1016/j.jacc.2018.02.054.

The article was submitted to the journal on 12.04.2021

DOI: 10.15825/1995-1191-2021-2-60-66

A CLINICAL CASE OF USING THERAPEUTIC PLASMA EXCHANGE FOR THE TREATMENT OF RECURRENT FOCAL SEGMENTAL GLOMERULOSCLEROSIS IN A CHILD AFTER KIDNEY TRANSPLANTATION

I.A. Miloserdov[1, 2], V.S. Bogdanov[1], P.M. Gadzhieva[1], D.A. Saydulaev[1], A.A. Kartashev[1], E.G. Kulikova[1], I.E. Pashkova[1]

[1] Shumakov National Medical Research Center of Transplantology and Artificial Organs, Moscow, Russian Federation

[2] Sechenov University, Moscow, Russian Federation

Background. Focal segmental glomerulosclerosis (FSGS) of the graft in kidney recipients is a rare and difficult-to-diagnose post-kidney transplant complication, which can lead to graft loss and death of the recipient. A unified protocol is required for the treatment of this disease. **Materials and methods.** A 15-year-old female patient C. diagnosed with stage 5 chronic kidney disease as a result of steroid-resistant nephrotic syndrome with hematuria underwent a living related-donor kidney transplantation. On the third day after the operation, laboratory and imaging data showed kidney graft dysfunction. Patient examinations established the cause of the graft dysfunction – idiopathic nephrotic syndrome in FSGS. **Results.** For the treatment of recurrent FSGS, the patient had her immunosuppressive therapy converted from tacrolimus to cyclosporin A, and received two 500 mg rituximab injections. Ten sessions of therapeutic plasma exchange (Plasauto Sigma) were performed to remove antibodies to podocytes. During the therapy, diuresis was restored, creatinine and urea levels decreased. Six months after the kidney transplant, graft function was fully restored. **Conclusion.** The absence of recurrent FSGS within six months during a single course of therapeutic plasma exchange with its subsequent cancellation after restoration of graft function allows to recommend the developed method for the treatment of FSGS in pediatric patients after kidney transplantation.

Keywords: focal segmental glomerulosclerosis (FSGS), kidney transplantation, therapeutic plasma exchange, pediatrics, nephrology, immunosuppression.

INTRODUCTION

Focal segmental glomerulosclerosis (FSGS) is one of the most common morphological variants of chronic glomerulonephritis [1]. However, it is extremely rare in renal allograft recipients (RAR). Clinical manifestations, diagnosis, treatment techniques and long-term prognosis are insufficiently covered in the world literature and require further study.

Idiopathic, or primary, FSGS is characterized by typical sclerosis in a segment of the renal glomerulus along with fusion of the small podocyte pedicel. In addition to hereditary genetic abnormalities, other factors can also cause podocyte damage and be the cause of primary FSGS [2].

Idiopathic FSGS recurs in 20–50% of recipients (up to 80% if recurrence occurred in a previous renal graft). Sclerosis may not be evident at the onset of recurrence, and light microscopy may show normal glomerular architectonics. Recurrence is suspected when a patient with confirmed primary FSGS in his own kidney or previous renal transplant develops proteinuria and/or elevated serum creatinine levels, usually shortly after transplantation.

Secondary FSGS usually does not recur. The causes of secondary FSGS are genetic mutations, viruses (HIV, parvovirus B19, cytomegaloviruses, Epstein–Barr virus, etc.), medications and drugs (interferon-α, adriamycin, doxorubicin, etc.), structural and functional changes in the glomeruli (renal dysplasia, arterial hypertension, etc.), malignant tumors, and some nonspecific FSGS-like changes caused by renal scarring in glomerular diseases [3].

The clinical manifestations of FSGS are:

- Nephrotic syndrome (70% of patients), persistent proteinuria without nephrotic syndrome (30%).
- Mixed nephrotic syndrome combined with microhematuria.
- Arterial hypertension (50%).
- Acute renal failure (25–50%).
- Steroid-resistant course (80%) [4, 5].

Corresponding author: Vasily Bogdanov. Address: 1, Shchukinskaya str., Moscow, 123182, Russian Federation. Phone: (916) 358-16-80. E-mail: dr.artline@gmail.com

The paper describes the postoperative period in a child who underwent kidney transplantation with relapsed FSGS, and the treatment method.

CLINICAL OBSERVATION

Recipient and donor baseline data

Clinical manifestations of renal failure (mixed nephrotic syndrome with arterial hypertension and macrohematuria) first appeared in the patient when he was 3 years old. He received prednisolone therapy for a long time with no significant clinical and laboratory response; a steroid-resistant clinical phenotype of chronic glomerulonephritis was found.

In June 2009, nephrobiopsy was performed, the biopsy result was uninformative, FSGS was not excluded. In November 2011, cyclosporine A therapy was started with temporary decrease in proteinuria levels, repeated series of methylprednisolone pulse therapy were performed. Mycophenolic acid preparations have been prescribed since June 2014. Complete clinical and laboratory remission was not achieved.

Renal failure gradually progressed. The last relapse was in June 2016 – complete mixed nephrotic syndrome (anasarca +8 kg), arterial hypertension up to 160/120 mm Hg.

Since July 2016, renal replacement therapy in the form of prolonged venovenous hemodiafiltration with further transfer of the patient to intermittent hemodialysis was started under emergency indications. A Tenckhoff catheter was implanted, but two weeks later the patient was transferred to peritoneal dialysis with a 4 exchange/day regime without any features. Ultrafiltration was unstable, ranging from 100 to 1400 mL. Since November 2017, the patient has been transferred to Baxter's peritoneal dialysis.

In May 2018, due to progression of secondary hyperparathyroidism, subtotal parathyroidectomy was performed. In December 2018, May 2019 and November 2019, episodes of dialysis peritonitis and anuria were observed for two years.

The donor was a woman (recipient's mother), 39 years old, blood group compatible (0(I) Rh+). She was overweight (BMI 29.4 kg/m^2). CKD-EPI glomerular filtration rate was 91 mL/min. She underwent a full examination as a potential kidney donor – no medical contraindications to donation were identified.

Transplantation and early postoperative period

In August 2020, the 15-year-old patient (blood group 0(I) Rh+, baseline height 148 cm, weight 36.1 kg) underwent a living-related left kidney transplantation to the right iliac region with graft ureteral stenting; graft function was immediate. Methylprednisolone 400 mg, basiliximab 20 mg were used as intravenous induction therapy. The initial maintenance immunosuppressive therapy included methylprednisolone 16 mg/day, tacrolimus 6 mg/day, and mycophenolic acid 720 mg/day.

Immediately after transplantation, RAR function was satisfactory during the first two days: diuresis was adequate for water load, serum creatinine was 131 μmol/L, and urea was 11.6 mmol/L. According to ultrasound findings, RAR volume was 102 cm^3, vascular resistance indices in the main, segmental, and arch arteries of RAR were within 0.6–0.7.

On the third day after operation, creatinine level increased to 142 μmol/L and urea to 13.6 mmol/L in the blood serum, diuresis rate decreased. Biopsy was impossible due to pronounced hypocoagulation, against the background of anticoagulant therapy as part of the postoperative heparin protocol. In order to prevent acute cellular rejection, a course of pulse therapy (methylprednisolone 500 mg intravenously) for three days, and immunoglobulin antithymocyte 500 mg for two days was conducted. The therapy had no effect.

Diagnosis and treatment of recurrent FSGS

On day 7 following kidney transplantation, daily urine output decreased to 500 mL, arterial hypertension appeared with blood pressure elevations to 160/90 mmHg. According to laboratory tests, serum creatinine was 294 μmol/L, urea was 20.1 mmol/L, total protein was 52.7 g/L, albumin was 32.5 g/L, and urine protein was 19.2 g/L. According to ultrasound findings, RAR volume increased to 170 cm^3, vascular resistance indices were within 0.8–0.85. Taking into account the findings of the examination, a recurrence of the underlying disease cannot be ruled out. RAR punch biopsy findings revealed moderate acute tubular necrosis, microcirculatory disorders characteristic of calcineurin inhibitor toxicity, and antibody-mediated rejection 0 (AMR 0). Results of immunological examination for glomerulonephritis in systemic vasculitis, systemic lupus erythematosus, and antiphospholipid syndrome were negative.

Based on the history (acute glomerulonephritis at the age of 3.5 years with clinical phenotype – steroid-resistant nephrotic syndrome with arterial hypertension and erythrocyturia), clinical signs (edema syndrome, arterial hypertension), laboratory results (increase in creatinine and urea levels, decrease in albumin and total protein, massive proteinuria) and imaging (deterioration in intrarenal blood flow and increase in graft size) investigation methods, "RAR dysfunction, recurrent FSGS" was diagnosed.

Due to increasing hyperhydration and rise in serum creatinine and urea levels, hemodialysis sessions were initiated, antithymocyte immunoglobulin therapy was cancelled on day 9 after transplantation, therapeutic plasma exchange (TPE) sessions were initiated, human

immunoglobulin was injected in the days between plasma exchange procedures.

On day 18 after transplantation, immunosuppressive therapy was converted – tacrolimus was withdrawn, cyclosporine A was initiated at 5 mg/kg/day dose, then rituximab 500 mg was introduced, tablet corticosteroid therapy with prednisolone 60 mg/m^2/day was started. Two days later, pulse therapy with methylprednisolone 500 mg daily for 5 days was initiated.

Against the background of this therapy, there was gradual recovery of diuresis (to 150 mL by September 9), reduction of interdialysis day azotemia (serum creatinine level decreased from 718 μmol/L to 607 μmol/L, urea from 32.8 mmol/L to 27.2 mmol/L), and improvement in general well-being.

On day 22 after transplantation, a repeated graft punch biopsy was performed (due to an increase in the volume of the renal graft and an increase in the resistance index according to ultrasound). No data on cellular and antibody-mediated rejection were obtained. Electron microscopy of the biopsy specimen was performed – the picture is most consistent with nephropathy of minimal changes in the form of podocyte small process disease, focal-segmental glomerulosclerosis/hyalinosis cannot be ruled out (not detected in the material).

On day 27, diuresis was restored (more than 1 liter per day). On day 28 after transplantation, the final hemodialysis session was performed (7 sessions in total), after which there was an increase in serum creatinine and urea levels for two days, then a decrease. The average volume of treated plasma per procedure was 0.98 (0.88 to 1.11) of circulating plasma. Fresh frozen plasma (FFP) of identical blood group was used as replacement fluid.

Parameters of TPE procedures performed on the patient are shown in Table.

In addition, the level of proteinuria in the single portion of urine decreased to 1.8 g/L. The dynamics of laboratory indicators are shown in Fig. 1.

On day 31 after kidney transplantation, the recipient completed a TPE course. In order to induce remission, 500 mg of rituximab was administered again.

Table

Therapeutic plasma exchange parameters

Procedure No.	1	2	3	4	5	6	7	8	9	10
Days after kidney transplantation, days	9	11	15	17	18	22	25	29	31	33
Patient weight, kg	35	39	40	40	40	39.2	39.6	40	39.7	39.8
Circulating blood, mL	2450	2730	2800	2800	2800	2744	2772	2800	2779	2786
Circulating plasma, mL	1788	2102	2066	2066	2066	2058	2079	2100	2084	2089.5
FFP for replacement, mL	1380	1710	1800	1770	1770	1700	1920	1920	2050	2020
NaCl 0.9% for replacement, mL	200	50	0	0	0	100	0	0	0	0
Albumin 10% for replacement, mL	200	200	200	200	200	200	200	200	0	200
Processed plasma, L	1.57	1.85	2	1.97	2	2	2.02	2.11	2.31	2.22
Processed plasma, circulating plasma	0.88	0.88	0.97	0.95	0.97	0.97	0.97	1.00	1.11	1.06
Maximum pump rate, mL/min	65	65	55	65	65	70	65	70	70	70
Heparin during the procedure, units	1750	1750	2250	2000	1750	1250	2250	2250	2250	2250

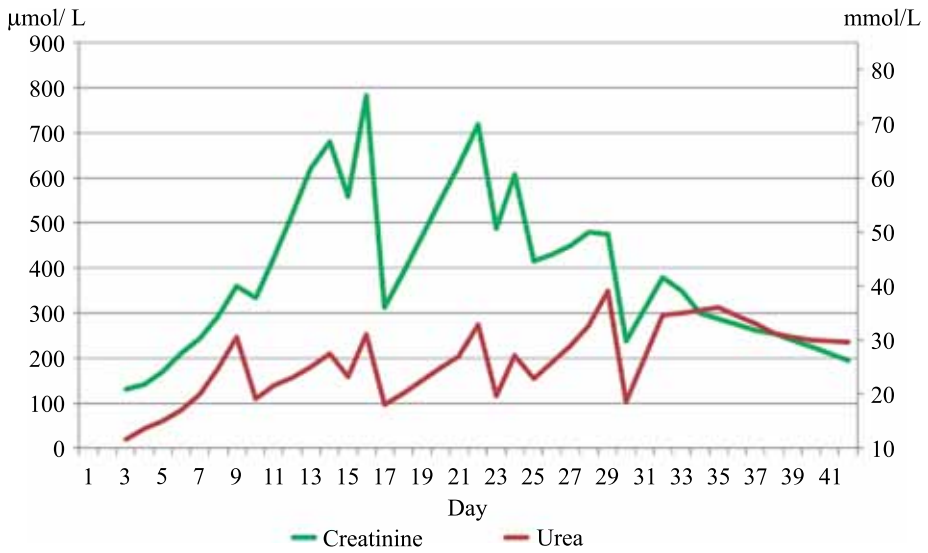

Fig. 1. Kidney recipient laboratory parameters

Thus, against the background of the therapy (10 TPE procedures, the second administration of rituximab, prednisolone 60 mg/m²/24 hours, cyclosporine A 5–8 mg/kg/day), a pronounced positive trend was noted.

Long-term postoperative period

On day 42 after transplantation, inpatient treatment was completed: diuresis was adequate to water load, serum creatinine was 196 μmol/L, urea was 29.6 mmol/L (decrease over time), proteinuria was 0.39 g/L, vascular resistance indices were within 0.75–0.8 (according to ultrasound results).

During outpatient follow-up, further improvement in the child's general condition, and normalization of clinical and laboratory parameters, were observed. At follow-up examination 3 months after discharge, serum creatinine level was 130 μmol/L, urea was 15.7 mmol/L, daily proteinuria was 0.373 g, vascular resistance indices were within 0.6–0.7.

DISCUSSION

The presented clinical case raises a number of questions concerning the diagnosis and treatment of diseases with a high recurrence rate.

The main problem in diagnosing FSGS in a kidney recipient was the inability to establish the initial cause of renal failure. A biopsy was performed at the first manifestation of the disease (at the age of 4 years), but electron microscopy was not performed; therefore, biopsy results were not fully informative. A biopsy performed at a more mature age (e.g., before transplantation at age 15) may not be informative due to the age of the lesion.

Prior to kidney transplantation, the patient underwent genetic examination to rule out genetically determined FSGS. A panel of seven permeability factors (CD40, PTPRO, CGB5, FAS, P2RY11, SNRPB2, and APOL2) could predict posttransplant FSGS recurrence with 92% accuracy [6], but our study was negative.

The non-specificity of the clinical picture of RAR dysfunction in the early postoperative period, as well as the lack of necessary anamnestic data resulted in delayed diagnosis and delayed (7 days after transplantation) performance of punch biopsy of the RAR. The fragment obtained during punch biopsy also lacked specific markers characteristic of FSGS. However, absence of histological signs of injury during the first week after transplantation is characteristic of podocytopathies.

Thus, the following clinical findings were established on day 7 after transplantation:

- Arterial hypertension (150/100 mmHg) against the background of a 4-component antihypertensive therapy;
- increase in peripheral edema, increase in the patient's body weight;
- laboratory-confirmed RAR dysfunction (creatinine up to 550 μmol/L and urea up to 27 mmol/L);
- massive proteinuria (up to 20 g/L);
- erythrocyturia (with microscopy, erythrocytes occupy the entire field of view);
- hypoproteinemia (total protein level 52.7 g/L) and hypoalbuminemia (albumin level 32.5 g/L) against the background of continuous albumin infusion (up to 20 g per day);
- deterioration of intrarenal blood flow according to ultrasound.

This clinical picture is characteristic of mixed nephrotic syndrome. Given that corticosteroid therapy had no effect, and there were no significant changes according

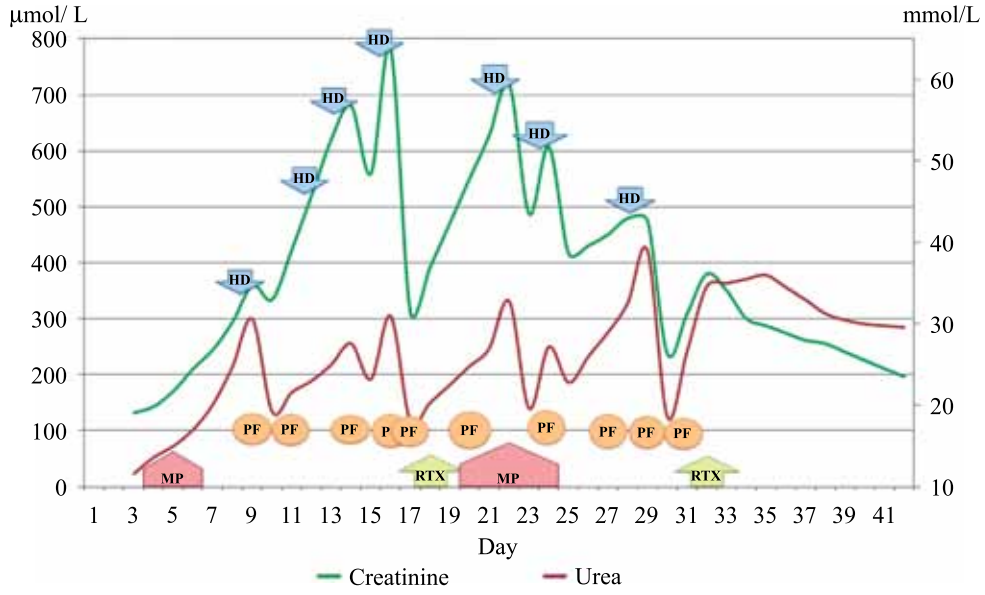

Fig. 2. Main components of treatment: HD – hemodialysis session, MP – methylprednisolone pulses 500 mg intravenously, RTX – rituximab 500 mg intravenously, PF – plasmapheresis sessions

to RAR biopsy data, the patient was diagnosed as having recurrent FSGS.

Currently, plasmapheresis and rituximab are the main methods for treating recurrent FSGS in world practice [7–9]. The main components of the therapy are shown in Fig. 2.

The volume and regimens of plasmapheresis procedures, as well as the type of procedure, are not defined and vary depending at the hospital where the patient is being treated.

We chose TPE because of patient safety and its effectiveness as an antibody removal method. TPE procedures allow to remove most of the protein structures of the plasma, while FFP replacement allows to maintain or compensate for protein and plasma clotting factor deficiencies.

The use of double cascade filtration (DCF) was abandoned because its use in the early postoperative period leads to massive bleeding due to removal of plasma clotting factors. Besides, protein loss during DCF against the background of proteinuria, characteristic of FSGS, also leads to a worsening of the clinical picture.

The FSGS immuno-pathomechanism is associated with a large number of permeability factors, many of which have not yet been identified. Due to the inability to identify the exact substrate that caused the recurrence of idiopathic FSGS, the use of immunoadsorption was abandoned.

There is no exact data in the literature on how many and how much plasmapheresis procedures should be performed. Given the pathogenesis of the disease, it is assumed that after removal of circulating antibodies from the body, there is no need for plasmapheresis procedures.

According to the latest guidelines by the American Society for Apheresis (ASFA), TPE procedures should be initiated when symptoms of recurrent FSGS occur daily or once every 2 days. The recommended volume of replacement is 1.5 to 2 circulating plasma volume (CPV) [8]. Rudnicki M. reports that the best results were obtained in patients who received 3–4 TPE procedures per week TPE, with 1–2 CPV volume before the onset of remission. The total number of treatments ranged from 8 to 12 [9].

Interest in rituximab as a potential drug for the treatment of nephrotic syndrome followed the observation of a dramatic reduction in proteinuria in children with nephrotic syndrome treated with rituximab for idiopathic thrombocytopenic purpura [10] and post-transplant lymphoproliferative disorder.

Over the past 10 years, the use of rituximab in recurrent FSGS has expanded considerably due to good outcomes [11, 12].

In addition, since rituximab selectively suppresses B-lymphocytes, it has a direct protective effect on podocytes. Rituximab is able to protect acid sphingomyelinase-like phosphodiesterase 3b (SMPDL3b) as well as acid sphingomyelinase (aSMase) by binding to the SMPDL3b protein at podocyte lipid bridges, which can be a target for FSGS permeability factor and which is identifiable by rituximab [13, 14]. Rituximab in combination with TPE appears to be more effective than reported by clinical cases [15, 16].

Cyclosporin A was chosen as a drug for supportive immunosuppressive therapy based on its features contributing to stabilization of the actin cytoskeleton in podocytes [17].

The chosen treatment tactics for the kidney recipient with FSGS made it possible to achieve remission within 18 days, restoring graft function.

CONCLUSION

Recurrent idiopathic FSGS in renal allograft recipients is a complex clinical problem due to the objective difficulty of diagnosis and the lack of a single standard of treatment. As part of differential diagnosis, data on the original disease of native kidneys as well as results of electron microscopy of the RAR biopsy are of key importance.

The presented clinical case of successful use of TPE in combination with rituximab and basic immunosuppressive therapy to treat recurrent FSGS in a child after kidney transplantation demonstrates the safety and efficacy of the developed method. The proven treatment regimen for recurrent FSGS can be recommended for application in clinical practice.

The authors declare no conflict of interest.

REFERENCES

1. *Saran R et al.* US renal data system 2016 annual data report: Epidemiology of kidney disease in the United States. *Am J Kidney Dis*. 2017; 69 (Suppl 1): A7–A8.
2. *Canaud G, Delville M, Legendre C.* Recurrence of Focal and Segmental Glomerulosclerosis After Transplantation. *Transplantation.* 2016; 100: 284–287.
3. *Murkamilov IT, Sabirov IS, Fomin VV, Murkamilova ZhA.* Fokal'no-segmentarnyy glomeruloskleroz: sovremennoe sostoyanie problemy. *Arkhiv vnutrenney meditsiny*. 2020; 1: 38–46.
4. *Bobkova IN, Kozlovskaya LV, Tsygin AN, Shilov EM.* Klinicheskie rekomendatsii po diagnostike i lecheniyu fokal'no-segmentarnogo glomeruloskleroza. *Nefrologiya*. 2015; 19 (1).
5. *Rosenberg AZ, Kopp JB.* Focal segmental glomerulosclerosis. *Clin J AM Soc Nophrol*. 2017.
6. *Delville M et al.* A circulating antibody panel for pretransplant prediction of FSGS recurrence after kidney transplantation. *Sci Transl Med.* 2014; 6.
7. *Uffing A et al.* Recurrence of FSGS after Kidney Transplantation in Adults. *CJASN*. Feb 2020; 15 (2): 247–256.
8. *Schwartz J et al.* Guidelines on the Use of Therapeutic Apheresis in Clinical Practice – Evidence-Based Approach from the Writing Committee of the American So-

ciety for Apheresis: The Seventh Special Issue. *Journal of Clinical Apheresis*. 2016; 31: 213–214.
9. *Rudnicki M.* FSGS Recurrence in Adults after Renal Transplantation. *Biomed Res Int.* 2016; 2016: 3295618.
10. *Nozu K, Iijima K, Fujisawa M et al.* Rituximab treatment for posttransplant lymphoproliferative disorder (PTLD) induces complete remission of recurrent nephrotic syndrome. *Pediatr Nephrol*. 2005; 20: 1660–1663. doi: 10.1007/s00467-005-2013-7.
11. *Cravedi P, Kopp JB, Remuzzi G.* Recent progress in the pathophysiology and treatment of FSGS recurrence. *Am J Transplant*. 2013; 13: 266–274.
12. *Araya CE, Dharnidharka VR.* The factors that may predict response to rituximab therapy in recurrent focal segmental glomerulosclerosis: a systematic review. *J Transplant*. 2011; 2011: 374213.
13. *Fornoni A, Sageshima J, Wei C, Merscher-Gomez S, Aguillon-Prada R, Jauregui AN et al.* Rituximab targets podocytes in recurrent focal segmental glomerulosclerosis. *Sci Transl Med*. 2011; 3: 85ra46.
14. *Reiser J, Fornoni A.* Rituximab: a boot to protect the foot. *J Am Soc Nephrol*. 2014; 25: 647–648.
15. *Tsagalis G, Psimenou E, Nakopoulou L, Laggouranis A.* Combination treatment with plasmapheresis and rituximab for recurrent focal segmental glomerulosclerosis after renal transplantation. *Artif Organs*. 2011; 35: 420–425.
16. *Hristea D, Hadaya K, Marangon N, Buhler L, Villard J, Morel P, Martin PY.* Successful treatment of recurrent focal segmental glomerulosclerosis after kidney transplantation by plasmapheresis and rituximab. *Transpl Int*. 2007; 20: 102–105.
17. *Li X et al.* Cyclosporine A protects podocytes via stabilization of cofilin-1 expression in the unphosphorylated state Exp Biol Med (Maywood). 2014 Aug; 239 (8): 922–936.

The article was submitted to the journal on 12.04.2021

DOI: 10.15825/1995-1191-2021-2-67-75

A COMPREHENSIVE SURGICAL APPROACH TO THE TREATMENT OF DEEP STERNAL WOUND INFECTION AFTER HEART TRANSPLANTATION

V.M. Zakharevich[1, 2], V.A. Mitish[3–5], T.A. Khalilulin[1, 2], A.R. Zakiryanov[1], D.S. Ivanov[1], A.M. Goltz[1], A.A. Sukhatchev[1], K.S. Kiryakov[1], O.A. Pozdnyakov[1], N.Y. Zacharevich[1]

[1] Shumakov National Medical Research Center of Transplantology and Artificial Organs, Moscow, Russian Federation

[2] Sechenov University, Moscow, Russian Federation

[3] Research Institute of Emergency Pediatric Surgery and Traumatology, Moscow, Russian Federation

[4] National Medical Research Center of Surgery named after A.V. Vishnevsky, Moscow, Russian Federation

[5] Peoples' Friendship University of Russia, Moscow, Russian Federation

Deep wound infection of the anterior chest wall tissues in patients after transsternal cardiac surgery despite intensive developments in surgical techniques and improvement of antibacterial chemotherapy, remains a genuine concern worldwide [1]. The incidence of this complication in the general population ranges from 0.5 to 4% [2, 3]. Despite developed approaches in the treatment of cardiac surgery patients, the treatment of deep sternal wound infection and surrounding tissues following a heart transplantation still remains a rather serious and pressing challenge. This paper presents a clinical observation of a heart transplant recipient, complicated by deep postoperative wound infection. The strategy of staged surgical treatment of sternal osteomyelitis consisted of surgical wound debridement, local wound debridement with vacuum dressings, and reconstructive surgery at the final stage (sternal reosteosynthesis, plasty of the anterior chest wall wound with displaced skin and fascial flaps).

Keywords: heart transplantation, wound infection, sternum, mediastinitis, immunosuppressive therapy, anterior chest wall wound plasty, reosteosynthesis.

INTRODUCTION

Deep wound suppuration in the anterior chest wall after sternotomy as a complication after heart surgery has remained a pressing problem for many decades, especially in the group of heart recipients for whom immunosuppressive therapy is an integral part of the treatment process [1].

Preoperative risk factors include gender, age, bad habits (smoking, alcohol, and drug addiction), diabetes mellitus, and a history of chronic diseases [5]. Intraoperative risks are caused by the urgency of the surgery, sternotomy errors, wound edge retraction techniques, incorrect sternal osteosynthesis, use of soft tissue reduction method, and repeated surgical access (resternotomy, cardiolysis) [11]. The most important intraoperative risk factors for deep wound infection are the volume of blood loss, cardiopulmonary bypass duration, compression (ischemia) in the surgical wound area, traumatic sternal hemostasis technique, use of wax and an electrocoagulator in the spongy sternum area [6]. Postoperative risk factors include sternal instability, sternal ischemia, sternal suture eruption, resternotomy, prolonged mechanical ventilation, cardiac massage, low cardiac output, respiratory distress syndrome, immunosuppression, and decompensation of chronic diseases [12].

The pathogenesis of this complication encompasses a wide range of pathological processes, as well as many perioperative risk factors. Wound infection is characterized by translocation and contamination by pathological microorganisms of wound edges and walls, including the dermis and subcutaneous adipose tissue, with the development of local inflammation, as well as purulent discharge. Deep postoperative wound infection is a serious complication involving various areas of the subcutaneous adipose tissue, fascia, sternum, ribs, and soft tissues of the retrosternal space [2].

The pathological flora found in the wound discharge cultures is mainly represented by St. aureus, St. epidermidis and gram-negative bacteria [3, 4]. High virulence and resistance of hospital microbial strains to antibacterial chemotherapy pose serious challenges in the selection of etiotropic and pathogenetic therapy, and prolong hospitalization time and treatment cost [7], which creates a "vicious circle" for the patient and the attending physician. Deep wound infection after heart transplantation increases mortality by up to 32% [8, 9].

Corresponding author: Denis Ivanov. Address: 1, Shchukinskaya str., Moscow, 123182, Russian Federation. Phone: (499) 190-60-34. E-mail: divanovs@gmail.com

Currently, there are various surgical methods for replacing anterior chest wall tissue defect forming after surgical treatment of a purulent-necrotic focus. However, they all come with certain risks. For example, plasty with the greater omental flap is associated with high traumatic effect, the risk of developing necrosis, peritonitis, as well as the development of thoraco-abdominal hernia [11]. Myoplasty with the pectoralis major flaps is associated with high trauma and development of necrosis, and the operation is often followed by severe pain syndrome and impaired motor function [12].

One of the most effective and credible ways to treat postoperative osteomyelitis of the sternum and ribs was the staged surgical treatment strategy developed by V.A. Mitish et al. [13, 14, 15]. The reconstructive stage consists in the use of local tissues to replace the anterior chest wall defect formed after surgical treatment. At the same time, local tissues are mobilized in the form of skin-fascial or skin-muscle formations, which are subsequently displaced into the defect. This strategy was the basis for successful treatment in patients after heart transplantation complicated by deep wound infection that required surgical treatment.

CASE STUDY

Patient Y., 59 years old, with complaints of shortness of breath with little physical exertion, swelling of the legs and abdomen, general weakness, right thoracic pain, was hospitalized in November 2019 at Shumakov National Medical Research Center of Transplantology and Artificial Organs in Moscow for examination to ascertain possibility of being a potential heart recipient. Medical history shows that the patient had repeated paroxysmal atrial fibrillation in 2002, 2003 and 2006. In December 2018, examination against the background of complaints of acute chest pain revealed extensive transmural myocardial infarction. As a result, thrombolysis was performed. In July 2019, his EchoCG showed a severe left ventricular aneurysm, and severe pulmonary hypertension. At the same time, coronary angiography was performed: the anterior interventricular branch of the left coronary artery was occluded in the proximal segment, the distal bed was contrasted retrogradely from the circumflex artery.

Upon admission to the cardiology department in October 2019, the patient's condition was assessed as moderate. There were manifestations of chronic heart failure (NYHA class III); right-sided hydrothorax, ascites, hypostatic pneumonia, and chronic kidney disease were noted. According to echocardiographic studies, the ejection fraction was 15%, and the final diastolic volume was 205 mL. Because it was impossible to perform reconstructive surgical treatment on the patient's heart and conservative therapy would be futile, it was decided to perform heart transplantation as the only possible treatment method. The patient was put on the heart transplant waiting list on November 18, 2019.

Against the background of antibacterial, massive diuretic, inotropic therapy, and puncture of the pleural cavities, the patient's condition improved. The severity of shortness of breath decreased, edema and ascites regressed, and the volume of fluid in the pleural cavities decreased. Chest CT showed gradual resolution of pneumonia.

On December 02, 2019, the patient underwent orthotopic heart transplantation. The early postoperative period proceeded against the background of myocardial insufficiency (requiring inotropic support) and renal failure, for which renal replacement therapy sessions were performed.

In the cardiac surgery department after transfer from the intensive care unit, the patient's condition remained hemodynamically stable. Examinations showed a satisfactory graft function. Coronary angiography revealed no hemodynamically significant lesions of the graft coronary arteries. Endomyocardial biopsy revealed no acute cellular and antibody-mediated rejection. There was no fever throughout the postoperative period. However, the patient still had renal insufficiency, which required repeated renal replacement therapy sessions, as well as a tendency to fluid accumulation in the pericardial cavity with signs of right heart compression. As a result, open drainage of the pericardial cavity from subxiphoidal access was performed on December 16, 2019.

On December 22, 2019, the patient was diagnosed with 5 cm of skin and soft tissue diastasis in the middle third of the postoperative suture. Immediate reduction of immunosuppressive therapy was performed - Mycophenolate mofetil was canceled and the antibiotic therapy was adjusted. Within seven days, no positive dynamics was observed. The wound increased in size both in width and length, and purulent discharge appeared. Computed tomography revealed sternum diastasis with osteomalacia at the body level, the xiphoid process and spread of the wound channel into the retrosternal tissue. Postoperative wound suppuration with sternal lesions was diagnosed. Therefore, there was a decision to surgically treat the purulent wound of the anterior chest.

In the operating room on December 30, 2019, the patient underwent wound revision. The wound cavity contained a cloudy purulent discharge, which also came from the retrosternal space. Sternal suture failure and signs of marginal necrosis and destruction of the sternal halves were diagnosed (Fig. 1). The sutures seams were removed. When the sternal halves were diluted, purulent mediastinitis was diagnosed (Fig. 2). Marginal resection of the affected areas of the body and the sternum handle was performed. The altered soft tissue areas were excised. The wound was treated with hydrogen peroxide solution and iodopyron. The operation was completed

by applying a vacuum dressing with pulsating vacuum aspiration (Fig. 3).

In the postoperative period, a culture of Pantoea agglomerans, Acinetobacter baumanni, sensitive to polycyclic antibiotics, such as Polymxin B and Colistin, were taken from the wound. Also, Staphylococcus epidermitis, sensitive only to Linezolid, Vancomycin and Moxifloxacin, was repeatedly found in the cultures from the wound discharge. Antibiotic therapy was adjusted in accordance with the obtained sensitivity of the isolated microorganisms during the entire period of local wound treatment.

Local treatment with NPWT (Negative pressure wound treatment) systems was carried out for 6 weeks.

Scheduled replacement of the vacuum aspiration system was performed in the operating room, during which we performed stage surgical treatment of soft tissue and sternum wounds, sanitation with an antiseptic solution for 10 minutes. Despite the ongoing treatment, the

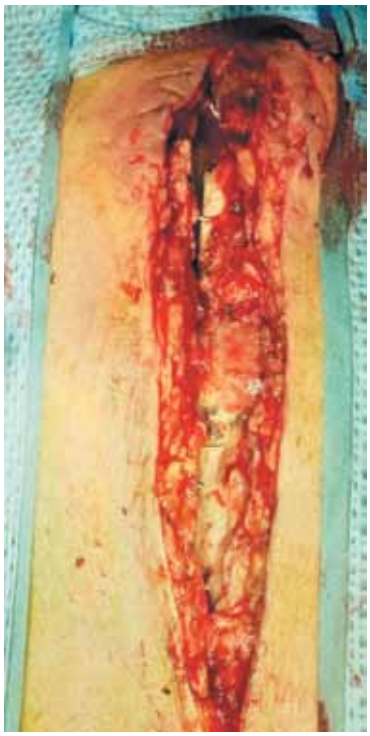

Fig. 1. View of the postoperative anterior chest wall wound before surgical treatment

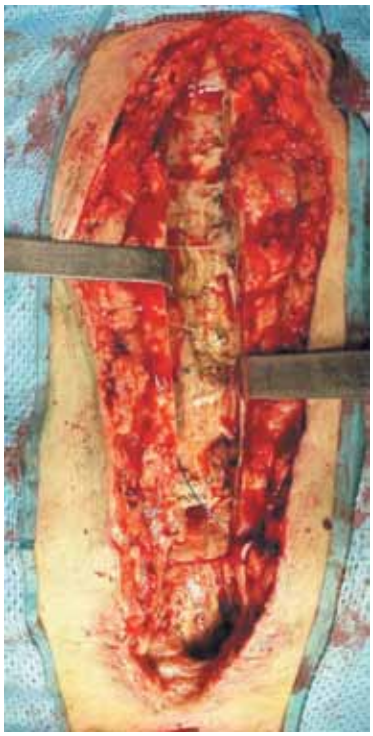

Fig. 2. View of the wound after removal of wire sutures and separation of sternal halves

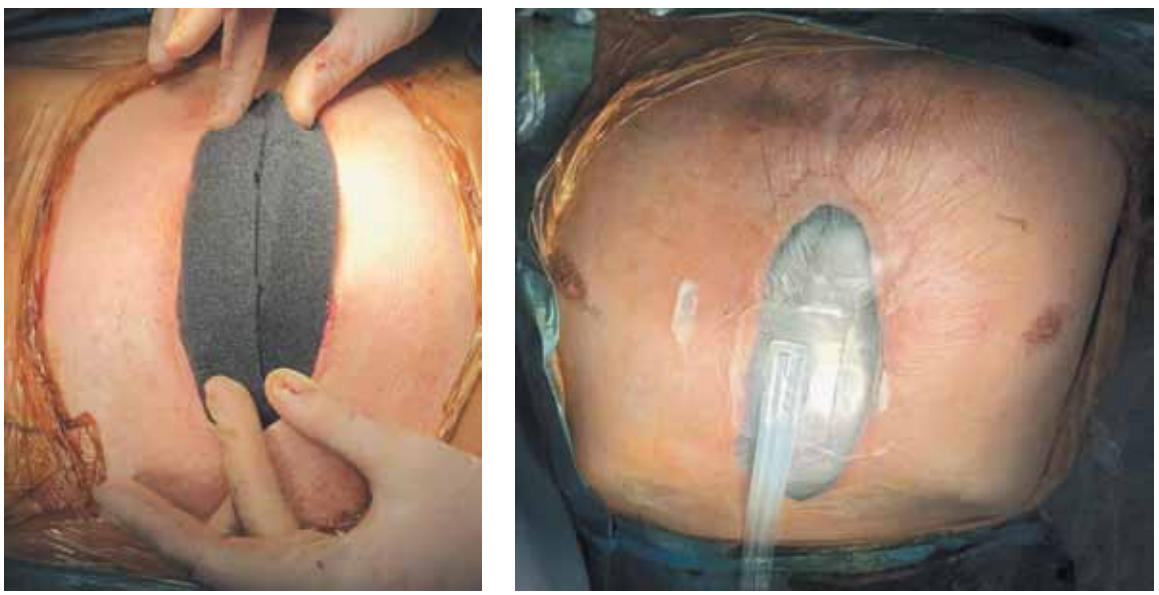

Fig. 3. Completion of surgical wound debridement by imposing a negative pressure wound therapy system

healing process of the postoperative wound had sluggish positive dynamics, the wound walls and bottom were partially filled with edematous granulation tissue, the foci of secondary necrosis appeared in some places (Fig. 4). The patient continued to remain asthenic, have anemia of mixed genesis, chronic kidney disease requiring renal replacement therapy. In the postoperative period, right-sided polysegmental pneumonia joined, which required short-term follow-up in the intensive care unit. All this significantly complicated the course of the wound process and prolonged the hospitalization period.

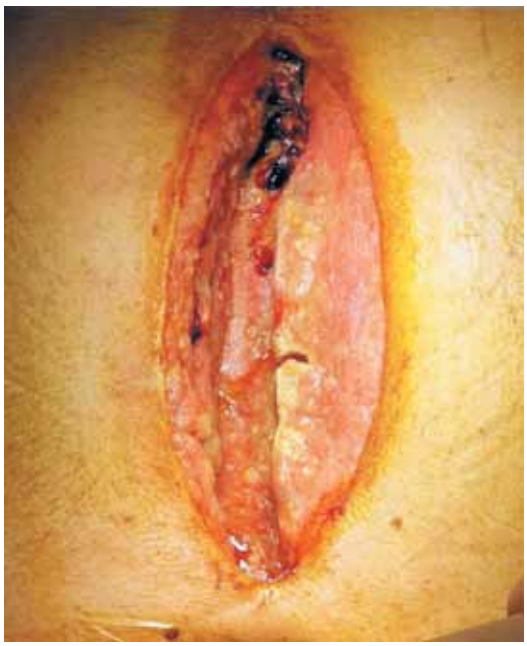

Fig. 4. Wound condition on day 45 after local treatment with NPWT

By the end of the second month after surgical treatment of the wound, the patient's general condition improved, and positive dynamics of the wound process and its transition to a regeneration phase were noted. The condition of the sternum is shown in Fig. 5.

After three times obtaining sterile cultures from the wound, it was decided to perform the second (reconstructive) stage of surgical treatment - sternal reosteosynthesis and replacement of the soft tissue wound defect in the anterior chest wall with displaced fasciocutaneous flap.

On March 30, 2020, under endotracheal anesthesia, the edges of the soft tissue and sternum wound were acutely treated in the operating room, and granulation areas were removed (Fig. 6). Both sternal halves were mobilized with opening of the pleural cavities (Fig. 7). The anterior mediastinum and pleural cavities were drained with silicone tubes. The sternum edges were brought together and juxtaposed. Sternal rheosteosynthesis was performed according to Robiscek, as well as 8 single oblique-transverse wire sutures (Fig. 8). Satisfactory frame function of the thorax was restored (Fig. 9). The size of the wound defect in the anterior chest wall soft tissue was 17 cm by 5 cm. Closing the wound by simply bringing the edges of the wound together was not possible. Therefore, it was decided to replace the wound defect with local tissues through extensive mobilization of the wound edges in the form of fasciocutaneous flaps.

In a blunt and sharp way, the integumentary tissues were separated from the sternum, the pectoralis major muscles and from the ribs in the lower part of the wound to a 10–12 cm width (Fig. 10).

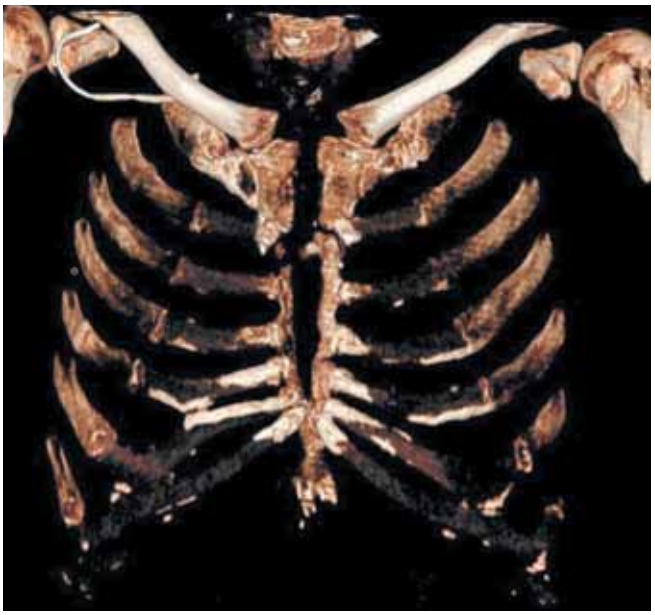

Fig. 5. Sternal diastasis at the manubrium level and with a bone defect at the body level. 3D reconstruction of CT scan

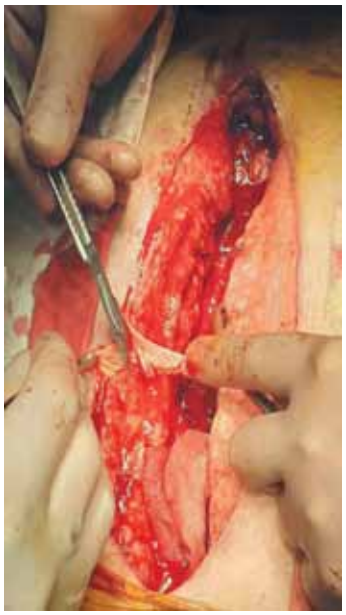

Fig. 6. Reconstructive surgery phase. Wound edges were excised. Granulation areas were removed, sternal edges were freshened

Using deep U-shaped sutures (in two rows on both sides), the mobilized wound edges were displaced toward the wound defect until they were completely juxtaposed (Fig. 11).

Thanks to the U-shaped tension and stay sutures, the wound edges matched without tension (Fig. 12). The subcutaneous adipose tissue was sutured with single absorbable nodular sutures. The wound edges were sutured with U-shaped skin sutures.

The postoperative period was uneventful. Ischemia, signs of inflammation and significant edema of the displaced integumentary tissues were not observed. The wound healed by primary intention. Antibacterial therapy with Moxifloxacin 400 mg once a day was carried out. According to multispiral chest CT scan on April 20, 2020, slight eruption of the first wire suture in the sternum handle area and 7 mm sternum handle diastasis were noted, which, however, did not affect sternal stability (Fig. 9). On day 14 after reconstructive surgery, the outer rows of U-shaped tension sutures on both sides were removed. After a significant decrease in the discharge along the drains on day 5, drains were removed from

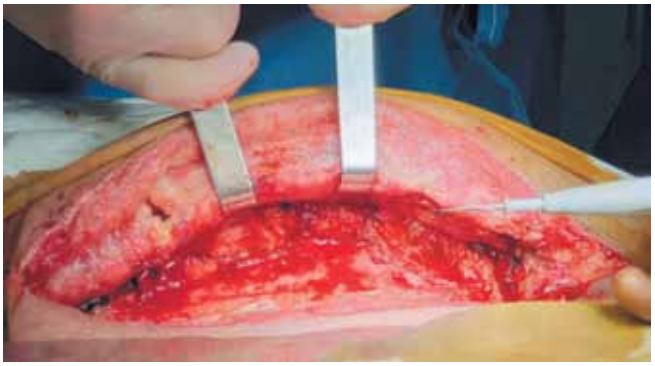

Fig. 7. The retrosternal space of both parts of the sternum was separated from adhesions by blunt and by sharp dissection

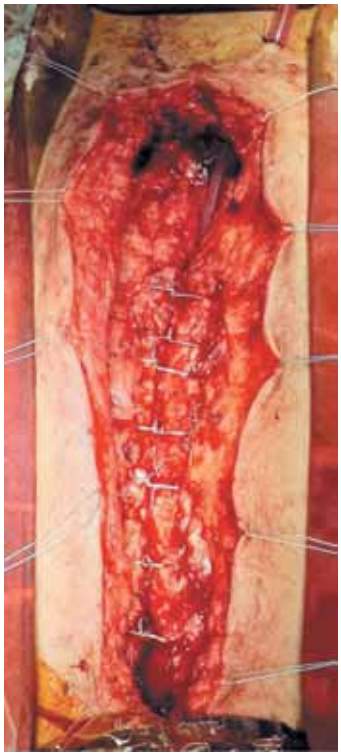

Fig. 8. Sternal reosteosynthesis with eight single transverse and one single longitudinal Robicsek wire sutures

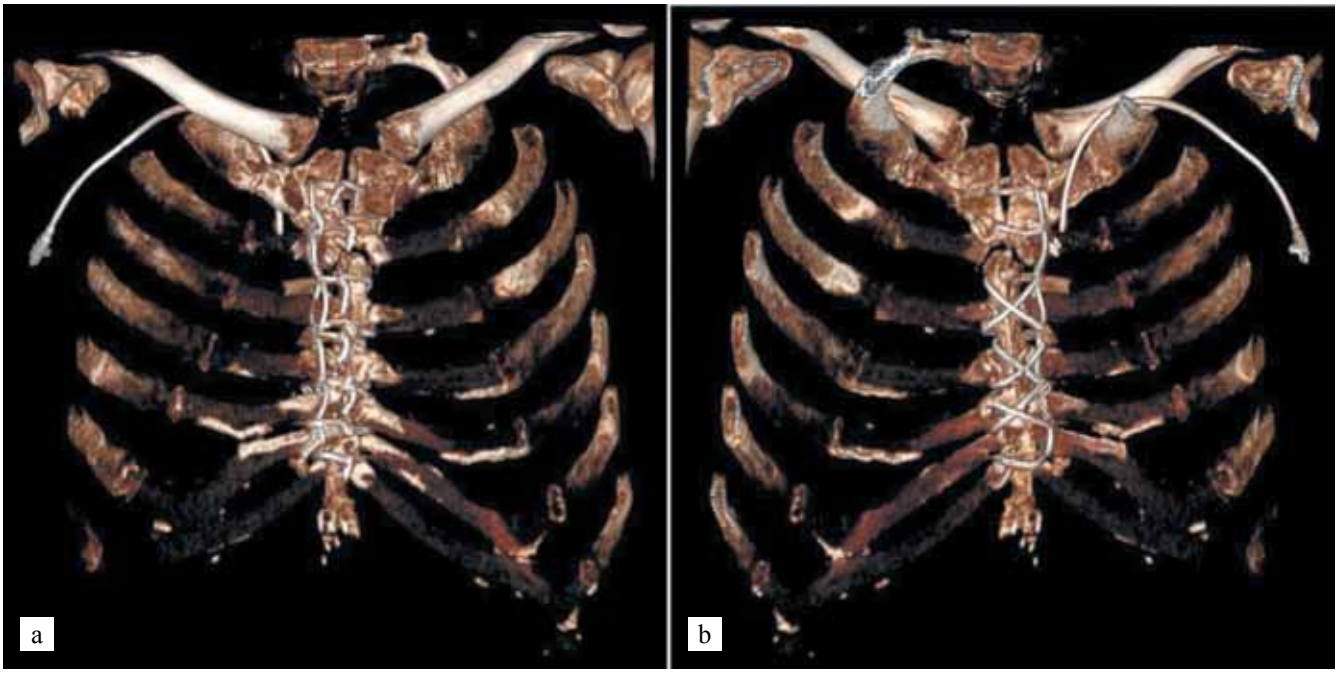

Fig. 9. Sternal reosteosynthesis by Robicsek technique: a) along the front and b) along the inner surfaces of the sternum. 3D reconstruction of CT scan

Fig. 10. Mobilization of wound edge as a fasciocutaneous flap using electrocoagulation

the anterior mediastinum and pleural cavities, and on day 18 after surgery, the inner rows of tension sutures and skin sutures were removed (Fig. 13).

The patient was discharged on day 115 of hospitalization in a satisfactory condition, with no complaints, and with the wound completely healed under outpatient observation by a cardiologist and a surgeon.

CONCLUSION

Surgical complications in the form of deep wound infection after median sternotomy can lead to major consequences for patients, including death. The risks of adverse outcomes are particularly high in patients with a high degree of cardiac cachexia, which are mostly recipients awaiting heart transplantation. In the first months after transplantation, immunosuppressive therapy is the most aggressive, which greatly reduces the body's immune response and reparative capacity. In such a situation, the success of treatment of severe infected wounds threatening the development of generalized infection largely depends on the experience and capabilities of a large team of different specialists. The use of standard methods of treating deep sternal wound infection used in thoracic practice cannot be a universal method for this cohort of patients.

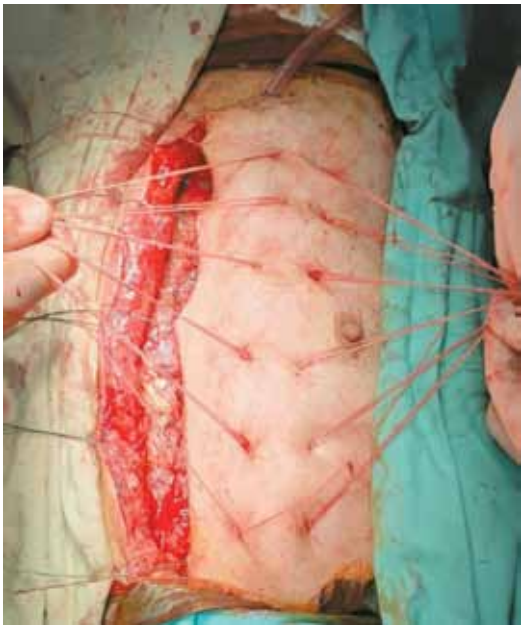

Fig. 11. Displacement of the mobilized full-thickness integumentary tissues of the anterior chest wall into the wound defect using deep U-shaped (flat-topped) sutures

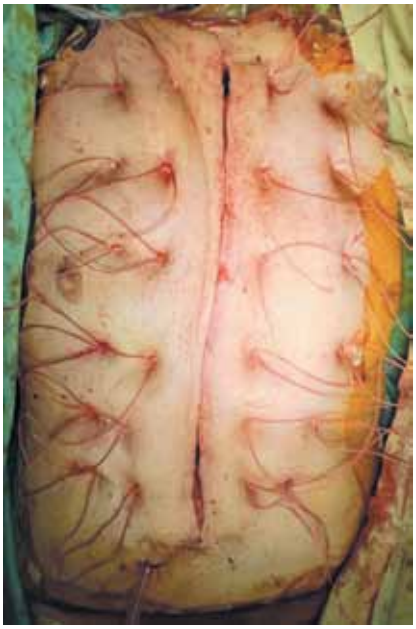

Fig. 12. Replacement of wound defect with local tissues

Fig. 13. View of the anterior chest wall on day 18 after reconstructive surgery. Wound healing by primary intention

The combined approach to surgical treatment of deep sternal wound infection in a heart recipient developed by us, combining such methods as surgical treatment of a purulent-necrotic focus, use of vacuum aspiration with scheduled dressings and replacements of the vacuum aspiration system, transition to "open" management of postoperative wound without vacuum aspiration, with daily dressings, selection of antibiotic therapy based on the obtained cultures, transition to single-component immunosuppression and reduction of serum tacrolimus levels to minimal therapeutic values, staged approach to surgical treatment (serial debridement of the postoperative wound and use of a vacuum aspiration system in the first stage and with subsequent osteosynthesis and soft tissue plasty of the anterior chest wall with displaced fasciocutaneous flaps), allows to successfully handle deep sternal wound infection in heart recipients under immunosuppression.

The authors declare no conflict of interest.

REFERENCES

1. *Vestergaard RF.* Effect of Hemostatic Material on Sternal Healing After Cardiac Surgery. *The Annals of thoracic surgery*. 2014; 97 (1): 153–160.
2. *Rehman SM.* Risk factors for mediastinitis following cardiac surgery: the importance of managing obesity. *Journal of Hospital Infection*. 2014; 88 (2): 96–102.
3. *Risnes I, Abdelnoor M, Almdahl SM, Svennevig JL.* Mediastinitis after coronary artery bypass grafting risk factors and long-term survival. *Ann Thorac Surg*. 2010; 89: 1502–1509.
4. *Tang GHL, Maganti M, Weisel RD, Borger MA*. Prevention and management of deep sternal wound infection. *Semin Thorac Cardiovasc Surg*. 2004; 16: 62–69.
5. *Sa MP, Soares EF, Santos CA.* Risk factors for mediastinitis after coronary artery bypass grafting surgery. *Rev Bras Cir Cardiovasc*. 2011; 26: 27–35.
6. *Diez C, Koch D, Kuss O*. Risk factors for mediastinitis after cardiac surgery – a retrospective analysis of 1700 patients. *J Cardiothorac Surg*. 2007; 2: 23.
7. *Ye X.* Incidence and costs of bleeding-related complications in French hospitals following surgery for various diagnoses. *BMC health services research*. 2013; 13 (1): 186.
8. *Ariyaratnam P, Bland M, Loubani M.* Risk factors and mortality associated with deep sternal wound infections following coronary bypass surgery with or without concomitant procedures in a UK population: a basis for a new risk model? *Interact Cardiovasc Thorac Surg*. 2010; 11: 543–546.
9. *Kunal S.* Mediastinitis in cardiac surgery: A review of the literature. *International Journal of Medicine and Biomedical Research*. 2013; 1 (2): 97–103.
10. *Gautier SV, Khomyakov SM.* Donorstvo i transplantatsiya organov v Rossiyskoy Federatsii v 2015 godu. VIII soobshchenie registra Rossiyskogo transplantologicheskogo obshchestva. Transplantologiya: itogi i perspektivy. Tom VII. 2015 god / Pod red. S.V. Gautier. M.–Tver': Triada, 2016. 448.
11. *Abboud CS, Wey SB, Baltar VT.* Risk factors for mediastinitis after cardiac surgery. *Ann Thorac Surg*. 2004; 77 (2): 676–683.
12. *Ku CH, Ku SL, Yin JC.* Risk factors for sternal and leg surgical site infections after cardiac surgery in Taiwan. *Am J Epidemiol*. 2005; 161: 661–671.
13. *Mitish VA, Zakharevich VM, Merzlyakov VYu, Popov VA, Skopin AI.* Aktivnoe khirurgicheskoe lechenie posleoperatsionnogo osteomielita grudiny i reber posle koronarnykh i kardiokhirurgicheskikh operatsiy. *Byulleten' NTsSSKh A.N. Bakuleva RAMN. Serdechno-sosudistye zabolevaniya*. 2005; 6 (S5): 77.
14. *Mitish VA, Usu-Vuyyu OYu, Paskhalova YuS, Ushakov AA, Zvyagin AA, Orudzheva SA, Zhestkov MS.* Opyt khirurgicheskogo lecheniya khronicheskogo posleoperatsionnogo osteomielita grudiny i reber posle mini-invazivnoy revaskulyarizatsii miokarda. *Rany i ranevye infektsii*. 2015; 2 (2): 46–57.
15. *Mitish VA, Usu-Vuyyu OYu, Paskhalova YuS, Ushakov AA, Magomedova SD, Baltun LA i dr.* Opyt khirurgicheskogo lecheniya patsientov vysokogo riska vsledstvie khronicheskogo posleoperatsionnogo osteomielita grudiny i reber. *Rany i ranevye infektsii*. 2017; 4 (3): 14–22.

The article was submitted to the journal on 11.03.2021

DOI: 10.15825/1995-1191-2021-2-76-83

NON-ALCOHOLIC WERNICKE'S ENCEPHALOPATHY IN A KIDNEY TRANSPLANT RECIPIENT

R.O. Kantariya, O.N. Vetchinnikova, A.V. Vatazin, L.A. Sherman

Vladimirsky Moscow Regional Research Clinical Institute, Moscow, Russian Federation

Background. Non-alcoholic Wernicke's encephalopathy occurs in various somatic conditions with thiamine deficiency, excessive excretion of thiamine, or impaired thiamine metabolism. Very few cases of this pathology have been described in chronic kidney disease (CKD). We present a unique case of non-alcoholic Wernicke's encephalopathy in a patient with a kidney transplant is presented. **Past medical history.** The patient underwent kidney transplantation in 2008. Outpatient follow-up by a nephrologist was irregular. Renal graft function remained relatively stable: blood creatinine 200–240 μmol/L, estimated glomerular filtration rate 40–30 mL/min, tacrolimus plasma concentrations tended to increase (5.7–7.6–8.4–10.4 ng/mL); repeated graft biopsy (in 2015 and in 2017) determined the chronic toxicity of calcineurin inhibitors. The patient's condition worsened in late January 2020: body temperature increased to 38°C, nausea, vomiting, loose, watery stools for up to 5 times per day, 8 kg weight loss, decreased diuresis. A few days later, double vision, shaky gait and then immobility appeared. Biochemical examination results: potassium 3.8 mmol/L, sodium 139 mmol/L, alpha-amylase 159 units/L (norm 0–100 units/L), creatinine 242 mmol/L, urea 13.2 mmol/L; ultrasound signs of pancreatitis. Magnetic resonance imaging (MRI) of the brain: bilateral diffuse lesions of the midbrain, thalamus, and cerebellum. Based on the clinical picture and on brain MRI results, Wernicke's encephalopathy was diagnosed. Parenteral administration of thiamine had a good effect. **Conclusion.** Possible mechanisms of the development of Wernicke's encephalopathy in a patient were discussed. Vigilance is required regarding this disease when metabolic disorders occur in patients with CKD.

Keywords: Wernicke's encephalopathy, kidney transplantation, pancreatitis, thiamine.

Wernicke's encephalopathy is a rare severe degenerative brain damage first described by German psychiatrist Carl Wernicke in 1881 as acute superior haemorrhagic polio-encephalitis in two men suffering from alcoholism and a woman with pyloric stenosis [1]. Thiamine (vitamin B1) deficiency underlies the disease, but this association became known much later than the first observations described by C. Wernick in the middle of the last century [2]. Thiamine is a water-soluble vitamin that is not synthesized in the body; its daily requirement depends on carbohydrate intake – 1–2 mg for a healthy person. Total thiamine reserves in the body are relatively small – 30–50 mg – and are completely depleted after 4–6 weeks in the absence of thiamine intake. Thiamine is required by cell membranes to maintain osmotic gradient, and is involved in glucose metabolism and neurotransmitter synthesis. Vitamin deficiency can be twofold: exogenous (due to insufficient intake from food) and endogenous (due to impaired absorption of the vitamin in the gastrointestinal tract or its increased excretion). Another possible mechanism for the onset of Wernicke's encephalopathy is the inhibition of thiamine conversion into thiamine pyrophosphate – the active part of alpha-ketoglutarate dehydrogenase, pyruvate dehydrogenase and transketolase – enzymes that ensure normal metabolism of nervous tissue. Therefore, in case of thiamine reduction in the body, the most pronounced changes occur in the brain, where the activity of oxidative metabolism is very high: lack of energy leads to reduced glucose utilization by neurons and damage in their mitochondria [2].

The exact prevalence of the disease is unknown; diagnosis is often established only at autopsy. In general, the incidence of Wernicke's encephalopathy is estimated at 0.4–2.8%, with a lower incidence of 0.04–0.13% for that of non-alcoholic origin [3]. The most common cause of Wernicke's encephalopathy is alcoholism. Non-alcoholic Wernicke encephalopathy occurs in many clinical situations, most often associated with malnutrition or acute metabolic stress. In particular, thiamine deficiency can be experienced by patients suffering from cancer, sepsis, those undergoing surgical procedures, etc. [3, 4]. Despite the indicated rarity of this condition, only in the last few years a large number of clinical observations of Wernicke's encephalopathy in patients not abusing alcohol have been described: with gastrointestinal disorders of various origins (surgery, cancer, pregnancy, etc.), fasting or strict dietary restrictions (strict adherence to fasting), malnutrition, anorexia nervosa, brain injury, encephalitis with lesions of the basal nuclei and temporal lobes, and carbon monoxide poisoning [5–13]. It is of interest to observe Wernicke's encephalopathy in patients

Corresponding author: Olga Vetchinnikova. Address: 61/2, Schepkina str., Moscow, 129110, Russian Federation. Phone: 8 (495) 684-57-81. E-mail: olg-vetchinnikova@yandex.ru

who underwent liver, bone marrow, hematopoietic stem cell transplantation [14–16]. At the same time, according to PubMed search engine results, Wernicke's encephalopathy is rarely described in chronic kidney disease (CKD), although this disease is characterized by a wide variety of metabolic disorders. We have encountered only a small series of observations in patients receiving dialysis therapy [17–21]. We present a unique case of non-alcoholic Wernicke encephalopathy, which developed against the background of metabolic disorders in a patient with a kidney transplant. This is the first report of its kind; we have not found any such description in any other available published report.

***Patient N.**, born in 1988, from a distant Moscow suburb, has been observed at the kidney transplantation ward of Vladimirsky Moscow Regional Research Clinical Institute in Moscow since 2007. The patient considers himself sick since 2006, when his blood pressure increased to 250/160 mm Hg and he developed peripheral edema (lower extremities). Examination revealed increased blood creatinine levels to 300 μmoL/l (estimated glomerular filtration rate (eGFR) 25 mL/min). Chronic glomerulonephritis was diagnosed (without histological confirmation), stage 4 CKD, nephroprotective and symptomatic therapy was administered. In August 2007, due to the development of end-stage chronic renal failure, long-term hemodialysis therapy was initiated. A year later (November 6, 2008), cadaveric kidney transplantation was performed, immunosuppressive therapy was conducted according to the standard protocol: basiliximab 40 mg, metipred 1000 mg, prednisolone 30 mg/day, tacrolimus at 0.2 mg/kg/day starting dose until the target concentration was reached and mycophenolic acid 1440 mg/day. Graft function was delayed; 3 hemodialysis sessions were performed. Diuresis was restored in a week with a gradual decrease in azotemia levels (Table 1). Ultrasound examination of the kidney transplant was unremarkable. The patient was discharged a month later in a satisfactory condition, with stable graft function.*

The patient was readmitted 1.5 months later due to deterioration of the condition: loss of appetite, diffuse abdominal pain, vomiting, persistent diarrhea, low-grade fever. On admission, the patient's condition was moderate, body temperature 37.6 °C, dry skin, and visible mucous membrane. Respiratory rate was 22/min, with no peculiarities on lung auscultation. BP 85/55 mm Hg, pulse 120/min, low-filled. The abdomen was moderately swollen, painful on palpation in the epigastric region. There were no acute abdominal symptoms. Renal graft in the left iliac region, elastic, painless. Diuresis 1000 mL/day. Complete blood count: hemoglobin 10^9 g/L, white blood cells 1.3 × 10^9/L, neutrophils 0.5 × 10^9/L, platelets 95 × 10^9/L. Hematologist's conclusion: grade 4 neutropenia. Blood electrolytes: sodium 137 mmol/L, potassium 3.4 mmol/L, calcium, phosphorus within normal range. Total bilirubin, liver enzymes, alkaline phosphatase, glucose, and blood lipids were within the reference values. Serum amylase level was 257 U/L (normal 0–100), blood creatinine and urea were respectively 600 μmol/L, and 34 mmol/L. Bacteriological examination of stool: Candida pp 10^6, E. coli 10^9, Ps. vulgaris 10^6 CFU/ml. The test result for cytomegalovirus, Epstein–Barr virus, hepatitis was negative. Ultrasound examination of the renal graft was unremarkable, abdominal organs – signs of acute pancreatitis. The patient was examined by a gastroenterologist with the following diagnosis: acute pancreatitis, intestinal dysbiosis. In general, the patient's clinical and laboratory symptoms were consistent with acute pancreatitis, acute graft injury, and grade 4 neutropenia. The therapy administered included intravenous infusion of saline, antibiotics, including antifungal and antiviral, a proton pump inhibitor, antispasmodic drugs, and a prebiotic. Mycophenolic acid was canceled, granulocyte colony-stimulating factor (filgrastim) was prescribed, methylprednisolone in a total dose of 1000 mg was administered. A few days later, the patient's condition improved: body temperature returned to normal, vomiting stopped, stool normalized, abdominal pain regressed, blood pressure 115/85 mm Hg, daily urine output increased to 2.5 L, blood creatinine and urea levels decreased to 330 μmol/L and 26 mmol/L, respectively, with a further decrease, white blood cells 5.0 × 10^9/L, platelets 167 × 10^9/L. A week later, renal graft biopsy was performed with the following conclusion: the histological picture

Table 1

Results of laboratory examination of patient N. in the early postoperative period after kidney transplantation

Indicator	Kidney transplantation, Nov. 6, 2008		
	Nov. 13, 2008	Nov. 21, 2008	Dec. 2, 2008
Diuresis, mL/day	2000	3600	3400
Creatinine, μmol/L	790	390	180
Urea, mmol/L	27	30	20
Hemoglobin, g/L	100	96	101
Bilirubin, μmol/L	4.0	7.8	9.7
AST, units/L	21	12	10
ALT, units/L	40	18	9
Alkaline phosphatase, u/L	60	61	70
Albumin, g/L	43	40	36
Cholesterol, mmol/L	3.1	3.7	3.3
Uric acid, μmol/L	327	595	443
Glucose, mmol/L	4.0	5.2	4.9
Calcium, mmol/L	2.2	2.1	2.1
Phosphorus, mmol/L	2.8	2.1	1.1
Daily proteinuria, g	2.6	0.87	0.43
Tacrolimus serum concentration, ng/mL	7.2	8.6	10.3

is consistent with acute tubular necrosis of the donor organ. A month later, the patient was discharged in satisfactory condition with normal peripheral blood and biochemical parameters, with satisfactory graft function (blood creatinine 180 μmol/L, blood urea 9.3 mmol/L).

There was outpatient follow-up at the consultative and diagnostic center of Vladimirsky Moscow Regional Research Clinical Institute 1–3 times a year (Table 2). Tacrolimus dose was adjusted taking into account its serum concentration, which tended to increase; graft function remained relatively stable. In the fall of 2014, the patient independently stopped taking prednisolone, after which he developed peripheral edema (lower extremities), his blood pressure increased to 180/110 mm Hg; During examination, daily proteinuria was 2 g. In October 2015, a repeated biopsy of the renal graft was performed with the following conclusion: chronic graft nephropathy stage 1, chronic calcineurin inhibitor toxicity. The patient resumed taking prednisolone, tacrolimus dose was adjusted, and an angiotensin-converting enzyme inhibitor was prescribed. His condition stabilized, peripheral edema disappeared, blood pressure returned to normal 125–130/80 mmHg, proteinuria decreased to 1.2 g/day.

In July 2017, with increasing proteinuria, a third nephrobiopsy was performed with the following conclusion: chronic calcineurin inhibitor nephrotoxicity with diffuse global nephrosclerosis, chronic graft nephropathy stage 2.

Sudden deterioration at the end of January of the current year: body temperature increased to 38 °C, nausea, vomiting, loose, watery stools up to 5 times a day, up to 8 kg weight loss, decreased urine output. A few days later, double vision, shaky gait, then immobility appeared; the patient was admitted to an infectious diseases clinic at his place of residence. No evidence of acute infectious pathology was obtained. Complete blood count: hemoglobin 121 g/L, white blood cells 6.6 × 10^9/L, platelets 324 × 10^9/L; biochemical blood test: potassium 3.8 mmol/L, sodium 139 mmol/L, liver enzymes within normal values, creatinine 242 mmol/L, urea 13.2 mmol/L. Ultrasound examination of the abdominal organs and kidney transplant was unremarkable, except for the pancreas, which showed ultrasound signs of pancreatitis: the gland was enlarged, with indistinct contours, increased echogenicity and heterogeneous (blurred) structure. An increase in neurological symptoms was recorded, brain MRI was performed with the following conclusion: central pontine myelinolysis. The condition was regarded as a secondary autoimmune process, methylprednisolone pulse therapy methylprednisolone in a total dose of 3000 mg was administered. Simultaneously, symptomatic, neuroprotective, antibacterial therapy was administered. However, the patient's condition continued to deteriorate: he stopped swallowing solid food, hyperkinetic disorders appeared. The patient was transferred to the intensive care unit of Vladimirsky Moscow Regional Research Clinical Institute.

On admission, his condition was serious. He was conscious with a normosthenic physique. Reduced nutrition. His skin and mucous membranes were moist, pale pink. Vesicular breathing, no wheezing, respiratory rate 17 per minute. Muffled heart sounds, rhythmic. BP 150/80 mm Hg. Heart rate 90 beats/min, satisfactory filling. Moist tongue, coated with white plaque. Soft abdomen, painless on palpation. The liver was not enlarged. Peristalsis was audible. The graft was palpable in the left iliac region, elastic, and painless. Unassisted urination. Diuresis 1200 mL/day. Laboratory results are presented in Table 3.

Neurological status. The patient was conscious, on a Glasgow Coma Scale score of 15. Productive contact was difficult due to speech disorders. Speech with gross dysarthria. Nasal tone of voice (nasolalia). No meningeal signs. Correctly oriented, lethargic, apathetic, drowsy. Obeys simple commands. Emotionally labile, quickly exhausted. Hearing was not impaired. D = S eye slits, bilateral partial ptosis. Did not follow the hammerhead.

Table 2

Results of laboratory examination of patient N. at the outpatient follow-up stage

Parameter	Date of examination at the Consultative and Diagnostic Center, Vladimirsky Moscow Regional Research Clinical Institute										
	Aug. 27, 2009	Aug. 2, 2010	May 19, 2011	Nov. 29, 2012	Nov. 28, 2013	Nov. 20, 2014	Oct. 29, 2015	Nov. 24, 2016	July 24, 2017	Nov. 28, 2018	Aug. 5, 2019
Diuresis, mL/day	1700	–	1800	1900	1800	1800	2100	2300	2200	–	1800
Blood creatinine, μmol/L	210	220	190	180	240	210	180	206	210	270	240
eGFR, mL/min	38	36	42	44	31	37	43	36	35	26	30
Blood urea, mmol/L	9.2	11.1	9.7	10.5	11.6	12.1	12.4	10.8	9.2	18.2	17.8
Proteinuria, g/day	1.6	–	0.6	1.2	0.5	1.8	1.2	0.6	1.1	–	0.4
Tacrolimus serum concentration, ng/mL	6.4	6.5	8.4	4.9	5.4	6.6	7.6	8.5	7.3	7.6	6.5

Rounded pupils, D < S. Photoreactions: direct and concomitant, OD = OS = lively. Face was symmetrical, tongue along the midline. Pharyngeal reflex depressed, choking when swallowing. Raising the shoulders and turning the head were not impaired. Motor functions: amount of active and passive movement was not limited. Strength of arm muscles D = S = 5 points, legs D = S = 5 points. Tone in the extremities is physiological. Tendon and periosteal reflexes: from the hands D = S, lowered; knee D = S, lowered; Achilles D = S, lowered. No pathological foot marks. Coordination of movements: fingers – a nasal test was performed with pronounced coarse tremor and past-pointing, more on the left. No sensitive impairments.

A differential diagnosis between central pontine myelinolysis and Wernicke's encephalopathy was made. The absence of hyponatremia and hypoosmolarity in the patient throughout the disease, as well as the effect of methylprednisolone pulse therapy (3000 mg in total) made the diagnosis of central pontine myelinolysis and the autoimmune nature of this condition doubtful. Repeated brain MRI was performed: no volumetric masses were detected in the brain substance. In the midbrain, in the dorsal thalamus, in the superior cerebellar peduncle and paraventricularly around the fourth ventricle, as well as in the vermis and the anterior lobe of both cerebellar hemispheres, almost symmetrically, a pathological MR signal area – hyperintense MR signal on T2-weighted images, isointensive – on T1-weighted images, without volumetric effects on adjacent brain structures – was visualized. Diffusion-weighted imaging showed diffusion restriction from 2 symmetrically located foci in the midbrain due to edema. In the white matter of the cerebral hemispheres, multiple different-sized foci of the altered MR signal with fairly clear contours, up to 8 mm in maximum dimension, with a tendency for fusion of 2 lateral ventricles in the leuoaraiosis zone were detected. There was no dislocation of midline structures. All cerebrospinal fluid (CSF) pathways – basal cisterns, cerebral ventricles and external subarachnoid space along the cerebral hemispheres and cerebellum – were not dilated. The pituitary gland was not enlarged. The craniovertebral junction is correctly formed, the cerebellar tonsils were at the level of the foramen magnum plane. The paranasal sinuses were airy. The orbits were without pathological changes. Conclusion: MRI signs of Wernicke's encephalopathy: bilateral diffuse lesion of the midbrain, thalamus and cerebellum without volumetric effect on adjacent brain structures; focal white matter lesion is probably a manifestation of metabolic encephalopathy (Fig.).

Based on clinical symptoms, the presence of oculomotor disorders, ataxia, changes in mental status and characteristic MRI signs of brain injury, as well as given the onset of the disease, corresponding to a severe exacerbation of chronic pancreatitis, the patient was diagnosed with neurological Wernicke's encephalopathy. Treatment was prescribed according to the guidelines of the European Federation of Neurological Societies [22]: intramuscular thiamine hydrochloride 300 mg/day (10 days), 200 mg/day (10 days), 100 mg/day for 1 month, then oral benfotiamine 150 mg/day for 1 month; thioctic acid 600 mg/day, intravenous drip, followed by a switch to oral administration for 1 month; intramuscular pyridoxine hydrochloride 100 mg/day (10 days), intramuscular cyanocobalamin 1000 mcg/day (10 days).

The patient's condition improved against the background of the therapy, he became more active, his vision began to recover, and his speech improved. To continue treatment, the patient was transferred to a neurological hospital at the place of his residence. Six months later, he was examined at the consultative and diagnostic center of Vladimirsky Moscow Regional Research Clinical Institute with the following conclusions: satisfactory condition, neurological status without pathological changes, graft function remained reduced and stable: blood urea 14.1 mmol/L, blood creatinine 239 mmol/L, eGFR 30 mL/min, daily proteinuria 1.3 g, tacrolimus plasma concentration 6.6 ng/mL.

Table 3

Results of laboratory examination of patient N. at the last hospitalization

Indicator	At admission	At discharge
Content in the blood		
Creatinine, μmol/L	241	205
eGFR, ml/min	30	37
Urea, mmol/L	23.7	22.3
Tacrolimus, ng/ml	8.6	4.9
Alpha-amylase (norm 0–100 U/L)	153	69
Hemoglobin, g/L	119	126
Bilirubin, μmol/L	15.1	9.8
AST, units/L	22	17
ALT, units/L	12	12
Alkaline phosphatase, u/L	177 (norm 0–258 units/L)	68 (norm 30–120 units/L)
Albumin, g/L	41	45
Cholesterol, mmol/L	4.0	4.1
Osmolarity, mosmol/L	291	282
Sodium, mmol/L	141	138
Potassium, mmol/L	3.3	4.3
Ionized calcium, mmol/L	1.14	1.17
Phosphorus, mmol/L	1.62	1.2
Procalcitonin, ng/mL (norm 0–0.1)	0.2	–
Diuresis, mL/day	1200	2300
Daily proteinuria, g	1.5	1.1

DISCUSSION

So, our patient was diagnosed with Wernicke's encephalopathy, a severe brain injury caused by thiamine deficiency, in the long-term (after 11 years) post-transplant period. It is known that the latter occurs not only with chronic alcoholism, which our patient does not suffer from, but also with a number of other somatic diseases. In this case, the leading risk factor for Wernicke's encephalopathy was most likely acute exacerbation of chronic pancreatitis, as indicated by his increased serum amylase levels and pancreas ultrasound examination findings. Anorexia, repeated vomiting, and diarrhea caused by pancreatitis caused insufficient intake, excessive excretion of thiamine and its depletion in the body. There has been a reported case of non-alcoholic Wernicke encephalopathy in pancreatitis complicated by severe metabolic disorders [23]. In turn, the appearance of pancreatitis and gastroenterological disorders in our patient could be associated with tacrolimus toxicity. It is reported that up to 75% of patients taking this calcineurin inhibitor have some type of gastrointestinal issues [24]. In our patient, chronic calcineurin inhibitor toxicity had a long history and was confirmed by repeat renal graft biopsy. The patient's low compliance, possibly due to his youth and/or a far-away place of residence, made his dynamic examination and follow-up by a nephrologist irregular. Another mechanism of thiamine deficiency in our patient can be assumed to be a disorder in its phosphorylation,

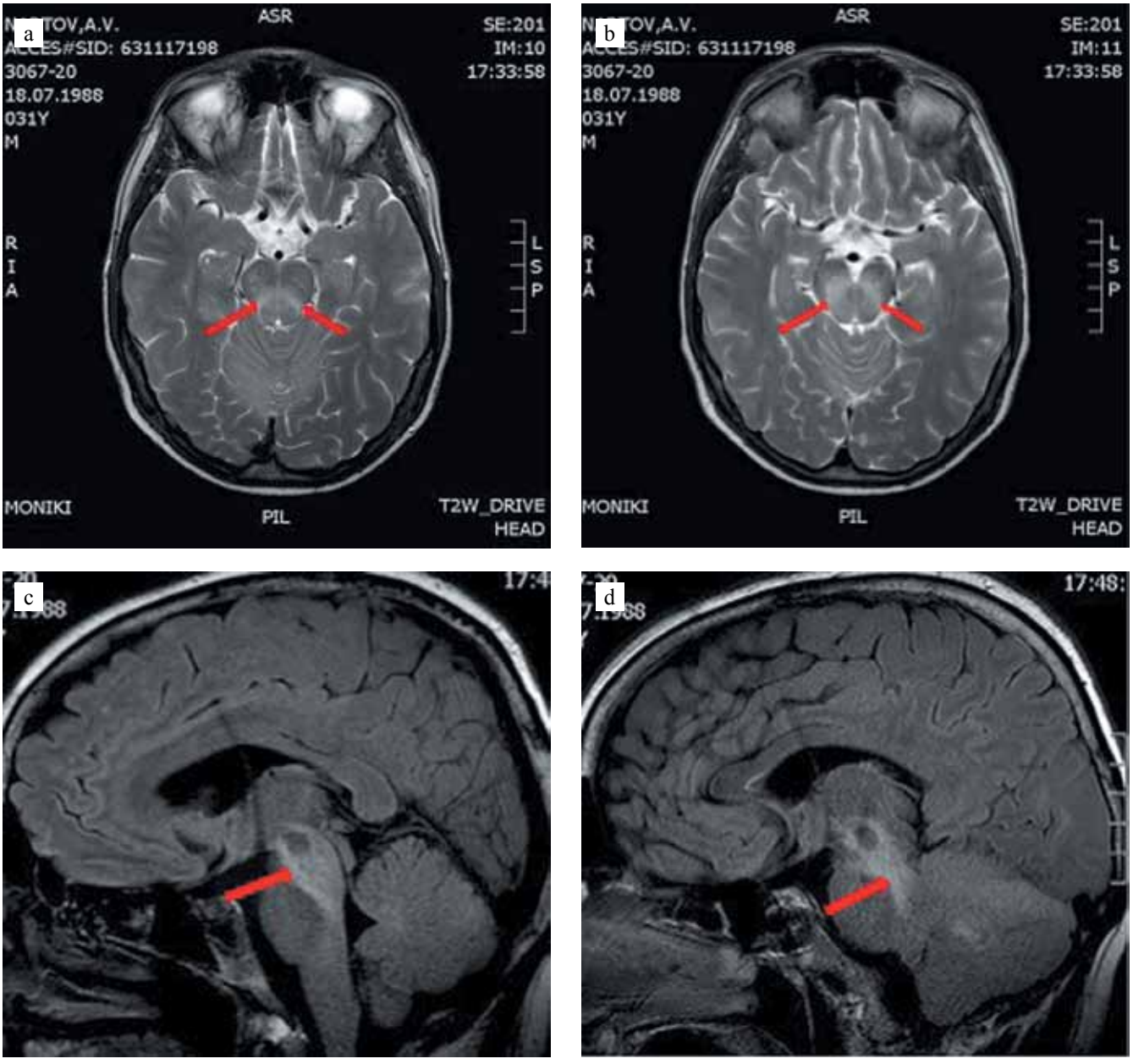

Fig. Non-contrast-enhanced magnetic resonance imaging of the brain of patient N.: a, b. T2-weighted (axial) images of the brain; c, d. diffusely weighted (sagittal) images of the brain. Symmetrical enhancement of the MR signal from the midbrain and thalamus (shown by arrows)

which occurs with the participation of magnesium [25, 26]. Decreased serum magnesium levels associated with inhibition of its tubular reabsorption under the influence of calcineurin inhibitors is more common in the early postoperative period but is also possible in the long term [27]. However, measuring the serum magnesium levels is not a routine biochemical test and has not been performed in this case.

Wernicke's encephalopathy in non-alcoholic patients has mainly complex clinical manifestations and atypical development of the disease [3, 5, 10, 11]. Our patient turned out to be an exception in this respect. In him, Wernicke encephalopathy manifested itself by the classical triad described by the author: oculomotor disorders, ataxia, and mental disorders, although this triad occurs in a third or half of patients [1, 3, 11]. It was the classical clinical symptoms, as well as the absence of hyponatremia episodes during the course of the disease, that served as the basis for diagnosis of Wernicke's encephalopathy and exclusion of central pontine myelinolysis. The diagnosis is usually verified by neuroimaging – brain MRI reveals a symmetrical medial thalamic lesion, which occurred in the patient we observed [5, 11]. Finally, the rapid response to parenteral thiamine administration provided additional supporting evidence in favor of Wernicke's encephalopathy.

If the timeliness of the diagnosis of Wernicke's encephalopathy is based on clinicians' awareness, alertness and familiarity with the predisposing factors and clinical symptoms of the disease, its prognosis depends on the earliest possible initiation of pathogenetic therapy, i.e. adequate thiamine administration. Delaying treatment or not initiating it at all can lead to Korsakoff's psychosis or even death [3, 5]. An important point of this observation was the correct diagnosis of Wernicke's encephalopathy and the immediate administration of thiamine, which led to a good outcome – complete disappearance of neurological symptoms in the patient.

CONCLUSION

This clinical case is the first description of Wernicke's encephalopathy in a kidney recipient. It indicates the complexity of diagnosis and the difficulty of differential diagnosis of this condition with central pontine myelinolysis, as well as the curability of this disease with the right management tactics. This case highlights the importance of being vigilant for Wernicke's encephalopathy in situations involving significant metabolic disorders that are common in CKD. Timely diagnosis and proper treatment will improve the prognosis.

The authors declare no conflict of interest.

ЛИТЕРАТУРА/REFERENCES

1. *Wernicke C.* Die akute hämorrhagische polioencephalitis superior. Fischer Verlag, Kassel. Lehrbuch der Gehirnkrankheiten für Ärzte und Studierende 1881; II: 229–242.
2. *Campbell ACP, Russell WR*. Wernicke's encephalopathy: the clinical features and their probable relationship to vitamin B deficiency. *Q J Med*. 1941; 10: 41–64.
3. *Ota Y, Capizzano AA, Moritani T, Naganawa S, Kurokawa R, Srinivasan A*. Comprehensive review of Wernicke encephalopathy: Pathophysiology, clinical symptoms and imaging findings. *Jpn J Radiol*. 2020 Sep; 38 (9): 809–820. doi: 10.1007/s11604-020-00989-3.
4. *Chamorro AJ, Rosón-Hernández B, Medina-García J-A, Muga-Bustamante R, Fernández-Solá J, Martín-González MC et al*. Differences between alcoholic and nonalcoholic patients with Wernicke encephalopathy: A multicenter observational study. *Mayo Clin Proc*. 2017; 92 (6): 899–907. doi: 10.1016/j.mayocp.2017.02.019.
5. *Semple D, Smyth R*. Oxford handbook of psychiatry. Oxford: Oxford University Press; 2013. 1057 p. doi: 10.1093/med/9780199693887.001.0001
6. *Doğan İG, Altiokka GU, Türker F, Saka B, Bilgiç B, Orhan EK*. Wernicke's encephalopathy due to non-alcoholic gastrointestinal tract disease. *Noro Psikiyatr Ars*. 2018; 55 (4): 307–314. doi: 10.29399/npa.23010.
7. *Mantero V, Rifino N, Costantino G, Farina A, Pozzetti U, Sciacco M et al*. Non-alcoholic Beriberi, Wernicke encephalopathy and long-term eating disorder: Case report and a mini-review. *Eat Weight Disord*. 2021 Mar; 26 (2): 729–732. doi: 10.1007/s40519-020-00880-0. Epub 2020 Mar 4.
8. *Oudman E, Wijnia JW, Oey M, van Dam M, Painter RC, Postma A*. Wernicke's encephalopathy in hyperemesis gravidarum: A systematic review. *Eur J Obstet Gynecol Reprod Biol*. 2019; 236: 84–93. doi: 10.1016/j.ejogrb.2019.03.006.
9. *Oudman E, Wijnia JW, Oey MJ, van Dam MJ, Postma A*. Preventing Wernicke's encephalopathy in anorexia nervosa: A systematic review. *Psychiatry Clin Neurosci*. 2018; 72 (10): 774–779. doi: 10.1111/pcn.12735.
10. *Yin H, Xu Q, Cao Y, Qi Y, Yu T, Lu W*. Nonalcoholic Wernicke's encephalopathy: A retrospective study of 17 Cases. *J Int Med Res*. 2019; 47 (10): 4886–4894. doi: 10.1177/0300060519870951.
11. *Liu Y-L, Xiao W-M, Liang M-Q, Wu Z-Q, Wang Y-Z, Qu J-F, Chen Y-K*. Clinical characteristics and magnetic resonance imaging findings in nine patients with nonalcoholic Wernicke's encephalopathy: A retrospective study. *Neuropsychiatr Dis Treat*. 2019; 15: 2433–2441. doi: 10.2147/NDT.S217237.
12. *Alizadeh L, Mostafavi Z, Jahanshahi A, Khani M, Nouri-Vaskeh M*. Wernicke encephalopathy following gastrojejunostomy: A case report and review of the literature. *Turk J Emerg Med*. 2019; 19 (4): 154–156. doi: 10.1016/j.tjem.2019.08.001
13. *Shah IA, Asimi RP, Kawoos Y, Wani M, Saleem T, Baba WN*. Nonalcoholic Wernicke's encephalopathy: A retrospective study from a tertiary care center in Northern India. *J Neurosci Rural Pract*. 2017; 8 (3): 401–406. doi: 10.4103/jnrp.jnrp_14_17.
14. *Xie B, Si Z-Z, Tang W-T, Qi H-Z, Li T*. Wernicke encephalopathy in a patient after liver transplantation: A Case re-

port. *World J Gastroenterol*. 2017; 23 (47): 8432–8436. doi: 10.3748/wjg.v23.i47.8432.
15. *Di Giuliano F, Picchi E, Scaggiante J, Ferrante P, Misciasci T, Da Ros V et al*. Posterior reversible encephalopathy syndrome and Wernicke encephalopathy in patient with acute graft-versus-host disease. *Radiol Case Rep*. 2019; 14 (8): 971–976. doi: 10.1016/j.radcr.2019.05.024.
16. *Xue S, Yuan L, Cheng H-Y, Yin Y-M, Gu J-Y, Zhang W-J, Wang J-B*. Four cases of Wernicke's encephalopathy following hematopoietic stem cell transplantation. *Zhongguo Shi Yan Xue Ye Xue Za Zhi*. 2018; 26 (3): 880–885. doi: 10.7534/j.issn.1009-2137.2018.03.042.
17. *Chen G, Chen LM, Li XM*. The 473rd case: Renal failure, abdominal pain, and mental abnormality. *Zhonghua Nei Ke Za Zhi*. 2020; 59 (1): 82–85. doi: 10.3760/cma.j.issn.0578-1426.2020.01.016.
18. *Ueda K, Takada D, Mii A, Tsuzuku Y, Saito SK, Kaneko T et al*. Severe thiamine deficiency resulted in Wernicke's encephalopathy in a chronic dialysis patient. *Clin Exp Nephrol*. 2006; 10: 290–293. doi: 10.1007/s10157-006-0440-9.
19. *Nakashima Y, Ito K, Nakashima H, Shirakawa A, Abe Y, Ogahara S et al*. Wernicke's encephalopathy that developed during the introduction period of peritoneal dialysis. *Intern Med*. 2013; 52: 2093–2097. doi: 10.2169/internalmedicine.52.9427.
20. *Kim CS, Bae EH, Ma SK, Kim SW*. The case seizure, ophthalmoplegia, and amnesia in a peritoneal dialysis patient. *Kidney Int*. 2016; 90 (6): 1389–1390. doi: 10.1016/j.kint.2016.06.015.
21. *Nishimura Y*. Wernicke's encephalopathy after cardiac surgery. *Asian Cardiovasc Thorac Ann*. 2018; 26 (4): 302–304. doi: 10.1177/0218492318772693.
22. *Galvin R, Bråthen G, Ivashynka A, Hillbom M, Tanasescu R, Leone MA*. EFNS guidelines for diagnosis, therapy and prevention of Wernicke encephalopathy. *Eur J Neurol*. 2010; 17 (12): 1408–1418. doi: 10.1111/j.1468-1331.2010.03153.x.
23. *Butt I, Ulloa N, Surapaneni BK, Kasmin F*. Refeeding syndrome and non-alcoholic Wernicke's encephalopathy in a middle-aged male initially presenting with gallstone pancreatitis: A clinical challenge. *Cureus*. 2019; 11 (7): e5156. doi: 10.7759/cureus.5156.
24. *Danovich GM*. Immunosupressivnye preparaty i protokoly dlya transplantatsii pochki. *Transplantatsiya pochki* / Per. s angl. pod red. Ya.G. Moysyuka. M.: GEOTAR-Media, 2014: 167–260.
25. *Sánchez-Larsen Á, Segura T, García-Muñozguren S, Peinado-Ródenas J, Zamarro J, Hernández-Fernández F*. Cerebral Vasospasm and Wernicke encephalopathy secondary to adult cyclic vomiting syndrome: The role of magnesium. *BMC Neurol*. 2016; 16 (1): 135. doi: 10.1186/s12883-016-0660-x.
26. *Coughlan JJ, Mross T, Wafer M, Liston R*. Thiamine refractory Wernickes encephalopathy reversed with magnesium therapy. *BMJ*. 2016. doi: 10.1136/bcr-2016-218046.
27. *Pochineni V, Rondon-Berrios H*. Electrolyte and acid-base disorders in renal transplant recipients. *Front Med*. 2018; 5: 261. doi 10.3389/fmed.201800261

The article was submitted to the journal on 3.11.2020

DOI: 10.15825/1995-1191-2021-2-84-87

RECONSTRUCTIVE PLASTIC SURGERY ON THE URINARY TRACT OF A KIDNEY TRANSPLANT

D.A. Saydulaev[1], V.S. Bogdanov[1], M.A. Petryaev[1], A.A. Kartashev[1], A.A. Zharikov[1], S.V. Sadovnikov[1], I.A. Miloserdov[1, 2]

[1] Shumakov National Medical Research Center of Transplantology and Artificial Organs, Moscow, Russian Federation

[2] Sechenov University, Moscow, Russian Federation

We present a clinical case of urolithiasis. A patient diagnosed with stage 5 chronic kidney disease due to autosomal dominant polycystic kidney disease after bilateral nephrectomy underwent kidney transplantation with ureteral graft stenting. Two months after the operation, a stone was found in the upper third of the ureteral graft, complicated by necrosis in this area. Reconstructive plastic surgery on the ureter of the transplanted kidney with removal of the ureteral stone achieved the desired clinical effect.

Keywords: urolithiasis, ureteroureteral anastomosis, kidney transplantation, urology.

INTRODUCTION

The main long-term urological complications after kidney transplantation include ureteral strictures (3–12.6%) and development of vesicoureteral reflux into the renal graft (5–20%) [1–3]. Urolithiasis in kidney transplantation is a rare urological complication, occurring at a rate of less than 1% [4], often not diagnosed on time due to renal denervation.

Despite the increasing possibilities of percutaneous correction of obstructions, there remains a certain category of patients requiring open surgical intervention. The indications for surgery are narrowing of the lumen over a significant area, complete ureteral obliteration or technical impossibility of performing percutaneous elimination of obstructions to urine outflow. In a number of patients, endoscopic methods and open surgical intervention fail to restore an adequate urine passage from the graft. Such patients have to live with nephrostomy drainage, which can often lead to recurrent pyelonephritis and premature loss of graft function as well as social maladjustment.

In the post-transplant period with obstructive uropathy, in case of ineffective drainage of the kidney followed by antegrade/retrograde bougienage and stenting of the graft ureter, reconstructive surgical interventions on the urinary tract of the transplanted kidney by open or laparoscopic methods are used [5–7]. Given the incidence and severity of urological complications in kidney transplant recipients, various methods of prevention and correction of urological complications are currently being developed both at the stage of preparing the end-stage chronic kidney disease patient for surgery and in the post-transplantation period [8].

RECIPIENT BASELINE DATA

***Male patient T.**, born in 1975 with episodes of increased blood pressure, was admitted at the clinic in 1991 with urolithiasis, kidney stones. Examination revealed multiple renal cysts, diagnosed as autosomal dominant polycystic kidney disease. Later, there were exacerbations of chronic pyelonephritis, gradual increase in renal insufficiency. In 2002, he was diagnosed with end-stage chronic kidney disease. Renal replacement therapy with long-term hemodialysis was initiated.*

In August 2019, laparoscopic bilateral nephrectomy was performed due to recurrent chronic pyelonephritis. The patient is on the waiting list for a deceased-donor kidney transplant.

TRANSPLANTATION AND EARLY POSTOPERATIVE PERIOD

In August 2020, a left kidney transplant was performed from a deceased donor to the right iliac region with graft ureteral stenting. He received tacrolimus, everolimus, and methylprednisolone as immunosuppressive therapy. Delayed graft function was noted in the postoperative period. Oliguria persisted for a long time, the level of azotemia decreased extremely slowly. Percutaneous needle biopsy of the graft showed that the causes of graft dysfunction were acute tubular necrosis, 50% nephrosclerosis. On day 23 after transplantation, the water-excreting function of the graft was restored, creatinine and urea levels decreased. Eleven hemodialy-

Corresponding author: Dzhabrail Saydulaev. Address: 1, Shchukinskaya str., Moscow, 123182, Russian Federation. Phone: (903) 750-00-85. E-mail: sdzhabrail@yandex.ru

sis sessions were performed. Graft function was restored on day 43.

DIAGNOSIS AND TREATMENT

Two months after kidney transplantation, the patient complained of pain around the kidney graft, decreased urine output. Ultrasound examination of the kidney graft showed that the pelvicalyceal system (PCS) was moderately dilated (renal pelvis 20 mm, calyces 5–7 mm). A hyperechoic mass with clear acoustic shadow was visualized in the projection of the ureteropelvic junction (UPJ) and the upper third of the ureter. Contrast-enhanced spiral CT scan was performed; a series of images visualized a concretion in the UPJ area, extravasation of the contrast agent into the retroperitoneal space (Fig. 1). As a result of examination, urolithiasis in the transplanted kidney, stone in the upper third of the graft ureter, necrosis in the graft ureter, and extravasation of urine were diagnosed.

To restore adequate urodynamics, it was decided that reconstructive surgery should be performed.

The retroperitoneal space was revised under endotracheal anesthesia. There was slight leakage of a light yellow liquid (urine), a culture was taken, electrolytes (potassium 9.5 mmol/L) were analyzed. On revision of the wound, a 2 cm long graft ureteral defect with a calculus (stone) in it was noted. The stone was removed (Fig. 2).

The necrotic section of the graft ureter was resected. It was decided to form an end-to-end uretero-ureteral anastomosis of the graft ureter. The proximal and distal ends of the ureter were intubated with ureteral stent #7CN (Fig. 3). A circular anastomosis was formed using a 5/0 monofilament thread.

EARLY POSTOPERATIVE PERIOD

On the first day after surgery, there was a decrease in urine output through the urethral catheter, an increase in the amount of discharge (urine) through a stand-by drainage tube. According to ultrasound findings, there was no fluid accumulation around the graft, and the PCS was not dilated. Based on the above, uretero-ureteral anastomosis failure was diagnosed. A decision was made to drain the PCS with a nephrostomy tube.

Percutaneous nephrostomy of the renal graft was performed under ultrasound control. The flow of pink-colored urine at a moderate rate via the nephrostomy drainage was observed.

On the third day after operation, the stand-by drainage tube was removed due to the absence of discharge.

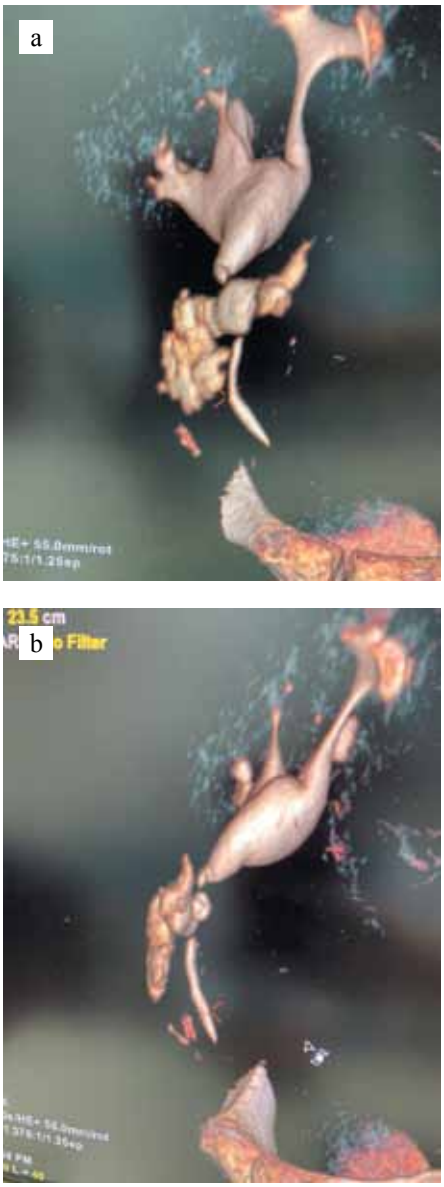

Fig. 1. Intravenous contrast-enhanced spiral CT imaging (urographic phase)

Fig. 2. Ureteral stone removed from the ureter graft

On day 14, the patient was discharged from the hospital with nephrostomy drainage (creatinine 250 μmol/L; urea 23.4 mmol/L) to restore renal graft function.

On day 30, the patient was admitted at the Shumakov National Medical Research Center of Transplantology and Artificial Organs in Moscow for antegrade pyeloureterography in the transplanted kidney.

Control antegrade pyeloureterography in the renal graft did not result in contrast agent extravasation, its passage into the bladder was timely. The nephrostomy drainage tube was removed. Control ultrasound scanning amid PCS drainage with urothelial stent did not show any dilatation.

Seven days after removal of the nephrostomy drainage tube, cystoscopy was performed, and the internal ureteral stent was removed.

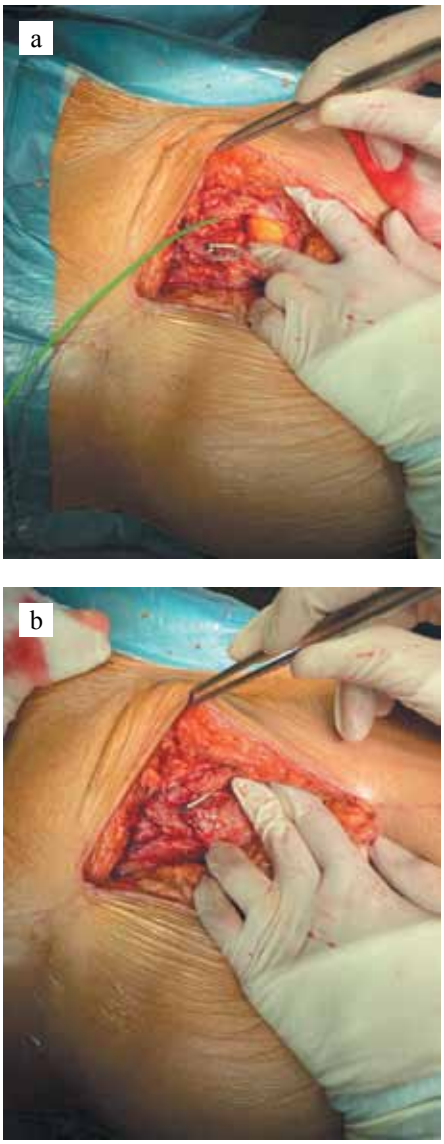

Fig. 3. Resection of the necrotic section of the ureter, formation of uretero-ureteral anastomosis of the ureteral graft

Control ultrasound examination of the renal graft showed no PCS enlargement, and blood flow velocities in the graft were satisfactory. No urodynamic abnormalities were found. Azotemia at the time of discharge was creatinine 130 μmol/L and urea 12.4 mmol/L.

DISCUSSION

In the intra- and postoperative period, the patient had no evidence of calculus in the graft PCS. A clinical presentation of acute renal colic in kidney recipients was impossible because of renal graft denervation. Due to lack of clinical manifestations, diagnosis of these cases may be delayed, which in turn would lead to long-term obstruction of the urinary tract, leading to impaired urodynamics, graft dysfunction, necrosis, and perforation of the graft ureter.

It was impossible to use the recipient's own ureter due to the previously performed bilateral nephrectomy as a result of autosomal dominant polycystic kidney disease and recurrent attacks of pyelonephritis. Formation of uretero-ureteral anastomosis with graft ureter stenting or permanent drainage of the graft with a nephrostomy tube were the only ways to restore adequate urine flow from the graft.

Due to the presence of calculus at the border between the UPJ and the upper third of the graft ureter with extravasation of urine, it was decided to perform reconstructive plastic surgery on the native urinary tracts of the renal graft. At the same time, a nephrostomy drainage was used to provide an opportunity for healing of the uretero-ureteral anastomosis.

CONCLUSION

Uretero-ureteral anastomosis formation in the upper third of the graft ureter with stenting and freeing up by the pelvicalyceal system with nephrostomy drainage can be used in perforative damage of the transplanted kidney ureter when using the native kidney ureter becomes impossible. The clinical effect achieved shows that the surgical tactics are correct. Hence, we recommend the technique for treatment of this rare post-kidney transplant urological complication.

The authors declare no conflict of interest.

REFERENCES

1. *Kayler L, Kang D, Molmenti E, Howard R.* Kidney transplant ureteroneocystostomy techniques and complications: review of the literature. *Transplant Proc*. 2010; 42 (5): 1413–1420.
2. *Lempinen M, Stenman J, Kyllönen L, Salmela K.* Surgical complications following 1670 consecutive adult renal transplantations: A single center study. *Scandinavian Journal of Surgery*. 2015; 104: 254–259.

3. *Palazzetti A, Oderda M, Dalmasso E, Falcone M, Bosio A, Sedigh O et al.* Urological consequences following renal transplantation: a review of the literature. *Urologia*. 2015; 82 (4): 211–218. doi: 10.5301/uro.5000132.
4. *Branchereau J, Karam G.* Management of urologic complications of renal transplantation. *European Urology Supplements*. 2016; 15: 408–414. doi: 10.1016/j.eursup.2016.08.001.
5. *Lucas JW, Ghiraldi E, Ellis J, Friedlander JI.* Endoscopic management of ureteral strictures: an update. *Current Urology Reports*. 2018; 19 (4): 24.
6. *Ooms LSS, Moelker A, Roodnat JI et al.* Antegrade balloon dilatation as a treatment option for posttransplant ureteral strictures: case series of 50 patients. *Experimental and Clinical Transplantation*. 2018; 16 (2): 150–155.
7. *Ozkaptan O, Sevinc C, Balaban M, Karadeniz T.* Minimally invasive approach for the management of urological complications after renal transplantation: single center experience. *Minerva Urologica e Nefrologica*. 2018; 70 (4): 422–428. doi: 10.23736/S0393-2249.18.03078-3.
8. *Choate HR, Mihalko LA, Choate BT*. Urologic complications in renal transplants. *Transl Androl Urol*. 2019; 8 (2): 141–147. doi: 10.21037/tau.2018.11.13.

The article was submitted to the journal on 23.04.2021

DOI: 10.15825/1995-1191-2021-2-88-94

A CASE REPORT ON INTRAPORTAL INJECTION OF AUTOLOGOUS BONE MARROW-DERIVED MONONUCLEAR CELLS AND LIVER TRANSPLANTATION IN A PATIENT WITH CIRRHOSIS

A.R. Sheraliev, A.A. Polikarpov, I.I. Tileubergenov, A.V. Moiseenko, D.A. Granov

Granov Russian Scientific Center of Radiology and Surgical Technology, St. Petersburg, Russian Federation

To date, liver transplantation remains the only effective treatment for patients with cirrhosis. Due to lack of other effective, alternative therapeutic methods, the search and development of new treatment technologies is problem number one. The development of cellular technologies is promising for use in clinical practice. Using this observation as an example, the safety and efficacy of cell therapy technology for prolonged stay on the liver transplant waiting list by a patient with cirrhosis is shown. After intraportal injection of autologous bone marrow-derived mononuclear cells, liver cirrhosis stabilized on the CTP and MELD-Na scales for 22 months of observation, which allowed the patient to wait for an organ and successfully undergo liver transplantation.

Keywords: autologous bone marrow-derived mononuclear cells, cell therapy, stem cells, intraportal injection, bone marrow, portal flowmetry, liver cirrhosis, liver transplantation.

INTRODUCTION

Liver cirrhosis (cirrhosis) is a terminal state of a chronic disease caused by various etiological factors, accompanied by severe inflammation, hepatocyte necrosis and liver fibrosis. This condition progresses irreversibly, leading to decompensation and death [1–3]. Currently, orthotopic liver transplantation (OLT) is the only radical treatment for cirrhosis [4–6].

However, in the Russian Federation, as in other countries, there is significant organ shortage and, as a result, higher number of waitlisted candidates [7, 8].

Thus, under limited transplant care and lack of effective drugs that increase the synthetic liver function, the search for and development of new technologies for treatment and support of patients with end-stage liver disease is an urgent task. This problem is relevant, including for patients who have been waitlisted for OLT. According to clninicaltrials.gov, 104 (26 completed) clinical trials using stem cells (SCs) in the treatment of liver diseases were conducted in 2020. However, reports on the method of SCs administration in cirrhosis are contradictory [9–12]. The authors describe both a simplified version of administration – into the peripheral vein, and an intra-arterial, intra-portal route of administration. In our observation, in a patient with end-stage cirrhosis, intraportal administration of SCs to achieve increased concentration in the liver was tested.

OBSERVATION

***Female patient**, 54 years old, diagnosed with cryptogenic hepatitis, cirrhosis, was included in the waiting list for liver transplantation in July 2015 at the Granov Russian Scientific Center of Radiology and Surgical Technology, St. Petersburg, Russia. While on the waitlist, she received standard drug therapy (hepatoprotectors, diuretics), while her liver function progressively deteriorated.*

In 2017, intraportal infusion of autologous bone marrow-derived mononuclear cells was proposed during a planned visit. Prior permission from the local ethics committee of the clinic was obtained. After signing the informed consent, the patient was examined (Table 1). The patient's initial status was assessed: Child-Turcotte-Pugh class B, MELD-Na 15. Contrast-enhanced spiral CT imaging of the chest, abdomen, and pelvis was performed, the liver vessels were assessed. No ascites and portal vein thrombosis were observed on tomograms. The recipient's baseline quality of life was assessed using the SF-36 questionnaire. The physical and psychological health scores were 45.14 and 41.55, respectively. Based on the data obtained, it was established that the patient had no contraindications according to the inclusion criteria (liver cirrhosis) and exclusion (no malignant neoplasm, portal vein thrombosis, active bacterial, viral infection) to the cell therapy procedure (Russian Federation patent RU2671560 C1 of November 2, 2018).

Subsequently, under general anesthesia in the operating room, 256 ml autologous bone marrow was aspirated from the posterior iliac crest using a 4G × 70 mm needle (TSUNAMI MEDICALL Italy).

After the bone marrow extraction procedure, the aspirate was sent in a transfusion bag in a thermocontainer to the laboratory, where mononuclear cell (MNC)

Corresponding author: Aslan Sheraliev. Address: 70, Leningradskaya str., St. Petersburg, 197758, Russian Federation. Phone: (950) 026-80-74. E-mail: sherali.aslan@gmail.com

isolation was carried out using an automated Maco Press Smart separator (Maco Pharma, France). We obtained 51.8 mL of MNC suspension. Then, we performed a qualitative analysis of MNCs and hematopoietic cell population with assessment of their viability using flow cytometry (Beckman Coulter, USA). The result is shown in Fig. 1. As an MNC medium, we used a 0.9% NaCL solution, a 20% human albumin solution, and 2500 IU of heparin solution. The cells were resuspended to a final volume of 93.8 mL.

About 2.5 hours after MNCs were obtained in the X-ray operating room under local anesthesia using ultrasound and X-ray navigation, the portal vein (PV) was punctured with a 22G needle (Cook Medical, USA). After removing the mandrel and obtaining blood from the lumen of the needle on a 0.35G-shaped guidewire

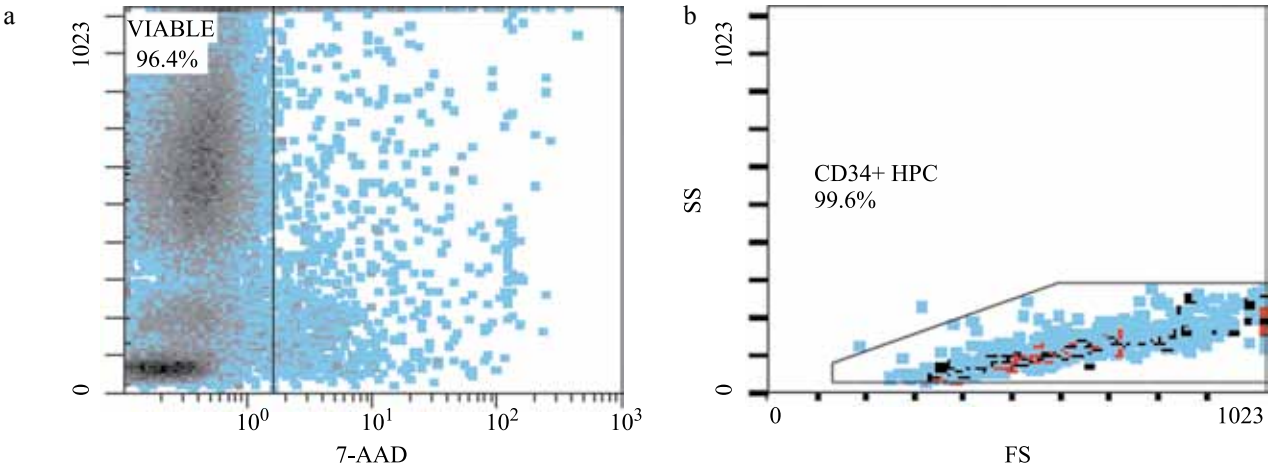

Fig. 1. Result of MNC suspension viability assessment by flow cytometry; a) viability of all MNC cells is 96.4%; b) viability of hematopoietic stem cells (CD34+) in MNC suspension is 99.6%

Table 1

Assessment of complete blood count and biochemistry panel results during the first 12 month of follow-up

	Before treatment	2 mths	4 mths	6 mths	8 mths	10 mths	12 mth	Units
White blood cells (WBC)	4.29	4.08	4.59	4.29	4.64	4.67	4.41	10^9/L
Red blood cells (RBC)	3.9	4.14	4.49	4.6	4.78	4.63	4.32	10^{12}/L
Hemoglobin (HGB)	109	113	127	127	131	128	135	g/L
Hematocrit (HCT)	33.1	34.4	38.8	38.9	38.3	39.4	37.1	%
Platelets (PLT)	88	77	83	101	104	95	105	10^9/L
Absolute neutrophil count (ANC)	2.27	2.14	2.65	2.52	2.75	2.62	2.51	10^9/L
Absolute lymphocyte count (LYMPH)	1.29	1.15	1.15	0.98	1.15	1.22	1.04	10^9/L
Absolute monocyte count (MONO)	0.46	0.57	0.6	0.57	0.5	0.61	0.51	10^9/L
Absolute eosinophil count (EO)	0.21	0.18	0.15	0.18	0.2	0.17	0.29	10^9/L
Absolute basophil count (BASO)	0.06	0.04	0.04	0.04	0.04	0.05	0.06	10^9/L
Glucose	5.55	5.42	5.43	5.95	5.57	6.97	5.26	mmol/L
Urea	2.7	3.3	3.9	3.6	3.8	4.3	4.5	mmol/L
Creatinine (Crea)	54	49.2	53.1	50.6	53.8	57.8	66.1	μmol/L
Total bilirubin	50	38.6	40.8	37.9	34.3	40.2	37.7	μmol/L
Direct bilirubin	28.4	20.2	20	17.9	16.7	16.6	15.5	μmol/L
AST	41	46	49	38	35	37	37	U/L
ALT	17	23	24	19	14	16	19	U/L
ALP	223	196	232	237	228	191	213	U/L
Potassium (K)	3.7	4.3	4.2	4.2	4.3	4.2	4.6	mmol/L
Sodium (Na)	141	139	142	140	137	139	142	mmol/L
Total protein	74	71	75	72	70	72	78	g/L
Albumin (ALB)	31	31	33	33	32	33	34	g/L
Quick prothrombin (Factor II)	53	56	57	53	58	56	55	%
Prothrombin time (PT)	18.4	17.8	17.7	18.2	17.2	17.5	18.8	sec.
INR	1.55	1.49	1.48	1.55	1.44	1.48	1.53	

(Starter, Boston, USA), a 4 F dilatation catheter (1 F = 0.33 mm, Cook Medical, USA) was inserted and angiography was performed from the v. portae with 15–20 mL of a water-soluble contrast agent (Omnipaque 350, Nycomed, USA). Next, a straight aortic catheter with 5 F lateral orifices (Cook Medical, USA) was placed on a metal guide (Storq, Cordis, USA). Taking into account the presence of collaterals caused by portal hypertension, before injecting the cell suspension, portal doppler flowmetry was performed using an automatic injector with 15–20 mL of a water-soluble contrast agent. The injection was performed at 0.5 mL/sec, 0.8 mL/sec, 1.0 mL/sec and 1.5 mL/sec to determine the optimal rate of selective perfusion of PV segmental branches. At 0.5 mL/sec injection rate, the PV segmental branches were not visualized, the contrast agent was discharged through the extrahepatic PV collaterals. At 0.8 mL/sec injection rate, uniform contrasting of all the PV segmental branches was achieved and the absence of blood flow along the collaterals was noted (Fig. 2). A 93.8 mL MNC suspension was injected from the portal vein bifurcation level at 0.8 mL/sec without loss of cells along the collaterals. The puncture canal was sealed with a hemostatic sponge, followed by removal of the catheter and fixation of aseptic dressing.

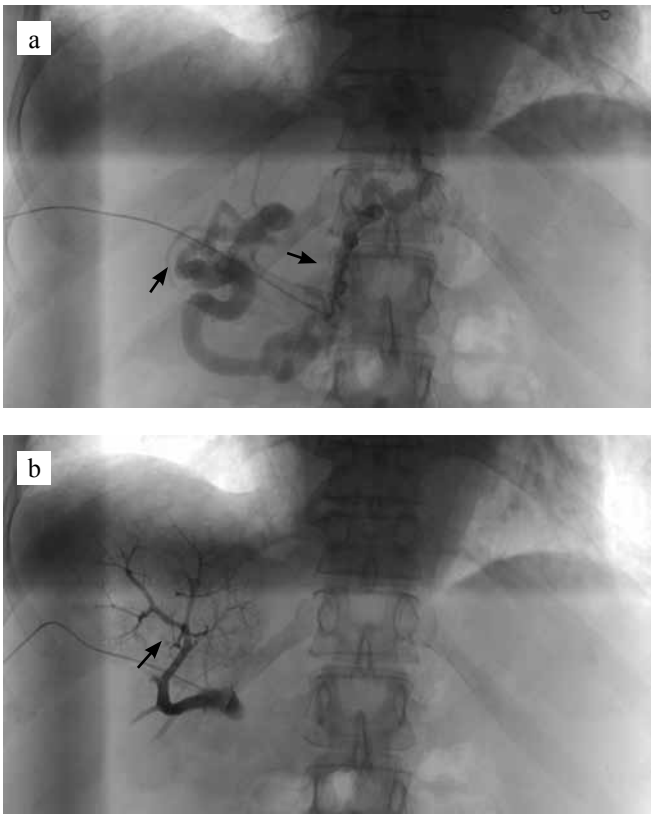

Fig. 2. Angiograms of the patient. a) portogram with contrast agent injection at the rate of 1 mL/sec and 1.5 mL/sec: the portal vein trunk and collaterals were visualized (black arrows); b) portogram with contrast agent injection at a rate of 0.8 mL/sec: only the portal vein segmental branches were perfused (optimal speed)

Ultrasound examination was performed after the operation. It found no bleeding at the manipulation site. There were no complications and clinically significant adverse events in the early postoperative period during the follow-up of the patient. The patient was discharged after 48 hours of hospital observation and control blood tests.

Then, every 2 months, the liver function indices were assessed according to the MELD-Na and CTP scales (Table 2), quality of life (Table 3).

During 22 months of follow-up, the patient's liver functional parameters improved: total bilirubin and hepatic transaminases levels decreased, albumin serum levels increased. The degree of liver failure according to CTP scale (7 points) and MELD-Na (14 points) was stabilized. The patient's quality of life indicators improved according to the SF-36 questionnaire (physical health – 56.44 points, mental health – 53.25 points).

Morphological assessment before the introduction of cells showed pronounced leukocytic infiltration, inflammation; the number of binuclear cells was 12 cells/mm^2, no mitoses were detected (Fig. 3). According to According to immunohistochemistry (IHC), the Ki67 marker expression was 2%, alpha-fetoprotein was not expressed.

Two months after the use of cell therapy, we performed repeated trepan biopsy of the liver from the same segment with subsequent morphological and IHC assessment (Fig. 5). There was decreased inflammatory infiltration, a significant increase in the number of binuclear

Table 2

Assessment of liver failure based on MELD-Na and CTP scales

Observation period	MELD-Na, points	Child-Turcotte-Pugh, points
Before treatment	15	Class B – 8
2 months	14	Class B – 8
4 months	15	Class B – 8
6 months	14	Class B – 7
8 months	14	Class B – 7
10 months	14	Class B – 7
12 months	15	Class B – 8
18 months	14	Class B – 7
22 months	14	Class B – 7

Table 3

Quality of life assessment (SF-36 questionnaire)

Observation period	Physical health	Mental health
Before treatment	45.14	41.55
1 month	47.00	45.00
4 months	50.53	48.48
8 months	54.43	52.09
12 months	54.77	39.78
18 months	51.10	46.11
22 months	56.44	53.25

cells from 12 to 19 cells/mm^2. No mitoses were detected. Ki67 expression was 3% (no significant dynamics), alpha-fetoprotein was not expressed.

After 22 months of follow-up after MNC was injected, the patient underwent OLT from a postmortem donor using the piggyback implantation technique with preservation of the retrohepatic section of the recipient's inferior vena cava.

There were no post-transplant complications. Graft function was satisfactory. The patient is alive and regularly monitored at the outpatient transplant center.

DISCUSSION

OLT remains the main radical treatment for cirrhosis patients. A longer wait for donor organ entails a higher waitlist mortality. Prior to OLT, patients receive only drug therapy in order to correct blood liver function. The lack of competitive effective therapy prompts the search for other ways to solve this problem. Regenerative medicine and cell therapy may serve as the most likely method of reducing liver failure mortality.

The safety and efficacy of stem cells in cirrhosis has been proven in clinical trials in a limited sample of patients [11–14]. However, in the process of human stem cell therapy, researchers face three main questions: how to obtain SCs, the administration-delivery route, and the choice of a cell population to achieve the best therapeutic effect.

In our case, the source of SCs was autologous bone marrow-derived mononuclear cells obtained from a patient with cirrhosis. Apparatus separation of the MNC made it possible to obtain a cell suspension with high viability.

According to a literature review, the authors have not previously detailed and substantiated the rate of cell administration and the advantages of the portal route of administration in the presence of venous collaterals [15–18].

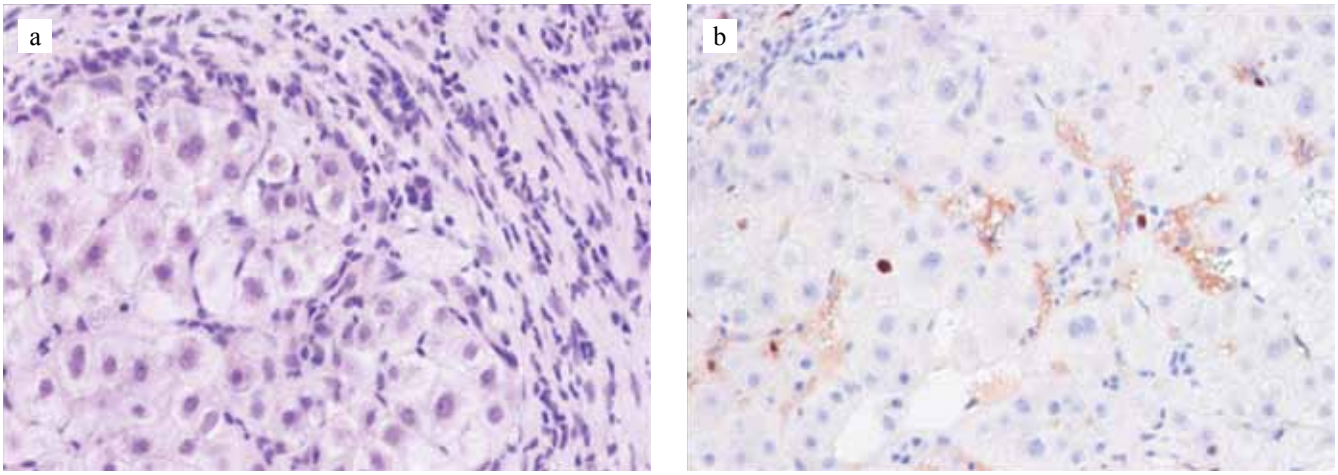

Fig. 3. Histological examination of liver biopsies before MNC infusion: a) infiltration by WBC, inflammation; b) IHC, expression of the Ki67 marker – 2%, alpha-fetoprotein was not expressed

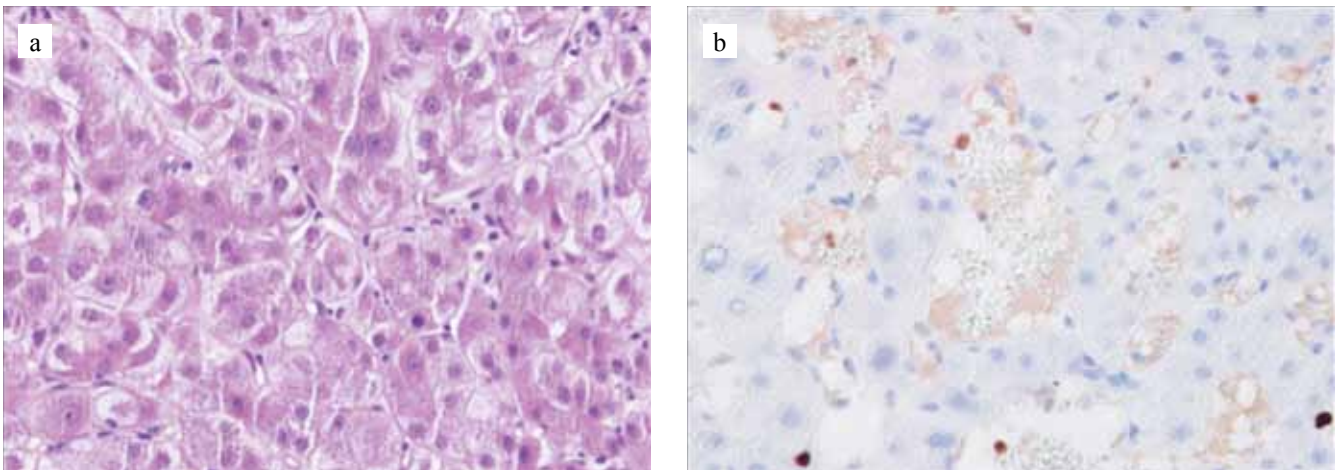

Fig. 4. Histological examination of liver biopsies after MNC infusion (2 months): a) infiltration by WBC and inflammation decreased, the number of binucleated cells increased (19 cells/mm^2). b) IHC, expression of the Ki67 marker – 3%, alpha-fetoprotein was not expressed

In the presented clinical case, we have demonstrated the portal doppler flowmetry technique, which allows to prevent the loss of cell suspension through the portosystemic venous collaterals when administered via the portal vein.

CONCLUSION

This proven cell therapy technology is safe and allows to improve liver function and stabilize the course of cirrhosis according to prognostic scales CTP (from 8 to 7), MELD-Na (from 15 to 14) while on the OLT waiting list.

The study on targeted delivery of a cell suspension to the liver through the portal vein suggests the need for a personalized approach in the use of cell therapy. A further randomized study on an enlarged sample of patients will be of great scientific interest.

The authors declare no conflict of interest.

REFERENCES

1. *Alexandrov VN, Kamilova TA, Kalyuzhnaya LI, Krivent-zov AV, Firsanov DV, Chirsky VS et al*. Cell therapy in liver cirrhosis. *Bulletin of the Russian Military Medical Academy*. 2014; 1 (45): 197–202. (In Russ.).
2. *Ivashkin VT, Mayevskaya MV, Pavlov CS, Sivolap YuP, Lunkov VD, Zharkova MS et al*. Management of adult patients with alcoholic liver disease: clinical guidelines of the Russian Scientific Liver Society. *Russian Journal of Gastroenterology, Hepatology, Coloproctology*. 2017; 27 (6): 20–40. (In Russ.). doi.org/10.22416/1382-4376-2017-27-6-20-40.
3. *Goldberg D, Ditah IC, Saeian K, Lalehzari M, Aronsohn A, Gorospe EC et al*. Changes in the prevalence of hepatitis C virus infection, nonalcoholic steatohepatitis, and alcoholic liver disease among patients with cirrhosis or liver failure on the waitlist for liver transplantation. *Gastroenterology*. 2017; 152 (5): 1090–1099. doi.org/10.1053/j.gastro.2017.01.003.
4. *Granov AM, Granov DA, Zherebtsov FK, Gerasimova OA, Borovik VV, Osovskikh VV et al*. Liver Transplantation. A Single Center Experience of 100 Cases. *Russian Journal of Transplantology and Artificial Organs*. 2012; 14 (4): 11–16. (In Russ.).
5. *Gautier SV*. Liver Transplantation in Russia: 25-year experience and current solutions. *Russian Journal of Transplantology and Artificial Organs*. 2015; 7 (2): 93–95. (In Russ). doi: 10.15825/1995-1191-2015-2-93-95.
6. *Pais R, Barritt 4th AS, Calmus Y, Scatton O, Runge T, Lebray P et al*. NAFLD and liver transplantation: current burden and expected challenges. *Journal of hepatology*. 2016; 65 (6): 1245–1257. doi.org/10.1016/j.jhep.2016.07.033.
7. *Gautier SV, Moysyuk YG, Khomyakov SM*. Organ Donation and Transplantation in the Russian Federation in 2014 7th Report of National Register. *Russian Journal of Transplantology and Artificial Organs*. 2015; 17 (2): 7–22. (In Russ.). doi.org/10.15825/1995-1191-2015-2-7-22.
8. *Gautier SV, Khomyakov SM*. Organ Donation and Transplantation In Russian Federation In 2017 10th Report of the National Registry. *Russian Journal of Transplantology and Artificial Organs*. 2018; 20 (2): 6–28. (In Russ.). doi.org/10.15825/1995-1191-2018-2-6-28.
9. *Yannaki E, Anagnostopoulos A, Kapetanos D, Xagorari A, Iordanidis F, Batsis I et al*. Lasting amelioration in the clinical course of decompensated alcoholic cirrhosis with boost infusions of mobilized peripheral blood stem cells. *Exp Hematol*. 2006; 34: 1583–1587. doi.org/10.1016/j.exphem.2006.06.012.
10. *Peng L, Xie DY, Lin BL, Liu J, Zhu HP, Xie C et al*. Autologous Bone Marrow Mesenchymal Stem Cell Transplantation in Liver Failure Patients Caused by Hepatitis B: Short-Term and Long-Term Outcomes. *Hepatology*. 2011; Sept: 820–828. doi.org/10.1002/hep.24434.
11. *Newsome PN, Fox R, King AL, Barton D, Than NN, Moore J et al*. Granulocyte colony-stimulating factor and autologous CD133-positive stem-cell therapy in liver cirrhosis (REALISTIC): an open-label, randomised, controlled phase 2 trial. *Lancet Gastroenterol Hepatol*. 2018; 3: 25–36. doi.org/10.1016/S2468-1253(17)30326-6.
12. *Chung SJ, Lee TY, Lee YH, Baik K, Jung JH, Yoo HS et al*. Phase I Trial of Intra-arterial Administration of Autologous Bone Marrow-Derived Mesenchymal Stem Cells in Patients with Multiple System Atrophy. 2020. doi: 10.21203/rs.3.rs-62544/v1.
13. *Feng Y, Wang AT, Jia HH, Zhao M, Yu H*. A Brief Analysis of Mesenchymal Stem Cells as Biological Drugs for the Treatment of Acute-on-Chronic Liver Failure (ACLF): Safety and Potency. *Current Stem Cell Research & Therapy*. 2020; 15 (3): 202–210. doi.org/10.2174/1574888X15666200101124317.
14. *Sakai Y, Takamura M, Seki A, Sunagozaka H, Terashima T, Komura T et al*. Phase I clinical study of liver regenerative therapy for cirrhosis by intrahepatic arterial infusion of freshly isolated autologous adipose tissue-derived stromal/stem (regenerative) cell. *Regenerative Therapy*. 2017; 6: 52–64. doi.org/10.1016/j.reth.2016.12.001.
15. *Am Esch JS 2nd, Knoefel WT, Klein M, Ghodsizad A, Fuerst G, Poll LW et al.* Portal Application of Autologous CD133+ Bone Marrow Cells to the Liver: A Novel Concept to Support Hepatic Regeneration. *Stem Cells*. 2005; 23: 463–470. doi.org/10.1634/stemcells.2004-0283.
16. *Levicar N, Pai M, Habib NA, Tait P, Jiao LR, Marley SB et al*. Long-term clinical results of autologous infusion of mobilized adult bone marrow derived CD34+cells in patients with chronic liver disease. *Cell Proliferation*. 2008; 41: 115–125.
17. *Mahmoud SZ, Abdo EF, Helal SR, Eldien HS, Abdeltawab D, Abd-Elkader AS*. Clinical and laboratory outcomes of stem cell transplantation in patients with decompensated liver cirrhosis: single-arm pilot trial. *Journal of Current Medical Research and Practice*. 2019; 4 (1): 44. doi: 10.4103/JCMRP.JCMRP_30_18.
18. *Kotkas IE*. Changes in the hemodynamics of the liver after its resection with the use of cellular technologies. *Medicina i zdravoohraneyie v sovremenom obshestve: Supplement*. 2020: 38. (In Russ.).

The article was submitted to the journal on 2.12.2020

DOI: 10.15825/1995-1191-2021-2-95-103

NUMERICAL AND EXPERIMENTAL JUSTIFICATION OF TRANSCATHETER AORTIC VALVE PROSTHESIS DESIGN

E.A. Ovcharenko[1], K.Yu. Klyshnikov[1], A.A. Shilov[1], N.A. Scheglova[2], T.V. Glushkova[1], D.V. Nushtaev[3], L.S. Barbarash[1]

[1] Research Institute for Complex Issues of Cardiovascular Diseases, Kemerovo, Russian Federation
[2] LOGEEKS Ltd., Novosibirsk, Russian Federation
[3] Severstal Management, Moscow, Russian Federation

Objective: to justify the design of a self-expanding transcatheter aortic valve prosthesis based on a biomaterial stabilized with ethylene glycol diglycidyl ether using numerical simulation and a series of field experiments with working prototypes to determine the consistency of the proposed design solutions. **Material and methods.** Numerical computer models of a developed aortic valve prosthesis intended for transcatheter implantation, as well as prototypes of the most promising concepts for a series of field tests, were used in the work. Computer 3D models were subjected to numerical analysis in the Abaqus/CAE environment (Dassault Systemes, France) based on the finite element method with iterative design optimization and repeated numerical experiments. Physical prototypes of the transcatheter prosthesis were subjected to a series of mechanical tests for axial and radial compression, as well as tests on a Vivitro hydrodynamic stand (Vivitro Labs, Canada) under simulated normal flow. All studies were carried out in a comparative aspect with a similar transcatheter aortic valve prosthesis (control), the CoreValve™ bioprosthesis (Medtronic, Inc., USA). **Results.** Computer simulation demonstrates the stress-strain state values that do not significantly exceed the critical levels (628 and 756 MPa versus the threshold value 1080 MPa) for two basic concepts of support frames. The fatigue strength based on the calculation of the mean and alternating stresses corresponding to normo- and hypertensive states based on the Goodman diagrams, did not reveal any evidence that the threshold values (destruction area after 200 million cycles) were exceeded. The hydrodynamic characteristics of working prototypes made on the basis of computer models correspond to the testing data of CoreValve™ clinical bioprosthesis: the effective orifice area was 1.97 cm^2, the mean transprosthetic gradient was 8.9 mm Hg, the regurgitant volume was 2.2–4.1 mL per cycle depending on the prototype model. **Conclusion.** Generally, experiments carried out showed the consistency of the concepts, including from the point of view of implementation of the leaflet apparatus based on xenogeneic tissues treated with ethylene glycol diglycidyl ether.

Keywords: transcatheter prosthesis, aortic stenosis, finite element method, fluid dynamics, numerical simulation.

INTRODUCTION

Transcatheter aortic valve replacement (TAVR) is a minimally invasive approach, which has gained considerable acceptance in the last decade. The procedure is intended for patients with high-risk aortic stenosis, who are not eligible for surgical replacement due to significant risks associated with comorbidity and recipient age. Being much less invasive than the surgical alternative, TAVR can shorten the rehabilitation period and provide treatment for aortic stenosis in high- to moderate-risk patients [1].

Common to all FDA- and CE-approved TAVR devices is the valve material, which is made of glutaraldehyde-fixed equine or porcine pericardium. Nevertheless, the existing pool of prosthetic dysfunctions, based on this type of preservation – first of all, calcification [2] and structural degeneration [3] – prevents us from concluding that such prostheses have significantly long functioning period, and, therefore, that they can be used for low-risk patient groups. [4], for which the prosthesis should last longer. Among the methods of xenograft stabilization for cardiovascular surgery in Russia, ethylene glycol diglycidyl ether (EGDE), which is more resistant to calcification due to its chemical structure [5], has been highly recommended, and the clinical results of the use of EGDE-based heart valve prostheses confirm its durability [6]. Potentially, TAVR constructions based on this type of stabilization should not be inferior to existing glutaraldehyde-treated prostheses in terms of mechanical properties and hemodynamics. This work

Corresponding author: Kirill Klyshnikov. Address: 6, Sosnovy Boulevard, Kemerovo, 650002, Russian Federation. Phone: (923) 516-68-66. E-mail: KlyshnikovK@gmail.ru

presents an experimental justification of the design of a self-expanding transcatheter aortic valve prosthesis based on an EGDE-stabilized biomaterial.

MATERIALS AND METHOD

Design input

Based on studies on TAVR features and results, analysis of design solutions of existing transcatheter valves and their shortcomings (analysis of the literature of the current state) [7, 8], analysis of new experimental prostheses [9, 10], as well as analysis of regulator requirements, the basic design characteristics of medical products were determined. The main prerequisites for the design of aortic valve prosthesis were:

– The prosthesis represents a stent-type support frame, on which three symmetrical leaflets, made of biological material and a veneer in the inflow area, are mounted.
– Structurally, the prosthesis consists of three interconnected zones that provide the functions – (1) fixation in the lumen of the annulus fibrosus or dysfunctional prosthesis; (2) preservation of the symmetrical geometry of the cusp and the possibility of its closure; (3) ensuring fixation in the sinotubular articulation area while maintaining the geometry of the cusp unchanged.
– The technology chosen for the support frame was the use of a self-expanding structure based on a superelastic titanium nickelide alloy. This solution, highly recommended in the clinical practice of TAVR, additionally, would not require the development of a complex delivery system, as in the case of alternative solution, balloon implantation.
– The prosthesis cusp must not interfere with the packaging into the delivery system, hence, have a minimum thickness, while maintaining sufficient strength and providing the necessary closure zone (co-optation), which is ensured by using EGDE-stabilized porcine xenopericardium.

The original geometry of the support frame should allow laser cutting from a small-diameter 6 mm (18 Fr) tube for subsequent packaging in a minimal profile delivery system.

Concepts

Components of the developed prosthesis were designed through a series of numerical experiments to assess the main functional characteristics – radial forces, stress-strain state, and fatigue-strength characteristics. For this purpose, two primary concepts of a stent-based support frame were developed: "classical" and "inclined" cell topology. The main difference in the second case was the inclination of three cell rows – two in the inflow area and one in the outflow. Such a feature, presumably, should provide a special pattern for subsequent pre-implantation packaging into the delivery system – due to the twisting of the support frame. Support frame models, implemented in the form of two-dimensional sweeps for subsequent formation of volumes, were built in the SolidWorks (Dassault Systemes, France) design software (computer-aided design).

Numerical Simulation

The resulting concepts were subjected to numerical analysis in the Abaqus/CAE environment (Dassault Systemes, France) based on the finite element method with iterative design optimization and repeated numerical experiments. For this purpose, C3D8 hex element grid (a general-purpose 3D hexagonal element, fully integrated with 8 nodes, n = 105,000) was obtained on the basis of three-dimensional models. The study was performed for a series of load tests, including:

1) Giving the final shape to the support frame (Fig. 1, a, b) from the initial 6 mm to the final geometry of variable diameter, fitting size 25 mm for the area containing the cusps. The criterion for the consistency of the design was the absence of elements with high stress values exceeding the ultimate strength of the material (σ = 1522.4 MPa [11]).
2) Axial stiffness test of the inflow area (Fig. 1, b) to assess fixation forces at 75% relative to the original diameter. The resulting stress-strain curves were evaluated.
3) Radial compression test (Fig. 1, b) to assess the force with which the device will exert pressure on the annulus fibrosus in the implanted state, in particular, in the cardiac conduction system passage area, i.e. the area responsible for the occurrence of the left bundle branch block.
4) The cyclic fatigue test based on the average and alternating stress diagrams – the ability of the structure to withstand prolonged alternating load – demonstrated for the final models the ability to operate without node destruction under the action of normal and elevated pathological pressures – up to 160 mmHg (0.21 kPa).

Real-life experiments

The developed drawings of the support frames formed the basis for the prototypes of two versions of the TAVR prosthesis: one based on the "classical" design and two based on the "inclined" design (Fig. 2, a). Titanium nickelide tubes with 6 mm diameter and 0.5 mm wall thickness were manufactured by laser cutting, with subsequent shaping by heat treatment with a phase trans-

formation temperature of 17 ± 3 °C and surface treatment by mechanical and electrochemical polishing.

The obtained support frames were subjected to a series of mechanical tests for axial and radial compression in comparison with the control – a CoreValve™ bioprosthesis support frame (Medtronic, Inc., USA) of the same standard size. For this purpose, the specimens were placed in plate clamps or radial grips of ZwickRoell universal testing machine (ZwickRoell, Germany) and compressed by 75% in axial (Fig. 3, a) and radial (Fig. 3, b) directions, with registration of force-deformation curves.

To create the cusp and the lining, the templates were designed, according to which the necessary components were made by laser cutting using the thickness mapping of EGDE-stabilized porcine xenopericardium. Then, by consecutive mounting of all elements of the prosthesis on the support frame with the help of sutures according to well-known methods, working prototypes of prostheses (Fig. 2, b) were made for hydrodynamic tests under real-life experiments on a stand. Hydrodynamic characteristics were studied in a Vivitro pulsating flow setup (Vivitro Labs, Canada), in which normal blood flow was simulated: 70 mL stroke volume, 5 L/min cardiac output, and 120/80 mm Hg pressure. Results: the effective orifice area, maximum and mean transprosthetic gradients, and regurgitant volume were recorded for 10 steady-state cycles. A 25-size commercial CoreValve™ bioprosthesis was used as control values.

RESULTS

Numerical simulation

The following characteristics were obtained from numerical analysis of load tests:

1) Giving the final shape to the support frame from the initial 6 mm to the final geometry of variable diameter, up to 22–31 mm with a fitting size of 25 mm did

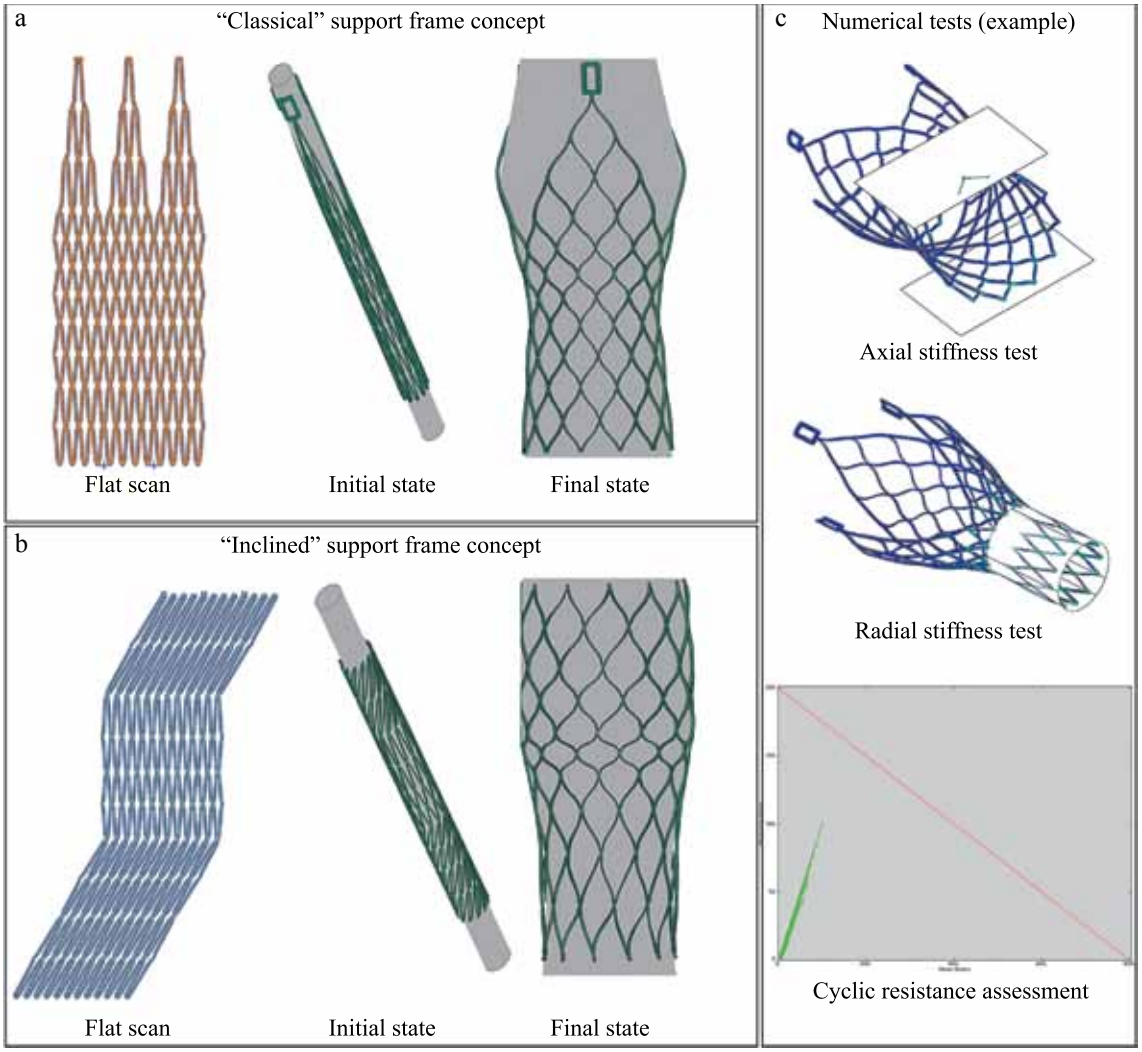

Fig. 1. Two primary concepts of a support frame based on stents "classical" (a) and "inclined" (б) topology of cells, computer models: initial flat sketch for laser cutting machine; initial state, similar to the manufactured one; final state obtained by the finite element method; в – an example of numerical tests for design optimization: axial stiffness test with slabs; radial stiffness test with a cylindrical surface; alternating stress diagram for evaluating cycle durability

not cause a critical increase in the stress-strain state of the nodes: the average weighted value of node stress was 341 (110–628) and 258 (53–756) MPa depending on the concept at the threshold level (1080 MPa), taken as the ultimate strength of titanium nickelide (Fig. 4, b).

2) The axial stiffness test (Fig. 4, a) of the inflow area yielded values ranging from 11.3 to 17.1 N as the total force to estimate the fixation forces.
3) The radial compression test (Fig. 4, a) showed similar findings, with radial forces for the "classical" and "inclined" concepts – 12.4 and 16.8 N, respectively, with slightly higher values for the CoreValve™ bioprosthesis (up to 21.3 N) [12].
4) Cyclic fatigue test showed that the resulting alternating stresses do not exceed 36–50 MPa. The average stress variations, taking into account the previously formed stress-strain state, are 410–513 MPa – below the ultimate fatigue strength (S-N curves 400 MPa [13]).

Real-life experiments

It was shown that the maximum axial force in the case of the developed support frames was 12.8–15.6 mm, depending on the geometry and, in general, weakly depended on the frame area. For the control case, the CoreValve™ bioprosthesis, there was a clear dependence of forces on the prosthesis area: 12.4 N for the inflow area and 7.58 N for the outflow area. The 75% radial compression force generated for the experimental prostheses was also shown to be weakly dependent on the prosthesis area, being 11.6–17.0 N, while in the control case it ranged from 20.6 N (inflow area) to 8.1 N (outflow area). In all cases, a clear hysteresis dependence of the frame properties under loading and unloading was obtained – formation of a specific stress-strain curve loop that is characteristic of titanium nickelide. It was shown that the ranges of forces created by the support frames in a real-life experiment, firstly, agree with the findings of numerical experiments, which made it possible to verify computer simulation, and secondly, agree well with the properties of the commercial CoreValve™ prosthesis, which is widely used in in TAVR clinical practice in Russia.

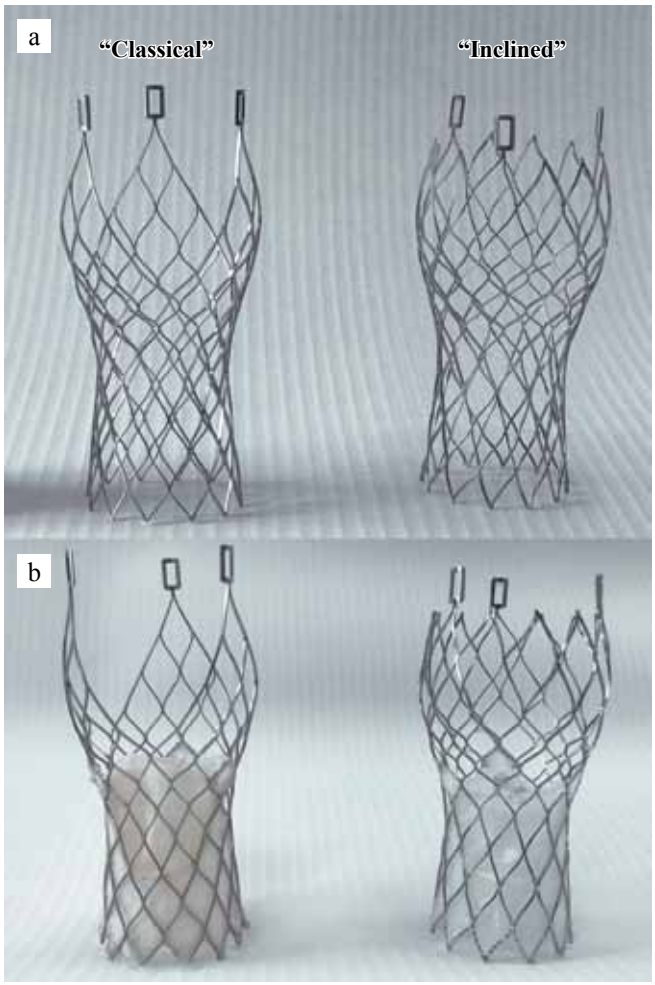

Fig. 2. Supporting frames and prototypes of TAVR-prostheses, containing a valve apparatus and facing of the inflow zone, of two concepts: based on the "classic" cell and "inclined"

Quantitative results of the hydrodynamic study are shown in Table.

DISCUSSION

Designing a new transcatheter aortic valve prosthesis is a complex task that requires investigation and justification of the geometry and properties of all its components – the support frame, the cusp, and the subsequent

Table

Hydrodynamic characteristics of the studied prostheses

Indicator	"Classical" design	"Inclined" design	Control
Effective orifice area, cm^2	2.17 ± 0.32	1.97 ± 0.21	2.34 ± 0.11
Maximum transprosthetic gradient, mm Hg	13.9 ± 6.5	17.5 ± 8.8	10.4 ± 6.2
Mean transprosthetic gradient, mm Hg	7.1 ± 3.8	8.9 ± 4.3	5.1 ± 2.1
Regurgitant volume, mL/cycle	2.2 ± 1.8	4.1 ± 2.3	2.8 ± 2.6

Note. All data are presented as mean ± standard deviation, calculated over 10 steady-state hydrodynamic cycles.

validation of the assembled structure. The present study demonstrates an analysis of the two most important risks for TAVR – excessive pressure on the areas of the cardiac conduction system around the annulus fibrosus and hemodynamic efficiency. The first aspect determines the possibility of conduction abnormalities – primarily atrioventricular block resulting from mechanical compression, while the second determines the development of para- and transprosthetic regurgitation due to loose engagement of the prosthesis with the surrounding tissues or violations of the leaflet geometry. Clinical experience with the use of self-expanding TAVR prostheses demonstrates the prevalence of these two effects in the complication structure of this type of prosthetic repair [14].

The study of mechanical properties and stress-strain states through numerical and real-life experiments, demonstrates the consistency of the proposed concepts. The arising internal forces (stress) do not reach critical values, constituting much lower amplitudes even for loaded structural nodes. The value of such a "safety margin", on one hand, does not cause risk of failure of the prosthesis sections, even with additional loads (bends during the passage of the patient's vascular bed), on the other hand, it makes it possible for in-depth optimization of the design: changes in the geometric parameters of the cell, i.e., potential reduction in the prosthesis diameter in the pre-implantation state – the delivery system profile. External forces generated by the support frame in the radial and axial directions are largely consistent with the control – the CoreValve™ clinical bioprosthesis, which, despite complications, has a high evidence base for its effectiveness. It can be assumed that the proposed design will demonstrate similar fixation results in the aortic valve lumen. The concepts show lower radial forces in the annulus fibrosus, suggesting a lower risk of compression of the conduction system. However, this thesis should be confirmed by an extended series of experiments, including assessing the fixation reliability. Fatigue modeling data showed a slight change in the stress in the systole-diastole cycle for both models, suggesting that the frame is functioning in an "infinite" range and predicting com-

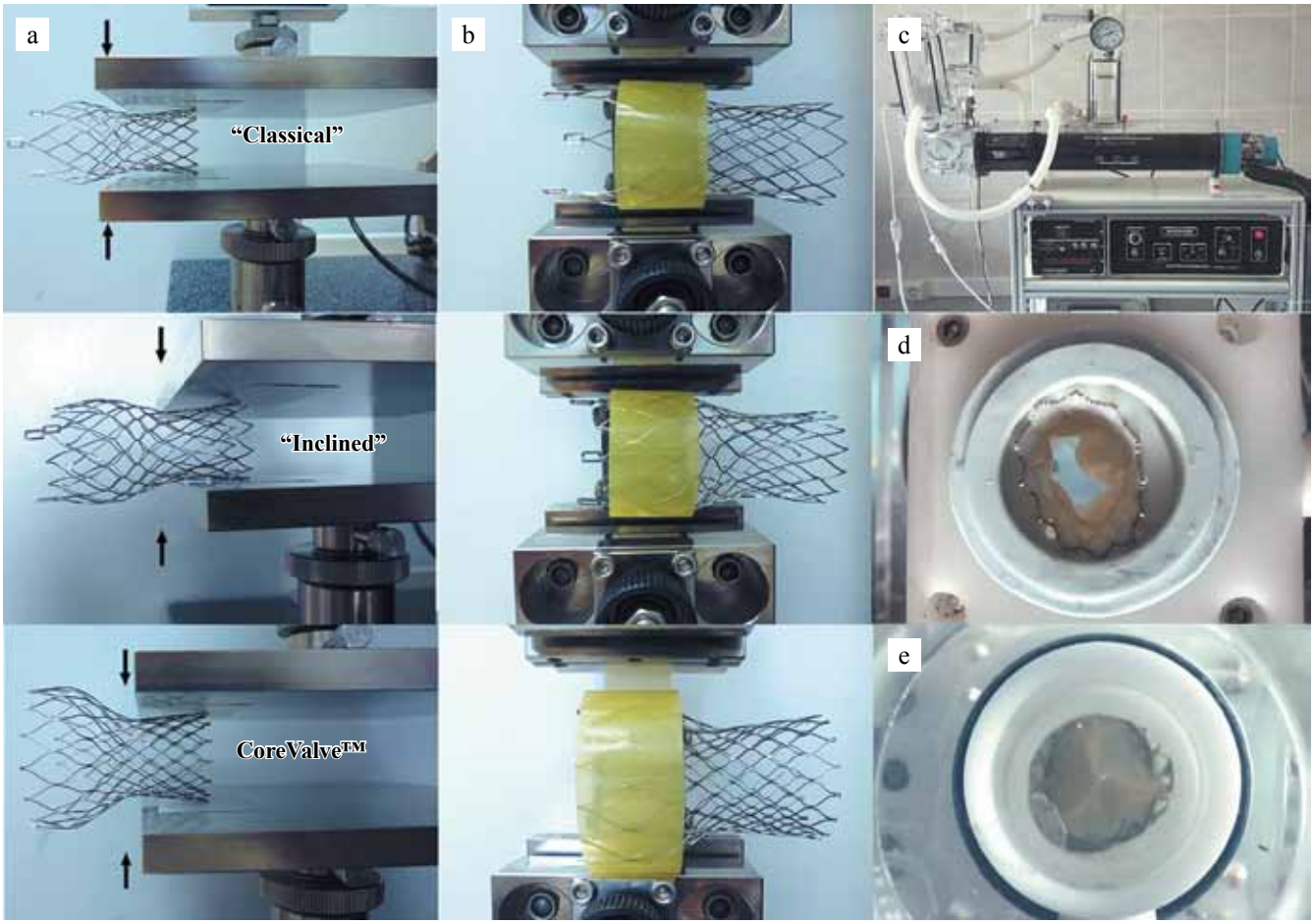

Fig. 3. Setting up full-scale experiments with prototypes of supporting frames and working prototypes of an assembled prosthesis: а – study of mechanical properties in a universal testing machine for axial compression; б – the same for radial compression; в – stand for hydrodynamic testing of prostheses; г – view from the inflow zone of the prototype valve prosthesis installed in the hydrodynamic stand; д – view from the outlet zone to the closed flap apparatus

pliance with the requirements to withstand 200 million systole-diastole cycles without failure.

In vitro hydrodynamic characteristics are the main indicator of bioprosthesis performance; in a comparative aspect, they show generally satisfactory results. Comparison of the performance of glutaraldehyde-stabilized xenopericardial leaflets (CoreValve™ control bioprosthesis) and the concepts in question based on EGDE-stabilized biomaterial confirmed the acceptability of the latter for TAVR prostheses. Quantitative characteristics – effective orifice area and the transprosthetic gradient determining the opening of the cusp, indicate sufficient elasticity and mobility of the leaflets. The regurgitant volume, comparable both with bioprostheses for open intervention [15, 16], and with the control, in turn, confirms the cusp closure tightness and creation of tight contact with the annulus fibrosus in vitro model.

CONCLUSION

The series of studies carried out demonstrates the consistency of the developed support frame concepts, including from the point of view of implementing the cusp based on EGDE-treated xenotissues. Validation of working prototypes in the hydrodynamic evaluation unit in a comparative aspect with the clinical specimen of a similar TAVR bioprosthesis confirmed the satisfactory functional characteristics of the models developed.

The study was funded by a grant from the Russian Science Foundation (project No. 18-75-10061) on the topic "Research and Implementation of the Concept of Robot-Assisted Minimally Invasive Aortic Valve Repair".

The authors declare no conflict of interest.

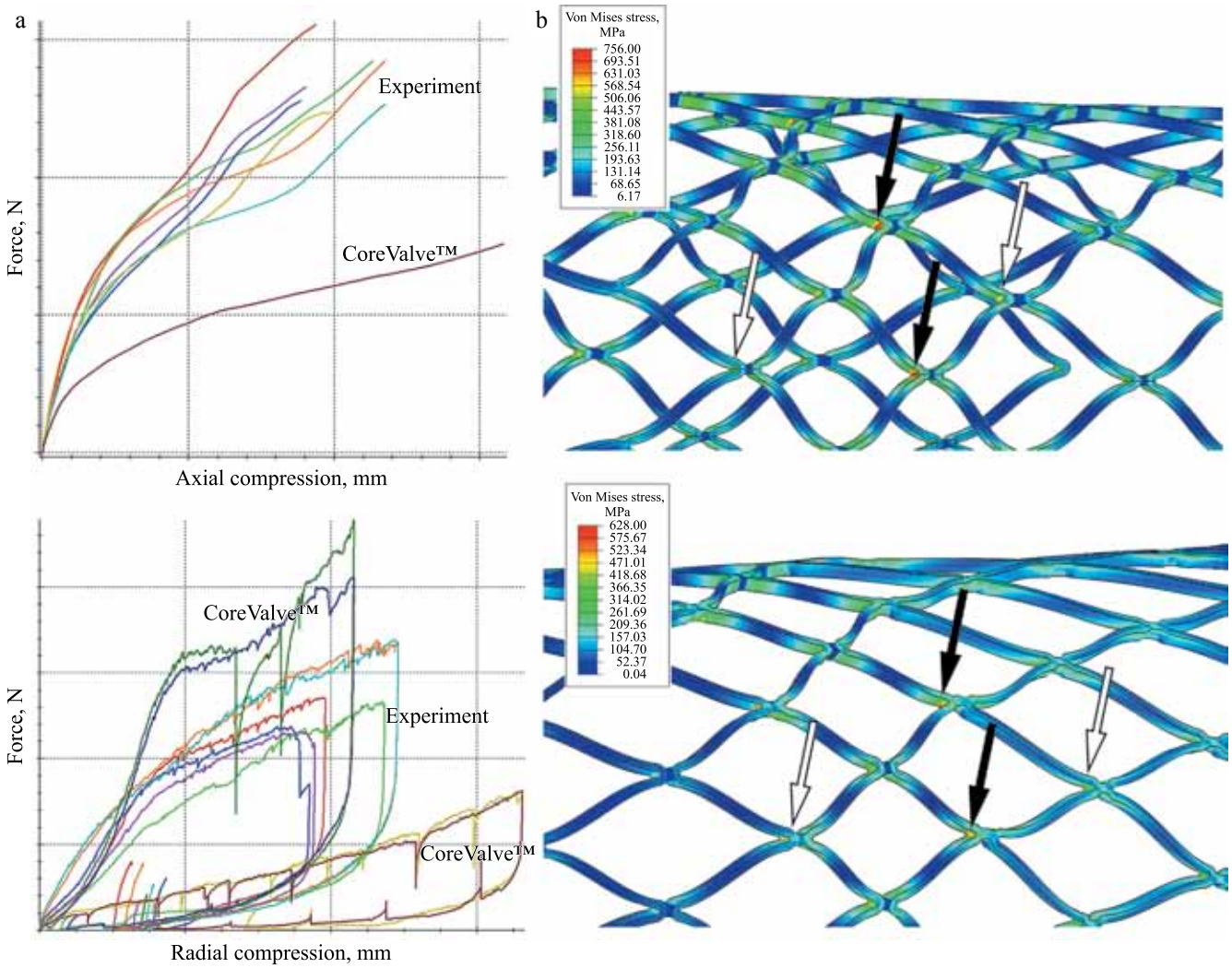

Fig. 4. Test results: a – full-scale assessment of mechanical properties in a universal testing machine in comparison with a control – a commercial bioprosthesis CoreValve ™; б – numerical assessment of the stress-strain state of the support frame models, black arrows indicate nodes with maximum von Mises stress values, white – with moderate ones

REFERENCES

1. *Kamioka N, Wells J, Keegan P, Lerakis S, Binongo J, Corrigan F et al.* Predictors and clinical outcomes of nextday discharge after minimalist transfemoral transcatheter aortic valve replacement. *JACC Cardiovasc Interv.* 2018; 11: 107–115. doi: 10.1016/j.jcin.2017.10.021.
2. *Rodriguez-Gabella T, Voisine P, Puri R, Pibarot P, Rodes-Cabau J.* Aortic bioprosthetic valve durability: incidence, mechanisms, predictors, and management of surgical and transcatheter valve degeneration. *J Am Coll Cardiol.* 2017; 70: 1013–1028. doi: 10.1016/j.jacc.2017.07.715.
3. *Wang M, Furnary AP, Li HF, Grunkemeier GL.* Bioprosthetic aortic valve durability: a metaregression of published studies. *Ann Thorac Surg.* 2017; 104: 1080–1087. doi: 10.1016/j.athoracsur.2017.02.011.
4. *Dasi LP, Hatoum H, Kheradvar A, Zareian R, Alavi SH, Sun W et al.* On the mechanics of transcatheter aortic valve replacement. *Ann Biomed Eng.* 2017; 45: 310–331. doi: 10.1007/s10439-016-1759-3.
5. *Zhuravleva IYu, Karpova EV, Oparina LA, Kabos N, Ksenofontov AL, Zhuravleva AS et al.* Xenopericardum, preserved by di- and pentaepoxides: molecular mechanisms of crosslinking and mechanical properties of biomaterial. *Circulatory pathology and cardiac surgery.* 2018; 22 (3): 56–68. doi: 10.21688/1681-3472-2018-3-56-68. [In Russ, English abstract].
6. *Barbarash LS, Rogulina NV, Rutkovskaya NV, Odarenko YuN, Kokorin SG.* Experience with the use of epoxy-treated biological prostheses in mitral valve disease in patients younger than 65 years of age. *Thoracic and cardiovascular surgery.* 2019; 61 (2): 114–122. doi: 10.24022/0236-2791-2019-61-2-114-122. [In Russ, English abstract].
7. *Rotman OM, Bianchi M, Ghosh RP, Kovarovic B, Bluestein D.* Principles of TAVR valve design, modelling, and testing. *Expert Rev Med Devices.* 2018; 15 (11): 771–791. doi: 10.1080/17434440.2018.1536427.
8. *Cahill TJ, Chen M, Hayashida K, Latib A, Modine T, Piazza N et al.* Transcatheter aortic valve implantation: current status and future perspectives. *Eur Heart J.* 2018; 39 (28): 2625–2634. doi: 10.1093/eurheartj/ehy244.
9. *Bogachev-Prokofiev AV, Zhuravleva IYu, Sharifulin RM, Zheleznev SI, Demidov DP, Kliver EE, Karaskov AM. In vitro* implantation of the first domestic transcatheter prosthesis in the native mitral valve. *Circulatory pathology and cardiac surgery.* 2018; 22 (1): 22–28. [In Russ, English abstract].
10. *Rotman OM, Kovarovic B, Chiu WC, Bianchi M, Marom G, Slepian MJ, Bluestein D.* Novel Polymeric Valve for Transcatheter Aortic Valve Replacement Applications: *In vitro* Hemodynamic Study. *Ann Biomed Eng.* 2019; 47 (1): 113–125. doi: 10.1007/s10439-018-02119-7.
11. *Marrey R, Baillargeon B, Dreher ML, Weaver JD, Nagaraja S, Rebelo N, Gong XY.* Validating Fatigue Safety Factor Calculation Methods for Cardiovascular Stents. *J Biomech Eng.* 2018; 140 (6): 10.1115/1.4039173. doi: 10.1115/1.4039173.
12. *Tzamtzis S, Viquerat J, Yap J, Mullen MJ, Burriesci G.* Numerical analysis of the radial force produced by the Medtronic-CoreValve and Edwards-SAPIEN after transcatheter aortic valve implantation (TAVI). *Med Eng Phys.* 2013; 35 (1): 125–130. doi: 10.1016/j.medengphy.2012.04.009.
13. *Robertson SW, Pelton AR, Ritchie RO.* Mechanical fatigue and fracture of Nitinol. *International Materials Reviews.* 2012; 57 (1): 1–37. doi: 10.1179/1743280411Y.0000000009.
14. *Alfadhli J, Jeraq M, Singh V, Martinez C. Updates* on transcatheter aortic valve replacement: Techniques, complications, outcome, and prognosis. *J Saudi Heart Assoc.* 2018; 30 (4): 340–348. doi: 10.1016/j.jsha.2018.07.002.
15. *Klyshnikov KYu, Ovcharenko EA, Maltsev DA, Zhuravleva IYu. Comparative* characteristics of hydrodynamic indicators of bioprostheses of heart valves "UniLine" and "PeriCor". *Clinical physiology of blood circulation.* 2013; 1: 45–51. [In Russ, English abstract].
16. *Marquez S, Hon RT, Yoganathan AP.* Comparative hydrodynamic evaluation of bioprosthetic heart valves. *J Heart Valve Dis.* 2001; 10 (6): 802–811.

The article was submitted to the journal on 16.07.2020

DOI: 10.15825/1995-1191-2021-2-104-113

SUPERCRITICAL CARBON DIOXIDE AS A TOOL FOR IMPROVING THE BIOCOMPATIBLE PROPERTIES OF BIOPOLYMER AND TISSUE-SPECIFIC SCAFFOLDS FOR TISSUE ENGINEERING

E.A. Nemets[1, 2], A.E. Lazhko[3], A.M. Grigoryev[1], V.Yu. Belov[1, 2], V.A. Surguchenko[1], Yu.B. Basok[1, 2], A.D. Kirillova[1], V.I. Sevastianov[1, 2]

[1] Shumakov National Medical Research Center of Transplantology and Artificial Organs, Moscow, Russian Federation

[2] Institute for Biomedical Research and Technology, Moscow, Russian Federation

[3] Kurnakov Institute of General and Inorganic Chemistry, Moscow, Russian Federation

Objective: to investigate the efficacy of supercritical carbon dioxide (sc-CO_2) for enhancшtп the biocompatibility of biopolymer scaffolds from biodegradable materials and tissue-specific scaffolds from decellularized porcine liver slices (PLSs) or fine porcine cartilage particles (FPCPs). **Materials and methods.** Biopolymer scaffolds of a polyoxy(butyrate-co-valerate) and gelatin copolymer composition, 4 mm in diameter and 80 mm in length, were formed by electrospinning (NANON-01A, MECC CO, Japan) and stabilized by incubation in glutaraldehyde vapor for 48 hours at room temperature. For decellularization, PLSs and FPCPs were incubated under periodic stirring in buffer (pH = 7.4) solutions of sodium dodecyl sulfate (0.1%) and Triton X-100 with increasing concentrations (1, 2, and 3%). Treatment in a sc-CO_2 atmosphere was done at 150–300 bar pressure, 35 °C temperature, and 0.25–2.5 mL/min flow rate of sc-CO_2 for 8–24 hours. 10% ethanol was introduced as a polarity modifier. Cytotoxicity was studied according to GOST ISO 10993-5-2011. The growth of NIH/3T3 in the presence of samples was studied using an interactive optical system IncuCyte Zoom. **Results.** The effect of the sc-CO_2 flow rate and pressure, and the effect of addition of ethanol, on the biocompatibility of scaffolds was investigated. It was found that treatment at a low sc-CO_2 flow rate (0.25 mL/min) does not achieve the required cytotoxicity. Complete absence of cytotoxicity in biopolymer scaffolds was achieved in the presence of 10% ethanol, at a sc-CO_2 flow rate of 2.5 mL/min, 300 bar pressure and 35 °C temperature after 8 hours of treatment. Effective removal of cytotoxic detergents from decellularized liver occurs already at a 150-bar pressure and does not require the addition of ethanol. Adding ethanol to sc-CO_2 eliminates not only the cytotoxic, but also the cytostatic effect of tissue-specific scaffolds. **Conclusion.** Sc-CO_2 treatment is an effective way to enhance the biocompatibility of three-dimensional porous matrices produced using cytotoxic substances: bifunctional crosslinking agents for biopolymer scaffolds and surfactants in the case of tissue-specific matrices. Addition of ethanol as a polarity modifier improves the treatment efficiency by eliminating both cytotoxic and cytostatic effects.

Keywords: pig liver, pig cartilage, decellularization, biopolymer scaffolds, supercritical CO_2, polarity modifier, cytotoxicity, biocompatibility.

INTRODUCTION

The key challenge in creating tissue-engineered constructs for use in tissue and regenerative medicine is the development of biodegradable highly porous scaffolds (*synonyms:* matrices, scaffolds) that could enable specific cells to be delivered to an organ requiring correction and treatment, and ensure their long-term functioning in that organ.

Today, so many scaffolds possessing the necessary complex of physicomechanical and biological properties have been developed. In their manufacture, preference is given to high-molecular-weight natural materials. Collagen, which forms the main component of the extracellular matrix (ECM) and can stimulate reparative processes, and its partially denatured derivatives, such as gelatin, are most commonly used for this purpose [1, 2]. However, collagen scaffolds undergo extremely rapid (less than 1 month) resorption when injected into the body [3, 4]. In order to increase resorption time of biopolymer-based materials, a wide range of physical and chemical cross-linking methods have been developed [5–7]. Collagen crosslinking methods using bifunctional crosslinking agent, glutaraldehyde (GA), are the most widely used. Along with the high efficiency of biopolymer structure stabilization, crosslinking with GA comes with a number of side effects including cytotoxicity of the final product [8, 9].

In natural tissues, ECM is able to provide not only physical support to cells, but also send biological signals

Corresponding author: Evgeny Nemets. Address: 1, Shchukinskaya str., Moscow, 123182, Russian Federation. Phone: (903) 579-23-79. E-mail: evgnemets@yandex.ru

selectively supporting adhesion, proliferation, and differentiation of cells of a particular tissue or organ [10, 11]. In this regard, there is great interest in scaffolds made by decellularization, a process aimed at removing cells and genetic material from the tissue while preserving not only the structural but also tissue-specific properties of ECM. Currently, a wide range of different physical, chemical and biological methods are used for decellularization of organs and tissues, among which treatment with surface-active agents (surfactants) of ionic or non-ionic nature is the most common [12–14]. One of the significant disadvantages of surfactant use for organ and tissue decellularization is the need to wash them thoroughly in buffer solutions from residual detergents for a long time (at least 72 h) [12–15]. This increases the risk of washing out significant amounts of glycans and cytokines, and can lead to disruption of matrix recellularization processes [16]. Consequently, reducing the time of contact with the aqueous phase is necessary in terms of minimizing the risk of such complications.

Recently, there has been increased interest in the use of supercritical fluids (SCF) in the creation of scaffolds for tissue engineering and regenerative medicine [17–24]. Any substance at a temperature and pressure above the critical point goes into the SCF state (Fig. 1), at which the difference between the liquid and gas phases disappears. One of the most important properties of SCF is its ability to dissolve substances, and the dissolving power increases with increasing density. Since the SCF density increases with increasing pressure at a constant temperature, changing the pressure can affect its dissolving ability [25].

Of the known SCFs, supercritical carbon dioxide (sc-CO_2) is used most often in biomedical technologies (sc-CO_2). Sc-CO_2 can be treated at temperatures close to physiological values (35–40 °C), and does not require the use of additional organic solvents. At the end of treatment, the carbon dioxide is easily and practically

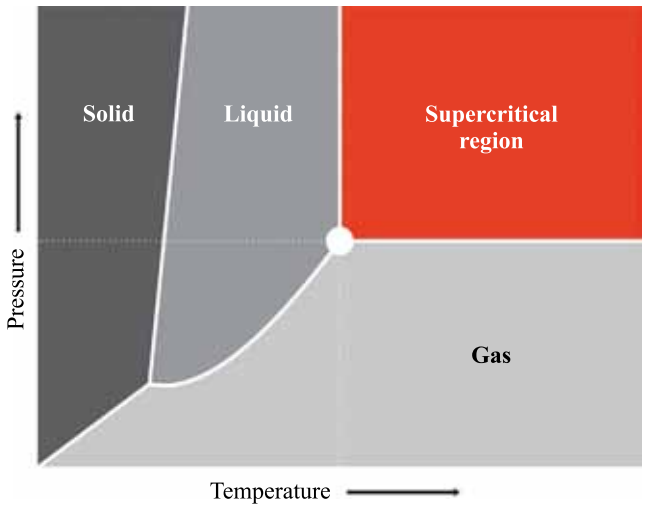

Fig. 1. Transition of substance into supercritical state

without residue removed by simple depressurization. At the same time, removal of toxic compounds soluble in sc-CO_2 (unreacted monomers and oligomers, surfactants, plasticizers, etc.) can occur, which leads to significant improvement in the biocompatible properties of the obtained materials [26].

Since carbon dioxide is a non-polar compound, to increase the efficiency of removal of polar phospholipid components of cell membranes, treatment with sc-CO_2 is performed in a hydrophilic agent, usually ethanol [27]. The addition of ethanol also makes it possible to increase the preservation of such important ECM components as collagens, glycosaminoglycans, adhesive proteins (fibronectin, laminin, etc.), as well as angiogenic factors during decellularization [28].

All this suggests that treatment with sc-CO_2 can facilitate the effective removal of cytotoxic surfactant residues and unreacted GA used in the matrix formation process for tissue engineering.

The **aim** of this work is to investigate the efficacy of sc-CO_2 to improve the biocompatibility of tubular porous scaffolds made of a copolymer composition of polyoxy(butyrate-co-valerate) and polyhydroxybutyrate-valerate-gelatin (PHBV-G) stabilized by GA and tissue-specific scaffolds made of porcine liver slices (PLSs).

MATERIALS AND METHODS

Obtaining scaffolds

Biopolymer porous tubular scaffolds (Fig. 2) from 10% (by weight) solutions of polyhydroxybutyrate-valerate (PHBV) and gelatin (type A) in hexafluoroisopropanol (all Sigma-Aldrich, USA), mixed in a 1:2 ratio (by volume), formed using electrospinning, NANON-01A unit (MECC CO, Japan). The voltage between the electrodes was 25 kV, the distance between the electrodes was 10 cm, the rod diameter was 4 mm, and the rod rotation speed was 500 rpm. The samples obtained from the composition (PHBV-G) were mechanically removed from the substrate, dried at 37 °C for 4–6 h, and vacuum-treated at 37 °C and residual pressure of 10–20 mm Hg within 18–24 hours.

Additional stabilization of the biopolymer scaffold structure by GA vapor (Serva, Germany) was performed by placing pre-swollen samples (distilled water, 24 h at room temperature) in a closed container (desiccator) containing a 25% GA solution, without direct contact of the sample with the GA solution, and incubated at room temperature for 48 h.

Decellularization of porcine liver and cartilage

Porcine liver was obtained at a slaughterhouse (Promagro Ltd, Russia) after slaughtering healthy animals (weight about 120 kg) in accordance with European Directive 64/433/EEC. After refrigerated transportation

(4 °C), the porcine liver was cut into PLSs 0.1 × 0.3 cm in size, frozen at –80 °C and stored at this temperature until decellularization began.

The hip and knee joints of the pigs were obtained at the slaughterhouse (Promagro Ltd, Russia) after the slaughter of healthy animals (weight about 120 kg) in accordance with the European Directive 64/433/EEC. After refrigerated transportation (4 °C), the cartilage was removed from articular surfaces with a scalpel, cut into 0.5 × 0.5 cm slices, frozen at –80 °C, and crushed under continuous liquid nitrogen cooling for 4 minutes at 25 Hz shaking frequency of the grinding jar using a CryoMill (Retch GmBH, Germany). Fractions of finely minced porcine cartilage particles (FMPCP) sized 30–100 μm were isolated by sifting the contents of the grinding jar through a set of sieves with appropriate cell size.

Decellularization of FMPCPs and PLSs was performed in three buffer solutions (phosphate-buffered saline (PBS), pH = 7.4) of 0.1% sodium dodecyl sulfate (SDS) and with increasing concentration (1%, 2%, and 3%) of Triton X-100 (all Sigma-Aldrich, USA) with periodic stirring (200 rpm, 3 times daily, 1 hour, at room temperature). After thorough washing from surfactants in three changes of PBS and subsequent incubation in buffer solution for 24 hours at room temperature, decellularized porcine liver slices (DPLSs) were transferred to cryotubes and stored at –80 °C until treatment with sc-CO_2.

Treatment with supercritical CO_2

Treatment in a sc-CO_2 atmosphere was done on a RESS-SAS unit (Waters corporation, USA) at T = 35 °C, 150 and 300 bar pressure, 0.25 and 2.5 mL/min sc-CO_2 feed rate for 8 or 24 hours. Ethanol at 10% concentration (by volume) was chosen as the polarity modifier.

Cytotoxicity study

Cytotoxicity of the test samples was assessed in vitro according to interstate standard GOST ISO 10993-5-2011 [29]. All procedures were performed under aseptic conditions. We used the NIH 3T3 mouse fibroblast cell line obtained from a collection of transplanted vertebrate somatic cells at Ivanovsky Institute of Virology, Moscow, Russia. The cells were seeded into 24- and 96-well flat-bottomed culture plates (Corning-Costar, USA) at a concentration of 8 × 10^4 cells/well and 2 × 10^4 cells/well, respectively, and incubated for 24 hours at 37 °C in a humid atmosphere containing 5 ± 1% CO_2 before an 80 ± 10% monolayer was formed.

At least three extracts and samples were prepared for each scaffold sample. Sodium chloride (NPK, Russia) was used as the extraction solution. The ratio of sample surface area to extraction solution volume was 3:1 cm^2/mL. Extraction time was 24 hours and temperature was 37 °C. The obtained extract was introduced into a 96-well plate with a formed cell monolayer in the volume of 100 μl/well.

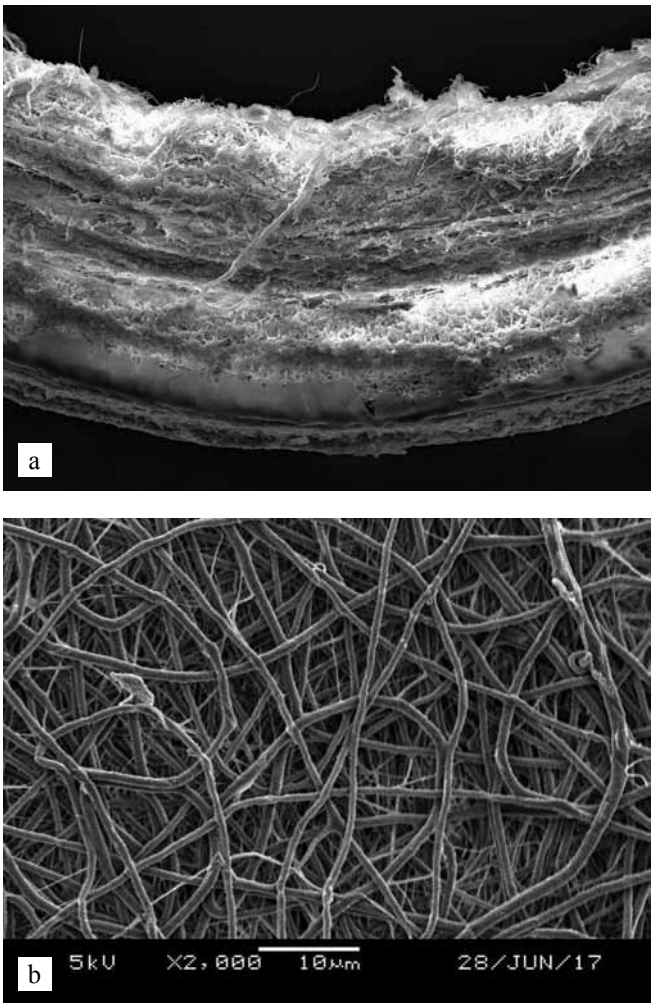

Fig. 2. Structure of a biopolymer porous tubular scaffold, d = 4 mm. a) a cross section (100× magnification); b) inner surface (2000× magnification)

For the cytotoxicity study by direct contact, the biopolymer scaffold samples (1 × 1 cm^2 and 0.1 cm thick) and tissue-specific matrices (5 mg weighed portion) were placed directly into a 24-well plate on the cell monolayer surface. The plates were incubated for 24 hours at 37 °C in a humid atmosphere containing 5 ± 1% CO_2.

On day 2 of incubation, we evaluated monolayer confluence (the degree of cell coverage of the substrate), as well as the degree of cell lysis using inverted binocular microscope MC 700 (Micros, Austria).

Negative control (K–) was DMEM culture medium with or without fetal calf serum, and the positive control (K+) was zinc solution in nitric acid: Zn 1–2 wt% in HNO_3 (Sigma-Aldrich, USA), diluted 1:100 with saline.

The results were analyzed according to the grading scale of the degree of cell reactivity:

Grade 0: No reaction, discrete intracytoplasmic granules observed, no cell lysis;

Grade 1: slight reaction, no more than 20% of cells are rounded (round, loosely attached, no intracytoplasmic granules);

Grade 2: mild reaction, no more than 50% of cells are lysed (round, loosely attached, no intracytoplasmic granules);

Grade 3: moderate reaction, no more than 70% of cells are lysed (round, loosely attached, no intracytoplasmic granules);

Grade 4: strong reaction, more than 70% of cells are lysed (almost completely destroyed monolayer).

Negative control – the degree of cell reaction is 0, cell reaction is None. Positive control – the degree of cell reaction is 3 or 4. The reactivity of the extract under study must not exceed grade 0 (reaction None).

The study of prolonged (up to 72 hours) cytotoxic effect under direct contact of the cells with the samples under study was performed using the IncuCyte Zoom interactive optical system for long-term cell research (Essen BioScience, USA). This complex allows you to incubate cells under standard conditions and microscopy the culture plate at specified time intervals with image photofixation. Analysis of the obtained images using the built-in software makes it possible to calculate the change in the cell monolayer confluence for each sample as a function of time.

The effect of cytotoxic residues on the proliferative activity of NIH 3T3 fibroblasts was studied using an interactive optical system IncuCyte Zoom, which allows real-time recording of cell growth curves on the surface of the culture plate during direct contact with the test sample.

Statistical data processing was performed using the standard Microsoft Excel software package. The level of statistical significance was $p < 0.05$.

RESULTS AND DISCUSSION

Before treatment with sc-CO_2, the cytotoxicity of the extracts was "moderate" (grade 3) in the case of biopolymer scaffolds and at grade 4 (acute cytotoxic reaction) for tissue-specific scaffolds.

After exposure to sc-CO_2, regardless of the choice of treatment mode, the extracts from biopolymer scaffolds as well as FMPCP and DPLS matrices were not cytotoxic (grade 0). At the same time, under conditions of direct contact with the NIH 3T3 monolayer, the samples showed cytotoxicity, whose severity depended on treatment conditions.

Treatment of scaffolds with sc-CO_2 at a low feed rate (0.25 ml/min) turned out to be little effective. The greatest reduction in the level of cytotoxicity to "mild" (level 2) was achieved after prolonged treatment (24 hours) of DPLS samples in sc-CO_2 medium with the addition of ethanol. However, this result does not meet the GOST ISO 10993-5-2011 standards.

Increasing the sc-CO_2 feed rate to 2.5 mL/min had a positive effect on the treatment efficiency of both biopolymer and tissue-specific scaffolds (Tables 1 and 2).

Treatment of biopolymer scaffolds with sc-CO_2 at 2.5 mL/min feed rate and 150 bar pressure was marginally effective even when ethanol was added (Table 1). Increasing the sc-CO_2 pressure to 300 bar was accompanied by a marked decrease in cytotoxicity to "insignificant" (level 1) after 24 hours of exposure (Table 1). Only the addition of ethanol into the sc-CO_2 composition makes it possible to achieve a complete absence of cytotoxic effect of biopolymer scaffolds at 300 bar pressure after 8 hours of treatment (Table 1).

In the case of DPLS scaffolds, increasing the sc-CO_2 feed rate has a more pronounced effect on reducing cytotoxicity (Table 2). In the case of samples treated for 24 hours with individual sc-CO_2 at 150 bar pressure, cytotoxicity decreases to "insignificant" (level 1). The addition of ethanol makes it possible to completely suppress the cytotoxicity of scaffolds already after 8 hours of sc-CO_2 treatment.

Increasing the pressure from 150 to 300 bar enhances the effect of treating DPLSs with sc-CO_2 (Table 2). Complete absence of cytotoxicity (level 0) was obtained after 8 hours of exposure to sc-CO_2 without adding ethanol.

It should be particularly noted that the samples treated with regimens that provided effective surfactant removal demonstrated the absence of cytotoxicity not

Table 1

Cytotoxicity of porous biopolymer scaffolds (sc-CO_2 feed rate 2.5 mL/min)

	Ethanol, %	Pressure, bar	Time, hour	Cytotoxicity
1	Control (without sc-CO_2 treatment)			Moderate (3)
2	–	150	8	Moderate (3)
3	–	150	24	Moderate (3)
4	10	150	8	Mild (2)
5	10	150	24	Mild (2)
6	–	300	8	Mild (2)
7	–	300	24	Insignificant (1)
8	10	300	8	None (0)
9	10	300	24	None (0)

only after 24 hours of direct contact with cells, but also under prolonged direct contact with cells for 72 hours.

The obtained results suggest that for effective washing from cytotoxic surfactant residues, DPLS treatment should be performed for 8 hours at 35 °C temperature, sc-CO_2 feed rate of 2.5 ml/min and a pressure of 300 bar in an atmosphere of pure carbon dioxide. A similar result can be achieved by treatment at a pressure of 150 bar with the addition of a polarity modifier (ethanol) to the supercritical fluid.

Methods of decellularization under the influence of detergents [12–15] involve a long (at least 72 hours) washing of obtained scaffolds from cytotoxic surfactants, which increases the risk of washing out significant amounts of bioactive molecules (glycosaminoglycans and cytokines) that play an important role in scaffold recellularization.

Table 2

Cytotoxicity of tissue-specific scaffold (sc-CO_2 feed rate 2.5 mL/min)

	Ethanol	Pressure, bar	Time, hour	Cytotoxicity
1	Control (without sc-CO_2 treatment)			Severes (4)
2	–	150	8	Mild (2)
3	–	150	24	Insignificant (1)
4	10%	150	8	None (0)
5	10%	150	24	None (0)
6	–	300	8	None (0)
7	–	300	24	None (0)
8	10%	300	8	None (0)
9	10%	300	24	None (0)

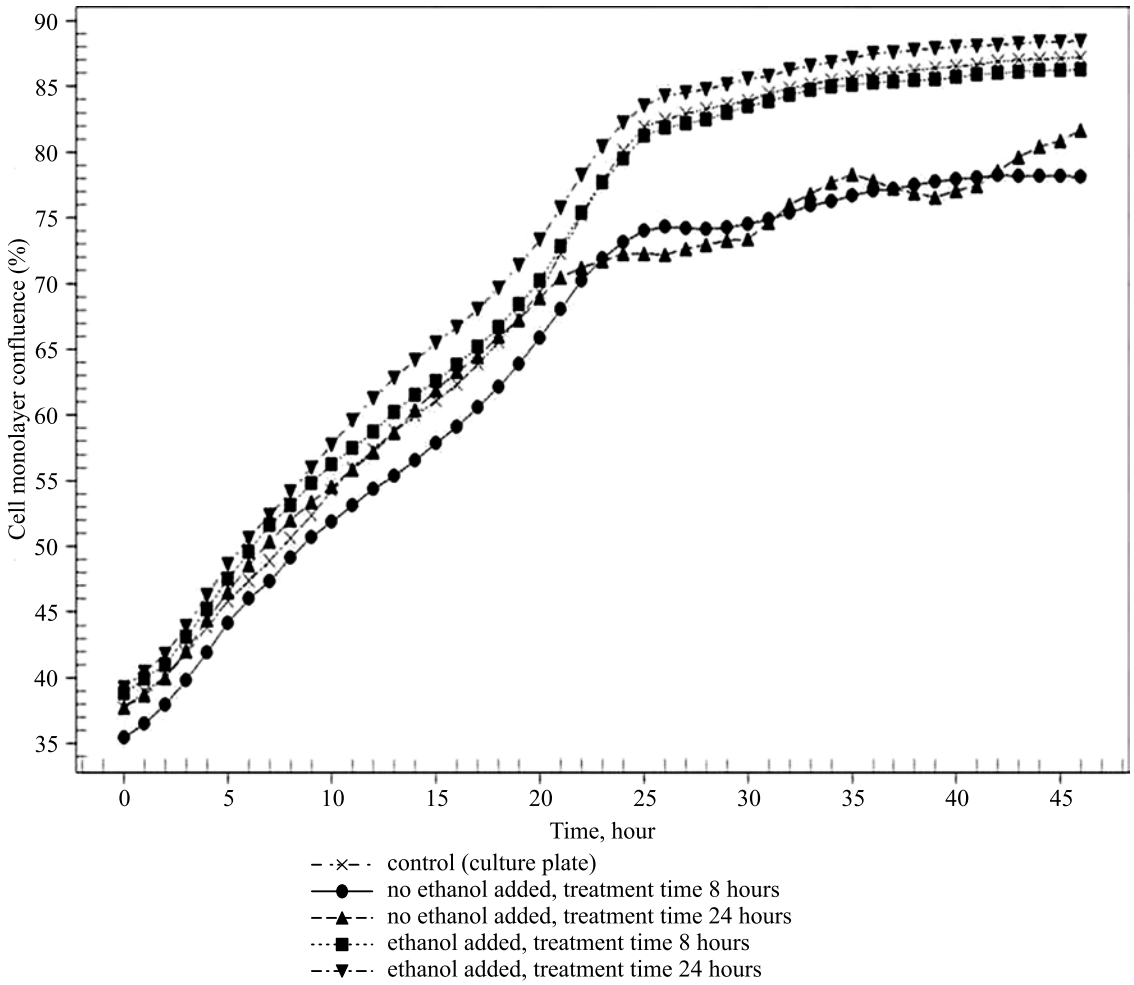

Fig. 3. Growth curve of NIH 3T3 cells in the presence of DPLS matrices, treated with sc-CO_2 (300 bar, 35 °C, sc-CO_2 feed rate 2.5 mL/min)

The use of SCF treatment can reduce to 24 hours the time of surfactant removal in an aqueous medium.

To reveal the effect of cytotoxic residues on cell proliferative activity, an additional study was performed using interactive optical system IncuCyte Zoom, which allows real-time recording of changes in cell proliferative activity in the presence of scaffolds.

For this study, samples were selected that demonstrated the absence of cytotoxic effect using the evaluation scale and were obtained under the same sc-CO_2 treatment conditions: feed rate 2.5 ml/min, pressure 300 bar (Table 2, samples 6–9).

A marked decrease in NIH 3T3 proliferative activity was observed immediately after the introduction of samples (20 hours after seeding the cells on the culture plate) in the case of sc-CO_2-treated samples without the addition of ethanol (Fig. 3). At the same time, ethanol-treated scaffolds did not induce a decrease in cell proliferation compared to the control (cells on culture plate.

Microscopic examination carried out after the end of the experiment to study the growth of NIH 3T3 in the presence of sc-CO_2-treated DPLS scaffolds in different regimens (Fig. 4) confirmed the absence of any signs of negative effects on cells (lysis, scoring), which once again confirms the conclusion made earlier that the samples studied have no cytotoxicity. However, the decrease in the proliferative activity of cells detected in contact with sc-CO_2-treated scaffolds without the addition of ethanol suggests the presence of a cytostatic effect in this case.

FMPCP scaffolds treated under conditions that are optimal for enhancing the biocompatibility of porcine liver scaffolds (sc-CO_2 2.5 ml/min with the addition of ethanol; 35 °C; 300 bar; 8 hours) also showed no cytotoxicity (level 0). Meanwhile, the presence of decellu-

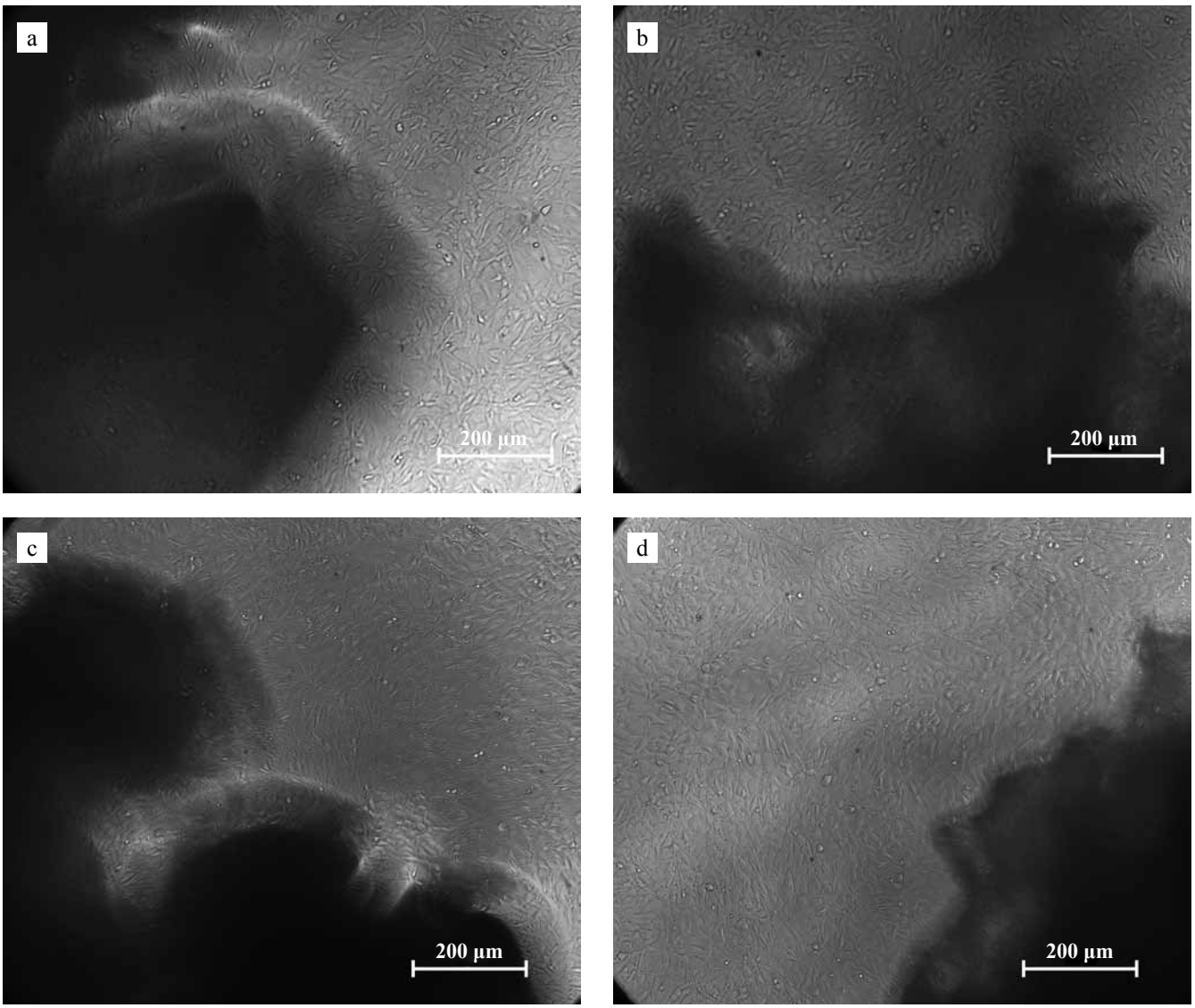

Fig. 4. Cell populations after 48 hours of culturing NIH 3T3 in the presence of sc-CO_2-treated PLS matrices (300 bar, 35 °C, 2.5 mL/min). a) sc-CO_2, 8 hours; b) sc-CO_2, 24 hours; c) sc-CO_2 + ethanol, 8 hours; d) sc-CO_2 + ethanol, 24 hours. 100× magnification

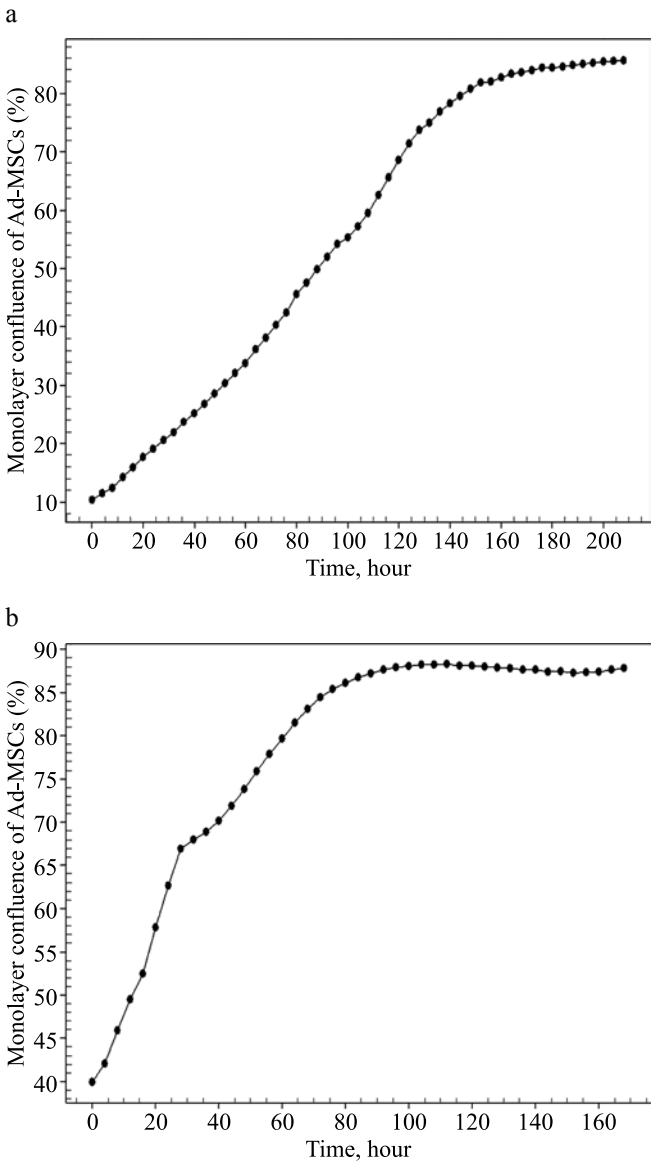

Fig. 5. Growth curve of NIH 3T3 cells on the surface of culture plate in the absence (a) and presence (b) of FMPCP matrices treated with supercritical fluids in the optimal mode (sc-CO_2 2.5 mL/min + ethanol, 300 bar, 35 °C, 8 hours)

larized fine cartilage particles not only has no cytostatic effect on human adipose tissue-derived mesenchymal stem cells (Ad-MSCs), but also demonstrates a stimulating effect on cell proliferation (Fig. 5): the time for the confluent monolayer level to rise to 80% in the presence of decellularized cartilage particles is noticeably shorter. Probably, the reason for this is the presence of signaling molecules in the decellularized cartilage matrix that accelerate Ad-MSC adhesion and proliferation, which coincides with experimental results described in reports [30].

Thus, from the point of view of suppression of both cytotoxic and cytostatic effect of tissue-specific matrices after decellularization using detergents, SCF treatment regimens based on carbon dioxide containing ethanol additives are therefore optimal. In our opinion, the reason for this is that both non-ionic (Triton X-100) and ionic (SDS) detergents are present in the composition of the decellularizing solution. Supercritical carbon dioxide is a nonpolar solvent whose efficiency, in terms of removing polar surfactant, is sufficient to eliminate cytotoxic effect, but not sufficient to suppress cytostatic effect. Addition of polar ethanol (polarity modifier) can reduce the SDS content to levels that are not capable of exerting a cytostatic effect.

CONCLUSION

Sc-CO_2 treatment is an effective way of enhancing the biocompatibility of three-dimensional porous matrices obtained using cytotoxic substances: bifunctional cross-linking agents for biopolymer scaffolds and surfactants, in the case of tissue-specific matrices FMPCP and DPLSs. Adding ethanol as a polarity modifier improves the treatment efficiency by eliminating both cytotoxic and cytostatic effects.

The work was supported by a grant (No. 21-15-00251) from the Russian Science Foundation.

The authors declare no conflict of interest.

REFERENCES

1. *Surguchenko VA*. The matrices for tissue engineering and hybrid organs. Biocompatible materials (textbook). Ed. by: V.I. Sevastianov, M.P. Kirpichnikov. M.: MIA, 2011. Chast' II: 199–228.
2. *Sevastianov VI, Basok YB, Grigor'ev AM, Kirsanova LA, Vasilets VN.* Formation of tissue-engineered construct of human cartilage tissue in a flow-through bioreactor. *Bull Exp Biol Med*. 2017; 164 (2): 269–273. doi: 10.1007/s10517-017-3971-z.
3. *Goissis G, Suzigan S, Parreira DR, Maniglia JV, Braile DM, Raymundo S.* Preparation and characterization of collagen-elastin matrices from blood vessels intended as small diameter vascular grafts. *Artif Organs*. 2000; 24: 217–223. doi: 10.1046/j.1525-1594.2000.06537.x. PMID: 10759645.
4. *Busra MFM, Lokanathan Y*. Recent development in the fabrication of collagen scaffolds for tissue engineering applications: A review. *Curr Pharm Biotechnol.* 2019; 20 (12): 992–1003. doi: 10.2174/1389201020666190731121016. PMID: 31364511.
5. *Oryan A, Kamali A, Moshiri A, Baharvand H, Daemi H.* Chemical crosslinking of biopolymeric scaffolds: Current knowledge and future directions of crosslinked engineered bone scaffolds. *Int J Biol Macromol*. 2018; 107 (Pt A): 678–688. doi: 10.1016/j.ijbiomac.2017.08.184.
6. *Kawecki M, Łabuś W, Klama-Baryla A, Kitala D, Kraut M, Glik J et al*. A review of decellurization methods caused by an urgent need for quality control of cell-free extracellular matrix' scaffolds and their role in regenerative medicine. *J Biomed Mater Res B Appl Biomater*. 2018; 106 (2): 909–923. doi: 10.1002/jbm.b.33865. PMID: 28194860.

7. *Rose JB, Pacelli S, Haj AJE, Dua HS, Hopkinson A, White LJ et al*. Gelatin-based materials in ocular tissue engineering. *Materials (Basel)*. 2014; 7 (4): 3106–3135. doi: 10.3390/ma7043106. PMID: 28788609.
8. *Nemets EA, Pankina AP, Sevastianov VI*. Comparative analysis of methods for increasing of biostability of collagen films. *Inorganic Materials: Applied Research*. 2017; 5: 718–722.
9. *Umashankar PR, Arun T, Kumari TV*. Short duration gluteraldehyde cross linking of decellularized bovine pericardium improves biological response. *J Biomed Mater Res*. 2011; 97 (3): 311–320. doi: 10.1002/jbm.a.33061. PMID: 21448995.
10. *Gattazzo F, Urciuolo A, Bonaldo P*. Extracellular matrix: a dynamic microenvironment for stem cell niche. *Biochim Biophys Acta*. 2014; 1840 (8): 2506–2519. doi: 10.1016/j.bbagen.2014.01.010. PMID: 24418517.
11. *Sun Y, Wang TL, Toh WS, Pei M*. The role of laminins in cartilaginous tissues: from development to regeneration. *Eur Cell Mater*. 2017; 34: 40–54. doi: 10.22203/eCM.v034a0.
12. *Shirakigawa N, Ijima H*. Decellularized tissue engineering. *Advanced Structured Materials*. 2017; 66: 185–226. doi: 10.1007/978-981-10-3328-5_5.
13. *Crapo PM, Gilbert TW, Badylak SF*. An overview of tissue and whole organ decellularization processes. *Biomaterials*. 2011; 32 (12): 3233–3243. doi: 10.1016/j.biomaterials.2011.01.057. PMID: 21296410.
14. *Gilpin A, Yang Y.* Decellularization strategies for regenerative medicine: From processing techniques to applications. *Biomed Res Int*. 2017; 2017: 9831534. doi: 10.1155/2017/9831534. PMID: 28540307.
15. *Gautier SV, Sevastyanov VI, Shagidulin MYu, Nemets EA, Basok YuB*. Tkanespetsificheskiy matriks dlya tkanevoy inzhenerii parenkhimatoznogo organa i sposob ego polucheniya. Patent na izobretenie RU 2693432 C2, 02.07.2019.
16. *Kawasaki T, Kirita Y, Kami D, Kitani T, Ozaki C, Itakura Y et al*. Novel detergent for whole organ tissue engineering. *J Biomed Mater Res A*. 2015; 103 (10): 3364–3373. doi: 10.1002/jbm.a.35474. PMID: 25850947.
17. *Song C, Luo Y, Liu Y, Li S, Xi Z, Zhao L et al*. Fabrication of PCL scaffolds by supercritical CO_2 foaming based on the combined effects of rheological and crystallization properties. *Polymers (Basel)*. 2020; 12 (4): 780. doi: 10.3390/polym12040780. PMID: 32252222.
18. *Nemets EA, Belov VJu, Ilina TS, Surguchenko VA, Pankina AP, Sevastianov VI*. Composite porous tubular biopolymer matrix of small diameter. *Perspektivnye materialy*. 2018; 9: 49–59. [In Russ, English abstract]. doi: 10.30791/1028-978X-2018-9-49-59.
19. *White LJ, Hutter V, Tai H, Howdle SM, Shakesheff KM*. The effect of processing variables on morphological and mechanical properties of supercritical CO_2 foamed scaffolds for tissue engineering. *Acta Biomater*. 2012; 8 (1): 61–71. doi: 10.1016/j.actbio.2011.07.032. PMID: 21855663.
20. *Antons J, Marascio MG, Aeberhard P, Weissenberger G, Hirt-Burri N, Applegate LA et al*. Decellularised tissues obtained by a CO_2-philic detergent and supercritical CO_2. *Eur Cell Mater*. 2018, 36: 81–95. doi: 10.22203/eCM.v036a07. PMID: 30178445.
21. *Casali DM, Handleton RM, Shazly T, Matthews MA*. A novel supercritical CO_2-based decellularization method for maintaining scaffold hydration and mechanical properties. *J Supercrit Fluids*. 2018; 131: 72–81. doi: 10.1016/j.supflu.2017.07.021.
22. *Huang YH, Tseng FW, Chang WH, Peng IC, Hsieh DJ, Wu SW et al*. Preparation of acellular scaffold for corneal tissue engineering by supercritical carbon dioxide extraction technology. *Acta Biomater*. 2017; 58: 238–243. doi: 10.1016/j.actbio.2017.05.060. PMID: 28579539.
23. *Gil-Ramírez A, Rosmark O, Spégel P, Swärd K, Westergren-Thorsson G, Larsson-Callerfelt AK et al*. Pressurized carbon dioxide as a potential tool for decellularization of pulmonary arteries for transplant purposes. *Sci Rep*. 2020; 10 (1): 4031. doi: 10.1038/s41598-020-60827-4. PMID: 32132596.
24. *Razgonova MP, Zaharenko AM, Sergievich AA, Kalenik TK, Golohvast KS*. Sverhkriticheskie fljuidy: teorija, jetapy stanovlenija, sovremennoe primenenie: uchebnoe posobie. SPb.: Lan', 2019. 192.
25. *Alekseev ES, Alent`ev AYu, Belova AS, Bogdan VI et al*. Supercritical fluids in chemistry. *Rus Chem Rev.* 2020; 89: 1337–1427. [In Russ, English abstract]. doi: 10.1070/RCR4932.
26. *Popov VK*. Implantaty v zamestitel'noj i regenerativnoj medicine kostnyh tkanej. *Biosovmestimye materialy (uchebnoe posobie)*. Pod red. V.I. Sevast'janova, M.P. Kirpichnikova. M.: MIA, 2011. Chast' II: 271–294.
27. *Ingrosso F, Ruiz-López MF.* Modeling Solvation in Supercritical CO_2. *Chemphyschem.* 2017; 18: 2560–2572. doi: 10.1002/cphc.201700434.
28. *Seo Y, Jung Y, Kim SH*. Decellularized heart ECM hydrogel using supercritical carbon dioxide for improved angiogenesis. *Acta Biomater*. 2018; 67: 270–281. doi: 10.1016/j.actbio.2017.11.046. PMID: 29223704.
29. GOST ISO 10993-5-2011 "Izdelija medicinskie. Ocenka biologicheskogo dejstvija medicinskih izdelij. Chast' 5. Issledovanija na citotoksichnost': metody *in vitro*".
30. *Sun Y, Yan L, Chen S, Pei M*. Functionality of decellularized matrix in cartilage regeneration: A comparison of tissue versus cell sources. *Acta Biomater.* 2018; 74: 56–73. doi: 10.1016/j.actbio.2018.04.048. PMID: 29702288.

The article was submitted to the journal on 8.04.2021

DOI: 10.15825/1995-1191-2021-2-114-121

COMPARATIVE ANALYSIS OF PHARMACOKINETIC PARAMETERS OF TRANSDERMAL AND INTRAMUSCULAR ADMINISTRATION OF GALAVIT®

E.G. Kuznetsova[1], O.M. Kuryleva[1], L.A. Salomatina[1], S.V. Kursakov[2], Z.Z. Gonikova[1], A.O. Nikolskaya[1], V.I. Sevastianov[1, 2]

[1] Shumakov National Medical Research Center of Transplantology and Artificial Organs, Moscow, Russian Federation

[2] Institute of Biomedical Research and Technology, Moscow, Russian Federation

Introduction. Immunomodulator Galavit® is a promising domestic drug for the prevention and treatment of various infectious diseases. Earlier, the authors have developed and investigated in vitro its new dosage form – transdermal therapeutic system (TTS). Positive results from experiments made it possible to proceed to the study of the pharmacokinetic parameters of Galavit® TTS in animals. **Objective:** to compare the pharmacokinetic parameters of intramuscular and transdermal administration of immunomodulator Galavit® in animal experiments. **Materials and methods.** Sodium aminodihydrophthalazinedione was used as a substance in the form of a powder to prepare a solution for intramuscular administration of 100 mg (trade name Galavit®, manufacturer SELVIM LLC). The pharmacokinetics of transdermal and intramuscular injections were studied in male Chinchilla rabbits weighing 4.5–5.0 kg. Serum sodium aminodihydrophthalazinedione concentrations in animals were determined by high-performance liquid chromatography using a specially developed technique. **Results.** In contrast to the injection method, a prolonged and uniform inflow of the drug substance (MP) into the body is observed for percutaneous administration of sodium aminodihydrophthalazinedione. The maximum serum Galavit® concentration for a 40 mg dose (0.172 ± 0.054 μg/mL) and for a 80 mg dose (1.16 ± 0.22 μg/mL) remained at a constant level for 9 and 8 hours, respectively. The relative bioavailability of the Galavit® transdermal therapeutic system was 0.65 and 1.06 for the same doses. **Conclusion.** Application of Galavit® 80 mg transdermal therapeutic system provides bioavailability that is similar to the intramuscular administration of this drug at the same dose. At the same time, its maximum serum concentration significantly decreases and the retention time of Galavit® in the body increases by more than 10 times, which can contribute to prolongation of the drug effect. Due to the current growing interest in the use of immunomodulator Galavit® for coronavirus infection COVID-19, the development and study of a new dosage form is a promising task.

Keywords: transdermal therapeutic system, sodium aminodihydrophthalazinedione, immunomodulator, pharmacokinetics.

INTRODUCTION

Over the past decades, scientific research in the development and implementation of highly active and competitive dosage forms in medical practice has been intensifying. More attention is being directed towards new systems and means for delivering medicinal substances with improved biopharmaceutical characteristics that increase therapeutic efficacy, tolerability and safety of drug therapy [1, 2]. One of these areas is the creation of transdermal therapeutic systems (TTS) – controlled-release dosage forms designed to continuously deliver the drugs they contain through intact skin into systemic circulation for a long (limited only by medical indications) time at a predetermined rate. The use of TTS increases the bioavailability of drugs, and also excludes the shortcomings of other methods by which it can be administered [3, 4].

Currently, the legitimacy and effectiveness of the use of immunotropic drugs that activate innate and adaptive immune systems for preventing and treating infectious diseases and a number of other diseases is widely discussed in the medical scientific literature [5].

A representative of this group of drugs is Russian synthetic drug Galavit® (aminodihydrophthalazinedione sodium is the active ingredient), which has immunomodulatory and pronounced anti-inflammatory properties.

Numerous studies have confirmed the efficacy of this drug in the complex immunocorrective therapy of patients with viral and bacterial pyoinflammatory diseases [6, 7]. For example, sodium aminodihydrophthalazinedione has been shown to reduce the severity of catarrhal and intoxication syndromes and significantly reduce duration in influenza diseases [8]. According to another study, this drug reduces the frequency and duration of

Corresponding author: Evgenia Kuznetsova. Address: 1, Shchukinskaya str., Moscow, 123182, Russian Federation. Phone: (499) 196-26-61. E-mail: kuzeugenia@gmail.com

infection, it reduces the need for antibiotic therapy and normalizes the immune status in children with frequent acute respiratory viral infection [9].

The authors have previously developed and investigated in vitro a transdermal therapeutic system [10, 11] containing sodium aminodihydrophthalazinedione. The results of the experiments showed the fundamental possibility of transdermal drug transfer, which made it possible to proceed to the study of TTS Galavit® in animals in vivo.

Creation of dosage forms includes a number of mandatory steps, one of which is the study of pharmacokinetics. An experimental study of the pharmacokinetic parameters of a drug allows one to predict the plasma drug concentration, choose an approximate dosing regimen, which is then adjusted during clinical trials [12]. Various methods can be used to determine the plasma drug concentration, which reliably monitor the concentration of a pharmacological agent under the selected conditions of a pharmacokinetic experiment and meet the general requirements of selectivity, accuracy, and reproducibility. The most commonly used method is high-performance liquid chromatography (HPLC) [13–15].

The **objective** of this work is to compare the pharmacokinetic parameters of intramuscular and transdermal administration of the immunomodulator Galavit® in animal experiments.

MATERIALS AND METHODS

Materials

The substance was sodium aminodihydrophthalazinedione in the form of a powder for preparing a solution for intramuscular administration of 100 mg (trade name Galavit®, manufacturer SELVIM LLC). Its molecular weight is 206 Da.

In the manufacture of laboratory samples of Galavit®, auxiliary substances and materials approved for medical use, and which meets the requirements of the current regulatory documentation were used.

The microemulsion composition with Galavit® included the following components: purified water (FS.2.2.0019.18), 0.9% sodium chloride solution (ESCOM, Russia), sodium dodecyl sulfate (AppliChem Panreac, Spain), apricot kernel oil (Desert Whale Jojoba Company Ltd., USA), α-tocopherol acetate (BASF SE, Germany), docusate sodium (Sigma, USA), Decaglyn PR-20 emulsifier (Nikko Chemicals Co., Ltd, Japan).

To create TTS Galavit®, the following components were selected: elastic microspongy material Foam tape 9773 (3M, USA), sorbent base PALV-01 (Palma Group of Companies, Russia), and Skotchpak 9730 film (3M, USA).

The following reagents were also used: sodium citrate (NPO RENAM, Russia), potassium phosphate 2-substituted, 3-water (Panreac, Spain), potassium phosphate 1-substituted (PCGroup, Russia), potassium hydroxide (Panreac, Spain), acetonitrile for chromatography (Panreac, Spain), trifluoroacetic acid (Merck, Germany), syringe filters (celluloseacetate, 0.45 μm, 25 mm, Agilent Technologies, Germany).

Equipment

Equipment used: disperser Heidolph DIAX 900 (Germany), ultrasonic homogenizer HeilscherUIS250V, analytical balance (GH-200 AND, Japan), centrifuge Hettich Rotina 38R (Germany), liquid chromatograph Agilent 1200 (Agilent Technologies, USA), equipped with UV detector, autosampler, degasser and column oven.

Methodology for pharmacokinetic study of Galavit® with intramuscular administration and with the use of transdermal therapeutic system

The study of the pharmacokinetics of sodium aminodihydrophthalazinedione with transdermal and intramuscular administration was performed on male Chinchilla rabbits weighing 4.5–5.0 kg.

The rabbits were obtained from the laboratory animal nursery belonging to Krolinfo Ltd. The producer provided a veterinary certificate for the latest animal health control. All experimental animals were bred on purpose and had not previously participated in a study. Quarantine period was 14 days. All manipulations with the animals were carried out in accordance with the rules adopted by the European Convention for the Protection of Vertebrate Animals Used for Experimental and other Scientific Purposes (ETS 123) Strasbourg, 1986).

The plasma concentration of sodium aminodihydrophthalazindione in rabbits during transdermal and intramuscular injections was studied according to the developed design. The animals were divided into four groups of 3 animals each. The first and second groups were injected once intramuscularly in doses of 40 and 80 mg; in the third and fourth groups, percutaneous administration of Galavit® in the same doses was studied.

TTS was applied to a pre-shaved area of the back skin at the base of the neck. The drug was glued to healthy skin no earlier than a day after the hair removal procedure.

Blood sampling of animals was performed before the drug was administered, as well as at discrete time intervals from the marginal ear vein into test tubes with 3.8% sodium citrate solution. Blood sampling times for TTS were 1, 2, 4, 6, 12, 15, 18, 20 and 24 hours of application. For the injectable form of the immunomodulator – 3, 6, 10, 20, 30, 40, 50 minutes, 1, 2, 3, 4, 5, 6, 7 hours after drug administration. Test tubes were centrifuged for 5 minutes at 1500 rpm, then plasma was carefully collected. The plasma levels of sodium aminodihydrophthalazinedione in the rabbits was measured by high-

performance liquid chromatography using a specially developed technique.

HPLC technique for quantifying plasma concentration of sodium aminodihydrophthalazinedione in the experimental animals

Sample preparation

Blood plasma was transferred into a 2.0 mL microcentrifuge tube and 200 µl of a 50% solution (by volume) of trifluoroacetic acid was added. The mixture was stirred on a vortex shaker for 2 minutes and centrifuged at 6000 rpm for 10 minutes. 500 µl of supernatant was transferred into a 1.5 mL HPLC microvial, 55 µL of a 50% potassium hydroxide solution (by weight) was added, and the mixture was stirred.

Chromatographic analysis

Chromatographic determination was performed on an Agilent 1200 liquid chromatograph under the following conditions:

Chromatographic column: Mediterranea Sea 18 25 × 0.46 cm, 5 µm (Teknokroma Analitica SA, Spain) with an 8 × 4 mm guard column filled with the same sorbent.

Mobile phase: acetonitrile: 0.015% solution (by volume) of trifluoroacetic acid, pH = 2.5 (15:85). The mobile phase was pre-filtered and degassed on a vacuum filtration device.

Mobile phase flow rate: 0.8 mL/min.

Elution mode: isocratic.

Column oven temperature: 25 °C.

Injected sample volume: 10 µL.

Detection: 221 nm.

Chromatography time: 16 min

Retention time: about 11.7 minutes.

Chromatograms were registered and processed using the ChemStation software (Agilent, USA). Results were statistically processed using Microsoft Office Excel 2003 software.

Lower limit of Galavit® quantification: 50.0 ng/mL.

Linearity range of the method: 50.0–2000 ng/mL.

Calculation of pharmacokinetic parameters

The pharmacokinetic method of study allows one to give a number of quantitative characteristics to absorption, metabolism (biotransformation), distribution and excretion of drugs from the body. For this, the following parameters were calculated:

- C_{max} – maximum plasma drug concentration (µg/mL).
- T_{max} – time to reach maximum drug concentration (h).
- AUC – total area under the plasma drug concentration-time curve from the moment it enters the body until complete elimination from the body (h·µg/mL).
- AUMC – total area under the curve of the product of time and plasma drug concentration from the moment it enters the body until its complete removal from the body (h^2·µg/mL).
- $T_{1/2}$ – drug elimination half-life – a period characterizing the rate of drug concentration decrease in the body fluids and tissues (h).
- MRT – mean residence time of drug in the body (h).
- β – elimination rate constant (h^{-1}).
- F – bioavailability. The relative bioavailability was determined by comparison with the bioavailability after intramuscular administration and was calculated using the formula:

$$F = \frac{AUC_{(TTS)} \times D_{(Injection)}}{AUC_{(Injection)} \times D_{(TTS)}},$$

where AUC is the area under the kinetic curve, D is the drug dose.

Pharmacokinetic parameters were estimated by a model-independent approach.

Statistical processing of results

Results were processed statistically in accordance with OFS.1.1.0013.15 "Statistical processing of chemical experiment results" using Microsoft Office Excel 2010 software. In addition, a two-sided Student's t-test was used [16]. Differences were considered statistically significant at $p < 0.05$.

RESULTS AND DISCUSSION

A comparative analysis of pharmacokinetic parameters in transdermal and intramuscular injections of immunomodulator Galavit® in vivo was carried out.

The averaged pharmacokinetic curves of sodium aminodihydrophthalazinedione with TTC application and intramuscular injection at 40 mg and 80 mg dose are shown in Figs. 1 and 2, respectively.

As seen in Fig. 1, with intramuscular injection of 40 mg of sodium aminodihydrophthalazinedione, the maximum plasma concentration was reached after 10 minutes and was about 11.6 ± 0.9 µg/mL. At 30 minutes, there was a sharp 2-fold decrease in the plasma drug concentration. After 2 hours, it decreased to 0.324 ± 0.050 µg/mL, and after 4 hours it was below the quantification limit. With transdermal administration of the same dose of the drug, the plasma concentration of the immunomodulator increased slowly. By the fourth hour, the drug content in the blood was 0.123 ± 0.037 µg/mL. After 6 hours, it reached a maximum level of 0.172 ± 0.054 µg/mL and remained constant within the statistical error for the next 9 hours ($p > 0.05$). Further, we noted a gradual decrease in the plasma drug levels. By 24 hours of application, plasma concentration of sodium aminodihydrophthalazinedione in the animals was 0.099 ± 0.034 µg/mL.

When the dose of sodium aminodihydrophthalazindione was increased to 80 mg, the maximum plasma drug level after intramuscular injection increased 2-fold and was 23.2 ± 1.0 μg/mL by 10 minutes (Fig. 2). One hour after injection, there was a sharp drop to 3.82 ± 0.42 μg/mL. After 7 hours, concentration of the immunomodulator was below the quantification level. With percutaneous administration of Galavit®, the maximum concentration was 1.16 ± 0.22 μg/mL 6 hours after the start of application of the transdermal system. Note that from 4 to 12 hours of the study, the plasma drug concentration in the animals was almost constant ($p > 0.05$).

Thus, with percutaneous administration of sodium aminodihydrophthalazinedione, we observed prolonged and uniform flow of the drug substance into the blood, while maintaining its concentration in the blood at a constant level for 8–9 hours.

Note that with intramuscular administration of immunomodulator Galavit®, a 2-fold increase in the dose resulted in a 2-fold increase in the maximum plasma drug concentration. In the case of percutaneous administration, the same two-fold dose change caused a 6.7-fold increase in the maximum plasma drug level. Such an increase in the diffusion flux of the drug through the skin,

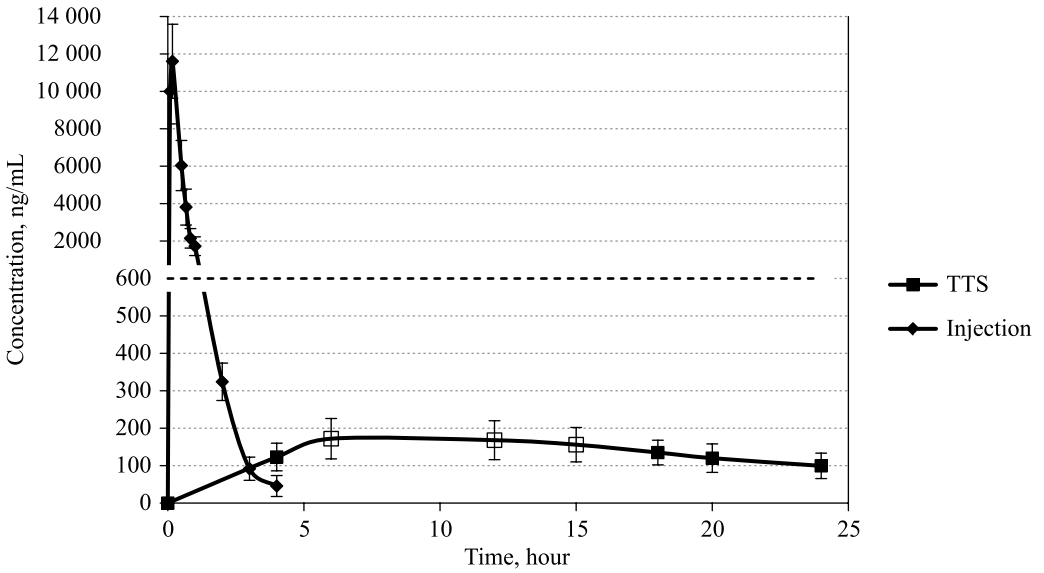

Fig. 1. Averaged dynamics of the concentration (±σ) of sodium aminodihydrophthalazinedione in the blood plasma of experimental animals with intramuscular and transdermal administration of a 40 mg dose. Differences in point values (□) are statistically insignificant ($p > 0.05$)

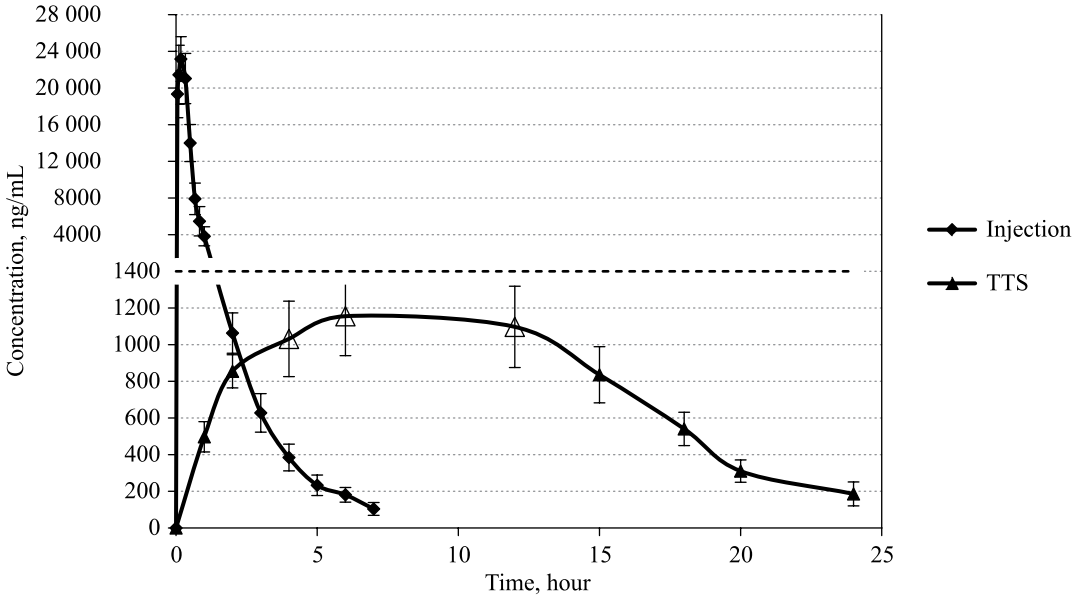

Fig. 2. Averaged dynamics of the concentration (±σ) of sodium aminodihydrophthalazinedione in the blood plasma of experimental animals with intramuscular and transdermal administration of a 80 mg dose. Differences in point values (Δ) are statistically insignificant ($p > 0.05$)

disproportionate to the increase in the drug content in TTS Galavit®, should be taken into account when selecting a therapeutic dose in a transdermal form.

The calculated pharmacokinetic parameters of sodium aminodihydrophthalazinedione at a single transdermal and intramuscular administration of two different doses to experimental animals are presented in Table.

Table

Pharmacokinetic parameters of sodium aminodihydrophthalazinedione in rabbits with transdermal and intramuscular administration

Parameters	Administration route, dose			
	Transdermal		Intramuscular	
	40 mg (n = 3)	80 mg (n = 3)	40 mg (n = 3)	80 mg (n = 3)
C_{max}, μg/mL	0.172	1.155	11.6	23.2
T_{max}, h	6	6	0.17	0.17
β, 1/h	0.0702	0.1686	2.74	1.81
$T_{1/2}$, h	9.8	4.6	0.25	0.38
AUC, h·μg/mL	4.7	18.6	7.21	17.54
AUMC, h^2·μg/mL	39.4	187.7	3.98	14.71
MRT, h	8.4	10.1	0.55	0.84

The decrease in sodium aminodihydrophthalazindione concentration in the blood after the steady-state period with TTC application was characterized by $T_{1/2}$ half-life, which was approximately 9.8 hours for a 40 mg dose and 4.6 hours for a 80 mg dose. The mean residence time of drug in the body (MRT) was approximately 8.4 hours and 10.1 hours for the lower and higher drug content in the TTS, respectively.

With intramuscular administration of the immunomodulator, the $T_{1/2}$ half-life was 0.25 hours and 0.38 hours, and the MRT was 0.55 hours and 0.84 hours for 40 mg and 80 mg doses.

Analyzing the results obtained, we can conclude that the use of a transdermal therapeutic system compared to intramuscular injection increases the mean residence time of drug in the body by more than 12–15 times. The half-life also increases by more than 10 times.

The calculated relative bioavailability of Galavit® transdermal therapeutic system was 0.65 for 40 mg and 1.06 for 80 mg. These results indicate that with an increase in the drug dose, the bioavailability of the transdermal therapeutic system becomes equal to the bioavailability of the immunomodulator when administered intramuscularly.

CONCLUSION

In the course of this work, the pharmacokinetics of intramuscular and transdermal administration of sodium aminodihydrophthalazinedione at 40 mg and 80 mg doses were studied in animals in vivo.

It was shown that application of Galavit® 80 mg transdermal therapeutic system provides a bioavailability that is equal to the bioavailability obtainable when this drug is administered intramuscularly at the same dose. Meanwhile, maximum plasma drug concentration decreases significantly and its residence time in the body increases by more than 10 times. This can help in prolonging the drug effect. Changes in drug concentration in the blood during application of TTS occurs gradually over several hours, in contrast to a sharp jump during intramuscular administration. This is an undisputed advantage of the Galavit® transdermal system in the case of long-term use for prophylaxis and supportive therapy.

It should be noted that at present, there is increased interest in the use of Galavit® in COVID-19 infection. Specifically, there was a recent report on the effectiveness of the drug in preventing moderate and severe forms of COVID-19 among medical workers under high risk of contracting SARS-COV-2 infection [17]. In this regard, the authors consider it promising to develop and study the domestic transdermal dosage form of immunomodulator Galavit®.

The authors declare no conflict of interest.

REFERENCES

1. *Sampiev AM, Nikiforova EB, Davitavjan NA.* Sovremennye dostizhenija v razrabotke i primenenii innovacionnyh lekarstvennyh sredstv. *Novye tehnologii*. 2012; 2: 247–254. [In Russ, English abstract].
2. *Leonova MV*. Novye lekarstvennye formy i sistemy dostavki lekarstvennyh sredstv: osobennosti peroral'nyh lekarstvennyh form. Chast' 1. *Lechebnoe delo.* 2009; 2: 21–31. [In Russ].
3. *Vasil'ev AE, Krasnjuk II, Ravikumar S, Tohmahchi VN.* Transdermal'nye terapevticheskie sistemy dostavki lekarstvennyh veshhestv (obzor). *Himiko-farmacevticheskij zhurnal*. 2001; 35: 29–42. [In Russ].
4. *Beregovyh VV, Pjatigorskaja NV, Prudkevich JuA, Kedik SA.* Transdermal'nye terapevticheskie sistemy dostavki lekarstvennyh sredstv. *Vestnik MITHT*, 2012; 7 (5): 17–22. [In Russ].
5. *Haitov RM.* Immunomoduljatory: mify i real'nost'. *Immunologija*. 2020; 41 (2): 101–106. [In Russ]. doi: 10.33029/0206-4952-2020-41-2-101-106.
6. *Djadina KS, Zemskov AM, Berezhnova TA, Mihajlova MD, Zemskova VA, Dobrosockih GV.* Perspektivy immunoterapii gnojno-vospalitel'nyh zabolevanij. *Vestnik novyh medicinskih tehnologij*. Jelektronnoe izdanie. 2020; 2: 81–89. [In Russ, English abstract]. doi: 10.24411/2075-4094-2020-16625.
7. *Luss LV, Martynov-Radushinskij AA*. Vtorichnaja immunnaja nedostatochnost'. Vsegda li nuzhny immunomoduljatory? *Medicinskij sovet*. 2014; 2: 40–45. [In Russ]. doi: 10.21518/2079-701X-2014-2-40-45.
8. *Sologub TV, Osinovec OJu*. Primenenie immunomodulirujushhego preparata galavit v kompleksnoj terapii grippa. *Klinicist.* 2012; 2: 76–80. [In Russ, English abstract].
9. *Rumjancev AG, Shherbina AJu.* Jeffektivnost' preparata galavit u chasto i dlitel'no bolejushhih detej starshe

6 let. *Rossijskij vestnik perinatologii i pediatrii*. 2008; 6: 100–101. [In Russ, English abstract].

10. *Kuznecova EG, Kuryleva OM, Salomatina LA, Sevast'janov VI.* Jeksperimental'noe issledovanie diffuzii immunomoduljatora Galavit® v model'noj sisteme. *Razrabotka i registracija lekarstvennyh sredstv*. 2020; 9 (1): 92–97. [In Russ, English abstract]. doi: 10.33380/2305-2066-2020-9-1-92-97.
11. *Kuznecova EG, Kuryleva OM, Salomatina LA, Sevast'janov VI.* Primenenie sinteticheskoj i biologicheskoj test-sistem pri razrabotke transdermal'nyh terapevticheskih sistem. *Perspektivnye materialy*. 2020; 8: 49–59. [In Russ, English abstract]. doi: 10.30791/1028-978X-2020-8-49-58.
12. Rukovodstvo po provedeniju doklinicheskih issledovanij lekarstvennyh sredstv. Chast' pervaja / Pod red. A.N. Mironova. M.: Grif i K, 2012. 944 s.
13. Farmacevticheskaja razrabotka: koncepcija i prakticheskie rekomendacii. Nauchno-prakticheskoe rukovodstvo dlja farmacevticheskoj otrasli. Pod red. S.N. Bykovskogo. M.: Pero, 2015.
14. *Zherdev VP, Voronina TA, Garibova TL, Kolyvanov GB, Litvin AA, Sariev AK i dr.* Ocenka farmakokinetiki i jeffektivnosti fenazepama u krys pri transdermal'nom i jenteral'nom sposobah vvedenija. Jeksperimental'naja i klinicheskaja farmakologija. 2003; 66 (1): 50–53. [In Russ].
15. *Narasimha Murthy S, Hiremath SR.* Clinical pharmacokinetic and pharmacodynamic evaluation of transdermal drug delivery systems of salbutamol sulfate. *Int J Pharm*. 2004; 287 (1–2): 47–53.
16. *Basok YB, Salomatina LA, Tikhobaeva AA, Sevastianov VI.* A Pharmacokinetic Study of Caffeine Transdermal Therapeutic Systems. *Advanced Metals, Ceramics and Composites* (ed. H. Tu, K. Solntsev, R. Zhou), Yunnan Publ. Group Corp., Kunming, China. 2013: 175–177.
17. *Sergienko VI, Bondareva IB.* Matematicheskaya statistika v klinicheskikh issledovaniyakh. M.: GEOTAR-MED, 2001: 256.
18. *Kolesov SV, Gorbatjuk DS, Panteleev AA, Bernakevich AI, Ukolov KJu*. Profilaktika srednih i tjazhelyh form COVID-19 aminodigidroftalazindionom natrija (Galavit®) u medicinskogo personala "krasnoj zony". *Immunologija.* 2020; 41 (6): 527–539. [In Russ]. doi: 10.33029/0206–4952-2020-41-6-527-539.

The article was submitted to the journal on 9.03.2021

DOI: 10.15825/1995-1191-2021-2-122-136

EVALUATION OF THE BIOCOMPATIBILITY AND ANTIMICROBIAL PROPERTIES OF BIODEGRADABLE VASCULAR GRAFTS OF VARIOUS POLYMER COMPOSITION WITH ATROMBOGENIC AND ANTIMICROBIAL DRUG COATING

L.V. Antonova[1], E.O. Krivkina[1], V.N. Silnikov[2], O.V. Gruzdeva[1], M.A. Rezvova[1], T.N. Akentieva[1], T.V. Glushkova[1], V.O. Tkachenko[3], V.M. Sakharova[1], L.S. Barbarash[1]

[1] Research Institute for Complex Problems of Cardiovascular Diseases, Kemerovo, Russian Federation
[2] Institute of Chemical Biology and Fundamental Medicine, Novosibirsk, Russian Federation
[3] Budker Institute of Nuclear Physics, Novosibirsk, Russian Federation

Creation of vascular grafts with atrombogenic and antimicrobial coating is a very important area. **Objective:** to evaluate the biocompatibility and antimicrobial properties of biodegradable vascular grafts of various polymer compositions with atrombogenic and antimicrobial drug coating. **Materials and methods.** Modification of the surface of the biodegradable vascular grafts was performed through complexation with polyvinylpyrrolidone, which was polymerized with polymer scaffold surface by means of ionizing radiation at 10 and 15 kGy. Physical and mechanical properties, as well as hemocompatibility were evaluated. Bacteriological studies were carried out using test strains of gram-negative and gram-positive microorganisms: *Klebsiella pneumoniae spp. ozaena* No. 5055, *Escherichia coli* ATCC 25922, *Staphylococcus aureus* ATCC 25923, *Proteus mirabillis* ATCC3177, *Pseudomonas aeruginosa*. **Results.** There was no influence of modifying manipulations with ionizing radiation on the physical and mechanical characteristics of biodegradable prostheses. Vascular grafts with atrombogenic and antimicrobial coatings exhibited atrombogenic properties upon contact with blood, reducing platelet aggregation by 5–7 times ($p < 0.05$). Also decrease in adhesion and platelets deformation index was found on the surface of drug-eluting scaffolds (for PCL-based prostheses, the latter decreased by 1.9 times relative to unmodified counterparts ($p < 0.05$), for PHBV/PCL-based prostheses – by 1.3 times relative to unmodified counterparts and 1.5 times relative to scaffolds with polyvinylpyrrolidone ($p < 0.05$). Bacteriological studies revealed a local inhibitory effect in the place where scaffolds with cationic amphiphile were applied on agar. No growth retardation zones were identified. Polymeric composition of the scaffolds and the used dose of ionizing radiation did not lead to a difference in the bacteriostatic properties of the scaffolds with amphiphile. **Conclusion.** A full cycle of surface modification of biodegradable polymer prostheses based on both PCL and PHBV/PCL composition resulted in significant increase in the atrombogenic and antimicrobial properties of prostheses and did not worsen the physical-mechanical and biocompatible properties of the structures being developed.

Keywords: biodegradable polymers, small diameter vascular grafts, atrombogenic drug coating, cationic amphiphile.

INTRODUCTION

Vascular tissue engineering is one of the promising modern areas involved in the development of effective blood vessel prostheses [1]. There are various approaches to tissue engineering of blood vessels, but all of them are aimed at creating a functional vascular implant with a structure similar to the organization of native artery tissues and demonstrating patency in the long-term postoperative period. The basis of such vascular grafts is artificial tubular matrix, most often made of biodegradable natural and/or synthetic polymers with high biocompatibility. The matrix is a scaffold that is populated by autologous cells in vitro or in situ.

Widespread use of vascular grafts in medicine has intensified the need for polymeric materials with antibacterial properties. It is difficult to establish the exact etiology of prosthetic vascular graft infection, since in most cases it is multifactorial [2]. Microbial contamination of the prosthetic vascular graft can occur either exogenously or endogenously (bacteremia) [3, 4]. Despite the placement of a sterile prosthetic vascular graft in an uninfected field, about 20% of them become infected, increasing the percentage of subsequent graft occlusion to 27% [5]. These circumstances require additional antimicrobial and anti-thrombogenic protection of the vascular graft surface.

Corresponding author: Larisa Antonova. Address: 6, Sosnovy Boulevard, Kemerovo, 650002, Russian Federation. Phone: (905) 906-04-51. E-mail: antonova.la@mail.ru

Pathogenic microbial adhesion to the surfaces with subsequent cell growth and colonization leads to biofilm formation with high resistance to antibiotics and host defense mechanisms [6, 7], which in clinical practice leads to the need for prosthesis replacement. This creates inconvenience and increases the risk for the patient. The most effective way to prevent biofilm formation on the surface of the prosthetic material is to prevent the adhesion of bacterial cells at the initial stage of infection of the prosthetic material. This can be achieved by replacing conventional prosthetic materials with antimicrobial biocompatible polymers [8, 9].

In combination with the general problems of decreasing effectiveness of antibacterial drugs due to the emergence of multidrug-resistant bacteria, the development of a prosthetic vascular graft with high antibacterial activity and low probability of inducing drug resistance becomes extremely urgent. A way out of this situation can be the approach of introducing an antibacterial drug directly into the prosthesis structure. On one hand, this approach solves the problem of local drug delivery and, on the other hand, ensures the effect of the drug on microorganisms before they form biofilms.

Over the past decade, hydrogels, three-dimensional polymeric networks obtained from water-soluble or biodegradable natural or synthetic polymers in which the antibacterial agent is bound to the polymer matrix through non-covalent interactions, have been widely used for drug delivery and prolonged release of drugs [10].

The most attractive compounds with antimicrobial activity to which microorganisms do not develop resistance are cationic amphiphiles (CAms) – molecules with one or more positively charged groups and lipophilic fragments [11, 12]. These compounds are synthetic analogues of naturally occurring cationic antimicrobials: they can also disrupt transmembrane potential, cause leakage of cytoplasmic contents and, ultimately, cell death [13]. Most of these compounds are highly effective against both Gram-positive and Gram-negative bacteria (including antibiotic-resistant strains), along with good selectivity in respect of mammalian cells. The possibility of obtaining amphiphiles that destroy bacterial membranes and, at the same time, have other bacterial targets significantly reduces the likelihood of resistance to such compounds. The high stability of these compounds, including in physiological fluids, combined with the low cost of their synthesis, makes these compounds the most promising candidates for the role of low molecular weight modifiers of polymeric materials with antibacterial properties.

The creation of a tissue-engineered vascular graft with a highly porous wall is extremely important for the full migration of cells into the prosthesis wall from the bloodstream and surrounding tissues and subsequent cell proliferation and differentiation in the vascular direction. However, a prosthetic graft with such surface architectonics is certainly capable of provoking thrombus formation. Therefore, additional modification of the surface of tissue-engineered highly porous small-diameter vascular grafts with drugs with antiaggregant and anticoagulant activity can prevent the initiation of thrombosis after implantation of such prostheses into the vascular bed.

The aim of the study was to evaluate the biocompatibility and antimicrobial properties of biodegradable vascular grafts of various polymer compositions with anti-thrombogenic and antimicrobial drug coating.

MATERIALS AND METHODS

Fabrication of biodegradable vascular grafts

Two varieties of 4 mm diameter polymeric tubular scaffolds were made by electrospinning: from 12% poly(ε-caprolactone) solution, (PCL; Sigma-Aldrich, USA) and from a polymer composition of 2% poly(3-hydroxybutyrate-co-3-hydroxyvalerate) solution, (PHBV, Sigma-Aldrich) and 12% poly(ε-caprolactone) solution, (PCL, Sigma-Aldrich) at 1:2 ratio. 1,1,1,3,3,3-hexafluoro-2-propanol (Sigma-Aldrich, USA) was used as a solvent. Electrospinning was performed on a Nanon-01A device (MECC, Japan). The following mode was selected for PCL-based graft fabrication: needle voltage 22 kV, polymer solution feed rate 0.5 mL/h, manifold rotation speed 1000 rpm, needle movement speed 60 mm/s, distance from the needle to the winding manifold 15 cm. For PHBV/PCL-based prosthetic grafts, the following mode was used: needle voltage 20 kV, polymer solution feed rate 0.5 mL/h, manifold rotation speed 1000 rpm, needle movement speed 60 mm/s, distance from needle to winding manifold 15 cm.

Formation of an anti-thrombogenic coating on the surface of biodegradable vascular graft

Additional modification of the surface of PCL- and PHBV/PCL-based grafts to increase thromboresistance was carried out according to our own original technique [14]. Hydrogel coating on the inner surface of the polymer graft was formed using radiation-induced graft polymerization. For this purpose, 4 mm-diameter PCL- and PHBV/PCL-based grafts were immersed for 30 minutes in a 5% solution of polyvinylpyrrolidone (PVP, K 90; PanReac AppliChem, Germany) in ethyl alcohol with complete filling of the graft inner channel. Next, the grafts were removed from the solution and dried horizontally for 24 hours in air at room temperature. For PVP-based grafting to the graft surface, the products were placed in glass tubes that were filled with inert argon gas, sealed with paraphilm, and irradiated with ionizing radiation in two different modes (with a total absorbed dose of 10 and 15 kGy) using a pulsed linear gas pedal ILU-10 with 5 MeV 50 kW beam energy (Budker Institute of Nuclear Physics, Russia). Thus, the vascular grafts were sterilized simultaneously with the

modification; therefore, further manipulations to form the drug coating were carried out under sterile conditions. Non-grafted polymer was washed with injection water for 60 minutes. The grafting quality was evaluated by attenuated total reflectance spectroscopy of the inner surface of the modified grafts on a Bruker Vertex 80v (Germany) instrument with an ATR attachment (Germany) in 4000–500 cm^{-1} spectral range.

To create a drug coating, two substances were chosen – iloprost and cationic amphiphile 1,5-bis-(4-tetradecyl-1,4-diazoniabicyclo[2.2.2]octan-1-yl)pentane tetrabromide without additional reactive groups.

Iloprost (Ilo, Bayer, Germany) is a drug registered in the Russian Federation and approved for medical use. It is a synthetic analog of prostacyclin, inhibits platelet aggregation, adhesion and release reaction; restores impaired microcirculation by induction of vasodilation, inhibition of platelet activation, activation of fibrinolysis, endothelial repair and protection; inhibits adhesion and migration of white blood cells after endothelial damage.

Cationic amphiphiles (A) in general, and 1,5-bis-(4-tetradecyl-1,4-diazoniabicyclo[2.2.2]octan-1-yl)pentane tetrabromide (Nano Tech-C, Russia) in particular, possess ribonuclease activity and, consequently, high antibacterial and antiviral activity [15–17]. An additional argument in favor of choosing this compound is the fact that it has passed all the necessary tests and is used in veterinary medicine as antiviral drug Triviject (Trionis-Vet LLC, Russia) in the form of an injection solution.

Cationic amphiphile, 1,5-bis-(4-tetradecyl-1,4-diazoniabicyclo[2.2.2]octan-1-yl)pentane tetrabromide without additional reactive groups (compound 3, Fig. 1), was synthesized as described earlier [16]. The nuclear magnetic resonance (1H NMR) spectrum of the obtained compound (3) is consistent with the literature data [16].

Addition of iloprost and cationic amphiphile 1,5-bis-(4-tetradecyl-1,4-diazoniabicyclo[2.2.2]octan-1-yl)pentane tetrabromide to the hydrogel coating was performed by complexation. A sterile modifying solution containing cationic amphiphile (A) at 0.25 mg/mL concentration was prepared. For this purpose, 0.025 g of amphiphile 1,5-bis-(4-tetradecyl-1,4-diazoniabicyclo[2.2.2]octan-1-yl)pentane tetrabromide was dissolved in 1 to 2 mL of methanol. The resulting solution was slowly added to a flask with sterile water for injection while stirring and the volume was brought to 98 mL. After that, 2 mL of iloprost (Ilo) was added to the solution at 20 μg per 100 mL (0.2 μg/mL). To attach the drugs to the PVP coating, the vascular grafts were incubated in the modifying solution containing the drugs for 30 minutes. Then, the finished PCL/PVP/Ilo/A and PHBV/PCL/PVP/Ilo/A vascular grafts were air-dried under sterile conditions and placed in sterile storage containers.

PCL and PHBV/PCL samples were unmodified controls; PCL/PVP and PHBV/PCL/PVP samples exposed to 10 kGy and 15 kGy of ionizing radiation were used as comparison groups. All work was carried out inside a sterile box. The list of experimental and control groups is presented in Table 1.

Table 1

Types of polymer samples

Name of samples	
PHBV/PCL	PCL
PHBV/PCL/PVP-10 kGy	PCL/PVP-10 kGy
PHBV/PCL/PVP-15 kGy	PCL/PVP-15 kGy
PHBV/PCL/PVP/Ilo/A-10 kGy	PCL/PVP/Ilo/A-10 kGy
PHBV/PCL/PVP/Ilo/A-15 kGy	PCL/PVP/Ilo/A-15 kGy

Assessment of physical and mechanical properties

The mechanical properties of the biodegradable vascular grafts before and after additional anti-thrombogenic drug coating were evaluated under uniaxial tension on a Z-series universal testing machine (Zwick/Roell) using a transducer with 50 N nominal force. The crosshead movement speed during the test was 50 mm/min. The ultimate tensile strength of the material was estimated as the maximum tensile stress (MPa) prior to failure. The

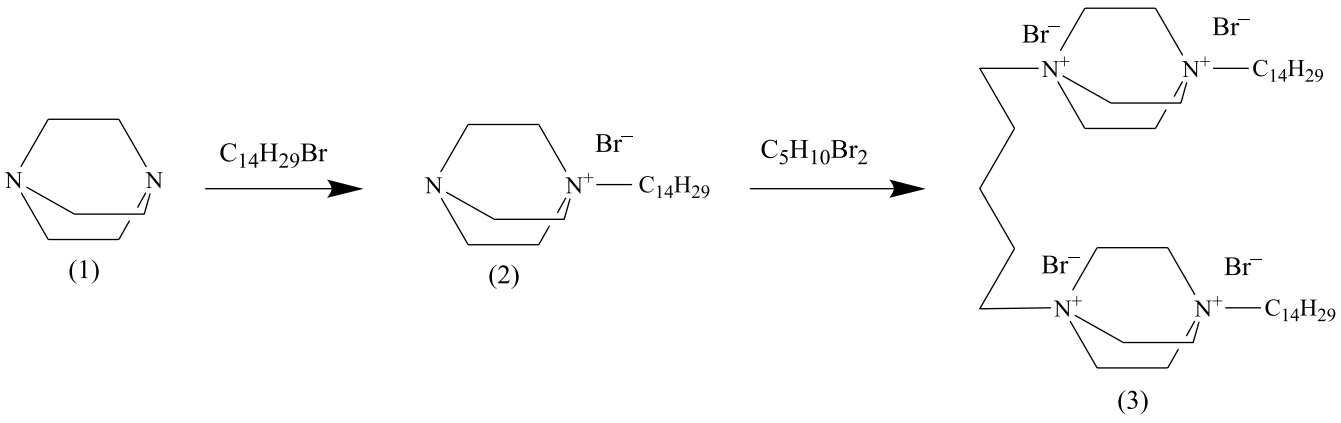

Fig. 1. Synthesis scheme for 1,5-bis-(4-tetradecyl-1,4-diazoniabicyclo[2.2.2]octan-1-yl)pentane tetrabromide

stress-strain properties of the material were evaluated by the relative elongation before failure (%) and Young's modulus (MPa), which was determined in the physiological pressure range (80 to 120 mmHg). Intact sheep carotid artery was used as the control.

Hemocompatibility assessment

Erythrocyte hemolysis

Hemolysis of erythrocytes after contact with the surface of polymeric samples was studied according to the ISO 10993.4 standard. Fresh donor blood was used, to which sodium citrate 3.8% was added in a 1:9 ratio (citrate:blood). 25 cm^2 polymer samples of 5 pieces for each type of material were placed in weighing bottles containing 10 mL of saline. The weighing bottles were incubated in the thermostat at 37 °C for 120 minutes. Saline and distilled water were used as positive and negative controls, respectively. Two hours after incubation, 200 μL of citrate blood was added to each weighing bottle and placed again in the thermostat for 60 min at 37 °C. After incubation, polymer samples were removed from the weighing bottles into appropriate tubes and centrifuged for 10 minutes at 2800 rpm to precipitate erythrocytes. The optical density of the obtained solutions was measured on a GENESYS 6 spectrophotometer (Thermo SCIENTIFIC, USA) at 545 nm.

The degree of hemolysis (H) in % was calculated using the formula [18, 19]:

$$H\ (\%) = \frac{D_t - D_{ne}}{D_{pe} - D_{ne}} \times 100\%,$$

where, D_t is the optical density of the sample incubated with the test material, D_{ne} is the optical density of positive control, and D_{pe} is the optical density of the sample after 100% hemolysis.

The mean optical density when measuring saline with blood (positive control), equal to 0, was taken as complete absence of hemolysis. The mean optical density of the device when measuring distilled water with blood (negative control), which was 0.279, was taken as 100% hemolysis.

Platelet aggregation

The study was performed according to the ISO 10993.4 standard. Fresh donor blood was used, to which sodium citrate 3.8% was added in a 1:9 ratio (citrate:blood). To obtain platelet-rich plasma (PRP), blood was centrifuged for 10 minutes at 1000 rpm. Platelet-poor plasma (PPP) was obtained by repeated centrifugation of PRP for 20 minutes at 4000 rpm. The PPP was used to calibrate the instrument. Intact PRP served as a positive control. Measurements were taken spontaneously without aggregation inducers. Ca^{+2} ion level was restored in citrated blood using $CaCl_2$ solution with 0.025 M molecular mass, after which the measurements were taken. The sample/reagent ratio was 250 μL of PRP + 25 μL of $CaCl_2$. The time of contact of the tested samples with PRP was 3 minutes. Measurement of maximum platelet aggregation was performed on a semi-automatic platelet aggregation analyzer "APAST 4004" (LABiTec, Germany).

Platelet adhesion

Samples of 0.5 cm^2 polymer matrices (n = 2) were incubated for 2 hours at 37 °C in 300 μL of PRP obtained from fresh citrated donor blood when centrifuged for 10 minutes at 1200 rpm. The samples were then washed with phosphate-buffered saline (PBS) (pH – 7.4) to remove non-adherent plasma components. The samples were then fixed in a 2% glutaraldehyde solution for 24 hours, washed with PBS, and dehydrated in a series of alcohols of ascending concentration from 30% to 100% for 15 minutes each, followed by drying at room temperature. The samples were then mounted on special tables using carbon tape and a conductive (Au/Pd) coating was formed on their surface using an EM ACE200 vacuum unit (Leica Mikrosysteme GmbH, Austria). We used the 8 most characteristic fields selected at random for the analysis. The adhesive ability of the material surface was evaluated by the number of platelets per 1 mm^2, by the predominance of platelet type on the surface, and by their deformation index (DI), which was calculated using the formula [18–20]:

DI = (Type I count × 1 + Type II count × 2 + Type III count × 3 + Type IV count × 4 + Type V count × 5) / total platelet count

Types of platelets depending on activation:

I Disc-shaped platelet, no deformity;
II Platelet is enlarged with the rudiments of pseudopodia in the form of protrusions;
III Platelet significantly enlarged, irregularly shaped, with pronounced pseudopodia, platelets tend to accumulate into larger conglomerates;
IV Proliferated platelet, cytoplasm proliferating between the pseudopodia;
V Platelet in the form of a stain with granules, due to proliferation of cytoplasm, the pseudopodia cannot be identified.

Bacteriological examinations

The following microbial strains were used for bacteriological examination: Klebsiella pneumonia spp. ozaena 5055, Escherichia coli ATCC 25922, Staphylococcus aureus ATCC 25923, Proteus mirabillis ATCC3177, Pseudomonas aeruginosa ATCC27853. These microorganisms were chosen for the experiment because they are the most common in infectious complications in cardiac surgery. Sensitivity of control microbial strains to the polymer matrices under study was measured using a disk-diffusion method to assess the sensitivity of bacteria

to cationic amphiphile (A) introduced into the matrix by complexation with PVP at 0.25 mg/mL concentration. Microbial suspension was prepared by direct suspension of the colonies in sterile isotonic solution to a 0.5 density according to the McFarland turbidity standards. No later than 60 minutes later, the bacterial suspension was applied to agar plates by stroking in three directions over the entire agar surface so that the strokes could adhere tightly to each other. The polymer matrix discs were spread no later than 15 minutes after inoculation of the plates. The plates were incubated in the thermostat at 35–36 °C for 24–48 hours.

Statistical analysis

Data were statistically processed using the Prism 7 software (GraphPad, USA). The nature of distribution in the samples was assessed using the Kolmogorov–Smirnov test. Data were presented as median and percentiles (Me, 25–75%). Kruskal–Wallis H test with FDR correction was used for multiple comparisons; differences were considered significant at significance level $p < 0.05$.

RESULTS

Results of graft polymerization of polyvinylpyrrolidone

In the IR spectra of PVP-modified and unmodified PHBV/PCL matrices, there were bands of C=O (ether carbonyl) stretching vibrations at 1724 cm^{-1}, C–O stretch bands were observed at 1278 and 1054 cm^{-1}, (Fig. 2), [21]. In the spectra of all samples under study, we also observed low intensity bands at 2942 cm^{-1} and 2865 cm^{-1}, corresponding to asymmetric vibrations of the methylene-oxygen group (CH_2–O) and symmetric vibrations of the methylene group (CH_2–), respectively, (Fig. 2) [22]. In contrast to unmodified samples, the spectra of PVP-modified matrices contained a 1654 cm^{-1} band related to the carbonyl amide group of the pyrrolidine ring [23], indicating grafting of the polymer to the surface of the vascular graft (Fig. 2). The absence of changes in the position and intensity of characteristic bands in the infrared spectrum of PHBV/PCL indicates an insignificant effect of modification conditions, in particular, ionizing radiation on the structure of the material. A similar picture was obtained in the study of PCL-based polymer vessels.

Physical and mechanical properties

Assessment of the long-term permeability of the developed prosthetic vascular grafts under is planned to be performed on a sheep model. Therefore, in the process of studying the physical and mechanical properties of the prostheses, the sheep carotid artery was chosen as an additional comparison group.

The procedure of polymerization of intermediate PVP polymer with PCL-based matrix surface using ionizing radiation at 10 and 15 kGy decreased the strength limit by 1.6 times ($p < 0.05$) and slightly increased the Young's modulus of these matrices (Table 2).

Meanwhile, modification of PHBV/PCL matrices by PVP had no effect on their strength properties but resulted in a 1.9-fold increase in Young's modulus ($p < 0.05$). Subsequent modification with amphiphile and iloprost by complexation did not affect the strength index of the PVP-modified PCL matrices, but decreased the stiffness of the PHBV/PCL matrices acquired during polymerization with PVP. Thus, the procedure for forming a drug coating on the surface of PHBV/PCL and PCL vascular grafts involving ionizing radiation did not result in a significant change in the physical and mechanical characteristics of the grafts.

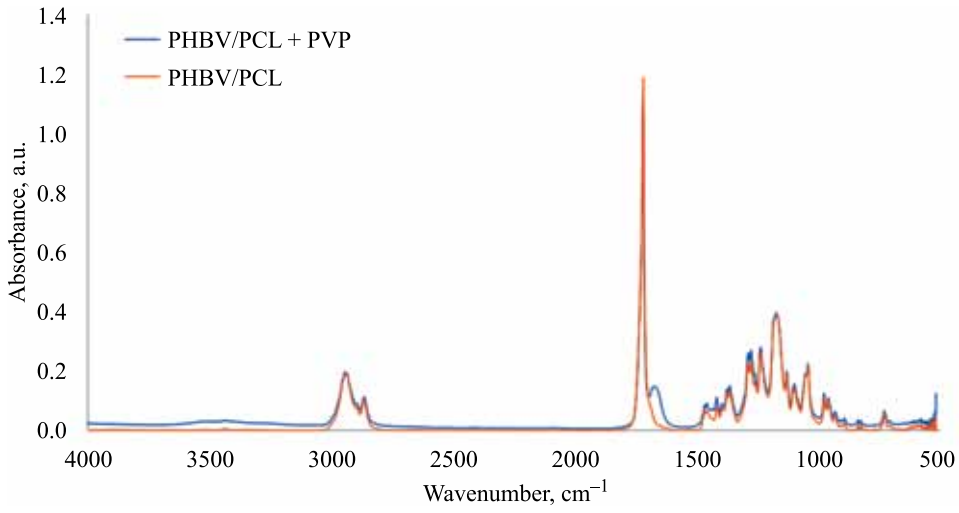

Fig. 2. IR spectra of PVP-modified and unmodified inner surface of a polymer vascular graft using PHBV/PCL as an example

Hemocompatible properties

The study of platelet aggregation activity revealed that there are statistically significant differences between intact PRP and all the matrix groups studied (Table 3).

When comparing the two types of unmodified matrices PHBV/PCL and PCL, no significant differences were found. Polymerization of the matrix surface with PVP under 15 kGy ionizing radiation slightly increased platelet aggregation to the matrix surface (Table 3). However, subsequent complexation of polymerized PVP with iloprost and amphiphile decreased platelet aggregation 6- to 7-fold compared with the results of intact PRP (Table 3; $p < 0.05$). This significant decrease in platelet aggregation appears to be related to the action of iloprost. The presence of amphiphile at a 0.25 mg/mL dose did not result in significant increase in platelet aggregation.

Hemolysis of erythrocytes did not exceed the permissible 2% when erythrocytes came into contact with the surface of all matrix varieties (Table 3). There were no significant differences between the groups either.

Platelet adhesion

After contact of unmodified matrices PHBV/PCL and PCL with intact PRP, platelet count on the surface of PCL matrices was 3 times higher than on the PHBV/PCL surface (Table 4, Fig. 3, Fig. 4). Type II and III platelets predominated on unmodified matrices. However, platelet DI after contact with the PCL surface was 1.4 times higher ($p < 0.05$) than that of platelets contacting the surface of PHBV/PCL matrices (Table 4).

After polymerization of the surface of PCL-based matrixes with PVP at radiation dose of 10 and 15 kGy, no significant changes in the degree of platelet adhesion relative to unmodified PCL matrices were observed (Table 4, Fig. 3). However, the increase in the proportion of type IV platelets using 15 kGy radiation is noteworthy.

Table 2

Mechanical properties of polymer tubular scaffolds before and after modification in comparison with sheep carotid artery

Sample type	n	Tension, MPa	Relative extension, %	Young's modulus, MPa
Sheep carotid artery	14	1.2 (1.06–1.9)	158.5 (126.0–169.5)	0.49 (0.39–0.66)
PHBV/PCL	7	3.99 (3.71–4.23)•	1438.0 (1403.0–1510.0)•	11.52 (10.66–12.21)•
PCL	7	5.84 (5.56–6.13)•	1391.0 (1350.0–1413.0)•	9.33 (9.23–9.55)•
PHBV/PCL/PVP-10 kGy	7	3.74 (3.5–3.83)•	1302.0 (1234.0–1360.0)*•	22.39 (21.59–23.71)*•
PHBV/PCL/PVP-15 kGy	7	3.61 (3.23–4.01)•	1202.0 (1120.0–1298.0)*•	19.8 (18.23–20.9)*•
PCL/PVP-10 kGy	7	3.56 (3.51–3.7)*•	1297.0 (1258.0–1342.0)*•	10.66 (10.37–11.01)*•
PCL/PVP-15 kGy	7	3.75 (3.48–4.01)*•	1183.0 (1157.0–1215.0)*•	12.86 (11.86–14.06)*•
PHBV/PCL/PVP/Ilo/A-10 kGy	7	3.57 (3.28–3.93)•	1258.0 (1200.0–1392.0)*•	15.24 (14.78–15.84)*•
PHBV/PCL/PVP/Ilo/A-15 kGy	7	3.89 (3.88–3.99)•	1364.0 (1343.0–1393.0)*•	14.55 (13.22–15.24)*•
PCL/PVP/Ilo/A-10 kGy	7	3.77 (3.66–3.87)*•	1421.0 (1380.0–1467.0)•▲	9.54 (9.43–9.76)•▲
PCL/PVP/Ilo/A-15 kGy	7	4.02 (3.8–4.18)*•	1454.0 (1433.0–1458.0)*•▲	10.15 (9.82–10.57)*•▲

* – $p < 0.05$ relative to PHBV/PCL or PCL; • – $p < 0.05$ relative to the sheep carotid artery; ▲ – $p < 0.05$ relative to 15 kGy PHBV/PCL-PVP radiation or 15 kGy PCL-PVP radiation.

Table 3

Maximum aggregation of human blood platelets after contact with modified and unmodified polymer matrices

Sample type	Maximum platelet aggregation, % Me (25%–75%)	Degree of red blood cell hemolysis, % Me (25%–75%)
PHBV/PCL	87.23 (83.95–89.84)*	0.504 (0.0–1.01)
PCL	87.23 (83.27–89.35)*	0.504 (0.0–1.01)
PHBV/PCL/PVP-10 kGy	85.8 (84.37–89.03)*	0.704 (0.5–1.01)
PHBV/PCL/PVP-15 kGy	88.53 (86.59–89.37)*	0.2 (0.0–0.5)
PCL/PVP-10 kGy	83.51 (82.68–86.60)*	0.2 (0.0–0.5)
PCL/PVP-15 kGy	90.12 (82.57–90.60)*	0.704 (0.5–1.01)
PHBV/PCL/PVP/Ilo/A-10 kGy	12.1 (11.05–12.78)**	0.2 (0.0–0.5)
PHBV/PCL/PVP/Ilo/A-15 kGy	12.18 (11.15–12.24)**	0.5 (0.0–0.5)
PCL/PVP/Ilo/A-10 kGy	10.86 (9.04–11.39)**	0.504 (0.0–1.01)
PCL/PVP/Ilo/A-15 kGy	10.7 (10.38–17.23)**	0.404 (0.0–1.01)
Intact platelet-rich plasma (PRP)	74.65 (72.45–75.31)	–

* – $p < 0.05$ relative to intact PRP; ** – $p < 0.05$ relative to unmodified PCL and PHBV/PCL matrices.

Grafting of PVP to the surface of PHBV/PCL matrices increased the degree of platelet adhesion almost 2-fold regardless of the radiation dose used (Table 4, Fig. 4) with some increase in type IV platelet count when 15 kGy radiation dose was used. However, platelet DI after polymerization of the matrix surface with PVP did not undergo significant changes.

Analysis of PCL/PVP/Ilo/A-10 kGy matrix surface after contact with intact PRP revealed significant decrease in both adhered platelet count and platelets DI relative to the PCL/PVP-10 kGy matrices – 1.5-fold and 1.7-fold, respectively ($p < 0.05$). At contact with the surface of the PCL/PVP/Ilo/A-15 kGy matrix, the studied parameters decreased 1.3- and 1.5-fold, respectively.

Formation of an anti-thrombogenic and antimicrobial drug coating Ilo/A on the surface of PHBV/PCL/PVP-15 kGy matrices reduced the count of adhered platelets by 1.5 times and the count of type III platelets by 2 times with prevalence of type I and II platelets on the surface of PHBV/PCL/PVP/Ilo/A-10 kGy and PHBV/PCL/PVP/Ilo/A-15 kGy matrices of type I and II platelets, which resulted in a 1.5-fold decrease in platelet DI ($p < 0.05$).

Results of bacteriological examination

Figs. 5 and 6 present the photos obtained when evaluating the bacteriostatic properties of matrices with different polymer composition, containing cationic amphiphile at a 0.25 mg/mL concentration at radiation doses of 10 and 15 kGy. The bacteriostatic properties of unmodified matrices were studied in a comparative aspect. It was found that in all samples containing cationic amphiphile, suppression of the growth of Klebsiella pneumonia spp. ozaena No. 5055, Escherichia coli ATCC 25922, Staphylococcus aureus ATCC 25923, Proteus mirabillis ATCC3177, Pseudomonas aeruginosa ATCC27853 had local inhibitory effect on the site of matrix application on agar. No growth retardation zones were detected (Figs. 5 and 6). The polymer composition of the matrices and the ionizing radiation dose used did not lead to a difference in the bacteriostatic properties of the amphiphilic matrices.

The unmodified matrices had no bacteriostatic effect: colonies continued to grow at the site where the matrices were applied (Fig. 5, 6).

In order to check the ability of the matrices to induce hemolysis of erythrocytes, Mueller–Hinton blood agar was used (Fig. 7). K. pneumonia does not have hemolytic properties, so this particular microorganism was chosen. As a result, there was no hemolysis both around the matrices and in the area of its location (Fig. 7).

Table 4

Platelet adhesion indicators after contact with polymer matrices PHBV/PCL and PCL depending on the surface modification variant

Sample type	Platelet type, %					Platelet count per 1 mm^2 **Me** (25–75%)	Strain index **Me** (25–75%)
	I	II	III	IV	V		
PHBV/PCL	7.7	30.8	53.8	7.7	0.0	**578.0** (0.0–1349.0)	**1.75** (0.0–2.9)
PCL	4.7	46.5	41.9	4.7	2.3	**1734.0** (866.9–3179.0)*	**2.5** (2.0–2.7)*
PHBV/PCL/PVP-10 kGy	49.0	1.0	48.0	2.0	0.0	**953.0** (1.0–2689.0)*	**1.85** (0.0–2.9)
PHBV/PCL/PVP-15 kGy	3.0	27.3	45.5	21.2	3.0	**1156.0** (0.0–3082.0)*	**1.91** (0.0–2.9)
PCL/PVP-10 kGy	8.1	64.9	16.2	10.8	0.0	**1927.0** (96.3–3082.0)**	**2.2** (0.5–2.5)
PCL/PVP-15 kGy	12.5	25.5	12.5	50.0	0.0	**1728.0** (846.4–3058.0)$^{\sigma}$	**1.9** (0.0–2.8)
PHBV/PCL/PVP/Ilo/A-10 kGy	25.0	50.0	21.6	3.4	0.0	**768.6** (0–1366.0)	**1.3** (0.0–2.6)**
PHBV/PCL/PVP/Ilo/A-15 kGy	12.5	62.5	18.8	6.2	0.0	**770.6** (0–1445.0)$^{\sigma}$	**1.3** (0.0–2.4)$^{\sigma}$
PCL/PVP/Ilo/A-10 kGy	3.7	56.0	31.4	8.9		**1310.0** (0.0–3176.0)$^{\alpha}$	**1.3** (0.0–2.6)$^{\#\,\alpha}$
PCL/PVP/Ilo/A-15 kGy	4.7	6.3	71.8	17.2		**1349.0** (0.0–3275.0)	**1.3** (0.0–2.8)$^{\#\,\beta}$

* – $p < 0.05$ relative to the parameters of the PHBV/PCL scaffold; ** – $p < 0.05$ relative to the parameters of the PHBV/PCL/PVP-10 kGy matrix; $^{\sigma}$ – $p < 0.05$ relative to the parameters of the PHBV/PCL/PVP-15 kGy matrix; $^{\#}$ – $p < 0.05$ relative to the parameters of the PCL scaffold; $^{\alpha}$ – $p < 0.05$ relative to the parameters of the PCL/PVP-10 kGy matrix; $^{\beta}$ – $p < 0.05$ relative to the parameters of the PCL/PVP-15 kGy matrix.

DISCUSSION

Surface modification of PCL- and PHBV/PCL-based biodegradable vascular grafts is done by forming a PVP hydrogel coating on their inner surface, which is capable not only of binding drugs as a result of complexation, but also of temporarily (until its complete resorption) occupying the pore cavity, which significantly reduces the risk of platelet adhesion to the surface of the graft after its implantation into the vascular bed. In addition, the

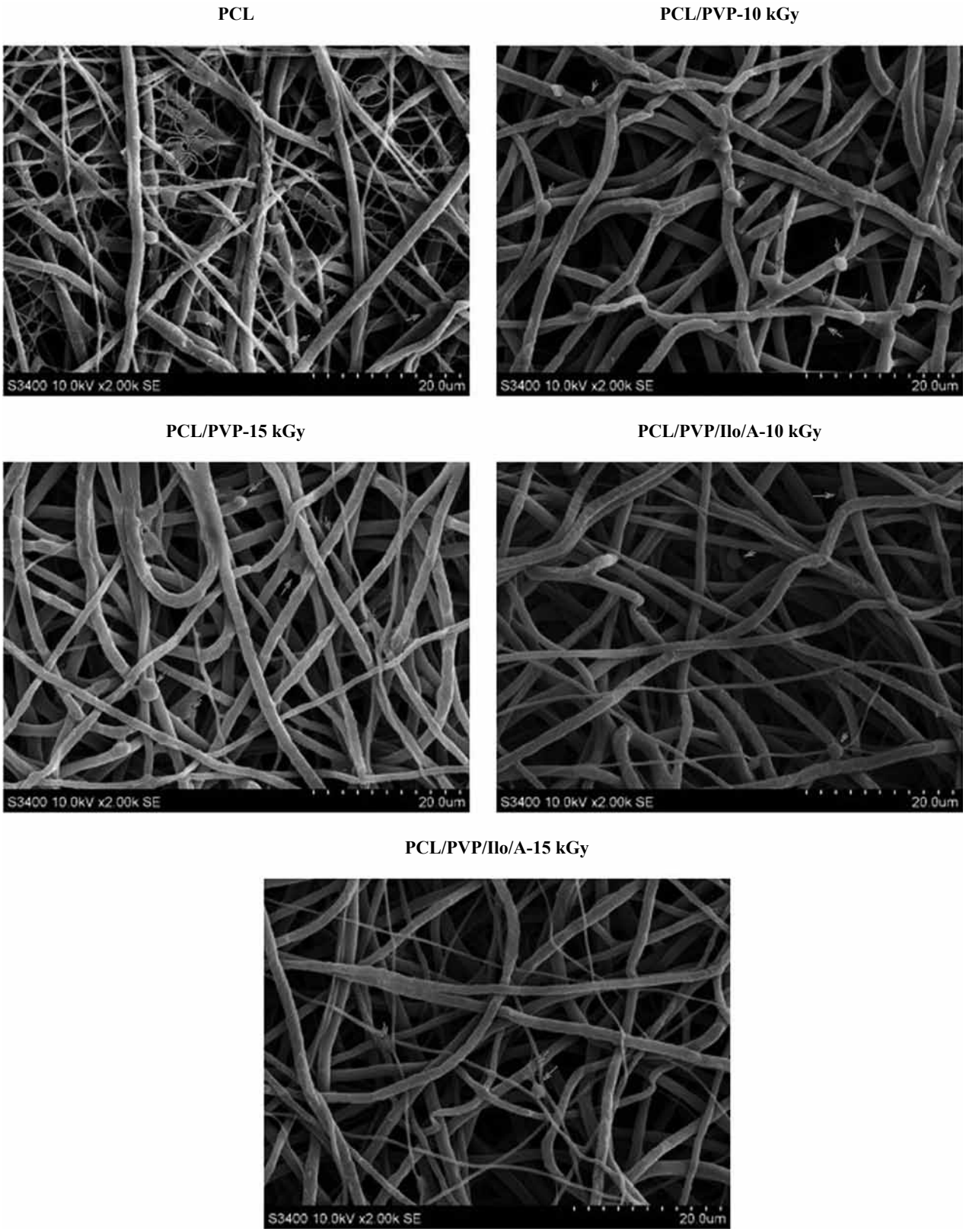

Fig. 3. Surface of PCL matrices after contact with platelet-rich plasma, 2000× magnification. Arrows and circles indicate platelets

known hydrophilicity of PVP contributes to the reduction of the degree of adhesion of protein molecules and blood cells, in particular, platelets, as well as prevention of conformational changes in protein structures. The mobility of macromolecular chains in hydrogels also determines the high rate of desorption of protein molecules, which enhances the anti-thrombogenic potential of PVP [24].

PVP was sewn onto the surface of biodegradable grafts using the radiation-induced graft polymerization method using total absorbed doses of 10 and 15 kGy. At

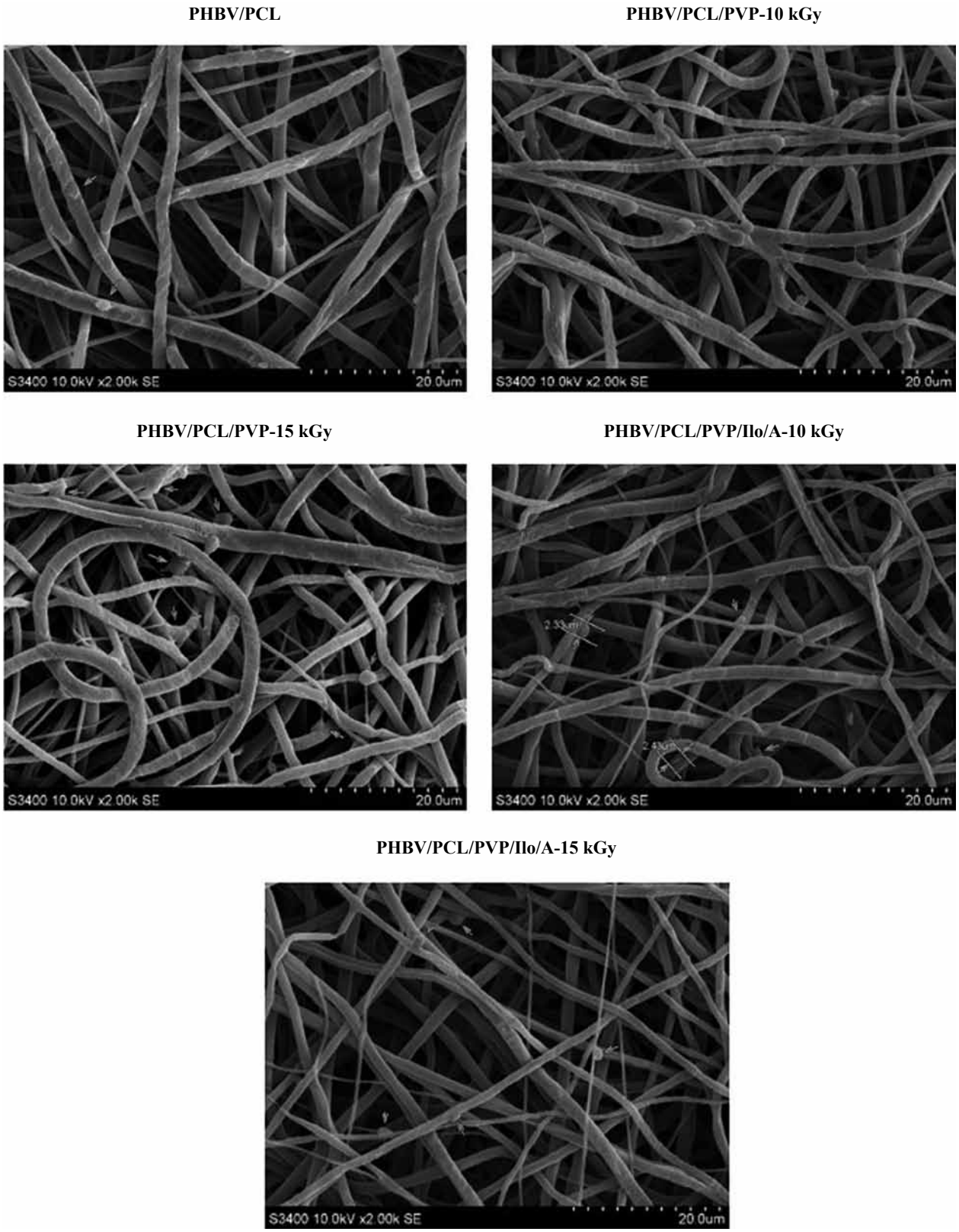

Fig. 4. Surface of PHBV/PCL matrices after contact with platelet-rich plasma, magnification 2000×. Arrows and circles indicate platelets

the same time, the 15 kGy dose was used to sterilize the products. However, ionizing radiation can affect biocompatibility properties. The use of 15 kGy total absorbed dose has been shown not to significantly increase platelet adhesion and deformation, with no significant change in the physical and mechanical properties of the grafts. Nevertheless, the subsequent stages of washing and drug adhesion by complexation neutralized these negative aspects of ionizing radiation with respect to the increase in platelet adhesion and deformation. Consequently, the

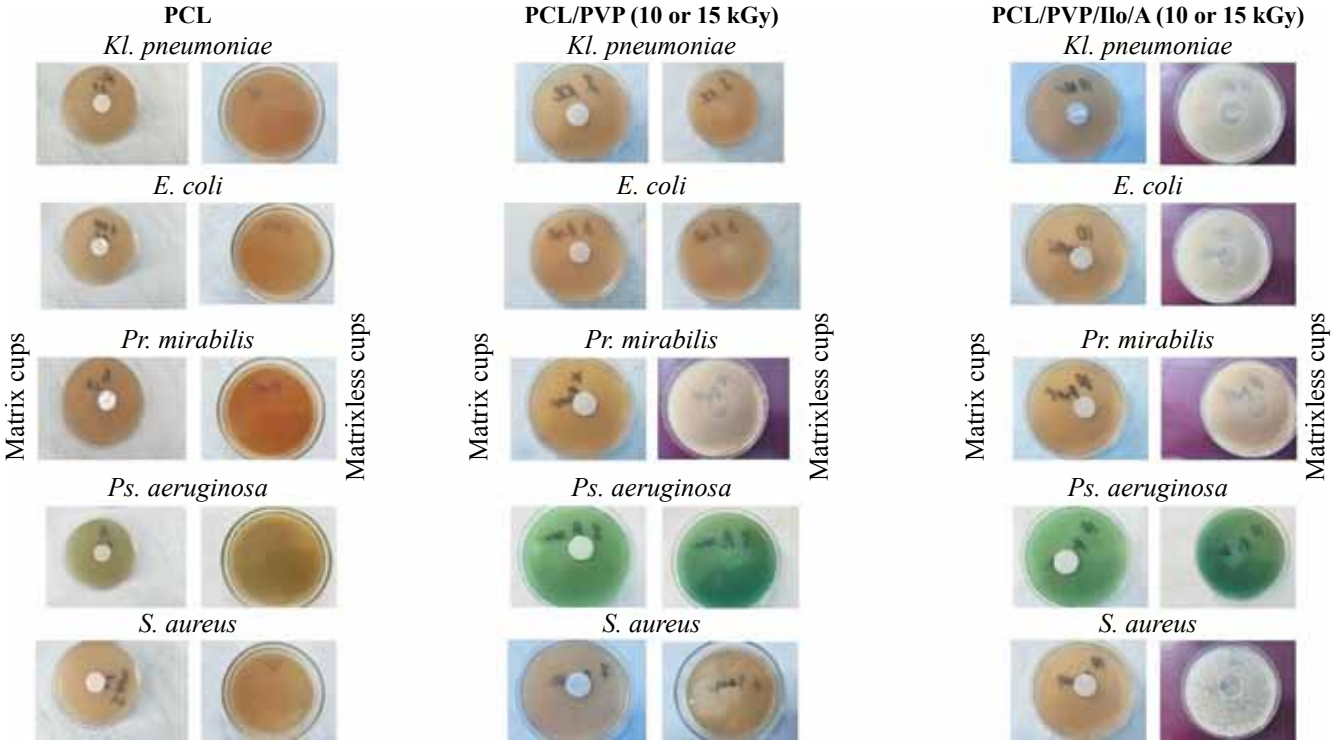

Fig. 5. Bacteriostatic properties of PCL scaffolds before and after modification with cationic amphiphile and iloprost

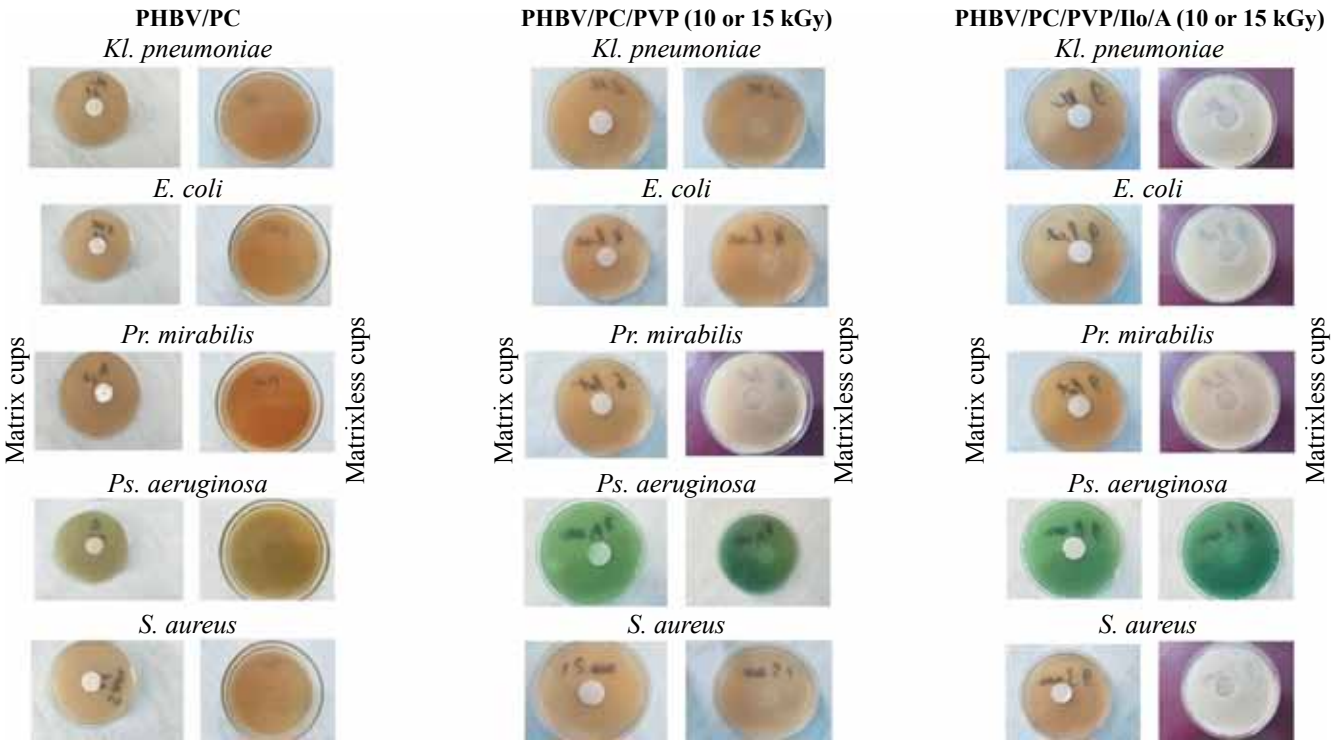

Fig. 6. Bacteriostatic properties of PHBV/PCL scaffolds before and after modification with cationic amphiphile and iloprost

subsequent choice of a 15 kGy radiation dose would be preferable, since, without adversely affecting the biocompatibility of the final product, it allows to simultaneously polymerize polyvinylpyrrolidone with the surface of biodegradable grafts and sterilize the grafts.

Based on PVP ability to form complexes, attachment of drugs to the free reactive groups of the PVP-based hydrogel is done by complexation. This method of drug incorporation, unlike covalent binding, allows for maximum preservation of the biological activity of drugs without creating steric hindrances and without blocking the molecule binding centers with blood clotting factors. The efficacy of iloprost and 1,5-bis-(4-tetradecyl-1,4-diazoniabicyclo[2.2.2]octan-1-yl)pentane tetrabromide after complexation with PVP has been proven both in hemocompatibility tests and in bacteriological examinations. A significant decrease in platelet adhesion to the surface of drug-eluting grafts compared to the unmodified counterparts and matrices with polymerized PVP was revealed. Cationic amphiphilic polymer matrices exhibited convincing bacteriostatic properties at the site where the matrices were applied on the agar without causing hemolysis.

CONCLUSION

A full cycle of surface modification of PCL- and PHV/PCL-based biodegradable polymer grafts resulted in a significant increase in the anti-thrombogenic and antimicrobial properties of prosthetic grafts and did not worsen the stress-strain and biocompatible properties of the developed constructs.

The study was carried out with financial support from the Russian Science Foundation (grant No. 20-15-00075 "Development of a biodegradable small-diameter vascular graft with an anti-thrombogenic and antimicrobial coating").

The authors declare no conflict of interest.

REFERENCES

1. *Taggart DP.* Current status of arterial grafts for coronary artery bypass grafting. *Ann. Cardiothorac Surg.* 2013; 2 (4): 427–430. doi: 10.3978/j.issn.2225-319X.2013.07.21. PMID: 23977618.
2. *Altun G, Pulathan Z, Hemsinli D.* Obturator bypass in the treatment of prosthetic graft infection: Classic but still effective. *Turk Gogus Kalp Damar Cerrahisi Derg.*

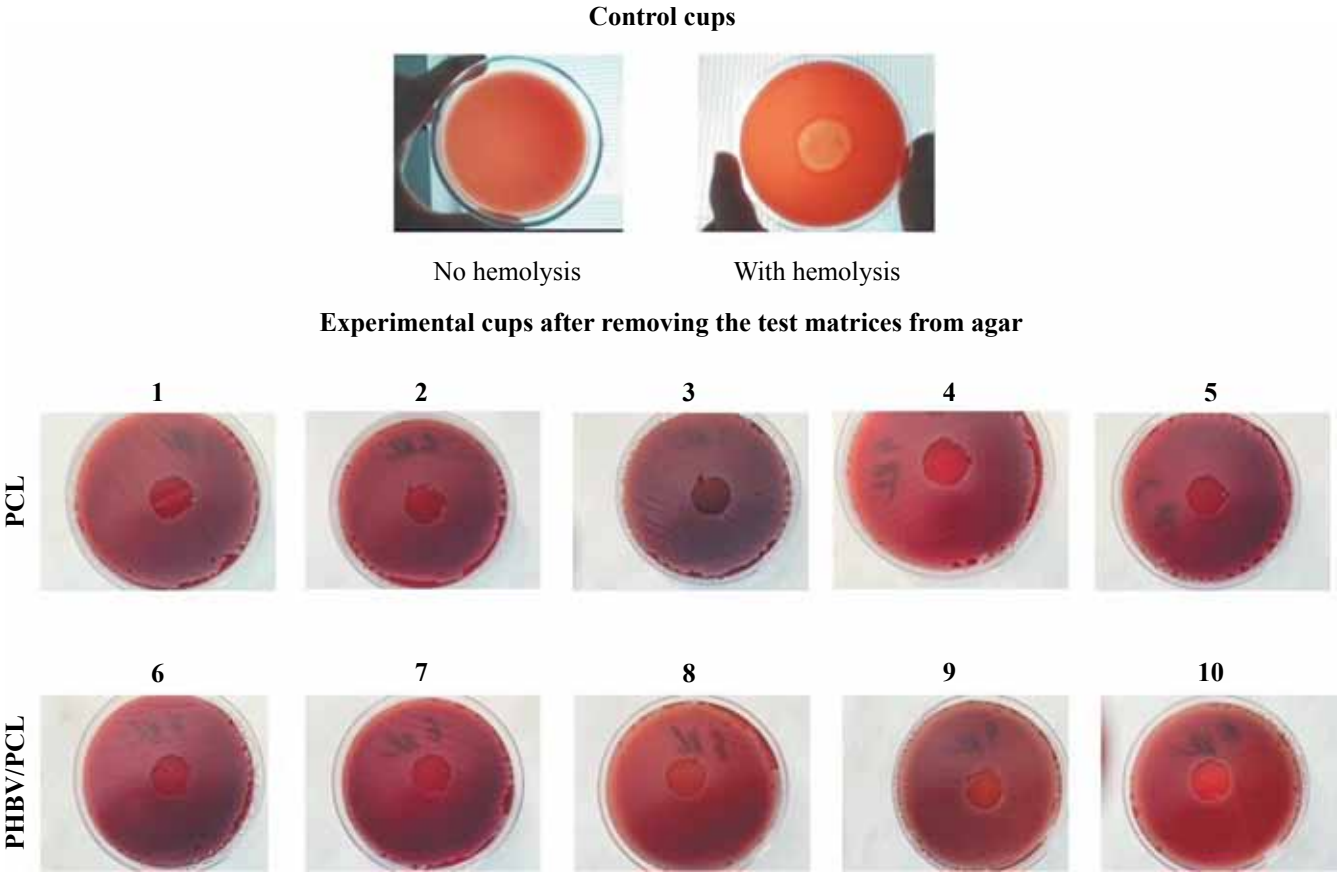

Fig. 7. Delayed growth of K. pneumonia and absence of hemolysis at the location of polymer scaffolds: 1 – PCL; 2 – PCL/PVP-10 kGy; 3 – PCL/PVP-15 kGy; 4 – PCL/PVP/Ilo/A-10 kGy; 5 – PCL/PVP/Ilo/A-15 kGy; 6 – PHBV/PCL; 7 – PHBV/PCL/PVP-10 kGy; 8 – PHBV/PCL/PVP-15 kGy; 9 – PHBV/PCL/PVP/Ilo/A-10 kGy; 10 – PHBV/PCL/PVP/Ilo/A-15 kGy

2018; 26 (3): 480–483. doi: 1010.5606/tgkdc.dergisi.2018.15744. PMID: 32082784.
3. *Gentili A, Di Pumpo M, La Milia DI, Vallone D, Vangi G, Corbo MI et al.* A Six-Year Point Prevalence Survey of Healthcare-Associated Infections in an Italian Teaching Acute Care Hospital. *Int J Environ Res Public Health.* 2020; 17 (21): 7724. doi: 10.3390/ijerph17217724. PMID: 33105772.
4. *Welborn MB, Valentine RJ.* Vascular infection. In Vascular Medicine; 2006. p. 859–879. *Elsevier Inc.* doi: 10.1016/B978-0-7216-0284-4.50067-1.
5. *Sousa JV, Antunes L, Mendes C, Marinho A, Gonçalves A, Gonçalves Ó et al.* Prosthetic vascular graft infections: a center experience. *Angiologia e Cirurgia Vascular.* 2014; 10 (2): 52–57. doi.org/10.1016/S1646-706X(14)70050-3.
6. *Aslam S, Darouiche RO.* Role of antibiofilm-antimicrobial agents in controlling device-related infections. *Int J Artif Organs.* 2011; 34 (9): 752–758. doi: 10.5301/ijao.5000024. PMID: 22094553.
7. *Geipel U.* Pathogenic organisms in hip joint infections. *Int J Med Sci.* 2009; 6 (5): 234–240. doi: 10.7150/ijms.6.234. PMID: 19834588.
8. *Staneviciute E, Na'amnih W, Kavaliauskas P, Prakapaite R, Ridziauskas M, Kevlicius L et al.* New *in vitro* model evaluating antiseptics' efficacy in biofilm-associated *Staphylococcus aureus* prosthetic vascular graft infection. *J Med Microbiol.* 2019; 68 (3): 432–439. doi: 10.1099/jmm.0.000939. PMID: 30735113.
9. *Zhao G, Hochwalt PC, Usui ML, Underwood RA, Singh PK, James GA et al.* Delayed wound healing in diabetic (db/db) mice with *Pseudomonas aeruginosa* biofilm challenge: a model for the study of chronic wounds. *Wound Repair Regen.* 2010; 18 (5): 467–477. doi: 10.1111/j.1524-475X.2010.00608.x. PMID: 20731798.
10. *Ng VW, Chan JM, Sardon H, Ono RJ, García JM, Yang YY et al.* Antimicrobial hydrogels: a new weapon in the arsenal against multidrug-resistant infections. *Adv Drug Deliv Rev.* 2014; 78: 46–62. doi: 10.1016/j.addr.2014.10.028. PMID: 25450263.
11. *Ghosh C, Haldar J.* Membrane-Active Small Molecules: Designs Inspired by Antimicrobial Peptides. *Chem Med Chem.* 2015; 10 (10): 1606–1624. doi: 10.1002/cmdc.201500299. PMID: 26386345.
12. *Molchanova N, Hansen PR, Franzyk H.* Advances in Development of Antimicrobial Peptidomimetics as Potential Drugs. *Molecules.* 2017; 22 (9): 1430. doi: 10.3390/molecules22091430. PMID: 28850098.
13. *Ghosh C, Haldar J.* Membrane-Active Small Molecules: Designs Inspired by Antimicrobial Peptides. *ChemMedChem.* 2015; 10 (10): 1606–1624. doi: 10.1002/cmdc.201500299. PMID: 26386345.
14. *Antonova LV, Sevostyanova VV, Rezvova MA et al.* Technology of producing functionally active biodegradable small-diameter vascular prostheses with drug coating: patent # 2702239. Proprietor: Federalnoe gosudarstvennoe byudzhetnoe nauchnoe uchrezhdenie "Nauchno-issledovatelskij institut kompleksnykh problem serdechno-sosudistykh zabolevanij" (NII KPSSZ) (RU); № 2019119912; effective date for property rights: 25.06.2019; registration date: 07.10.2019, Bull. № 28. [In Russ].
15. *Fedorova AA, Azzami K, Ryabchikova EI, Spitsyna YE, Silnikov VN, Ritter W et al.* Inactivation of a non-enveloped RNA virus by artificial ribonucleases: honey bees and acute bee paralysis virus as a new experimental model for *in vivo* antiviral activity assessment. *Antiviral Res.* 2011; 91 (3): 267–277. doi: 10.1016/j.antiviral.2011.06.011. PMID: 21722669.
16. *Yarinich LA, Burakova EA, Zakharov BA, Boldyreva EV, Babkina IN, Tikunova NV et al.* Synthesis and structure-activity relationship of novel 1,4-diazabicyclo[2.2.2] octane derivatives as potent antimicrobial agents. *Eur J Med Chem.* 2015; 95: 563–573. doi: 10.1016/j.ejmech.2015.03.033. PMID: 25867737.
17. *Burakova EA, Saranina IV, Tikunova NV, Nazarkinaa ZK, Laktionova PP, Karpinskaya LA et al.* Biological evaluation of tetracationic compounds based on two 1,4-diazabicyclo[2.2.2]octane moieties connected by different linkers. *Bioorg Med Chem.* 2016; 24 (22): 6012–6020. doi: 10.1016/j.bmc.2016.09.064. PMID: 27720324.
18. *Ye X, Wang Z, Zhang X, Zhou M, Cai L.* Hemocompatibility research on the micro-structure surface of a bionic heart valve. *Biomed Mater Eng.* 2014; 24 (6): 2361–2369. doi: 10.3233/BME-141049. PMID: 25226936.
19. *Shen X, Su F, Dong J, Fan Z, Duan Y, Li S. In vitro* biocompatibility evaluation of bioresorbable copolymers prepared from L-lactide, 1, 3-trimethylene carbonate, and glycolide for cardiovascular applications. *J Biomater Sci Polym Ed.* 2015; 26 (8): 497–514. doi: 10.1080/09205063.2015.1030992. PMID: 25783945.
20. *Jung F, Braune S, Lendlein A.* Haemocompatibility testing of biomaterials using human platelets. *Clin Hemorheol Microcirc.* 2013; 53 (1–2): 97–115. doi: 10.3233/CH-2012-1579. PMID: 22954639.
21. *Bai J, Dai J, Li G.* Electrospun composites of PHBV/pearl powder for bone repairing. *Progress in Natural Science: Materials International.* 2015; 25 (4): 327–333. doi: 10.1016/j.pnsc.2015.07.004.
22. *Lyu JS, Lee JS, Han J.* Development of a biodegradable polycaprolactone film incorporated with an antimicrobial agent via an extrusion process. *Sci Rep*. 2019; 9 (1): 20236. doi: 10.1038/s41598-019-56757-5. PMID: 31882928.
23. *Mireles LK, Wu MR, Saadeh N, Yahia H, Sacher E.* Physicochemical Characterization of Polyvinyl Pyrrolidone: A Tale of Two Polyvinyl Pyrrolidones. *ACS Omega.* 2020; 5 (47): 30461–30467. doi: 10.1021/acsomega.0c04010. PMID: 33283094.
24. *Källrot M, Edlund U, Albertsson AC.* Surface functionalization of degradable polymers by covalent grafting. *Biomaterials.* 2006; 27 (9): 1788–1796. doi: 10.1016/j.biomaterials.2005.10.010. PMID: 16257444.

The article was submitted to the journal on 12.04.2021

DOI: 10.15825/1995-1191-2021-2-137-146

COMPARATIVE ANALYSIS OF PROTOCOLS FOR DECELLULARIZATION OF CORNEAL LENTICULAR TISSUE

S.A. Borzenok[1, 2], S.V. Kostenev[1], A.V. Doga[1], A.V. Shatskikh[1], V.G. Li[1], D.S. Ostrovskiy[1], M.K. Khubetsova[1]

[1] S. Fyodorov Eye Microsurgery Federal State Institution, Moscow, Russian Federation
[2] A.I. Evdokimov Moscow State University of Medicine and Dentistry, Moscow, Russian Federation

Shortage of donor corneas is a burning issue in ophthalmology. That is why there is a search for new alternative ways for treating corneal diseases. Decellularization technologies make it possible to create corneal tissue-engineered constructs that can adrress the issue of donor corneal shortage. **Objective:** to conduct a comparative analysis of effective methods for treating the corneal lenticula and to create an optimized and standardized decellularization protocol. **Materials and methods.** Corneal stromal lenticules obtained after ReLEx SMILE surgery were chosen for the study. Lenticule parameters: thickness 77–120 microns, diameter 6.5 mm. We used 3 protocols for the treatment of lenticules: 1) treatment with 1.5 M sodium chloride with nucleases (NaCl); 2) 0.1% SDS (SDS); 3) treatment with Trypsin-EDTA solution, followed by double washing in a hypotonic Tris buffer solution with nucleases (Trypsin-EDTA). Optical properties of lenticles were determined spectrophotometrically, where the samples before decellularization served as a control. Fluorescence imaging of nuclear material in the original cryosections was performed using Hoechst dye. The state of collagen fiber ultrastructure was assessed by scanning electron microscopy. The quantitative DNA content in fresh lenticules and in lenticules after treatment was analyzed. **Results.** All three decellularization protocols effectively removed nuclear and cellular material; the residual DNA content was <50 ng/mg. However, the Trypsin-EDTA protocol led to significant damage to the extracellular matrix structure, which negatively affected the transparency of corneal tissue-engineered constructs. Transparency of samples for the NaCl protocol was close to native lenticules. Conclusion. To create a corneal tissue-engineered construct, NaCl decellularization protocols appear to be optimized and can be used to treat various corneal diseases.

Keywords: cornea, tissue engineering, decellularization, lenticula.

INTRODUCTION

Technical advances in refractive surgery have led to the development of a femtosecond laser vision correction method using ReLEx SMILE technology (Refractive Lenticule Extraction & Small Incision Lenticule Extraction). During operation, the surgeon first uses a laser to form a disc-shaped portion of the corneal stroma (the lenticule), which is then extracted through a micro incision. Such lenticule parameters as thickness and diameter depend on the initial corrected myopia or myopic astigmatism [1].

Lenticule reimplantation has been shown to restore stromal volume and refractive anomalies after surgery (refractive lenticule extraction), as shown in monkey and rabbit models [2, 3]. Correction of farsightedness and keratoconus with intrastromal lens implantation has also been reported [4–6].

It is worth noting that the current severe shortage of donor material underlies the search for new directions in the treatment of corneal disorders. It is generally recognized that tissue engineering is an alternative to allotransplantation, therefore, the use of lenticules seems to be a promising and effective technique. However, residual cellular components of the lenticules place this graft in the category of true grafts, which, as is known, can lead to rejection reaction.

The modern view of allogeneic transplantation implies the preparation of suitable acellular, non-immunogenic tissues for subsequent transplantation to the recipient. Decellularization is a promising direction in tissue engineering, allowing for maximum removal of cells and genetic material, thereby reducing the risk of graft immunity reaction. However, it should be noted that damage to the extracellular matrix (ECM) should be minimized, since preservation of the framework and structural and functional properties of ECM is fundamental to effective use of decellularized organs and tissues [7, 8]. Various decellularization protocols described in the literature employ physical, enzymatic, and chemical methods to release ECM from cells [9].

Corresponding author: Valeriy Li. Address: 59a, Beskudnikovsky Boulevard, Moscow, 127486, Russian Federation. Phone: (916) 071-38-80. E-mail: inferno_03@mail.ru

In the studies by Gary Hin-Fai Yam et al., the authors used donor corneas as a source of 70 μm thick stromal lenticules created by femtosecond laser [10]. The authors compared decellularization protocols, both with isolated application of 0.1% sodium dodecylsulfate (SDS), 0.1% Triton X-100, 1.5 M NaCl, and in combination with nucleases of various concentrations. By spectrophotometry, a transmittance similar to the control was obtained in the 1.5 M NaCl group followed by the 0.1% SDS group. When evaluating immunohistochemistry data, it was found that after treatment with 0.1% SDS, there was no luminescence of the nuclei, while in the groups using 0.1% Triton X-100, 1.5 M NaCl and 1.5 M NaCl with nucleases 2 U/ml, luminescence was preserved. DNA content in the 0.1% SDS group was 20.71 ± 4.3 ng DNA per 1 mg dry weight of the sample; the length of extracted DNA fragments was less than 200 base pairs, which corresponded to the indicative criteria for the effectiveness of organ and tissue decellularization suggested by Crapo et al. [11].

In an experiment on rabbits, Chinese researchers created a construct of decellularized lenticules glued together with fibrin glue for carrying out anterior lamellar keratoplasty [12]. These stromal lenticules were extracted from the human cornea by ReLEx SMILE surgery (with ≥100 μm thickness and 6.6 mm diameter). The treatment protocol used was 1.5 M NaCl with 5 U/ml DNase and 5 U/ml RNase solution. This protocol was borrowed from the work of Shafiq et al, where the authors reported its successful application on whole donor human corneas for cell removal [13].

In a recent study, Huh M.I. et al. used donor corneas from which stromal lenticules were extracted using ReLEx SMILE (100 μm thickness, 8 mm diameter). Decellularization protocols used included washing in Triton X-100, SDS or trypsin-EDTA solution under various concentrations: 0.1%, 0.25%, 0.5%. Then washing was done in hypotonic, isotonic, and hypertonic tris-buffer solutions followed by washing in nuclease solution. Finally, the wash cycle was repeated in Tris-buffer solutions [14].

Of the protocols, decellularization with hypotonic 0.25 and 0.5% trypsin-EDTA followed by washing in hypotonic tris-buffer with nucleases showed the lowest DNA contents. Spectrophotometry revealed that the group using 0.5% trypsin-EDTA and hypotonic Tris-buffer had the best transparency. Scanning electron microscopy data in this group revealed that the ECM after treatment was undisturbed.

Thus, we can conclude that there are many corneal lenticular decellularization protocols today. However, despite all the diversity, there is still no clear understanding of the preferred protocol.

PURPOSE OF THE STUDY

In our study, we compared effective lenticular treatment methods in order to optimize and standardize the decellularization protocol.

MATERIALS AND METHODS

Before the Smile operation, voluntary informed consent for further use of donor lenticular tissue was obtained from all patients. The mean age of patients was 27.3 ± 5.4 years. All patients underwent SMILE surgery for myopia and complex myopic astigmatism. The spherical equivalent before the SMILE surgery was –4.72 ± 0.86 diopters. For decellularization, lenticules with 77–120 μm thickness and 6.5 mm diameter were used.

The material was taken in the operating room at the head office of Fyodorov Eye Microsurgery Federal State Institution in Moscow. The ReLex SMILE eye surgery was carried out under local drip anesthesia using a VisuMax femtosecond laser (500 kHz pulse frequency, 160 nJ pulse energy). First, the base of the lenticule was formed, and then its "lid". The lenticule diameter was 6.5 mm, while the lid diameters were 7.5 mm and 7.6 mm. The resulting lenticule was transferred into a pre-prepared vial containing dispersed viscoelastic (DV) containing 3.0% sodium hyaluronate and 4.0% chondroitin sulfate weighing 600,000 Daltons. Next, the vial with samples was transferred into a container and transported to the laboratory at the Center for Fundamental and Applied Biomedical Problems, Fyodorov Eye Microsurgery Federal State Institution. In the laboratory, studies were carried out under sterile conditions in vitro (n = 145). Table 1 shows the distribution of lenticules in the experiment.

Table 1

Distribution of lenticules by type of work

Lenticule assessment methods	Number of lenticules
Spectrophotometry	45
Histology	20
Immunohistochemistry	20
Scanning electronic	20
Microscopy	40
DNA analysis	145

Decellularization of the lenticule

Before decellularization, the lenticules were washed of DV in PBS solution (three times) for 5 minutes each. Three solution variants were used for decellularization. They differed in components, exposure time, and concentration. As a result, four groups were formed, where

three groups were experimental and one was the control (Table 2).

Transparency of native and decellularized lenticules

Spectral transmission of lenticule from 380 to 780 nm wavelength was determined using a Multiskan GO spectrophotometer (Thermo Scientific, USA); data were collected in 10 nm increments. Spectral transmission for the same samples was performed in two stages. At the first stage, native lenticules were measured – the control group. At the second stage, the transparency of the three experimental groups after treatment was investigated.

According to literature, glycerol (glycerin) is used to eliminate nonspecific lenticular edema after decellularization. In this study, DV approved for clinical use in ophthalmology was used for this purpose. After dehydration in DV for 1 hour, the samples were transferred to a 96-well plate starting from the second well, with the first well containing no lenticule. A volume of 250 μl of DV was added to each well and evenly distributed along its bottom. Then the 96-well plate was inserted into a spectrophotometer chamber to measure the transmittance K_p (%). As a calculated value for statistical analysis of the data, we used the average for the entire group of 41 transparency points of the obtained spectrum. For this, K_o was first calculated as follows:

$$K_o = \frac{K_1}{K_2} \times 100\ \%,$$

where K_o – transmittance for each of 41 spectral points within one sample in the group; K_1 – transmittance in the well containing the sample; K_2 – transmittance in the well not containing the sample.

K_c was then calculated as follows:

$$K_c = \frac{\Sigma K_o}{N},$$

where K_c – average transmittance for each of 41 spectral points of all samples in the group; ΣK_o – aggregate value of measurements of each sample in the group; N – total number of samples in the group.

K_p was then calculated as follows:

$$K_п = \frac{\Sigma K_c}{41},$$

where K_p – average transmittance for all 41 spectral points of the group as a whole; ΣK_c – aggregate value of the average transmittance; 41 – number of spectral points, which corresponds to a 380 to 780 nm wavelength, in 10 nm increments.

Histological evaluation of native and decellularized lenticules

The lenticules were fixed in a 10% solution of neutral formalin, then washed with running water, dehydrated in alcohols of ascending concentration, and embedded in paraffin. Next, a series of 2–3 μm thick histological sections were performed using hematoxylin and eosin stain, Van Gieson's stain, and alcian blue stain to assess the content of glycosaminoglycans in the tissues. The preparations were studied on an ix81 inverted microscope (Olympus, Japan) at 40× magnification, followed by photographing.

Using immunohistochemistry (IHC), we studied the expression of collagen types I, III, V and VI, characteristic of the corneal stroma and being the main ECM component. For this purpose, native and treated samples were first placed in Shandon Cryomatrix medium (Ther-

Table 2

Description of decellularization protocols

№	Active components	Description of method
1	Native lenticules	
2	0.1 % SDS (SDS)	Incubation in 0.1% sodium dodecyl sulfate (SDS) solution (Sigma-Aldrich) for 24 hours at room temperature. Samples were then washed in phosphate-buffered saline (PBS) with continuous shaking in a shaker and at 4 °C temperature, with PBS replacement every 24 hours
3	1.5 M NaCl + DNAase 5 U/ml and RNase 5 U/ml (NaCl)	Incubation in 1.5 M sodium chloride solution for 48 hours, with replacement of NaCl solution every 24 hours. Samples were then incubated in a DNase 5 U/mL (Sigma-Aldrich) and RNase 5 U/mL (Sigma-Aldrich) solution for 48 hours. Samples were then washed in PBS solution for 72 hours, with replacement every 24 hours. The treatment procedure was carried out at room temperature and with continuous shaking in a shaker
4	0.25% Trypsin-EDTA (Thermo fisher) + hypotonic Tris buffer solution (pH 7.2) + DNAase 50 U/mL and RNase 1 U/mL + hypotonic Tris buffer solution (Trypsin-EDTA)	Incubation in 0.25% Trypsin-EDTA solution for 48 hours, then 1 hour in a hypotonic Tris buffer solution (pH 7.2), then in a DNase 50 U/mL and RNase 1 U/mL solution for 24 hours. The samples were then washed in hypotonic Tris buffer solution (pH 7.2) for 1 hour. The decellularization procedure was performed at 37 °C temperature and with continuous shaking in a shaker

mo scientific, uk) and frozen at –30 °C temperature in an HM525 NX cryostat (Thermo scientific, UK). Then 10 μm-thick cryostat sections were made and transferred to Polysine slides (Thermo Scientific, UK), at the rate of four sections per slide. The following primary antibodies were used: type I collagen (Rabbit 1:200, ab34710, Abcam), type III collagen (Mouse 1:100, ab6310, Abcam); collagen type V (Rabbit 1:100, ab114072, Abcam); collagen type VI (Rabbit 1:200, ab6588, Abcam). Secondary antibodies Alexa Fluor 488 (1:250, ab150077, Goat Anti-Rabbit IgG, Abcam) and Alexa Fluor 594 (1:250, ab150116, Goat Anti-Mouse IgG, Abcam) were used to identify the above markers. After removal of secondary antibodies, the Hoechst dye (O150, PanEko) was used to assess nuclear staining. The results were evaluated using a laser scanning confocal microscope "Fluo View FV10i" (Olympus, Japan) 100×.

Evaluation of the ultrastructure of collagen fibers by scanning electron microscopy

Samples were dehydrated in acetone solution at an ascending concentration of 10%; 30%; 50%; 70%; 90%; 100% (three times) for 10 minutes each. The samples were then subjected to critical drying using a desiccant dryer (Critical Point Dryer Qurum k850, Quorum Technologies, UK). Then the samples were sputtered with gold (5 nm layer thickness, assay 999) using a sputtering device (Smart Coater SPI, SPI Supplies, USA) and analyzed using a scanning electron microscope – 6000plus (Jeol, Japan). The samples were analyzed at ten randomly selected points in a high vacuum mode 1000× (10 kV power).

Measurement of DNA content

DNA was extracted from samples using the DNeasy Blood & Tissue Kit (QIAGEN, Germany) according to the manufacturer's recommendations. The DNA content was counted using a Qubit 2.0 fluorometer (Invitrogen, USA) and a Qubit dsDNA HS (High-Sensitivity) Assay Kit (Invitrogen, USA). Measurement was carried out according to the manufacturer's instructions.

Statistical analysis

The mean with standard deviation (M ± SD) and median with interquartile range (Me (1–3 quartiles)) were used as descriptive statistics for variables. Normality of distribution of variables was assessed using the Shapiro–Wilk test. Homogeneity of variances was assessed using the Bartlett's test.

Independent samples were compared using the Kruskal–Wallis test followed by Dunn's post-hoc test or Welch's t-test for non-normally and normally distributed samples (with heterogeneous variances), respectively. In all cases, the Holm's correction for multiple comparisons was used. Results were considered statistically significant at $p < 0.05$.

Data was statistically processed using statistical computing environment R version 4.0.2 (R Foundation for Statistical Computing, Vienna, Austria). The data was visualized using GraphPad Prism 8.4.3 (GraphPad Software, Inc., USA).

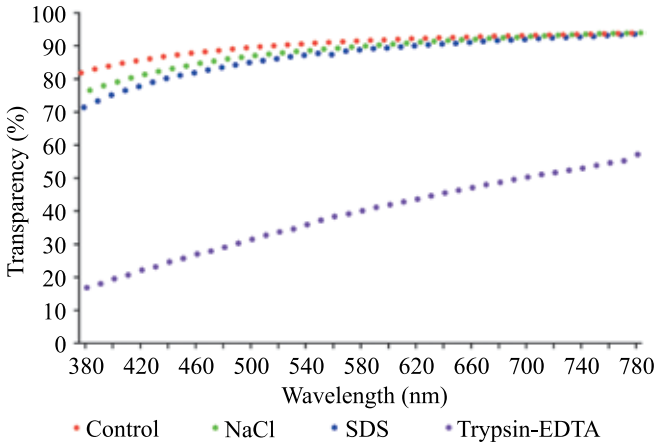

Fig. 1. Average spectral transmittance (%) at 380 to 780 nm wavelength

RESULTS

Transparent properties of the lenticule

The study showed that transparency was significantly reduced in the Trypsin-EDTA group compared to the control group, and the results in the NaCl group were the closest to the control (Fig. 1). There were statistically significant differences in groups SDS/Control (86.85 ± 3.34 vs. 90.39 ± 5.11; (87.46 (84.33–89.63)) vs. (91.49 (86.64–93.80)); $p < 0.03$); Trypsin-EDTA/Control (38.70 ± 8.78 vs. 90.39 ± 5.11; (43.74 (33.56–44.86)) vs. (91,49 (86,64–93,80)); $p < 0.0001$); also when comparing NaCl/Trypsin-EDTA (88.63 ± 2.56 vs. 38.70 ± 8.78; (89.12 (88.59–90.06)) vs. (43,74 (33,56–44,86)); $p < 0.0001$); SDS/Trypsin-EDTA (86.85 ± 3.34 vs. 38.70 ± 8.78; (87.46 (84.33–89.63)) vs. (43.74 (33.56–44.86)); $p < 0.003$).

Histological staining of lenticules

Histological staining with H&E, Van Gieson and alcian blue revealed complete removal of cells, cell nuclei and the absence of significant structural damage in the resulting acellular matrix in the SDS and NaCl groups. In the Trypsin-EDTA group, there was noticeable significant damage to the matrix structure against the background of complete absence of cells and cell nuclei (Fig. 2).

Immunohistochemical staining of lenticules

Fluorochromation of nuclei with Hoechst dye showed that the lenticules that were treated stained negatively. Meanwhile, a characteristic luminescence of the nuclei was determined in the control group. Also, according to IHC data, there was positive expression of collagen types I, III, V and VI in the control and experimental groups (Fig. 3).

Results of scanning electron microscopy

When analyzing the thickness of collagen fibers of the samples, differences were found both between the experimental groups and the control, as well as when comparing the experimental protocols in pairs with each other. In the NaCl/Control pair comparison, the thickness was (1.96 ± 0.46 vs. 2.30 ± 0.40; (1.9 (1.69–2.21)) vs. (2.26 (2.03–2.63)); p = 0.00013). Groups SDS/Control (1.36 ± 0.25 vs. 2.30 ± 0.40; (1.36 (1.21–1.47)) vs. (2.26 (2.03–2.63)); p < 0.0001). For Trypsin-EDTA/Control protocols (4.19 ± 0.56 versus 2.30 ± 0.40; (4.13 (3.85–4.54)) versus (2.26 (2.03–2.63)); p < 0.0001). Pairwise comparison of the protocols for NaCl, SDS, Trypsin-EDTA between each other revealed statistically significant differences (p < 0.0001). In Fig. 4, it can be seen that the SDS group is mainly represented by frayed fibrils, due to lack of sufficient volume of collagen fibers. In the Trypsin-EDTA group, there is a noticeable thickening of collagen fibers, which is caused by gross disturbance of their ultrastructure. Slight changes in the state of collagenous fibers were detected in the NaCl group.

DNA analysis

Pairwise comparison of groups by Welch's t-test (with Holm's correction) revealed a statistically significant difference, both between the experimental groups and the control, and between the experimental groups: NaCl/Control (39.34 ± 8.65 vs. 132.18 ± 44.17; (41.99 (38.57–44.67)) vs. (128.5 (102.02–154.48)); p < 0.0002); SDS/Control (37.07 ± 6.19 vs. 132.18 ± 44.17; (39.74 (36.72–42.75)) versus (128.5 (102.02–154.48)); p <

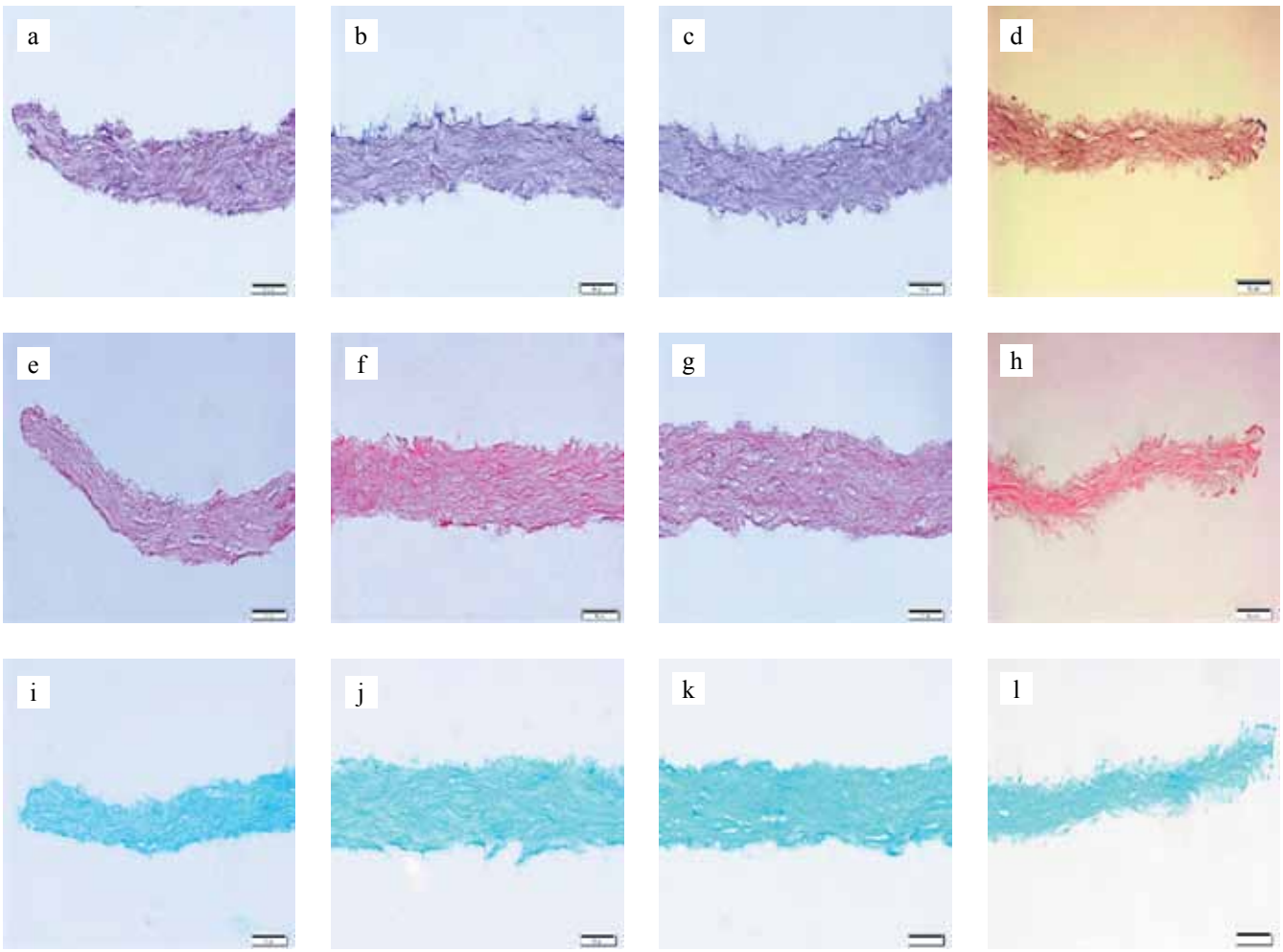

Fig. 2. Histological picture of native and decellularized lenticules. H&E stain: а – control, б – NaCl, в – SDS, г – Trypsin-EDTA; Van Gieson's stain: д – control, е – NaCl, ж – SDS, з – Trypsin-EDTA; Alcian blue stain: и – control, к – NaCl, л – SDS, м – Trypsin-EDTA; ×40

0.0001); Trypsin-EDTA/Control (13.42 ± 7.4 versus 132.18 ± 44.17; (11.45 (8.47–16.86)) versus (128.5 (102.02–154.48)); $p < 0.0001$). Comparison of experimental groups with each other revealed statistically significant differences for the NaCL/SDS groups ($p < 0.002$), for the SDS/Trypsin-EDTA groups ($p < 0.0006$), and for the NaCl/Trypsin-EDTA groups ($p < 0.0001$).

DISCUSSION

At the moment, there is an active search for an effective tissue-engineered corneal construct (TECC) as an alternative to donor corneal transplantation in conditions of severe corneal shortage.

Developing a decellularization protocol is a complex and routine technique. There are many detailed descriptions in the literature of various decellularization protocols for such organs as small intestine, pericardium, heart valves, liver, skin, bladder, and cornea [15, 16]. The effectiveness of decellularization mainly depends on the type of tissue. Unlike thicker organs or tissues, corneal tissue is thinner in thickness and has a specific structural organization, whose preservation is an extremely important condition for decellularization [17]. In this study, we used corneal lenticular tissue obtained during the ReLEX SMILE surgery. To assess decellularization, apart from the decellularization criteria suggested by Crapo et al., we additionally assessed the corneal stromal transparency, the state of collagen fiber ultrastructure and the main ECM components, such as glycosaminoglycans and total collagen [11].

In this study, the SDS and NaCl groups showed better results compared to the Trypsin-EDTA group as part of the pre- and post-treatment transparency assessment. The SDS group was statistically different from the control ($p < 0.005$), in contrast to the NaCl group ($p = 0.524$), which showed transparency results similar to the control group. On histological and immunohistochemical studies, all protocols were effective in removing nuclei. However, significant damage to the main ECM components was observed in the Trypsin-EDTA group, while these ECM components were preserved in the SDS and NaCl groups.

The thickness of the ultrastructure of collagen fibers was found to be highest in the trypsin-EDTA group and lowest in the SDS protocol. NaCl-treated lenticules showed a result closest to that of the control group.

Residual DNA content in all treatment groups was less than 50 ng/mg, which is in line with those suggested

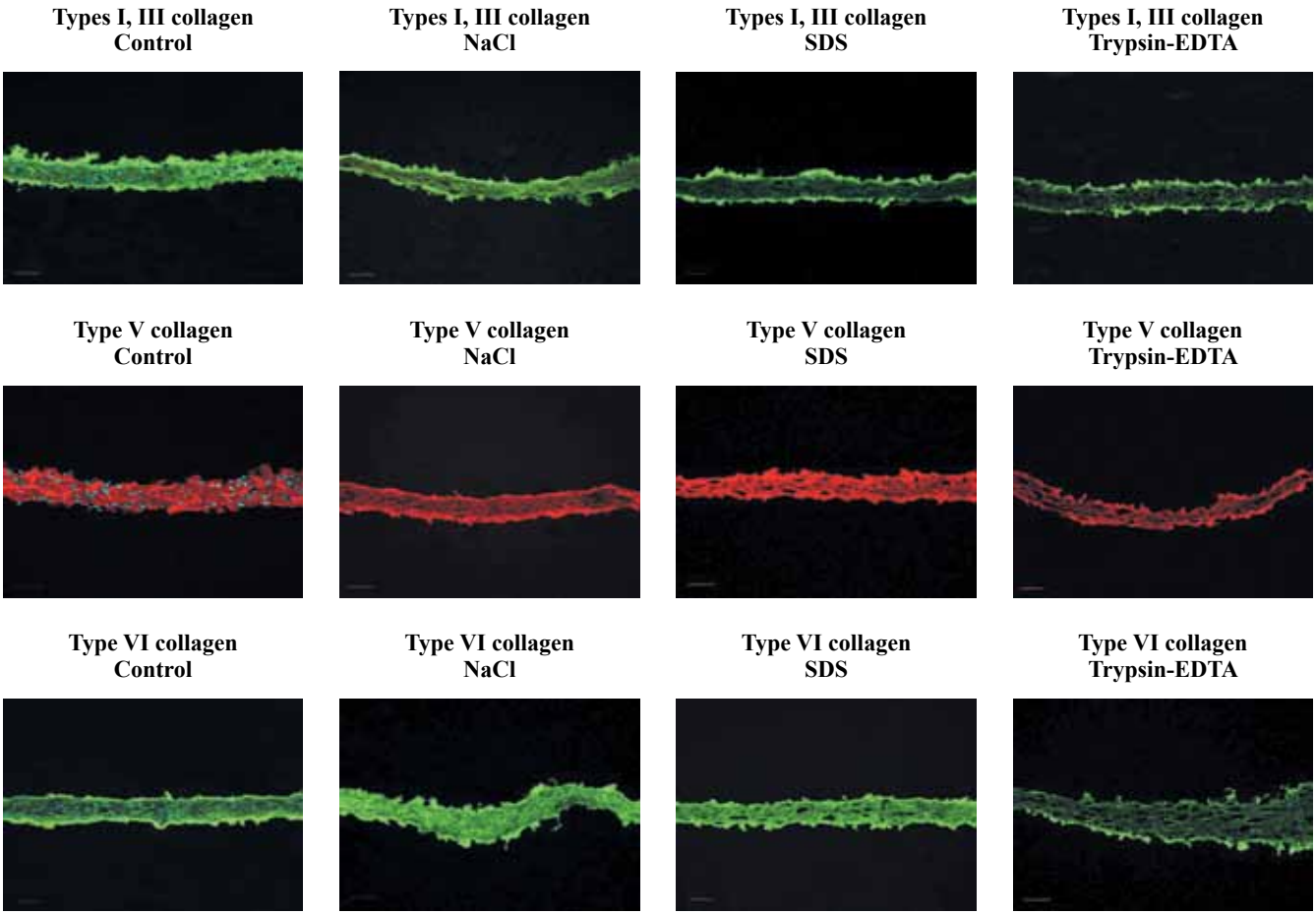

Fig. 3. Immunohistochemistry of native and decellularized lenticules

by Crapo et al. requirements [11]. The Trypsin-EDTA group had the lowest residual DNA content.

Our study did not confirm the data from Huh M.I. et al., where 0.25% and 0.5% Trypsin-EDTA were used with nucleases and double washing in hypotonic buffer solution [14]. We believe that the combined effect of the complex components of this protocol, although it leads to better results in terms of reducing the residual DNA content, nevertheless, is destructive in relation to the ultrastructure of collagen fibers and ECM components. The destructive effect of trypsin and nucleases on the collagen structure of tissues has been reported [18].

The absence of cellular material, the preservation of the collagen structure and the main ECM components are key predictors for TECC. In our study, treatment with 1.5 M NaCl with nucleases showed good results on all evaluation parameters for TECC development.

CONCLUSION

Thus, a comparative assessment of the effectiveness of different decellularization protocols for creating a corneal lenticular matrix creation has led to the creation of optimized and standardized protocols. The results presented in this work open up wide opportunities for the future use of TECC. However, the issue of TECC data storage is still unresolved and requires separate future research in this direction.

The authors declare no conflict of interest.

REFERENCES

1. *Ganesh S, Brar S, Arra RR*. Refractive lenticule extraction small incision lenticule extraction: A new refractive surgery paradigm. *Indian J Ophthalmol*. 2018; 66 (1): 10–19. doi: 10.4103/ijo.IJO_761_17. PMID: 29283117.
2. *Angunawela RI, Riau AK, Chaurasia SS, Tan DT, Mehta JS*. Refractive lenticule re-implantation after myopic ReLEx: a feasibility study of stromal restoration after refractive surgery in a rabbit model. *Invest Ophthalmol Vis Sci*. 2012; 53 (8): 4975–4985. doi: 10.1167/iovs.12-10170. PMID: 22743323.
3. *Riau AK, Angunawela RI, Chaurasia SS, Lee WS, Tan DT, Mehta JS*. Reversible femtosecond laser-assisted myopia correction: a non-human primate study of lenticule re-implantation after refractive lenticule ext-

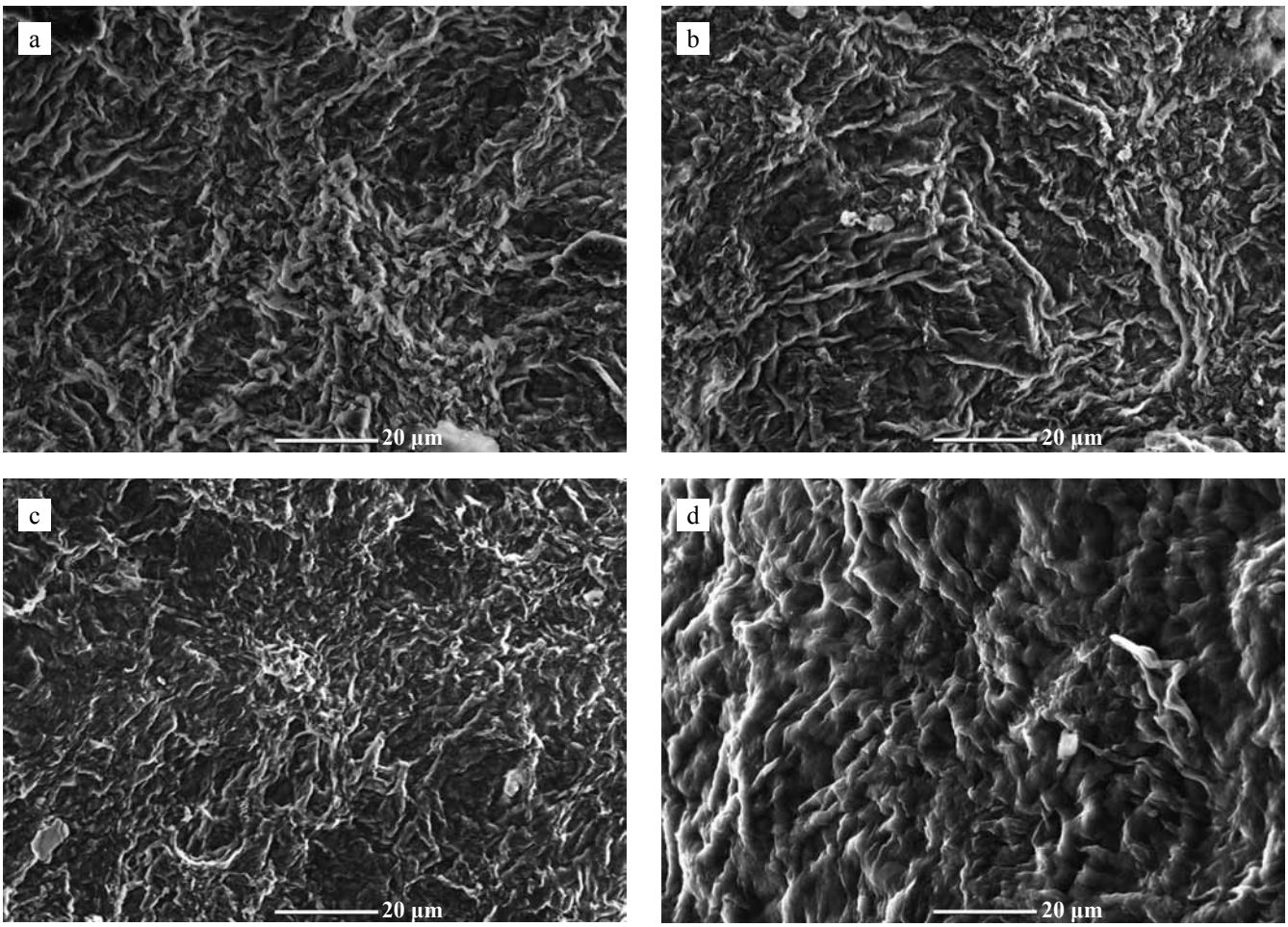

Fig. 4. Collagen ultrastructure of the ECM, where a is the Control, b is NaCl, c is SDS, and d is Trypsin-EDTA. Scanning electron microscopy 1000×

raction. *PLoS One*. 2013; 8 (6): e67058. doi: 10.1371/journal.pone.0067058. PMID: 23826194.

4. *Pradhan KR, Reinstein DZ, Carp GI, Archer TJ, Gobbe M, Gurung R.* Femtosecond laser-assisted keyhole endokeratophakia: correction of hyperopia by implantation of an allogeneic lenticule obtained by SMILE from a myopic donor. *J Refract Surg*. 2013; 29 (11): 777–782. doi: 10.3928/1081597X-20131021-07. PMID: 24203809.
5. *Sun L, Yao P, Li M, Shen Y, Zhao J, Zhou X*. The Safety and Predictability of Implanting Autologous Lenticule Obtained by SMILE for Hyperopia. *J Refract Surg*. 2015; 31 (6): 374–379. doi: 10.3928/1081597X-20150521-03. PMID: 26046703.
6. *Ganesh S, Brar S, Rao PA*. Cryopreservation of extracted corneal lenticules after small incision lenticule extraction for potential use in human subjects. *Cornea*. 2014; 33 (12): 1355–1362. doi: 10.1097/ICO.0000000000000276. PMID: 25343698.
7. *Bonvillain RW, Danchuk S, Sullivan DE, Betancourt AM, Semon JA, Eagle ME et al.* A nonhuman primate model of lung regeneration: detergent-mediated decellularization and initial *in vitro* recellularization with mesenchymal stem cells. *Tissue Eng Part A*. 2012; 18 (23–24): 2437–2452. doi: 10.1089/ten.TEA.2011.0594. PMID: 22764775.
8. *Ott HC, Matthiesen TS, Goh SK, Black LD, Kren SM, Netoff TI et al.* Perfusion-decellularized matrix: using nature's platform to engineer a bioartificial heart. *Nat Med*. 2008; 14 (2): 213–221. doi: 10.1038/nm1684. PMID: 18193059.
9. *Gilbert TW, Sellaro TL, Badylak SF.* Decellularization of tissues and organs. *Biomaterials*. 2006; 27 (19): 3675–3683. doi: 10.1016/j.biomaterials.2006.02.014. PMID: 16519932.
10. *Yam GH, Yusoff NZ, Goh TW, Setiawan M, Lee XW, Liu YC et al.* Decellularization of human stromal refractive lenticules for corneal tissue engineering. *Sci Rep*. 2016; 6: 26339. doi: 10.1038/srep26339. PMID: 27210519.
11. *Crapo PM, Gilbert TW, Badylak SF*. An overview of tissue and whole organ decellularization processes. *Biomaterials*. 2011; 32 (12): 3233–3243. doi: 10.1016/j.biomaterials.2011.01.057. PMID: 21296410.
12. *Yin H, Qiu P, Wu F, Zhang W, Teng W, Qin Z et al.* Construction of a Corneal Stromal Equivalent with SMILE-Derived Lenticules and Fibrin Glue. *Sci Rep*. 2016; 6: 33848. doi: 10.1038/srep33848. PMID: 27651001.
13. *Shafiq MA, Gemeinhart RA, Yue BY, Djalilian AR.* Decellularized human cornea for reconstructing the corneal epithelium and anterior stroma. *Tissue Eng Part C Methods*. 2012; 18 (5): 340–348. doi: 10.1089/ten.TEC.2011.0072. PMID: 22082039.
14. *Huh MI, Lee KP, Kim J, Yi S, Park BU, Kim HK.* Generation of Femtosecond Laser-Cut Decellularized Corneal Lenticule Using Hypotonic Trypsin-EDTA Solution for Corneal Tissue Engineering. *J Ophthalmol*. 2018; 2018: 2590536. doi: 10.1155/2018/2590536. PMID: 29805794.
15. *Badylak SF, Freytes DO, Gilbert TW.* Extracellular matrix as a biological scaffold material: Structure and function. *Acta Biomater*. 2009; 5 (1): 1–13. doi: 10.1016/j.actbio.2008.09.013. PMID: 18938117.
16. *Porzionato A, Stocco E, Barbon S, Grandi F, Macchi V, De Caro R.* Tissue-Engineered Grafts from Human Decellularized Extracellular Matrices: A Systematic Review and Future Perspectives. *Int J Mol Sci*. 2018; 19 (12): 4117. doi: 10.3390/ijms19124117. PMID: 30567407.
17. *DelMonte DW, Kim T.* Anatomy and physiology of the cornea. *J Cataract Refract Surg*. 2011; 37 (3): 588–598. doi: 10.1016/j.jcrs.2010.12.037. PMID: 21333881.
18. *Oh JY, Kim MK, Lee HJ, Ko JH, Wee WR, Lee JH.* Processing porcine cornea for biomedical applications. *Tissue Eng Part C Methods*. 2009; 15 (4): 635–645. doi: 10.1089/ten.TEC.2009.0022. PMID: 19249963.

The article was submitted to the journal on 9.03.2021

DOI: 10.15825/1995-1191-2021-2-147-157

PATHOGENETIC MECHANISMS, EPIDEMIOLOGY AND CLASSIFICATION OF ACUTE KIDNEY INJURY IN HEART TRANSPLANT RECIPIENTS

I.L. Poz[1], A.G. Strokov[1, 2], V.N. Poptsov[1], A.O. Shevchenko[1–3], S.V. Gautier[1, 2]

[1] Shumakov National Medical Research Center of Transplantology and Artificial Organs, Moscow, Russian Federation

[2] Sechenov University, Moscow, Russian Federation

[3] Pirogov Medical University, Moscow, Russian Federation

Kidney injury in heart transplant recipients is of a complex nature and bears the features of all types of cardiorenal interaction impairment. Pre-transplant renal dysfunction, perioperative acute kidney injury, as well as factors associated with graft and immunosuppression, determine the prevalence and severity of kidney pathology in this group of patients. This review examines the pathophysiology of kidney dysfunction in heart failure, the epidemiology, and criteria for acute kidney injury.

Keywords: cardiorenal syndrome, heart transplantation, epidemiology, criteria for acute kidney injury.

Heart disease and renal dysfunction are often interrelated. When the heart and kidneys are affected simultaneously, mortality, morbidity, as well as the complexity and cost of treatment increase significantly [1]. Mutual heart-kidney interaction syndrome has been known for a long time. However, until 2008 it had no clear definition and classification. This situation was corrected at an international conference facilitated by ADQI (Acute Dialysis Quality Initiative), where the opinions of leading experts in the field of nephrology, intensive care, cardiac surgery, cardiology, and epidemiology were reconciled.

Five types of cardiorenal syndrome (CRS) have been identified, which reflect all possible interdependent heart and kidney injury [2, 3]. At the same time, different types of CRS can be manifested at different stages of the disease in one patient. In some cases, there may be a vicious circle, where there is simultaneous or combined heart and kidney damage. A unique example of such a situation is kidney injury in heart transplant recipients, since at different stages of treatment, before and after transplantation, there could be manifestations of all CRS types: impaired kidney function with long-term heart failure (HF) at the preoperative stage; acute kidney injury (AKI) in the perioperative period against the background of cardiopulmonary bypass (CPB), heart graft dysfunction, use of cardiotonic drugs, mechanical support of the contractile function of the heart, immunosuppression; in some cases, renal damage has an outcome in the terminal stage with a continuing need for dialysis replacement therapy and persistence of such pathological mechanisms as suburemia, overhydration, chronic inflammation, bone and mineral disorders, anemia, and others, leading to the development in a heart graft characteristic of a chronic kidney disease (CKD) in the final, dialysis-dependent stage, changes in the form of cardiofibrosis, myocardial hypertrophy, calcification of heart valves and blood vessels.

MECHANISMS OF KIDNEY INJURY IN IMPAIRED CARDIAC FUNCTION

The pathophysiology of kidney injury in HF is complex, involving multiple pathological factors acting simultaneously (Fig.). Although a fall in cardiac output and renal perfusion has traditionally been considered as the main cause of HF-related renal dysfunction, the results of a number of major clinical trials do not support this position. For example, using an analysis of data from 118,465 patients with acute decompensated HF, Heywood et al. could not demonstrate an association between left ventricular systolic dysfunction and deterioration of kidney function [4]. According to the results of a study by K. Damman et al., in 2557 patients who underwent right heart catheterization, increased central venous pressure (CVP) was a predictor of mortality and was associated with low estimated glomerular filtration rate (eGFR), regardless of the cardiac index (CI) [5]. A number of studies suggest the presence of other pathophysiological mechanisms of renal dysfunction, particularly the effect of high right atrial pressure on venous congestion and venous hypertension. The same authors confirmed previously published data in a study of 2647 patients with systolic HF, in whom a decrease in the eGFR and mortality were associated with such manifestations of

Corresponding author: Iakov Poz. Address: 1, Shchukinskaya str., Moscow, 123182, Russian Federation.
Phone: (991) 245-55-61. E-mail: dr.poz@list.ru

venous stasis as ascites and increased pressure in the jugular vein [6]. According to the ESCAPE (Evaluation Study of Congestive Heart Failure and Pulmonary Artery Catheterization Effectiveness) study, which enrolled patients with decompensated HF, renal function depended neither on cardiac index, nor on pulmonary capillary wedge pressure, nor on systemic vascular resistance. However, it was associated with right atrial pressure [7].

Based on database analysis of a branch of the same study, Hanberg et al demonstrated that there is a statistically significant inverse correlation between CI and eGFR in patients with HF who underwent pulmonary artery catheterization [8].

In a study by Guglin et al. in 178 HF patients, eGFR correlated with high CVP and low renal perfusion pressure. EchoCG found that deterioration of renal function was associated with tricuspid regurgitation peak velocity, but not with left ventricular systolic function [9]. Maeder et al. reported that in patients with HF, tricuspid regurgitation severity was independently associated with the degree of impaired renal function [10]. At the same time, many studies that have analyzed right atrial pressure in HF have two shortcomings complicating interpretation of these data: severity of preexisting parenchymal renal disease and degree of reduction of left ventricular systolic function are not considered. It is possible that increased right atrial pressure becomes clinically significant for the onset of renal venous congestion only when the cardiac index is decreased. In an animal experiment simulating acute renal venous congestion (13 mm H_2O), renal dysfunction (decreased blood flow, eGFR, sodium and free water clearance) became less pronounced when systemic hemodynamics were restored to control values by transfusion [11]. Damman et al. report that in potential lung recipients with HF, due to pulmonary hypertension, right atrial pressure (RAP) and renal blood flow were independently correlated with radioisotope-measured eGFR. Moreover, the association with RAP was more pronounced in patients with reduced renal blood flow [12]. For instance, Uthoff et al. report that in patients with acute HF, the combination of arterial hypotension and high CVP was significantly associated with lower eGFR [13]. Thus, therapeutic measures aimed at reducing renal congestion will be most effective in patients with arterial hypotension.

The hemodynamic response to reduced systemic arterial pressure depends on endothelial function, which is impaired in both chronic kidney disease and heart failure. Reduced renal perfusion pressure stimulates the sympathetic nervous system and the renin-angiotensin-aldosterone system (RAAS). Angiotensin II and catecholamines cause glomerular arteriolar vasoconstriction that

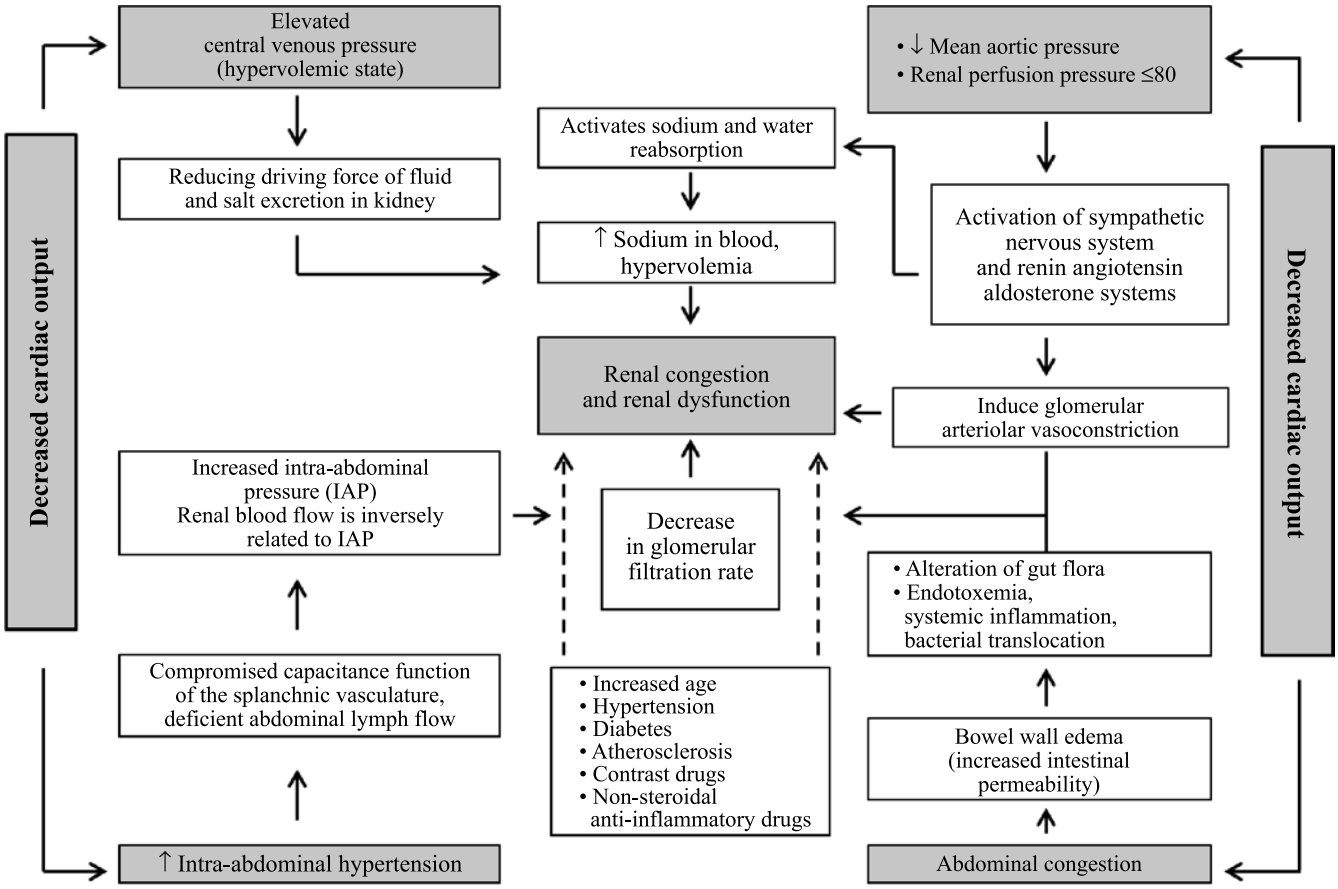

Fig. Pathophysiology of renal venous stasis and Impaired kidney function in heart failure (adapted from B. Afsar et al., 2016 [28])

reduces renal plasma flow [14]. Angiotensin II exerts a disproportionate vasoconstrictor effect on efferent arterioles, maintaining eGFR despite reduced renal plasma flow [15]. Thus, initially, the filtration fraction and eGFR were preserved, then the increase in angiotensin II and catecholamine production proves inadequate, which entails an even greater preglomerular vasoconstriction and reduction in eGFR [16]. This, in turn, activates sodium and water reabsorption in the proximal tubule, leading to even greater systemic and renal congestion; renal interstitial pressure increases; all capillary bed and tubules are compressed; local hypoxia develops. Increased pressure in the tubule lumen leads to a decrease in the transglomerular pressure gradient and exacerbates the decrease in eGFR [17].

In people without HF, the transient state of hypervolemia results in increased renal excretion of salt and fluid; this reduces the blood volume and cardiac output, normalizing blood pressure. However, in patients with HF, despite the hypervolemic state, elevated right atrial pressure and CVP negatively affect renal sodium excretion, creating a vicious cycle of sodium and fluid retention and HF build-up, which leads to even greater renal congestion [18].

Increased intra-abdominal pressure, blood congestion in the abdominal organs and interstitial space also play a role in impaired renal function. There is a negative correlation between the magnitude of renal blood flow and intra-abdominal pressure [19, 20]. According to a study by P.K. Harman et al., when the intra-abdominal pressure was elevated to 20 mmHg, GFR decreased to <25% of normal in experimental animals; when the intra-abdominal pressure was elevated to 40 mmHg, GFR fell to 7% of normal, while cardiac output was reduced to 37% of normal [21]. Compromised capacitance function of the abdominal organs and deficient abdominal lymph flow also contribute to elevated pressure in the right heart, which might additionally imply the occurrence of renal dysfunction [22]. In addition, disturbed intestinal microcirculation and barrier function, characteristic of HF, stimulate the production of cytokines that aggravate myocardial dysfunction, which in turn contributes to disturbed microcirculation [23]. Proinflammatory cytokines TNF and interferon-γ can disrupt the epithelial barrier function [24]. Subsequent entry of bacterial lipopolysaccharides into the bloodstream activates macrocytes and macrophages to produce proinflammatory mediators [24].

Inflammation can both contribute to the onset and be a consequence of renal venous stasis [25]. Inflammation causes vascular dysfunction through endothelial factors and increased arterial stiffness, decreased myocardial contractility due to functional suppression of contractility and myocardial cell death. P.C. Colombo et al. evaluated the effect of peripheral venous stasis induced by venous stress test on inflammation and endothelial activation. Venous arm pressure was increased to ~30 mmHg above the baseline level by inflating a tourniquet cuff around the dominant arm. Plasma interleukin-6 (IL-6), endothelin-1 (ET-1), angiotensin II, vascular cell adhesion molecule-1, and chemokine ligand 2 were significantly increased in the congested arm [26]. In HF and venous congestion, activation of RAAS and the sympathetic nervous system exacerbates the inflammatory response. According to experimental data from K. Iwata et al., RAAS activation leads to stimulation of nicotinamide adenine dinucleotide phosphate oxidase by angiotensin II, which leads to formation of reactive oxygen species.

All these processes promote progression of renal dysfunction and development of renal fibrosis [27].

Fibrosis is a common pathophysiological mechanism of cardiorenal syndrome. Disease-related injury to any organ triggers a complex cascade of cellular and molecular response, which culminates in tissue fibrosis. Although this fibrogenic response can be restrained for some time by adaptive mechanisms; in the case of prolonged damaging effects, sclerotic parenchyma, cellular dysfunction and, ultimately, functional insufficiency develop [29]. The cause of fibrotic processes, both in the heart and in the kidneys, is endothelial dysfunction arising from inflammation and oxidative stress, associated, in turn, with aging, arterial hypertension, diabetes mellitus and obesity, and leading to cardiovascular disease, HF and CKD [30]. Myocardial remodeling occurs after heart damage and involves the secretion of extracellular matrix proteins by myofibroblasts. This promotes cardiac fibrosis and preserves myocardial structure and function, but such a condition leads to chamber dilatation, cardiomyocyte hypertrophy, and apoptosis, and ultimately leads to the progression to heart failure [30]. In the kidney, tubulointerstitial fibrosis and dysfunction can be caused by differentiation of tubular epithelial cells into myofibroblasts through an epithelial-mesenchymal transition phenotype, leading to the cells losing their polygonal shape and epithelial markers and acquisition of a fibroblast phenotype with increased extracellular matrix synthesis (e.g. collagen I, III, fibronectin). Aldosterone can trigger a cascade of processes leading to cardiac, vascular, and renal fibrosis, mutually involving them in the development of cardiorenal syndrome. Experimental studies have supported such pathogenetic mechanisms. For example, in an experiment on rats, with AKI induced by bilateral renal ischemia/reperfusion, treatment with a mineralocorticoid receptor antagonist spironolactone prevented the activation of fibrotic and inflammatory processes, preventing the development of CKD [31, 32]. Of interest in this regard are the results obtained in the study of living kidney donors, who, 12 months after nephrectomy, developed a decrease in eGFR, accompanied by significant increase in left ventricular mass, confirmed by MRI, without development of arterial hypertension. Changes in eGFR were independently associated

with changes in left ventricular mass. Compared with the control group, the donors had a significantly increased concentration of fibroblast growth factor-23 and high-sensitivity C-reactive protein. However, the clinical relevance of these findings is unclear, as observational studies have shown favorable long-term outcomes for living kidney donors [33]. Nevertheless, studies of living kidney donors compared with controls suggest an increased risk of cardiovascular events and end-stage CKD [34, 35]. Elevated concentrations of highly sensitive cardiac troponin T and microalbuminuria were much more common in donors than in the control group [35]. Meanwhile, Paoletti et al. suggested that in 100 kidney transplant recipients, regression of left ventricular hypertrophy portends better long-term combined clinical outcome (death, any cardiovascular or renal event) [36].

In addition to these factors, activation of mineralocorticoid receptors through a number of mechanisms (inflammation; increased potassium levels in the blood, which has a proarrhythmic effect) promotes fibrotic changes in the heart, arteries, and kidneys. This process involves such mediators of inflammation and fibrosis as galectin-3 [31, 37], NGAL [38], stimulating growth factor ST2 [39] and cardiotropin-1 [40].

The pathophysiology of kidney injury after cardiac surgery with CPB is even more complex and multifactorial. Additional mechanisms affecting renal function in patients with chronic heart failure after such operations may include microembolization, metabolic and hemodynamic disorders, ischemia–reperfusion injury, and oxidative stress [41]. These mechanisms of injury may be interrelated and synergistic. The use of CPB has been associated with an alteration of vasomotor tone and a reduction in the renal parenchymal oxygen tension, and consequently, decreasing the renal perfusion pressure up to 30% and, hence, increasing the ischemia–reperfusion injury [42]. In addition, the formation of microemboli may be increased by the use of CPB. It is well known that emboli smaller than 40 μm are not effectively filtered by CPB-system filters and can damage renal capillaries directly. The release of free hemoglobin secondary to hemolysis is associated with renal tubular damage and coagulation activity dysfunction [41].

In cardiac recipients, nephrotoxic calcineurin inhibitors and risks associated with the use of organs from extended criteria donors are added to all of the described factors contributing to the onset of renal injury.

AKI EPIDEMIOLOGY AND CLASSIFICATIONS

AKI is a common complication occurring in more than 50% of patients within the first week after admission in the intensive care unit (ICU) [42]. According to M. Ostermann and J. Cerda, AKI-related mortality in the acute period is 24% in adults and 14% in pediatric patients [43]. Thus, it is 7 times higher than mortality in the non-AKI group of patients. Consequences of AKI include the need for renal replacement therapy (RRT), chronic kidney damage in about 20% of patients, and reduced quality of life. The additional cost of treating 1 patient with AKI requiring RRT in the United States averages $42,077 [44]. According to B.J. Moore and C.M. Torio, AKI accounts for 8–16% of all hospital admissions in the United States, which is about 13 million patients annually. The duration of hospitalization with a secondary diagnosis of AKI almost tripled from 2005 to 2014 [45]. According to Kerr et al., hospitalizations in 2014 for AKI patients in the UK incurred a cost of $1.3 billion, which was more than 1% of the total NHS budget [46].

Data on the incidence of AKI varies widely. In the past, more than 30 definitions of acute renal failure could be found in the literature. The diagnosis of acute renal failure was based on urine output and urea and creatinine as markers of eGFR reduction. The criteria for assessing the degree of renal dysfunction varied considerably among different authors. All these necessitated the development of a generally accepted classification of acute renal failure. For this purpose, the Acute Dialysis Quality Initiative (ADQI) expert group was formed in 2003. In 2004, ADQI presented the RIFLE classification, in which 5 stages of renal damage impairment were identified – Risk, Injury, Failure, Loss, End-stage kidney disease [47].

In 2007, members of the Acute Kidney Injury Network (AKIN) working group coined the term AKI (Acute Kidney Injury) to define a wide range of acute renal dysfunction from the earliest and mildest forms to cases where replacement therapy is required. The term AKI is intended to express the reversible nature of kidney injury in most cases. AKIN proposed a modification of RIFLE, which drew attention to the minimal increase in blood creatinine levels in a shorter period of time [48]. Finally, in 2012, in the clinical guidelines for the treatment of AKI, KDIGO, in turn, proposed again to increase the time period for assessing the degree of renal injury and drew attention to the delayed increase in blood creatinine levels in relation to renal dysfunction [49]. According to the KDIGO (Kidney disease: Improving Global Outcomes) clinical guidelines, AKI is a sudden decrease in kidney function in a period not exceeding 7 days, and CKD is pathological changes in the renal structure or function that last more than 90 days [49]. AKI should be considered as a systemic disease with long-term pathological effects on the heart, lungs, central nervous system, and especially the kidneys. The time interval between the onset of AKI and the development of CKD has been suggested to be called acute kidney disease. This term defines the course of the disease after AKI in patients with ongoing pathophysiological processes in the kidney. The main AKI classifications are shown in Table.

The addition of urine output as a criterion increases the incidence of AKI compared to a situation where se-

rum creatinine alone is assessed [50, 51]. Xuying Luo et al. analyzed the data of 3,107 patients who were consecutively admitted at the ICU over a 6-month period [52].

AKI was determined according to the RIFLE, AKIN and KDIGO classifications. KDIGO was the most sensitive for AKI detection (KDIGO 51%, RIFLE 46.9%, AKIN 38.4%). Meanwhile, the major limitation of these classifications is the use of serum creatinine levels as a marker of renal function. It is known that creatinine concentration can be influenced by factors not associated with glomerular filtration, such as gender, age, race, body surface area, diet, intake of certain drugs, as well as diabetes and liver disease [49]. Besides, a change in serum creatinine levels does not allow to identify the localization of renal injury, tubular or glomerular. To increase creatinine levels in the blood, a loss of about 50% of renal function is required.

As a consequence, it is detected 24–72 hours later than the concentration of a number of new biomarkers of kidney injury. These limitations facilitate the research of new substances that allow not only to predict and diagnose AKI, but also to identify the localization, type and etiology of injury, predict outcomes, and determine when to start treatment and ensure that it is monitored.

The currently known biomarkers make it possible to assess renal function (cystatin C [53], galectin-3 [54], proenkephalin [55]), predict AKI progression (interleukin-18 (IL18) [56]), neutrophil gelatinase-associated lipocalin (NGAL) [57], microRNA [58]), determine renal injury (NGAL, hepatic form of fatty acid binding protein (L-FABP) [59], microRNA, IL18, kidney injury molecule-1 (KIM-1) [60]), detect cell cycle inhibition (tissue inhibitor of metalloproteinase-2 and protein-7, which binds insulin-like growth factor (TIMP-2 and IGFBP-7) [61]) and, finally, determine the nephrotoxic effect of drugs (N-acetyl-glucosaminidase, gamma-glutamyl transpeptidase, alanine aminopeptidase) [62]. Although the use of most of the new biomarkers of kidney injury is still under study, their introduction into broad clinical practice is inevitable in the future. L-FABP is approved for use in Japan, NGAL is present in the European guidelines, and the TIMP-2 + IGFBP-7 combination is FDA approved in the United States [63].

Meanwhile, Klein et al. conducted a meta-analysis of 63 studies of new biomarkers in order to explore the possibility of using them in determining the onset of RRT in AKI. Unambiguous results were not obtained [64]. Biomarkers, which, according to the analysis, seem useful for predicting the use of RRT, are actually markers of kidney stress, damage and decreased glomerular filtration rate. From a clinical point of view, a decision to initiate RRT is not based on the severity of kidney injury, but on the presence of metabolic, electrolyte and volumetric disorders in the patient, as well as concomitant pathological conditions.

ACUTE KIDNEY INJURY IN HEART RECIPIENTS

Heart transplantation remains the only true "cure" for end-stage heart failure. Since 1967, when K. Barnard first performed a successful heart transplant (HTx), the number of such operations has been steadily increasing. By June 30, 2018, over 146,975 heart transplantations were performed in patients of all ages worldwide. According to the register of the International Society for

Table

Comparison of acute kidney injury scales

RIFLE		AKIN		KDIGO		Amount of urine
Stage	SCr	Stage	SCr	Stage	SCr	
RISK	1.5-fold increase or decrease in GF by >25%	1	Increase ≥26.5 μmol/L or 1.5–2-fold increase of baseline	1	Increase by 1.5–1.9 times or by ≥26.5 μmol/L of the baseline	<0.5 mL/kg/hour for 6–12 hours
INJURY	2-fold increase or decrease in GF by >50%	2	Increase by >2–3 times of the baseline	2	Increase by 2–2.9 times of the baseline	<0.5 mL/kg/hour for ≥12 hours
FAILURE	3-fold increase or SCr >354 μmol/L with rapid increase >44 μmol/L or GF decrease >75%	3	Increase by >3 times of baseline or SCr ≥354 μmol/L with rapid increase ≥44 μmol/L or RRT initiation	3	Increase by 3.0 times of the baseline or SCr ≥354 μmol/L or RRT initiation, or a decrease in GF to <35 mL/min/1.73 m^2 in patients <18 years of age	<0.5 mL/kg/hour for 24 hours or anuria for ≥12 hours
LOSS	Complete absence of renal function for >4 weeks					
END-STAGE KIDNEY DISEASE	Complete absence of renal function for >3 months					

RIFLE and KDIGO assess changes in SCr levels within 7 days, AKIN within 48 hours.

Heart and Lung Transplantation 2019, the 1- and 5-year survival rates of heart recipients were 81% and 69%, respectively [65].

Kidney injury is one of the most serious complications in both the early and late postoperative period, directly affecting treatment outcomes. According to numerous authors, the development of AKI and CKD is associated with longer ICU and hospital stay, higher incidence of infectious complications, acute graft rejection, and, in general, higher mortality rate [66, 67]. According to the results of a meta-analysis of 27 cohort studies with data from 137,201 heart recipients, the average incidence of AKI was 47.1% (4.5%–72.3%), the need for RRT was 12% (2.1%–39.06%). The incidence of AKI and severe AKI requiring RRT has increased in recent years. AKI after heart transplantation was associated with increased short-term and 1-year mortality (3.5 and 2.3-fold, respectively). AKI and AKI requiring a RRT were unfavorable prognostic factors in heart transplantation and were associated with a 13-fold increase in the risk of death within 90 days after surgery. Despite advances in transplantology in recent years, the risk of in-hospital mortality (and/or mortality within 90 days after surgery) and mortality within 1 year after transplantation has not changed over the past 20 years. This situation is probably due to liberalization of HTx indications and the use of organs from extended criteria donors [66]. Other results were published by Zijlstra et al, who analyzed data from 580 heart recipients who received transplants in Rotterdam from 1984 to 2013. The patients were divided into groups A (1984–1999) and B (2000–2013). Despite a significantly higher number of older donors in group B compared to group A (mean age 43 versus 29 years, donors over 50 years old 33% versus 2%, respectively), long-term survival was higher among group B recipients (90%, 86%, 81% and 68% by 30 days, 1 year, 5 years and 10 years, respectively, against 93%, 89%, 78%, and 53% in the same period in group A). In heart recipients who survived within 1 year after surgery, the 10-year survival was significantly higher in group B than in group A (80% versus 60%, respectively, $p < 0.0001$). In particular, this decrease was associated with a reduced incidence of kidney injury (14% in group A versus 4% in group B). According to the authors, such outcomes were achieved thanks to the use of new immunosuppression protocols, early prescription of statins regardless of cholesterol levels, active treatment of arterial hypertension and preemptive myocardial revascularization of the graft [68]. Since there are still no effective targeted pharmacotherapeutic for AKI, prevention, and early identification of patients at risk of AKI can potentially play an important role in improving treatment outcomes. Risk factors for AKI in heart transplantation have been studied by many authors. Preoperative ones include preexisting renal dysfunction, diabetes mellitus, older age of both donor and recipient, previous heart transplantation; Intra- and postoperative ones include graft ischemic time, surgery and CPB, large blood loss and much blood transfusions, mechanical circulatory support, functional heart graft failure [69–71]. According to Wang et al., who retrospectively analyzed heart transplants at 8 UK centers from 1995 to 2017, there was a steady increase in RRT use in the 30-day postoperative period – from 12% in 1995–2000 to 47.7% in 2011–2017. More frequent use of RRT was associated with older age of donors, higher number of recipients with urgent status, and more frequent use of mechanical (intra-aortic balloon pump, extracorporeal life support, assisted circulation) and inotropic support. Statistical analysis revealed RRT predictors in the post-transplant period: male gender, the need for left ventricular bypass and inotropic support before transplantation, intraoperative kidney dysfunction, and development of severe graft dysfunction after surgery. The use of organs from older donors increased the risk of requiring RRT. Besides, repeated surgical interventions and infectious complications were significantly associated with the need for RRT. As for the survival of recipients in this study, this indicator in the group of recipients with a need for RRT was lower than in other recipients only within 3 months after surgery. This difference was particularly pronounced in the early post-transplant period (71.6% and 94.7%, respectively) [72]. Meanwhile, according to Boyle et al., in the group of heart recipients with AKI requiring RRT, in-hospital mortality was 50% versus 1.4% in the group of recipients without AKI [73]. Guven et al. reported that the need for RRT within 30 days after transplantation was associated with higher mortality at 1 year after surgery (22% versus 8% in the group of recipients who did not require RRT) [74]. In a study by Romeo et al., this indicator in the group of heart recipients who received RRT within a month after surgery was also significantly higher than in other recipients (59.2% versus 5.8%) [75]. In all these studies, AKI requiring RRT served as a unifying risk factor for high mortality, but a common factor was also right ventricular failure – graft dysfunction [73–75].

Heart transplant recipients represent a unique population of patients in whom all types of cardio-renal syndrome can be observed at different stages of the pathological process. Over the past two decades, studies conducted among patients with severe heart failure have shown that venous congestion is a major damaging mechanism leading to the onset and progression of renal dysfunction, along with decreased cardiac output. It also activates the renin-angiotensin-aldosterone system with further sodium and water retention, inflammation with production of pro-inflammatory cytokines, endothelial dysfunction, fibrosis activation, and increased intra-abdominal pressure. In the meantime, clear data on the effect of such a mechanism in donor heart recipients are fragmentary. For example, several publications report that right ventricular failure in the early postoperative period is combined with

a high incidence of AKI requiring RRT with increased mortality. Introduction of precision methods for assessing and correcting hydration and volemic status in patients awaiting HTx and in cardiac recipients, would most likely reduce AKI incidence and improve transplantation outcomes. However, this requires further study.

The authors declare no conflict of interest.

REFERENCES

1. *Dasta JF, Kane-Gill S.* Review of the Literature on the Costs Associated With Acute Kidney Injury. *J Pharm Pract*. 2019 Jun; 32 (3): 292–302. doi: 10.1177/0897190019852556.
2. *Ronco C, House AA, Haapio M.* Cardiorenal syndrome: refining the definition of a complex symbiosis gone wrong. *Intensive Care Med*. 2008; 34 (5): 957–962. doi: 10.1007/s00134-008-1017-8.
3. *Ronco C, Bellasi A, Di Lullo L.* Cardiorenal Syndrome: An Overview. *Adv Chronic Kidney Dis.* 2018; 25 (5): 382–390. doi: 10.1053/j.ackd.2018.08.004.
4. *Heywood JT, Fonarow GC, Costanzo MR, Mathur VS, Wigneswaran JR, Wynne J et al.* High prevalence of renal dysfunction and its impact on outcome in 118,465 patients hospitalized with acute decompensated heart failure: a report from the ADHERE database. *J Card Fail.* 2007; 13: 422–430. doi: 10.1016/j.cardfail.2007.03.011.
5. *Damman K, van Deursen VM, Navis G, Voors AA, van Veldhuisen DJ, Hillege HL.* Increased central venous pressure is associated with impaired renal function and mortality in a broad spectrum of patients with cardiovascular disease. *J Am Coll Cardiol*. 2009; 53: 582–588. doi: 10.1016/j.jacc.2008.08.080.
6. *Damman K, Voors AA, Hillege HL, Navis G, Lechat P, van Veldhuisen DJ et al.* Congestion in chronic systolic heart failure is related to renal dysfunction and increased mortality. *Eur J Heart Fail.* 2010; 12: 974–982. doi: 10.1093/eurjhf/hfq118.
7. *Nohria A, Hasselblad V, Stebbins A, Pauly DF, Fonarow GC, Shah M et al.* Cardiorenal interactions: insights from the ESCAPE trial. *J Am Coll Cardiol.* 2008; 51: 1268–1274. doi: 10.1016/j.jacc.2007.08.072.
8. *Hanberg JS, Sury K, Wilson FP, Brisco MA, Ahmad T, Ter Maaten JM et al.* Reduced Cardiac Index Is Not the Dominant Driver of Renal Dysfunction in Heart Failure. *J Am Coll Cardiol*. 2016; 67 (19): 2199–2208. doi: 10.1016/j.jacc.2016.02.058.
9. *Guglin M, Rivero A, Matar F, Garcia M.* Renal dysfunction in heart failure is due to congestion but not low output. *Clin Cardiol.* 2011; 34: 113–116. doi: 10.1002/clc.20831.
10. *Maeder MT, Holst DP, Kaye DM.* Tricuspid regurgitation contributes to renal dysfunction in patients with heart failure. *J Card Fail.* 2008; 14: 824–830.
11. *Priebe HJ, Heimann JC, Hedley-Whyte J.* Effects of renal and hepatic venous congestion on renal function in the presence of low and normal cardiac output in dogs. *Circ Res.* 1980; 47: 883–890. doi: 10.1161/01.res.47.6.883.
12. *Damman K, Navis G, Smilde TD, Voors AA, van der Bij W, van Veldhuisen DJ et al.* Decreased cardiac output, venous congestion and the association with renal impairment in patients with cardiac dysfunction. *Eur J Heart Fail*. 2007; 9: 872–878. doi: 10.1016/j.ejheart.2007.05.010.
13. *Uthoff H, Breidthardt T, Klima T, Aschwanden M, Arenja N, Socrates T et al.* Central venous pressure and impaired renal function in patients with acute heart failure. *Eur J Heart Fail.* 2011; 13: 432–439. doi: 10.1093/eurjhf/hfq195.
14. *Blankstein R, Bakris GL.* Renal hemodynamic changes in heart failure. *Heart Fail Clin.* 2008; 4 (4): 411–423. doi: 10.1016/j.hfc.2008.03.006.
15. *Sambandam KK.* Effective use of loop diuretics in heart failure exacerbation: a nephrologist's view. *Am J Med Sci.* 2014; 347: 139–145. doi: 10.1097/MAJ.0b013e31828a2962.
16. *Ruggenenti P, Remuzzi G.* Worsening kidney function in decompensated heart failure: treat the heart, don't mind the kidney. *Eur Heart J.* 2011; 32: 2476–2478. doi: 10.1093/eurheartj/ehr242.
17. *Schrier RW.* Role of diminished renal function in cardiovascular mortality: marker or pathogenetic factor? *J Am Coll Cardiol.* 2006; 47: 1–8. doi: 10.1016/j.jacc.2005.07.067.
18. *Guazzi M, Gatto P, Giusti G, Pizzamiglio F, Previtali I, Vignati C, Arena R.* Pathophysiology of cardiorenal syndrome in decompensated heart failure: role of lung-right heart-kidney interaction. *Int J Cardiol.* 2013; 169: 379–384. doi: 10.1016/j.ijcard.2013.09.014.
19. *Cheatham ML, White MW, Sagraves SG, Johnson JL, Block EF.* Abdominal perfusion pressure: a superior parameter in the assessment of intra-abdominal hypertension. *J Trauma.* 2000; 49: 621–626; discussion 626–627. doi: 10.1097/00005373-200010000-00008.
20. *Bloomfield GL, Blocher CR, Fakhry IF, Sica DA, Sugerman HJ.* Elevated intraabdominal pressure increases plasma renin activity and aldosterone levels. *J Trauma.* 1997; 42: 997–1004; discussion 1004–1005. doi: 10.1097/00005373-199706000-00002.
21. *Harman PK, Kron IL, McLachlan HD, Freedlender AE, Nolan SP.* Elevated intra-abdominal pressure and renal function. *Ann Surg*. 1982 Nov; 196 (5): 594–597. doi: 10.1097/00000658-198211000-00015.
22. *Verbrugge FH, Dupont M, Steels P, Grieten L, Malbrain M, Tang WHW, Mullens W.* Abdominal contributions to cardiorenal dysfunction in congestive heart failure. *J Am Coll Cardiol.* 2013; 62: 485–495. doi: 10.1016/j.jacc.2013.04.070.
23. *Sandek A, Rauchhaus M, Anker SD, von Haehling S.* The emerging role of the gut in chronic heart failure. *Curr Opin Clin Nutr Metab Care. 2008*; 11: 632–639. doi: 10.1097/MCO.0b013e32830a4c6e.
24. *Sandek A, Anker SD, von Haehling S.* The gut and intestinal bacteria in chronic heart failure. *Curr Drug Metab.* 2009; 10 (1): 22–28. doi: 10.2174/138920009787048374.
25. *Ross EA.* Congestive renal failure: the pathophysiology and treatment of renal venous hypertension. *J Card Fail.* 2012; 18: 930–938. doi: 10.1016/j.cardfail.2012.10.010.

26. *Colombo PC, Onat D, Harxhi A, Demmer RT, Hayashi Y, Jelic S et al.* Peripheral venous congestion causes inflammation, neurohormonal, and endothelial cell activation. *Eur Heart J.* 2014; 35: 448–454. doi: 10.1093/eurheartj/eht456.
27. *Iwata K, Matsuno K, Murata A, Zhu K, Fukui H, Ikuta K et al.* Up-regulation of NOX1/NADPH oxidase following drug-induced myocardial injury promotes cardiac dysfunction and fibrosis. *Free Radic Biol Med.* 2018; 120: 277–288. doi.org/10.1016/j.freeradbiomed.2018.03.053.
28. *Afsar B, Ortiz A, Covic A, Solak Y, Goldsmith D, Kanbay M.* Focus on renal congestion in heart failure. *Clin Kidney J*. 2016; 9 (1): 39–47. doi: 10.1093/ckj/sfv124.
29. *Rockey DC, Bell PD, Hill JA.* Fibrosis: a common pathway to organ injury and failure. *N Engl J Med.* 2015; 372: 1138–1149. doi: 10.1056/NEJMra1300575.
30. *Travers JG, Kamal FA, Robbins J, Yutzey KE, Blaxall BC.* Cardiac fibrosis: the fibroblast awakens. *Circ Res*. 2016; 118: 1021–1040. doi: 10.1161/CIRCRESAHA.115.306565.
31. *Calvier L, Martinez-Martinez E, Miana M, Cachofeiro V, Rousseau E, Sádaba JR et al*. The impact of galectin-3 inhibition on aldosterone-induced cardiac and renal injuries. *JACC Heart Fail*. 2015; 3: 59–67. doi: 10.1016/j.jchf.2014.08.002.
32. *Lattenist L, Lechner SM, Messaoudi S, Le Mercier A, El Moghrabi S, Prince S et al*. Nonsteroidal mineralocorticoid receptor antagonist finerenone protects against acute kidney injury-mediated chronic kidney disease: role of oxidative stress. *Hypertension*. 2017; 69: 870–878. doi: 10.1161/HYPERTENSIONAHA.116.08526.
33. *Segev DL, Muzaale AD, Caffo BS, Mehta SH, Singer AL, Taranto SE et al*. Perioperative mortality and long-term survival following live kidney donation. *JAMA*. 2010; 303: 959–966. doi: 10.1001/jama.2010.237.
34. *Mjøen G, Hallan S, Hartmann A, Foss A, Midtvedt K, Øyen O et al.* Long-term risks for kidney donors. *Kidney Int*. 2014; 86: 162–167. doi: 10.1038/ki.2013.460.
35. *Moody WE, Ferro CJ, Edwards NC, Chue CD, Lin EL, Taylor RJ et al*. CRIB-Donor Study Investigators. Cardiovascular effects of unilateral nephrectomy in living kidney donors. *Hypertension*. 2016; 67: 368–377. doi: 10.1161/HYPERTENSIONAHA.115.06608.
36. *Paoletti E, Bellino D, Signori A, Pieracci L, Marsano L, Russo R et al.* Regression of asymptomatic cardiomyopathy and clinical outcome of renal transplant recipients: a long-term prospective cohort study. *Nephrol Dial Transplant.* 2016; 31: 1168–1174. doi: 10.1093/ndt/gfv354.
37. *Shevchenko OP, Ulybysheva AA, Gichkun OE, Mozheiko NP, Stakhanova EA, Kvan VS, Shevchenko AO*. Galectin-3 in heart transplant rejection and fibrosis. *Russian Journal of Transplantology and Artificial Organs*. 2019; 21 (3): 62–68. doi: 10.15825/1995-1191-2019-3-62-68.
38. *Tarjus A, Martínez-Martínez E, Amador C, Latouche C, El Moghrabi S, Berger T et al*. Neutrophil gelatinase-associated lipocalin, a novel mineralocorticoid biotarget, mediates vascular profibrotic effects of mineralocorticoids. *Hypertension.* 2015; 66: 158–166. doi: 10.1161/HYPERTENSIONAHA.115.05431.
39. *Martínez-Martínez E, Cachofeiro V, Rousseau E, Álvarez V, Calvier L, Fernández-Celis A et al.* Interleukin-33/ST2 system attenuates aldosterone-induced adipogenesis and inflammation. *Mol Cell Endocrinol.* 2015; 411: 20–27. doi: 10.1016/j.mce.2015.04.007.
40. *López-Andrés N, Rousseau A, Akhtar R, Calvier L, Iñigo C, Labat C et al.* Cardiotrophin 1 is involved in cardiac, vascular, and renal fibrosis and dysfunction. *Hypertension.* 2012; 60: 563–573. doi: 10.1161/HYPERTENSIONAHA.112.194407.
41. *Vives M, Hernandez A, Parramon F, Estanyol N, Pardina B, Muñoz A et al.* Acute kidney injury after cardiac surgery: prevalence, impact and management challenges. *Int J Nephrol Renovasc Dis.* 2019; 12: 153–166. doi: 10.2147/IJNRD.S167477.
42. *Chawla LS, Bellomo R, Bihorac A, Goldstein SL, Siew ED, Bagshaw SM et al.* Acute kidney disease and renal recovery: consensus report of the Acute Disease Quality Initiative (ADQI) 16 Workgroup. *Nat Rev Nephrol*. 2017; 13 (4): 241–257. doi: 10.1038/nrneph.2017.2.
43. *Ostermann M, Cerda J*. The burden of acute kidney injury and related financial issues. In: Ding X, Rosner MH, Ronco C, eds. Acute Kidney Injury – Basic Research and Clinical Practice. Basel, Switzerland: Contrib Nephrol, Karger; 2018: 100–112.
44. *Hoste EAJ, Kellum JA, Selby NM, Zarbock A, Palevsky PM, Bagshaw SM et al.* Global epidemiology and outcomes of acute kidney injury. *Nat Rev Nephrol*. 2018; 14 (10): 607–625. doi: 10.1038/s41581-018-0052-0.
45. *Moore BJ* (IBM Watson Health), *Torio CM* (AHRQ). Acute Renal Failure Hospitalizations, 2005–2014. HCUP Statistical Brief #231. Rockville, MD: Agency for Healthcare Research and Quality; 2017. https://www.hcup-us.ahrq.gov/reports/statbriefs/sb231-Acute-Renal-Failure-Hospitalizations.jsp.
46. *Kerr M, Bedford M, Matthews B, O'Donoghue D.* The economic impact of acute kidney injury in England. *Nephrol Dial Transplant.* 2014; 29 (7): 1362–1368. doi: 10.1093/ndt/gfu016.
47. *Kuitunen A, Vento A, Suojaranta-Ylinen R, Pettila V.* Acute renal failure after cardiac surgery: evaluation of the RIFLE classification. *Ann Thorac Surg.* 2006; 81: 542–546.
48. *Mehta RL, Kellum JA, Shah SV, Molitoris BA, Ronco C, Warnock DG, Levin A.* Acute Kidney Injury Network: report of an initiative to improve outcomes in acute kidney injury. *Crit Care.* 2007; 11: R31. doi: 10.1186/cc5713.
49. Kidney disease: Improving Global Outcomes (KDIGO) Acute Kidney Injury Work Group: KDIGO Clinical Practice Guideline for Acute Kidney Injury. *Kidney Inter Suppl*. 2012; 2: 1–138. doi: 10.1038/kisup.2012.1.
50. *Kellum JA, Sileanu FE, Murugan R, Lucko N, Shaw AD, Clermont G.* Classifying AKI by urine output versus serum creatinine level. *J Am Soc Nephrol.* 2015; 26 (9): 2231–2238.
51. *Salgado G, Landa M, Masevicius D, Gianassi S, San-Román JE, Silva L et al*. Acute renal failure according to the RIFLE and AKIN criteria: a multicenter study. *Med Intensiva.* 2014; 38 (5): 271–277. doi: 10.1016/j.medin.2013.04.007.

52. *Luo X, Jiang L, Du B, Wen Y, Wang M, Xi X.* Beijing Acute Kidney Injury Trial (BAKIT) workgroup. A comparison of different diagnostic criteria of acute kidney injury in critically ill patients. *Critical Care.* 2014; 18: R144. doi: 10.1186/cc13977.
53. *Yong Z, Pei X, Zhu B, Yuan H, Zhao W.* Predictive value of serum cystatin C for acute kidney injury in adults: a meta-analysis of prospective cohort trials. *Sci Rep.* 2017; 7: 41012. doi: 10.1038/srep41012.
54. *Shevchenko OP, Ulybysheva AA, Mozheiko NP, Gichkun OE, Stakhanova EA, Vasilieva VP, Shevchenko AO.* Diagnostic value of galectin-3 in heart transplant recipients with myocardial complications. *Russian Journal of Transplantology and Artificial Organs*. 2020; 22 (1): 8–15. doi: 10.15825/1995-1191-2020-1-8-15.
55. *Schulz C-A, Christensson A, Ericson U, Almgren P, Hindy G, Nilsson PM et al.* High level of fasting plasma proenkephalin-a predicts deterioration of kidney function and incidence of CKD. *J Am Soc Nephrol.* 2017; 28: 291–303. doi: 10.1681/ASN.2015101177.
56. *Lin X, Yuan J, Zhao Y, Zha Y.* Urine interleukin-18 in prediction of acute kidney injury: a systemic review and meta-analysis. *J Nephrol.* 2015; 28: 7–16. doi: 10.1007/s40620-014-0113-9.
57. *Hošková L, Franekova J, Málek I, Kautzner J, Szárszoi O, Jabor A et al*. Comparison of Cystatin C and NGAL in Early Diagnosis of Acute Kidney Injury After Heart Transplantation. *Ann Transplant*. 2016; 21: 329–245. doi: 10.12659/aot.896700.
58. *Velikiy DA, Gichkun OE, Shevchenko OP.* MicroRNAs in heart transplant recipients. *Russian Journal of Transplantology and Artificial Organs.* 2017; 19 (2): 126–132. (In Russ.) https://doi.org/10.15825/1995-1191-2017-2-126-132.
59. *Parr SK, Clark AJ, Bian A, Shintani AK, Wickersham NE, Ware LB. et. al.* Urinary L-FABP predicts poor outcomes in critically ill patients with early acute kidney injury. *Kidney Int.* 2015; 87: 640–648. doi: 10.1038/ki.2014.301.
60. *Bonventre JV.* Kidney injury molecule-1 (KIM-1): a urinary biomarker and much more. *Nephrol Dial Transpl.* 2009; 24: 3265–3268. doi: 10.1093/ndt/gfp010.
61. *Kashani K, Al-Khafaji A, Ardiles T, Artigas A, Bagshaw SM, Bell M et al.* Discovery and validation of cell cycle arrest biomarkers in human acute kidney injury. *Crit Care.* 2013; 17: R25. doi: 10.1186/cc12503.
62. *Teo SH, Zoltán, Endre ZH.* Biomarkers in acute kidney injury (AKI). *Best Pract Res Clin Anaesthesiol.* 2017; 31 (3): 331–344. doi: 10.1016/j.bpa.2017.10.003.
63. *Pickering JW, Endre ZH.* Bench to bedside: the next steps for biomarkers in acute kidney injury. *Am J Physiol – Ren Physiol.* 2016; 311: F717–721. doi: 10.1152/ajprenal.00268.2016.
64. *Klein SJ, Brandtner AK, Lehner GF, Ulmer H, Bagshaw SM, Wiedermann CJ, Joannidis M.* Biomarkers for prediction of renal replacement therapy in acute kidney injury: a systematic review and meta-analysis. *Intensive Care Med.* 2018; 44: 323–336. doi: 10.1007/s00134-018-5126-8.
65. *Khush KK, Cherikh WS, Chambers DC, Harhay MO, Hayes D Jr, Hsich E et al.* The International Thoracic Organ Transplant Registry of the International Society for Heart and Lung Transplantation: Thirty-sixth adult heart transplantation report – 2019; focus theme: Donor and recipient size match. *J Heart Lung Transplant*. 2019; 38 (10): 1056–1066. doi: 10.1016/j.healun.2019.08.004.
66. *Thongprayoon C, Lertjitbanjong P, Hansrivijit P, Crisafio A, Mao M, Watthanasuntorn K et al*. Acute Kidney Injury in Patients Undergoing Cardiac Transplantation: A Meta-Analysis. *Medicines (Basel)*. 2019; 6 (4): 108. doi: 10.3390/medicines6040108.
67. *Goltz AM, Zakharevich VM.* Retransplantatsiya serdtsa. *Transplantologiya: itogi i perspektivy*. Pod red. S.V. Gautier. M.–Tver': Triada, 2019: 271–290.
68. *Zijlstra LE, Constantinescu AA, Manintveld O, Birim O, Hesselink DA, van Thiel R et al*. Improved long-term survival in Dutch heart transplant patients despite increasing donor age: the Rotterdam experience. *Transpl Int*. 2015; 28: 962–971. doi: 10.1111/tri.12503.
69. *Tjahjono R, Connellan M, Granger E.* Predictors of Acute Kidney Injury in Cardiac Transplantation. *Transplant Proc*. 2016; 48 (1): 167–172. doi: 10.1016/j.transproceed.2015.12.006.
70. *García-Gigorro R, Renes-Carreño E, Peiretti MAC, López PA, Vela JLP, Rodríguez JG et al.* Incidence, Risk Factors and Outcomes of Early Acute Kidney Injury After Heart Transplantation: An 18-year Experience. *Transplantation*. 2018; 102 (11): 1901–1908. doi: 10.1097/TP.0000000000002293.
71. *Wang T-J, Lin C-H, Wei H-J, Wu M-J.* Long-Term Outcomes and Risk Factors of Renal Failure Requiring Dialysis after Heart Transplantation: A Nationwide Cohort Study. *J Clin Med*. 2020, 9 (8), 2455; https://doi.org/10.3390/jcm9082455.
72. *Wang L, Wang T, Rushton SN, Parry G, Dark JH, Sheerin NS.* The impact of severe acute kidney injury requiring renal replacement therapy on survival and renal function of heart transplant recipients – a UK cohort study. *Transpl Int*. 2020 Jun 16. doi: 10.1111/tri.13675.
73. *Boyle JM, Moualla S, Arrigain S, Worley S, Bakri MH, Starling RC et al*. Risks and outcomes of acute kidney injury requiring dialysis after cardiac transplantation. *Am J Kidney Dis.* 2006; 48 (5): 787–796. doi: 10.1053/j.ajkd.2006.08.002.
74. *Guven G, Brankovic M, Constantinescu AA, Brugts JJ, Hesselink DA.* Preoperative right heart hemodynamics predict postoperative acute kidney injury after heart transplantation. *Intensive Care Med*. 2018; 44: 588–597. doi: 10.1007/s00134-018-5159-z.
75. *Romeo FJ, Varela CF, Vulcano N, Pizarro R, Greloni G, Posatini R et al*. Acute Kidney Injury After Cardiac Transplantation: Foe or Common Innocent Bystander? *Transplant Proc*. 2018; 50 (5): 1489–1495. doi: 10.1016/j.transproceed.2018.03.106.

The article was submitted to the journal on 4.03.2021

DOI: 10.15825/1995-1191-2021-2-158-166

EARLY POSTOPERATIVE SEIZURES IN LIVER AND KIDNEY RECIPIENTS

O.M. Tsirulnikova[1, 2], A.V. Syrkina[2], I.A. Miloserdov[1, 2], I.E. Pashkova[2], S.Yu. Oleshkevich[2], I.B. Komarova[3]

[1] Sechenov University, Moscow, Russian Federation
[2] Shumakov National Medical Research Center of Transplantology and Artificial Organs, Moscow, Russian Federation
[3] Russian Medical Academy of Continuous Professional Education, Moscow, Russian Federation

Background. Transplantation is presently the only treatment for end-stage liver and kidney failure. Up to 42% of liver transplant recipients and up to 30% of kidney transplant recipients have neurological complications from the transplantation. Acute symptomatic seizures (ACS) occupy an important place in the structure of early postoperative neurological complications. Verification of the causes of seizures and management of the risk of relapse is presently a critical task. **Objective:** to review recent advances in ACS assessment, prevalence, and treatment approaches in liver and kidney transplant recipients. **Materials and methods.** The causes of ACS after liver and kidney transplant are diverse. Nonspecific causes of seizures such as dysmetabolic and volemic changes associated with transplantation are widely known. There are also specific syndromes associated with seizures in liver and kidney recipients, such as posterior reversible leukoencephalopathy syndrome, neurotoxicity of calcineurin inhibitors, hyponatremia in the final stage of liver failure, hypocalcemia in kidney recipients, etc. Diagnosis is made based on general rules, and treatment depends on the identified causes of seizures. Management of acute symptomatic seizures involves prescribing anticonvulsants according to the risk of seizure recurrence; immunosuppression is converted when neurotoxicity is identified. **Results.** The diagnostic algorithm, and often the treatment strategies, in ACS cases in liver and kidney recipients, are not clearly defined. **Conclusion.** Due to the multiple causes of ACS, there are differences in treatment tactics. Further accumulation and generalization of ACS outcome data will help in creating a convenient algorithm for rapid identification of the cause and the most effective treatment tactics.

Keywords: acute symptomatic seizures, seizures, liver recipient, kidney recipient, transplantation, neurological complications.

Organ transplantation is the only therapy for terminal and irreversible kidney and liver failure. Modern advances in surgical techniques, immunosuppression, and perioperative care have raised the 1-year survival rate to 90% [1, 2]. However, postoperative complications continue to occur. Neurological complications of orthotopic transplantation account for 9–42% [3].

Acute symptomatic seizures (ASS) rank second among neurological complications in liver or kidney recipients, second only to post-transplant encephalopathy [4], at 9–36% [5]. In survival studies, seizure syndrome still predicts fatal outcomes in solid organ recipients [6, 7]. In this regard, the issue of timely correction of ASS in the postoperative period of transplantation seems extremely relevant.

As defined by the International League Against Epilepsy, ASS are seizures occurring in close temporal relationship with an acute central nervous system insult, which may be toxic, metabolic, infectious, inflammatory, structural, or due to stroke [8]. The essential difference between ASS and seizures in epilepsy is the prognosis. With the situational nature, the risk of recurrent ASS is low, so long-term treatment with anticonvulsants is not required [8, 9].

ASS semiology can be quite varied. In adult recipients, it is usually represented by bilateral tonic-clonic seizures. In childhood, focal seizures are more common [10, 11]. ASS can recur throughout the day, becoming serial, or follow each other without regaining consciousness, which means development of status epilepticus. In patients with impaired consciousness, nonconvulsive status epilepticus recorded using an electroencephalogram is also possible [7].

Common causes of postoperative seizures include the proconvulsive effect of anesthetics [12], cerebral edema, refeeding syndrome [13], dysmetabolic and volemic changes, neurotoxicity of medications [14], anoxia, and structural brain damage. Liver and kidney recipients have additional causes of seizure syndrome.

Corresponding author: Alla Syrkina. Address: 1, Shchukinskaya str., Moscow, 123182, Russian Federation.
Phone: (903) 769-16-08. E-mail: AllaSyrk@gmail.com

The purpose of this review was to describe the features of ASS and approaches to their correction in patients after orthotopic liver and kidney transplantation.

ASS AFTER ORTHOTOPIC LIVER TRANSPLANTATION

Various authors have reported that the incidence of ASS after orthotopic liver transplantation (OLT) is 2.8–42% [4, 7, 10].

The range of causes of this complication in liver recipients in the early postoperative period is extensive and includes dysmetabolic disorders, neurotoxicity of calcineurin inhibitors, structural and infectious brain damage.

Most cases of ASS in the early post-OTP period are associated with immunosuppressants. For example, according to Derle E. et al. (2015), calcineurin inhibitors are responsible for ASS in 34% of cases [4]. Curiously, no correlation between excess immunosuppressors and occurrence of seizures has been found. ASS can develop even with normal blood levels [4]. Occurrence of a seizure syndrome is more common in the first week after OLT [11].

In 1%–10% of liver recipients, ASS is caused by vasogenic posterior cerebral edema [11, 15, 16]. On brain MRI, this is consistent with the picture of posterior reversible encephalopathy syndrome (PRES), also known as reversible posterior leukoencephalopathy syndrome (RPLS). In the pediatric population, this condition is less common than in adults [6, 10]. PRES is associated with direct neurotoxicity of calcineurin inhibitors [15, 17]. The mechanism of neurotoxicity of calcineurin inhibitors is poorly understood. In a study by Dohgu S. et al. (2004), cyclosporine promoted hyperpermeability of the blood-brain barrier by altering endothelial and astrocyte function [18]. Among the clinical manifestations of PRES are cortical blindness, seizure syndrome, depression of consciousness to coma without increased blood pressure.

In addition to calcineurin inhibitors, other drugs used in liver recipients in the postoperative period can also lead to neurotoxicity and ASS. Among them are isoniazid, methylprednisolone in combination with cyclosporine, imipenem, penicillamine, ciprofloxacin, acyclovir, etc [14, 19].

Metabolic causes of ASS (hypoglycemia, hypocalcemia, hypomagnesemia, hyponatremia, hypophosphatemia), according to Derle E. et al. (2015), were noted in 17.4% of cases [3, 4]. In liver recipients, preoperative hyponatremia is associated with end-stage liver failure. Plasma sodium levels below 115–120 mmol/L are associated with ASS [8, 20]. Rapid perioperative correction of hyponatremia can lead to such severe complications as central pontine and extrapontine myelinolysis (CPM and EPM) [21], the manifestations of which are: impaired consciousness, locked person syndrome, ophthalmoparesis, tetraparesis, and bulbar disorders [22]. An important metabolic cause is refeeding syndrome, when the introduction of parenteral or enteral nutrition after fasting is accompanied by hypophosphatemia, hypomagnesemia, hypokalemia, and thiamine deficiency. Clinical manifestations may include focal neurological symptoms, seizures, cerebral edema, and respiratory disorders.

Structural brain damage as a cause of seizure syndrome occurs in 13% of liver recipients [4]. Among them are hemorrhagic and ischemic cerebrovascular diseases (CVDs), brain abscess, and meningoencephalitis. Hemorrhagic or ischemic CVDs, according to Kim B. et al. (2007), occurs in 2–4% of liver recipients [23]. A higher risk of CVDs was noted in adult patients with pre-transplant diabetes mellitus [24].

Among Central nervous system infections, the herpes virus family is particularly relevant among liver recipients. Specifically, herpesvirus 6 can manifest with limbic encephalitis and seizures [25]. Progressive multifocal leukoencephalopathy (PML), a rare fatal demyelinating disease of the central nervous system caused by reactivation of the John Cunningham virus (JCV); it affects patients with pre-existing immunodeficiency [26–28]. The MRI picture may be similar to PRES, but the condition does not improve when immunosuppression dose is reduced or when immunosuppressants are converted, but continues to progress steadily [29].

Another cause of ASS in the early post-OLT period is sepsis. ASS against the background of sepsis occurs in 8.7% of patients [4]. Sepsis-associated encephalopathy is characterized by acute changes in mental status, cognitive functions, altered sleep/wake cycle, disorientation, impaired attention and/or disorganized thinking in the absence of direct evidence of brain infection [30]. Exaggerated motor activity with agitation and/or hallucinations can sometimes be observed, and agitation and drowsiness can occur alternately. Other but less frequent motor symptoms include asterix, tremor, and multifocal myoclonus [31].

The causes of ASS are often not limited to any one thing. A combination of two or more factors occurs in 26.1% of patients [4].

Diagnosis

There is no standard algorithm yet for identifying the causes of ASS in liver transplant recipients, but Shepard P.W. et al. (2012) suggest the following examinations: assessment of acid-base balance, serum electrolyte composition, including phosphorus and magnesium, neuroimaging to rule out circulatory disorders, electroencephalogram, lumbar puncture [32].

Treatment and prevention

Treatment of ASS in patients after OLT largely depends on the cause. So, in the case of neurotoxicity and

development of PRES, reducing the immunosuppression dose and converting the therapy are carried out [7, 17]. Ismail et al. (2017) describe a successful return of tacrolimus after complete restoration of neurological status in patients with tacrolimus-induced PRES [33].

Correction of metabolic disorders completely stops ASS. Slow correction of hyponatremia no faster than 15 mmol/L in 24 hours or 18 mmol/L in 48 hours avoids CPM and EPM [34].

As for anticonvulsants directly, levetiracetam is preferred because this drug does not affect hepatic enzymes, which allows the use of lower doses of immunosuppressants and avoids drug interactions [35]. In general, levetiracetam, gabapentin, pregabalin and lacosamide are the drugs of choice for the treatment of focal seizures in post-transplant patients. They have been shown to be quite effective and well tolerated [32]. Benzodiazepines, fosphenytoin, intravenous forms of levetiracetam, valproic acid, and lacosamide can be used when it is necessary to stop ASS [32]. Unfortunately, fosphenytoin and lorazepam for injection are not registered in the Russian Federation [36], and lacosamide is contraindicated for children under 16 years of age [37].

Chabolla D.R. et al. (2006) recommend anticonvulsant therapy for 1–3 months in patients without structural brain damage [38, 39]. In cases of structural brain damage, Shepard P.W. et al. (2012) use anticonvulsants for a long time [32] .

In order to prevent seizure syndrome, more authors suggest controlling metabolic parameters and the level of immunosuppressive drugs [4, 39]. When seizures occur before OLT, prescription of antiepileptic drugs is required only if there is a history of neurological disease, such as a history of traumatic brain injury or nontraumatic spontaneous intracranial hemorrhage. The Epilepsy Foundation of America suggests that seizures prior to OLT outside of existing epilepsy be considered acute symptomatic within stage 3–4 hepatic encephalopathy [40].

ASS risk factors in liver recipients

Balderramo D. et al. (2011) confirmed the correlation of calcineurin inhibitors neurotoxicity with hepatic failure before OLT, hyponatremia after OLT, OLT surgery time of more than 7 hours [41].

Later, in 2016, Wu S.-Y. et al. identified additional risk factors for neurological complications after OLT, such as hyponatremia, hepatic insufficiency (high MELD values), bacterial infection suffered the week before OLT, nutritional deficiency (BMI below 21.6 kg/m^2), overweight (BMI above 27.6 kg/m^2), renal failure, Child-Pugh class C cirrhosis, recipient age below 29 and over 60 years [42].

Tacrolimus levels above or equal to 8.9 ng/mL within 7 days were identified by Kumar S.S., Mashour G.A., and Picton P. in 2018 as a separate risk factor [3].

The risk of recurrent seizure in case of cerebrovascular disorders, transplant rejection, and sepsis is high, and anticonvulsants are recommended [32].

ASS AFTER ORTHOTOPIC KIDNEY TRANSPLANTATION

According to Sawhney H. et al. (2020), ASS develops in about 30% of kidney recipients in the early postoperative period [43]. The spectrum of causes of ASS includes, as well as in liver recipients, dysmetabolic disorders, drug neurotoxicity, structural and infectious brain damage. In addition, kidney recipients have specific causes of ASS, namely, hypertensive encephalopathy, disequilibrium syndrome and uremia [43].

Some of the most frequent causes of post-kidney transplant seizure syndrome are dysmetabolic disorders. According to Pochineni and Rondon-Berrios (2018), hypophosphatemia, hypomagnesemia, and hypocalcemia are associated with ASS [44]. According to Meena et al. (2020), hyponatremia developing in the first day after kidney transplantation is manifested as ASS [45]. Electrolyte parameters correlating with ASS are presented in Table 1.

Table 1

Barras P. et al. (2019): Critical values of biochemical indicators of ASS [46]

Indicator	Value
Sodium	<115 mmol/L
Ionized calcium	<5.0 mg/dL (<1.2 mmol/L)
Magnesium	<0.8 mg/dL (<0.3 mmol/L)
Phosphate	<2.5 mg/dL (<0.79 mmol/L)
Creatinine	>884 μmol/L

Malignant hypertension in patients with end-stage renal failure, with hemolytic uremic syndrome before and after kidney transplantation are associated with the development of PRES [47, 48]. The clinical picture is similar to tacrolimus-induced PRES, with high blood pressure additionally recorded. In hypertensive crisis, increased blood pressure level causes autoregulation failure of intracranial vascular tone and vasogenic edema of parietal and occipital brain lobes, manifested on MRI as symmetrical increase in MR signal from parietal and occipital areas in FLAIR and T2 modes [49]. On brain CT, these changes are hypodense [50]. Garg R.K. (2001) notes that the seizure syndrome distinguishes PRES from bilateral occipital infarcts [50].

Disequilibrium syndrome is associated with a sharp decrease in blood urea levels amid hemidialysis with fluid redistribution and occurrence of cerebral edema with depressed consciousness and seizures [51]. Bhandari B., Komanduri S. (2021) singles out the following predisposing factors: high urea nitrogen level above 60 mmol/L,

history of neurological diseases, hyponatremia, hemolytic uremic syndrome, and sepsis [51].

Uremic encephalopathy is characterized by decreased levels of consciousness, motor disorders, ataxia, and convulsions. Motor disorders in uremia, represented by tremor, asterixis and myoclonus, can be confused with ASS [52]. The Epilepsy Foundation of America reports that ASS occurs in one-third of patients with uremic encephalopathy [53]. Video-EEG monitoring allows for differential diagnosis, as there is no epileptiform activity in motor disorders [43].

Diagnosis

The diagnostic algorithm is not standardized; the following examinations are used in practice: blood gas, electrolytes, neuroimaging, and electroencephalography [32].

Treatment and prevention

Treatment of ASS in kidney recipients depends on the cause of the attack. Correction of electrolyte disturbances, stabilization of BP levels, dialysis, and use of benzodiazepines quickly stop the seizures. Stabilization of hypertension completely stops vasogenic cerebral edema in hypertensive PRES. Haughey D., Narsipur S.S. (2014) suggest the use of magnesium sulfate in this case [49], and Medeni S.S. et al. (2018) successfully used calcium channel blockers in a patient with atypical hemolytic uremic syndrome and hypertensive PRES. In the case of disequilibrium syndrome, Doorenbos C.J. (2001) suggests using 5 mL of 23% saline or 12.5 mL of intravenous mannitol to increase plasma osmolarity and reduce further osmotic shift, but this opinion is based on limited data [54]. Mistry K. (2019) recommends increasing dialysis time, reducing urea by 40% within 2 hours at the start of dialysis [55].

Chabolla D.R. et al. in 2006 developed a first aid protocol for ASS in kidney recipients, and in 2020 the protocol was slightly revised by Sawhney H. (2020) [43]. It is presented in Table 2.

Among anticonvulsant therapies, valproic acid is the drug of choice in kidney recipients. It should be noted that the drug is an inhibitor of liver enzymes and can alter the concentrations of immunosuppressants [43].

Valproic acid has several advantages over other anticonvulsants with respect to lever recipients: kidneys are not involved in its metabolism, dose adjustment is not needed depending on glomerular filtration rate (GFR), an additional dose is only required after high-flux hemodialysis, is effective for almost all types of seizures, can be administered intravenously, and can be used in children.

Levetiracetam can be used for ASS in kidney recipients because of its rapid anticonvulsant effect when administered intravenously. However, this drug requires dose adjustment depending on GFR and on the background of hemodialysis. Dose adjustments for anticonvulsants based on GFR are shown in Table 3.

Risk factors of ASS in kidney recipients

Due to the fact that ASS are one of the threatening early post-kidney transplant complications, the search for predictors of their development is of undoubted interest. It is assumed that preoperative EEG data may serve as one of the candidates for the role of a predictor. EEG changes in uremia were detected in 70% of cases and were represented by bifrontal slow-wave activity and 2-sided spike-and-wave activity of 3–6 Hz [56], which

Table 2

Practical approach to the management of bilateral tonic-clonic seizure in a kidney recipient (Chabolla D.R. et al., 2006 [39], modified by Sawhney H., 2020 [43])

<table>
<tr><td colspan="2">Acute onset of generalized tonic-clonic seizure</td></tr>
<tr><td colspan="2">Airway patency assessment, RR, HR</td></tr>
<tr><td colspan="2">Benzodiazepines</td></tr>
<tr><td>Seizure stopped</td><td rowspan="5">Continuous seizure or recurrent seizures without regaining consciousness – follow the epileptic status protocol</td></tr>
<tr><td>Eliminate or correct identified provocative factors</td></tr>
<tr><td>Neurological examination, EEG, brain MRI</td></tr>
<tr><td>If examination reveals no pathology, follow-up without antiepileptic therapy</td></tr>
<tr><td>If the examination reveals a pathology (EEG-epileptic activity or MR-structural lesion) or a spontaneous recurrent seizure occurs during follow-up without antiepileptic therapy – start anticonvulsant therapy</td></tr>
</table>

Table 3

Anticonvulsant doses depending on GFR [43]

GFR (mL/min)	60–90	30–60	15–30	<15	Hemodialysis
Levetiracetam	500–1000 mg twice/day	250–750 mg twice/day	250–500 mg twice/day	500–1000 mg once/day	Additional dose of 250–500 mg after dialysis
Valproic acid	No correction	No correction	No correction	No correction	Correction required for high-flux dialysis

is regarded as part of the existing encephalopathy. The representation of slow rhythms and specific EEG patterns correlates with the stage of CKD and may be a tool for recognizing subclinical uremic encephalopathy [57]. EEG changes are thought to be associated with high urea and chloride levels and low calcium levels [58]. However, EEG findings in studies have not been a reliable predictor of post kidney-transplant seizures but have correlated with developmental abnormalities [58]. Whereas postoperative EEG can be useful in diagnosing and determining treatment strategies when determining the cause of coma: nonconvulsive status epilepticus or encephalopathy, as well as in making differential diagnosis of epileptic and non-epileptic seizures [32]. According to the Lorie DH (2008) single-center study, pre-kidney transplant ASS did not predict pre-transplant recurrent seizure [58].

Since epileptic seizures can be triggered by fluctuations in blood sodium, calcium, magnesium and glucose, regardless of the underlying disease, these indicators may well be considered as predictors. Accordingly, Nardone R. et al. (2016) suggests that routine monitoring of blood electrolyte levels in case of dysmetabolic seizures is crucial for seizure control and prevents irreversible brain damage in patients [59].

Thus, the causes of acute symptomatic seizures developing in children after orthotopic liver and kidney transplantation are very diverse. Approaches to the correction of ASS and assessment of their prognostic significance largely depend on pathogenetic mechanisms. Most of the cases of this early-postoperative complication can be attributed to potentially manageable conditions. At the same time, as it was found out from the analyzed literature, there is currently no standardized diagnostic tactics for ASS. Accordingly, developing such a diagnostic tactic seems very relevant, as it can help to reduce the time for establishing a diagnosis and making decisions on treatment interventions.

The authors declare no conflict of interest.

REFERENCES

1. *Gautier SV, Tsiroulnikova OM, Moysyuk YG, Akhaladze DG, Tsiroulnikova IE, Silina OV et al.* Liver transplantation in children: six-year experience analysis. *Russian Journal of Transplantology and Artificial Organs*. 2014; 16 (3): 54–62. [In Russ, English abstract]. https://doi.org/10.15825/1995-1191-2014-3-54-62.
2. *Dutkowski P, Linecker M, DeOliveira ML, Müllhaupt B, Clavien P-A*. Challenges to liver transplantation and strategies to improve outcomes. *Gastroenterology*. 2015; 148 (2): 307–323. doi: 10.1053/j.gastro.2014.08.045.
3. *Kumar SS, Mashour GA, Picton P.* Neurologic Considerations and Complications Related to Liver Transplantation. *Anesthesiology*. 2018; 128 (5): 1008–1014. doi: 10.1097/ALN.0000000000002148.
4. *Derle E, Kibaroğlu S, Öcal R et al.* Seizure as a neurologic complication after liver transplant. *Exp Clin Transplant Off J Middle East Soc Organ Transplant*. 2015; 13 Suppl 1: 323–326. doi: 10.6002/ect.mesot2014.p176.
5. *Patchell RA*. Neurological complications of organ transplantation. *Ann Neurol*. 1994; 36 (5): 688–703. doi: 10.1002/ana.410360503.
6. *Menegaux F, Keeffe EB, Andrews BT et al.* Neurological complications of liver transplantation in adult versus pediatric patients. *Transplantation*. 1994; 58 (4): 447–450. doi: 10.1097/00007890-199408270-00010.
7. *Lee B, Min NH, Ham SY, Na S, Kim J.* Non-Convulsive Status Epilepticus following Liver Transplantation. *Korean J Crit Care Med*. 2016; 31 (1): 49–53. doi: 10.4266/kjccm.2016.31.1.49.
8. *Beghi E, Carpio A, Forsgren L et al.* Recommendation for a definition of acute symptomatic seizure. *Epilepsia*. 2010; 51 (4): 671–675. doi: 10.1111/j.1528-1167.2009.02285.x.
9. *Fisher RS, Acevedo C, Arzimanoglou A et al.* ILAE Official Report: A practical clinical definition of epilepsy. *Epilepsia*. 2014; 55 (4): 475–482. doi: 10.1111/epi.12550.
10. *Ameres M, Melter M, Zant R, Schilling S, Geis T*. Liver transplantation during infancy: No increased rate of neurological complications. *Pediatr Transplant*. 2018; 22 (8): e13304. doi: 10.1111/petr.13304.
11. *Gungor S, Kilic B, Arslan M, Selimoglu MA, Karabiber H, Yilmaz S*. Early and late neurological complications of liver transplantation in pediatric patients. *Pediatr Transplant*. 2017; 21 (3). doi: 10.1111/petr.12872.
12. *Lee JJ, Lim S, Lee YS et al.* Myoclonic movement after general anesthesia: A case report and review of the literature. *Medicine (Baltimore)*. 2018; 97 (12): e0141. doi: 10.1097/MD.0000000000010141.
13. *Nartailakov MA, Salimgaraev IZ, Panteleev VS et al.* Refeeding Syndrome in Surgical Patients. A Clinical Case Analysis. *Creative surgery and oncology*. 2019; 9 (2): 118–124. [In Russ, English abstract]. https://doi.org/10.24060/2076-3093-2019-9-2-118-124.
14. Toxins and Drugs Reported to Induce Seizures. Epilepsy Foundation. Accessed April 15, 2021. https://www.epilepsy.com/learn/professionals/resource-library/tables/toxins-and-drugs-reported-induce-seizures.
15. *Cruz RJ, DiMartini A, Akhavanheidari M et al.* Posterior reversible encephalopathy syndrome in liver transplant patients: clinical presentation, risk factors and initial management. *Am J Transplant Off J Am Soc Transplant Am Soc Transpl Surg*. 2012; 12 (8): 2228–2236. doi: 10.1111/j.1600-6143.2012.04048.x.
16. *Fernandez D, El-Azzabi T, Jain V et al.* Neurologic Problems After Pediatric Liver Transplantation and Combined Liver and Bowel Transplantations: A Single Tertiary Centre Experience. *Transplantation*. 2010; 90: 319–324. doi: 10.1097/TP.0b013e3181e5b7fc.
17. *Lunardi N, Saraceni E, Boccagni P et al.* Posterior reversible encephalopathy syndrome in the Intensive Care Unit after liver transplant: a comparison of our experience with the existing literature. Minerva Anestesiol. 2012; 78 (7): 847–850.

18. *Dohgu S, Yamauchi A, Nakagawa S et al.* Nitric oxide mediates cyclosporine-induced impairment of the blood-brain barrier in cocultures of mouse brain endothelial cells and rat astrocytes. *Eur J Pharmacol*. 2004; 505 (1–3): 51–59. doi: 10.1016/j.ejphar.2004.10.027.
19. *Chen H, Albertson TE, Olson KR.* Treatment of drug-induced seizures. *Br J Clin Pharmacol*. 2016; 81 (3): 412–419. doi: 10.1111/bcp.12720.
20. *Rudakova IG, Belova IA, Kel NV, Alakova MV.* Sudorogi obuslovlennye vodno-electrolitnym disbalansom i epilepsia. Problemy diagnostiki i terapii. *Nevroligiya. Neiropsihiatriya. Psihosomatica.* 2014; (S1): 45–47. [In Russ, English abstract]. doi.org/10.14412/2074-2711-2014-1S-45-47.
21. *Abbasoglu O, Goldstein RM, Vodapally MS et al.* Liver transplantation in hyponatremic patients with emphasis on central pontine myelinolysis. *Clin Transplant*. 1998; 12 (3): 263–269.
22. *Cascales Campos P, Ramirez P, Gonzalez R et al.* Central pontine and extrapontine myelinolysis: a rare and fatal complication after liver transplantation. *Transplant Proc*. 2011; 43 (6): 2237–2238. doi: 10.1016/j.transproceed.2011.06.052.
23. *Kim B-S, Lee S-G, Hwang S et al.* Neurologic complications in adult living donor liver transplant recipients. *Clin Transplant*. 2007; 21 (4): 544–547. doi: 10.1111/j.1399-0012.2007.00687.x.
24. *Gaynor JJ, Moon JI, Kato T et al.* A cause-specific hazard rate analysis of prognostic factors among 877 adults who received primary orthotopic liver transplantation. *Transplantation*. 2007; 84 (2): 155–165. doi: 10.1097/01.tp.0000269090.90068.0f.
25. *Abdel Massih RC, Razonable RR.* Human herpesvirus 6 infections after liver transplantation. *World J Gastroenterol*. 2009; 15 (21): 2561–2569. doi: 10.3748/wjg.15.2561.
26. *Tan CS, Koralnik IJ.* Progressive multifocal leukoencephalopathy and other disorders caused by JC virus: clinical features and pathogenesis. *Lancet Neurol*. 2010; 9 (4): 425–437. doi: 10.1016/S1474-4422(10)70040-5.
27. *Ozdemir F, Ince V, Baskiran A et al.* Progressive Multifocal Leukoencephalopathy after Three Consecutive Liver Transplantations. *Int J Organ Transplant Med*. 2015; 6 (3): 126–130.
28. *Anand P, Hotan GC, Vogel A, Venna N, Mateen FJ.* Progressive multifocal leukoencephalopathy: A 25-year retrospective cohort study. *Neurol Neuroimmunol Neuroinflammation*. 2019; 6 (6). doi: 10.1212/NXI.0000000000000618.
29. *Zivković S.* Neuroimaging and neurologic complications after organ transplantation. *J Neuroimaging Off J Am Soc Neuroimaging*. 2007; 17 (2): 110–123. doi: 10.1111/j.1552-6569.2007.00097.x.
30. *Beloborodova NB, Ostrova IV.* Sepsis-Associated Encephalopathy (Review). *General Reanimatology*. 2017; 13 (5): 121–139. [In Russ, English abstract]. doi: 10.15360/1813-9779-2017-5-121-139.
31. *Sonneville R, Verdonk F, Rauturier C et al.* Understanding brain dysfunction in sepsis. *Ann Intensive Care*. 2013; 3 (1): 15. doi: 10.1186/2110-5820-3-15.
32. *Shepard PW, St. Louis EK.* Seizure Treatment in Transplant Patients. *Curr Treat Options Neurol*. 2012; 14 (4): 332–347. doi: 10.1007/s11940-012-0180-y.
33. *Ismail D, Green J, Bannerman B et al.* Posterior Reversible Encephalopathy Syndrome (PRES) in Adult Multi-Visceral Transplant patients – Cambridge University Hospital experience. *Transplantation*. 2017; 101 (6S2): S137. doi: 10.1097/01.tp.0000521492.43465.8a.
34. *Dzyadzko AM, Katin ML, Rummo OO et al.* Central pontine myelinolysis after orthotopic liver transplantation (two case reports). *Russian Journal of Transplantology and Artificial Organs*. 2013; 15 (1): 89–95. [In Russ, English abstract]. https://doi.org/10.15825/1995-1191-2013-1-89-95.
35. *Glass GA, Stankiewicz J, Mithoefer A, Freeman R, Bergethon PR.* Levetiracetam for seizures after liver transplantation. *Neurology*. 2005; 64 (6): 1084–1085. doi: 10.1212/01.WNL.0000154598.03596.40.
36. Gosudarstvennyy reestr tsen na zhiznenno neobkhodimye i vazhneyshie lekarstvennye preparaty. Accessed April 22, 2021. http://farmcom.info/site/reestr?TnnName=%EA%E5%EF%EF%F0%E0.
37. Gosudarstvennyy reestr lekarstvennykh sredstv. Accessed April 22, 2021. https://grls.rosminzdrav.ru/Grls_View_v2.aspx?routingGuid=33129c9c-850c-4b0d-b9bf-fae2cfd5a55c&t=.
38. *Wijdicks EF, Plevak DJ, Wiesner RH, Steers JL.* Causes and outcome of seizures in liver transplant recipients. *Neurology*. 1996; 47 (6): 1523–1525. doi: 10.1212/wnl.47.6.1523.
39. *Chabolla DR, Wszolek ZK.* Pharmacologic management of seizures in organ transplant. *Neurology*. 2006; 67 (12 Suppl 4): S34–38. doi: 10.1212/wnl.67.12_suppl_4.s34.
40. Epilepsy Foundation. Accessed February 1, 2021. https://www.epilepsy.com/living-epilepsy/epilepsy-and/professional-health-care-providers/co-existing-disorders-69.
41. *Balderramo D, Prieto J, Cárdenas A, Navasa M.* Hepatic encephalopathy and post-transplant hyponatremia predict early calcineurin inhibitor-induced neurotoxicity after liver transplantation. *Transpl Int Off J Eur Soc Organ Transplant*. 2011; 24 (8): 812–819. doi: 10.1111/j.1432-2277.2011.01280.x.
42. *Wu S-Y, Chen T-W, Feng A-C, Fan H-L, Hsieh C-B, Chung K-P.* Comprehensive risk assessment for early neurologic complications after liver transplantation. *World J Gastroenterol*. 2016; 22 (24): 5548–5557. doi: 10.3748/wjg.v22.i24.5548.
43. *Sawhney H, Gill SS.* Renal transplant recipient seizure practical management. *World J Nephrol*. 2020; 9 (1): 1–8. doi: 10.5527/wjn.v9.i1.1.
44. *Pochineni V, Rondon-Berrios H.* Electrolyte and Acid-Base Disorders in the Renal Transplant Recipient. *Front Med*. 2018; 5. doi: 10.3389/fmed.2018.00261.
45. *Meena P, Bhargava V, Rana D, Bhalla A, Gupta A.* An Approach to Neurological Disorders in a Kidney Transplant Recipient. *Kidney 360*. 2020; 1 (8): 837–844. doi: 10.34067/KID.0002052020.
46. *Barras P, Siclari F, Hügli O, Rossetti AO, Lamy O, Novy J.* A potential role of hypophosphatemia for diag-

nosing convulsive seizures: A case-control study. *Epilepsia*. 2019; 60 (8): 1580–1585. doi: 10.1111/epi.16090.
47. *Giussani A, Ardissino G, Belingheri M et al.* Posterior reversible encephalopathy syndrome after kidney transplantation in pediatric recipients: Two cases. *Pediatr Transplant*. 2016; 20 (1): 68–71. doi: 10.1111/petr.12640.
48. *Medeni SS, Namdaroglu S, Cetintepe T et al.* An adult case of atypical hemolytic uremic syndrome presented with posterior reversible encephalopathy syndrome: Successful response to late-onset eculizumab treatment. *Hematol Rep*. 2018; 10 (3). doi: 10.4081/hr.2018.7553.
49. *Haughey D, Narsipur SS.* Posterior Reversible Encephalopathy Syndrome After Renal Transplant: A Simple Solution for a Complicated Patient. *Case Rep Nephrol Dial*. 2014; 5 (1): 20–25. doi: 10.1159/000366554.
50. *Garg RK.* Posterior leukoencephalopathy syndrome. *Postgrad Med J*. 2001; 77 (903): 24–28. doi: 10.1136/pmj.77.903.24.
51. *Bhandari B, Komanduri S.* Dialysis Disequilibrium Syndrome. In: StatPearls. StatPearls Publishing; 2021. Accessed April 16, 2021. http://www.ncbi.nlm.nih.gov/books/NBK559018/.
52. Uremic Encephalopathy: Practice Essentials, Pathophysiology, Epidemiology. Published online April 3, 2021. Accessed April 22, 2021. https://emedicine.medscape.com/article/239191-overview.
53. Uremic Encephalopathy. Epilepsy Foundation. Accessed April 22, 2021. https://www.epilepsy.com/living-epilepsy/epilepsy-and/professional-health-care-providers/co-existing-disorders/renal-disorders/uremic-encephalopathy.
54. *Doorenbos CJ, Bosma RJ, Lamberts PJ*. Use of urea containing dialysate to avoid disequilibrium syndrome, enabling intensive dialysis treatment of a diabetic patient with renal failure and severe metformin induced lactic acidosis. *Nephrol Dial Transplant Off Publ Eur Dial Transpl Assoc – Eur Ren Assoc*. 2001; 16 (6): 1303–1304. doi: 10.1093/ndt/16.6.1303.
55. *Mistry K*. Dialysis disequilibrium syndrome prevention and management. *Int J Nephrol Renov Dis*. 2019; 12: 69–77. doi: 10.2147/IJNRD.S165925.
56. *Hughes JR*. Correlations between EEG and chemical changes in uremia. *Electroencephalogr Clin Neurophysiol*. 1980; 48 (5): 583–594. doi: 10.1016/0013-4694(80)90293-x.
57. *Gadewar P, Acharya S, Khairkar P, Shukla S, Mahajan SN*. Dynamics of electroencephalogram (EEG) in different stages of chronic kidney disease. *J Clin Diagn Res JCDR*. 2015; 9 (3): OC25–27. doi: 10.7860/JCDR/2015/11257.5705.
58. *Hamiwka LD, Midgley JP, Hamiwka LA*. Seizures in children after kidney transplantation: has the risk changed and can we predict who is at greatest risk? *Pediatr Transplant*. 2008; 12 (5): 527–530. doi: 10.1111/j.1399-3046.2007.00813.x.
59. *Nardone R, Brigo F, Trinka E.* Acute Symptomatic Seizures Caused by Electrolyte Disturbances. *J Clin Neurol Seoul Korea*. 2016; 12 (1): 21–33. doi: 10.3988/jcn.2016.12.1.21.

The article was submitted to the journal on 22.04.2021

DOI: 10.15825/1995-1191-2021-2-167-176

CLINICAL FEATURES OF MALIGNANT TUMORS AGAINST THE BACKGROUND OF IMMUNOSUPPRESSIVE THERAPY IN HEART TRANSPLANT RECIPIENTS

L.B. Krougly[1], N.N. Koloskova[1], A.V. Nikulin[1], I.V. Pashkov[1], V.N. Poptsov[1], A.O. Shevchenko[1, 2]

[1] Shumakov National Medical Research Center of Transplantology and Artificial Organs, Moscow, Russian Federation

[2] Sechenov University, Moscow, Russian Federation

As the survival rate of cardiac recipients improves, higher incidence of malignancy in the late postoperative period becomes essential for their prognosis. Immunosuppressive therapy is one of the key prerequisites for successful transplantation. However, long-term use of immunosuppressive agents increases the incidence of malignant tumors compared to the general population. The risk of their development after organ transplantation increases by 2–4 times compared to the general population. For patients who have undergone transplantation since 2000, the risk of developing malignant neoplasms 1–5 years after surgery is estimated at 10–12%. Timely comprehensive examination of patients, development of new immunosuppression schemes, treatment of those predisposing to the development of malignant neoplasms and giving up harmful habits will reduce the risk of malignant tumors and help diagnose these serious complications at an early stage, which, in turn, will increase the life expectancy of solid organ (particularly the heart) recipients.

Keywords: heart transplantation, immunosuppressive therapy, malignant tumors.

INTRODUCTION

Heart transplantation (HTx) remains the most effective surgical treatment for refractory congestive heart failure. Provided that patient selection criteria are met, HTx can significantly increase patients' life expectancy, improve exercise tolerance and quality of life, and often allow patients to return to work. Apart from organ shortage, the main problems of transplantology are related to lack of effectiveness and safety of immunosuppressive therapy in the long term, which is associated with cellular and/or antibody-mediated graft rejection, infectious diseases, hypertension, renal failure, malignancies, and coronary artery vasculopathy in some patients [1].

In Russia, as elsewhere in the world, the most significant side effects of immunosuppressive therapy are malignancies, infectious complications, nephropathy, and diabetes mellitus [2].

According to the International Society for Heart and Lung Transplantation (ISHLT) report on HTx in adults, based on data submitted by 394 transplant centers observing 104,000 patients worldwide, the median survival after HTx was 8.5 years in recipients operated on between 1982 and 1992 and 10.9 years in recipients operated on from 1993 to 2003. The report concludes, however, that the improvement was mainly due to a decrease in mortality in the first year after HTx and that mortality at a later date did not fall significantly [3]. In 2018, there were reports showing that 16% of patients who lived 5 years after HTx and 28% of patients who lived 10 years after HTx were diagnosed with at least one case of malignancy in one location or the other. Moreover, malignancies are now the leading cause of death in patients who had HTx more than five years ago [4], confirming the importance of research on this topic. As short- and mid-term outcomes improve, long-term HTx complications, such as coronary artery vasculopathy and malignant tumors, become increasingly important. The risk of developing malignancies after organ transplantation is 2–4 times higher than in the general population, with the risk being higher in heart and/or lung recipients than in liver and/or kidney recipients [5–7]. For patients who have already had a transplant surgery, the risk of malignancy 1–5 years after HTx is estimated at 10–12% [8]. Despite the urgency of the problem, there have been relatively few studies on cancer incidence after heart transplantation. The incidence of malignant tumors after heart transplantation has varied widely in previous studies, ranging from 3% to 30%. This wide variation in results is mainly due to the different follow-up periods in different studies and the lack of detection of skin cancer, the most common post-transplant malignancy, in many large studies [9].

Corresponding author: Lev Krougly. Address: 1, Shchukinskaya str., Moscow, 123182, Russian Federation. Phone: (925) 022-00-44. E-mail: krouglylev@mail.ru

FEATURES OF THE COURSE OF CANCER IN PATIENTS WITH HEART TRANSPLANTS

According to the registry of the University Hospitals Leuven (Belgium), which included 563 patients who underwent primary heart transplantation over 25 years (1987–2013), malignant tumors of various localizations occurred in 181 patients (263 diagnosed cases of various tumors), which was 4511 cases per 100,000 patient-years. The mean age of the patients was 63 ± 11 years, the time after HTx was 7.7 ± 5 years. Screening for post-transplant malignancies was an integral part of follow-up and included clinical examination at each visit, annual chest x-ray, dermatologic examination, and gynecologic examination or prostate-specific antigen testing. Mammography and colonoscopy were performed according to current international guidelines [8]. The cumulative incidence of cancer 1, 5, 10, and 20 years after transplantation was 2% (95% confidence interval [CI], 0–4%), 14% (95% CI, 10–18%), 29% (95% CI, 25–33%), and 60% (95% CI, 52–68%), respectively. The most common cancer type was squamous cell skin cancer (58 patients, 22% of all cancers) and followed by basal cell skin cancer (51 patients, 19%). Many skin cancer patients had primary multiple tumors: 180 cases of squamous cell carcinoma in 58 patients and 111 cases of basal cell carcinoma in 51 patients. Forty-one patients (16%) had lung cancer, 30 (11%) had lymphoma, and 25 (10%) had prostate cancer. Increased risk factors for post-transplant malignancy in univariate Cox proportional hazards analysis were: having HTx before 2000 (hazard ratio [HR] 1.4; $P < 0.047$), older than 50 years at the time of HTx (HR 3.3; $P < 0.001$), male gender (HR 2.1; $P < 0.001$), history of smoking (HR 1.5; $P < 0.010$), immunosuppressive therapy with azathioprine (compared with mycophenolate mofetil, HR 1.4; $P < 0.044$) or with cyclosporine (compared with tacrolimus, HR 1.7; $P < 0.05$), coronary etiology of cardiomyopathy causing HTx (HR 1.4; $P < 0.024$).

Recipient's age at the time of transplantation was the most important risk factor, which is consistent with the data obtained from many registries. The risk of malignancy correlates both with age of patients after transplantation [10] and age of the general population [11]. A possible explanation is the aging of the immune system, which undermines the ability to defend against tumor cells. The aging of the immune system begins in early childhood with involution of the thymus, leading to decreased production of native T cells, and continues throughout life with gradual functional impairment of T cells. In older patients who have undergone HTx, the aging of the immune system is exacerbated by immunosuppressive therapy, which leads to increased risk of malignancy [12].

Another important risk factor was the male gender of the recipient. This was due in part to the higher incidence of prostate tumors in men compared to breast tumors and cervical cancer in women. However, the pattern was also observed after excluding these three diseases, which is consistent with other studies [13–15]. Curiously, the same differences in susceptibility to tumors are also observed in the general population [16]. This phenomenon may be caused by hormonal [17] and sex chromosome-specific effects on immune regulation [18], although the exact mechanisms of this phenomenon remain to be elucidated. Although the introduction of safer immunosuppressive therapy regimens and a reduced risk of cancer in patients operated on after 2000 is encouraging, the risk of malignancy in this localization remains high.

Not only are post-HTx malignant tumors more common than in the population, but they also usually have a poorer prognosis. The average survival for cancers of various localizations in HTx recipients is 2.9 years after diagnosis, which is significantly lower than the survival of patients with similar diseases in the general population [12, 19]. The incidence of tumors in this group of patients and the high mortality rate from them requires constant attention during the entire period of patient follow-up. Since immunosuppressive therapy is probably the most important modifiable risk factor for post-HTx cancer, individualizing immunosuppression may help reduce the risk of complications and, consequently, increase survival and life expectancy in this patient population [8].

A study at HUS Helsinki University Hospital (Finland) analyzed data from 479 adult heart transplant recipients transplanted in 1985–2014 (total of 4491.6 person-years of follow-up) and a mean follow-up of 7.8 years. Of all patients, 415 (86.6%) were alive 30 days and 386 (80.6%) one year after HTx. At the end of follow-up, 234 (48.9%) patients were alive. The mean age at the time of surgery was 52 years, 79.5% of the patients were male. A total of 267 cancers were reported in 143 patients during follow-up; the cumulative incidence after 1, 5, 10, and 20 years was 0.3%, 8.7%, 22.3%, and 52.4%, respectively. 96.3% of all malignant tumors were detected in men. The mean time from HTx to the development of cancer was 8.9 years. Among all patients, 21 had a history of malignancy of various localizations before HTx, of whom 11 (52.0%) were diagnosed de novo in the postoperative period. There were no recurrences of a previous malignancy [20].

Malignant tumors were classified as the cause of death in 52 patients, representing 21.2% of all deaths in the cohort during follow-up. There were only 2 deaths from malignancy within the first year after HTx, and 9 deaths within the first five years after HTx. The cancer risk ratio for the entire cohort of patients after HTx was 3.1 (95% CI 2.4–4.1), increasing slowly over time after HTx: 2.3 (95% CI 0.8–4.9) in the first five years after HTx, 3.0 (95% CI 1.6–4.1) 5.0) at 5–10 years, 3.3 (95% CI 2.2–4.8) at 10–20 years, and 4.6 (95% CI 2.0–8.8) at 20 years after HTx. HR to develop malignant tumour was

higher for men (3.3; 95% CI 2.5–4.3) than for women (1.8; 95% CI 0.5–4.7) and was highest in younger patients: 8.0 (95% CI 2.5–18.6) <40 years old with HTx, 5.8 (95% CI 3.3–9.3) in patients 40–49 years old, 2.0 (95% CI 1.3–3.2) in patients 50–59 years old, and 3.2 (95% CI 1.8–5.2) in patients over 60 years old at the time of malignant tumor detection. The study showed that the incidence of malignant tumors of different localizations in Finnish heart transplant recipients was six times higher and mortality three times higher than in the Finnish population as a whole, which is consistent with data from other studies [21, 22]. Basal cell carcinoma was the most common malignancy in the described cohort – more than half of all detected malignant tumors. Other cancers that were generally common in the Finnish population were also frequent: prostate cancer, lung cancer, and kidney cancer. Nevertheless, the incidence rate for all of them was significantly higher than that of the population, with the exception of prostate cancer. There were many cases of non-Hodgkin lymphoma (n = 36, HR 25.7) and lip and tongue cancer (HR 47.4 and 26.3, respectively).

Results of the study indicate that there is a high incidence of malignant tumors of various localizations among heart and/or lung recipients, the most common of which was squamous cell skin cancer [5, 23, 24]. Because oral cancers are associated with human papillomavirus (HPV) infection [25], chronic carriage of the virus on the background of immunosuppressive therapy has been recognized as a predisposing cause for the development of these cancers in heart recipients [26]. It has been suggested that HPV infection is a predisposing factor in the development of squamous cell skin cancer in heart transplant recipients [27].

The use of polyclonal antibodies to human lymphocytes for immunosuppression is thought to increase the risk of lymphoma and skin cancer. In recent years, along with a decrease in the use of polyclonal antibodies, a decrease in the incidence of lymphoma after heart and lung transplantation has been reported [28]. Squamous cell skin cancer was the most common and more aggressive type of cancer, which emphasizes the importance of regular skin examinations, especially because the disease tended to be more severe in solid organ recipients than in other patients [26]. Further studies are needed to determine the effect of immunosuppressive therapy regimens on the incidence of malignant tumors of various localizations, as well as to identify other possible risk factors for their occurrence in heart recipients.

The increased risk of malignancy in heart transplant recipients requires regular examinations and self-examination. Current guidelines in the Russian Federation include blood testing for Epstein–Barr virus (by polymerase chain reaction), measurement of prostate-specific antigen levels, mammography, and chest X-rays [2].

IMMUNOSUPPRESSIVE THERAPY AS A RISK FACTOR FOR MALIGNANCY AFTER HEART TRANSPLANTATION

Immunosuppressive therapy is one of the key conditions for a successful transplant surgery. However, many studies have reported that long-term use of immunosuppressants after transplantation increases the incidence of malignancy compared to the general population [12, 29].

Immunosuppressive therapy after HTx can be divided into induction and maintenance therapy. Induction immunosuppressive therapy is prescribed for a set period of time after surgery, while maintenance therapy is prescribed for life. Induction immunosuppressants that are used for HTx include rabbit antithymocyte globulin (ATG), equine ATG, and interleukin 2 receptor antagonists (basiliximab). According to the ISHLT registry, induction immunosuppressants were used in 52% of all patients with HTx in 2002 and 47% of all patients with HTx in 2012. In recent years, the preferred type of induction therapy has been ATGs or IL-2 receptor antagonists, which were administered in 27% and 21% of cases in 2002 and in 19% and 28% in 2012 [30]. The fact that only about half of all HTx recipients worldwide receive some form of induction therapy reflects the disagreement over its scope. The benefits include earlier reduction in glucocorticoid (GCS) doses and delayed initiation of calcineurin inhibitors (CIs) without a higher risk of rejection, as shown in randomized [30], retrospective [31] and prospective studies [32]. This avoids the side effects of GCS and the nephrotoxic effects of CIs. However, there are not yet enough large, randomized studies yet to draw conclusions about the safety and efficacy of immunosuppressive drugs used for induction therapy. Their long-term side effects are not yet fully understood, and there are concerns that they may increase the risk of infections and tumors [33]. To remove uncertainty about the potential benefits and harms of induction therapy for HTx, a Cochrane review was conducted in 2013 with a meta-analysis of 22 randomized trials [34]. Mortality and major complications, such as acute and chronic heart graft rejection reactions, development of infections, malignancies of various localizations, and decreased renal function, were studied. When comparing treatment regimens, acute graft rejection reactions were less common with induction therapy. Unfortunately, most of the studies included in the review did not last long enough to assess the risks of malignancy after HTx. Therefore, longer studies on this topic are needed to draw a definitive conclusion [35].

Maintenance immunosuppression after HTx usually consists of GCS, CIs (cyclosporine or tacrolimus) and mycophenolate mofetil, azathioprine or m-TOR inhibitor (everolimus or sirolimus). CIs inhibit the calcineurin enzyme in T cells, thereby preventing their proliferation and differentiation, while the antimetabolites

azathioprine and mycophenolate mofetil in turn inhibit the cell cycle of T and B cells, thereby having a more pronounced effect on both T and B cells [36]. According to the ISHLT registry, the frequency of CIs and antimetabolites in patients who survived 1 year after HTx has remained about the same since 2000 (98% and 88% respectively in 2000, 94% and 89% currently). At the same time, by 2012, cyclosporine was prescribed significantly less frequently than tacrolimus (13% versus 81% in patients who lived 1 year after HTx). The advantages of tacrolimus over cyclosporine were shown in a meta-analysis of 10 randomized trials involving 952 patients after HTx [35]. Tacrolimus was less likely to cause arterial hypertension, hyperlipidemia, hirsutism, and gingival hyperplasia, and in some studies, it was associated with lower overall post-HTx mortality. However, there were no significant differences between tacrolimus and cyclosporine in terms of appearance of malignancies and some other complications. Likewise, azathioprine is actively replaced by mycophenolate mofetil (3% versus 85% in patients surviving 1 year after HTx). Everolimus and sirolimus inhibit m-TOR (mammalian target of rapamycin), thereby reducing the proliferation and differentiation of T and B cells [36]. According to the ISHLT registry, the proportion of heart transplant recipients receiving an m-TOR inhibitor 1 year after transplantation increased from 3% in 2000 to 13% in 2012. M-TOR inhibitors are currently being studied for use in patients with chronic kidney disease and graft vasculopathy, but their use is limited by side effects, especially poor wound healing [37]. Everolimus is used not only after HTx but also in the treatment of some malignancies, such as renal cell carcinoma, pancreatic neuroendocrine tumors, and HER2-positive breast cancer [38–40]. The use of sirolimus in kidney recipients reduced the risk of malignant tumors [41, 42]. However, the risk of developing malignant tumors in patients treated with everolimus after HTx is poorly understood, although in a 2016 experimental study, retrospective follow-up of HTx patients showed promising results. At follow-up from March 1, 1990 to March 1, 2015 (mean period, 69.2 months) at the National Taiwan University Hospital in 454 patients receiving combined immunosuppressive therapy, including mycophenolate mofetil (n = 232) or everolimus (n = 222), malignancies were diagnosed in 27, of whom 23 (85%) received mycophenolate mofetil and 4 (15%) received everolimus. Everolimus therapy was significantly safer (9.91% vs. 1.80%, $P < 0.001$). The most common malignancies were lymphoma (n = 7), skin cancer (n = 5), and prostate cancer (n = 3). The 2-year overall survival after detection of malignant tumor did not differ significantly – 50% in the everolimus group and 47% in the mycophenolate mofetil group ($P = 0.745$). Perhaps the benefits of everolimus can be explained by the increased expression of E-cadherin, which promotes inhibition of cyclin-dependent kinase (CDK) $p27^{kip1}$, decreased cyclin D1 expression and cell cycle arrest of the tumor cell in the G1 phase, thus preventing tumor growth and metastatic progression [43].

MALIGNANT TUMORS OF VARIOUS LOCALIZATIONS IN HEART RECIPIENTS

Skin cancer is the most common malignancy seen in transplant recipients, accounting for 42% to 50% of all post-HTx tumors. The average interval between HTx and skin tumor diagnosis correlates with the age of the recipient at the time of transplantation. In general, patients over 50 years of age have a higher risk of developing the cancer than younger patients.

There are both external and internal risk factors for skin cancer. Ultraviolet radiation appears to be the main one [44], since skin cancer develops on areas exposed to prolonged and intense sun exposure, and is more frequently seen in patients exposed to high sun exposure after transplantation (>10,000 hours) [45, 46]. The incidence of skin cancer is directly correlated with the concentration of immunosuppressive drugs and the presence and frequency of rejection episodes in the first year after HTxx [47], more common in people with fair skin (Fitzpatrick type II), blue eyes, and blond or red hair [47, 48, 52]. The likelihood of developing skin cancer after HTx depends on gender [47].

The histologic pattern most often corresponds to squamous cell or basal cell carcinoma [49], localized to the head and neck (70%), trunk (9%), upper extremities (17%), or lower extremities (4%) [50]. Squamous cell carcinoma is 65–250 times more common in patients after HTx than in the general population, basal cell carcinoma is 10 times more common than in the general population [51]. The ratio of squamous cell carcinoma to basal cell carcinoma in the population is approximately 1:4, and the ratio of patients after HTx, by contrast, is 4:1 [48]. Squamous cell carcinoma is more severe in transplanted heart patients than in the general population; in addition, HTx patients have a higher risk of developing primary multiple cancer, risk of metastasis, perineural and lymphatic invasion, and local recurrence due to infectious diseases, especially infection with HPV [51, 52]. Patients with squamous cell carcinoma have a higher incidence of solar keratosis [52]. Another common skin cancer is melanoma, which occurs mostly in patients with fair skin, light hair and eyes, and a tendency to freckles. Heart recipients have a 1,633-fold increased risk of melanoma, and the prognosis of the disease is poor because of the development of long-term metastases [52].

The incidence of Kaposi sarcoma is much higher in patients who have had HTx, also higher than in the general population [48] with incidence rates ranging from 0.41% to 1.2% [53]. Herpes virus infection and the effect of immunosuppressive therapy have been cited as reasons for the increased incidence [49]. About 60% of

Kaposi sarcoma cases were nonvisceral (98% were skin tumors, 2% were oral or oropharyngeal tumors), and the remaining 40% were visceral – most often affecting the gastrointestinal tract, lungs, and lymph nodes. The prognosis for Kaposi sarcoma is poor, with a median survival of 23.6 months after diagnosis. Death occurs either directly from the disease progression or as a result of acute graft rejection [54].

Lymphoproliferative disease is the second most common cancer in HTx recipients [56] and the most common disease in pediatric heart transplant recipients [55]. Most cases occur within 1 year of HTx [44], the incidence in patients after HTx ranges from 1.5% to 11.4% [56], which is higher than in other organ recipients, and it is independent of factors such as age and gender, and does not increase over time, unlike other types of cancer [57, 58]. Epstein–Barr virus infection plays an important role in the pathogenesis of lymphoproliferative diseases, so their incidence remains high for 5 years after HTx [12, 59].

Lymphoproliferative diseases after solid organ transplantation are potentially malignant complications, affecting about 1% of recipients [60]. In contrast to the general population, the development of lymphoproliferative disease in HTx recipients affects not only the lymph nodes but also the liver, lungs, central nervous system, intestines, kidneys, and spleen. Gastrointestinal and respiratory organs are the most common target organs in pediatric heart transplant recipients [61]. Although lower doses of immunosuppressants are sufficient to achieve remission in some patients, most require rituximab and/or chemotherapy. Patients with relapsed lymphoma have a poor prognosis and require treatment with new drugs, such as PD-1 monoclonal antibody inhibitors nivolumab, pembrolizumab, or atezolizumab [62].

Solid tumors are relatively rare compared to skin tumors and lymphomas, but the prognosis for these diseases is also significantly worse than for skin tumors and lymphomas. The most common post-HTx solid organ cancer is lung cancer. The most important risk factor for its development, along with immunosuppressive therapy, is old age [63]. Non-small cell lung cancer is the most common type of lung tumor seen after heart transplantation, but there are also reports of mesothelioma and carcinoid tumors [55, 56, 64]. According to Goldstein et al. [56], the average interval from HTx to diagnosis of lung cancer, is 35.7 months. The prognosis for lung cancer patients depends on the stage, and is poor in the later stages of the disease. The main reasons of such high mortality include late detection, metastasis, and rapid tumor growth [65].

As for malignant tumors of other solid organs, the incidence of prostate and bladder cancer, according to a single-center study from the United States, is 0.79% [56]. Bladder malignancies have been shown to be among the most aggressive in cardiac transplant patients, with a higher incidence than in the general population. Continued smoking after transplantation, high blood levels of testosterone, and sexual activity are important risk factors. Adenocarcinoma is the most common type of prostate cancer [65]. The median interval between transplantation and tumor diagnosis is 36.5 months, and the median survival after diagnosis and treatment is 27 months. The leading cause of death in prostate cancer is metastasis to remote organs and tissues [55].

Salivary gland tumors are usually late in detection, extremely aggressive, and metastasize early [56, 65]. Adenocarcinoma is another frequent type of gastric and intestinal cancer in HTx recipients. Tumors of this type are also prone to rapid metastasis [55].

Renal cell cancer, breast and pancreatic adenocarcinomas, liver cancer, cervical cancer, and cholangiocarcinoma of the biliary tract are rarer types of malignancies seen after HTx [66].

CONCLUSION

The risk of malignant tumors of various localizations is significantly higher in heart recipients than in the general population. This is associated with immunosuppressive drugs, smoking, and patient age. Timely comprehensive examination of patients, development of new immunosuppression regimens, treatment of infections predisposing to the development of malignant tumors, and avoiding bad habits will help to reduce the risk of malignant tumors, enable diagnosis of complications at early stages, and thereby increase the life expectancy of recipients.

This research was partially supported by a grant (No. NSh-2598-2020.7) of the President of the Russian Federation for government support of leading scientific schools.

The authors declare no conflict of interest.

REFERENCES

1. *Ponikowski P, Voors A, Anker SD, Bueno H, Cleland JGF, Coast AJS et al*. ESC Guidelines for the diagnosis and treatment of acute and chronic heart failure: The Task Force for the diagnosis and treatment of acute and chronic heart failure of the ESC Developed with the special contribution of the HFA of the ESC. *Eur Heart J*. 2016; 37: 2186–2187. doi: 10.1093/eurheartj/ehw128.
2. *Gautier SV, Shevchenko AO, Poptsov VN*. Patsient s transplantirovannym serdtsem. Rukovodstvo dlya vrachey po vedeniyu patsientov, perenesshikh transplantatsiyu serdtsa. M.–Tver': Triada, 2014: 144. [In Russ].
3. *Stehlik J, Edwards LB, Kucheryavaya AY, Benden C, Christie JD, Dipchand AI et al*. International Society of Heart and Lung Transplantation. The Registry of the International Society for Heart and Lung Transplantation: 29th official adult heart transplant report 2012. *J Heart Lung Transplant*. 2012; 31: 1052–64. doi: 10.1016/j.healun.2012.08.002.

4. *Khush KK, Cherikh WS, Chambers DC, Goldfarb S, Hayes D Jr, Kucheryavaya AY et al*. The international thoracic organ transplant registry of the international society for heart and lung transplantation: thirty-fifth adult heart transplantation report – 2018; focus theme: multiorgan transplantation. *J Heart Lung Trans*. 2018; 37: 1155–1168. doi: 10.1016/j.healun.2018.07.022.
5. *Sampaio MS, Cho YW, Qazi Y et al*. Posttransplant malignancies in solid organ adult recipients: an analysis of the US National Transplant Database. *Transplantation*. 2012; 94: 990–998. doi: 10.1097/TP.0b013e318270bc7b.
6. *Krynitz B, Edgren G, Lindelöf B et al*. Risk of skin cancer and other malignancies in kidney, liver, heart, and lung transplant recipients 1970 to 2008 – a Swedish population-based study. *Int J Cancer*. 2013; 132: 1429–1438. doi: 10.1002/ijc.27765.
7. *Collett D, Mumford L, Banner NR et al*. Comparison of the incidence of malignancy in recipients of different types of organ: a UK Registry audit. *Am J Transplant*. 2010; 10: 1889–1896. doi: 10.1111/j.1600-6143.2010.03181.x.
8. *Youn J, Stehlik J, Wilk AR et al*. Temporal trends of *de novo* malignancy development after heart transplantation. *J Am Coll Cardiol*. 2018; 71: 40–49. doi: 10.1016/j.jacc.2017.10.077.
9. *Van Keer J, Droogné W, Van Cleemput J, Vörös G, Rega F, Meyns B et al*. Cancer After Heart Transplantation: A 25-year Single-center Perspective. *Transplantation Proceedings*. 2016; 48 (6): 2172–2177. doi: 10.1016/j.transproceed.2016.03.037.
10. *Jiang Y, Villeneuve PJ, Wielgosz A et al*. The incidence of cancer in a population-based cohort of Canadian heart transplant recipients. *Am J Transplant*. 2010; 10: 637–645. doi: 10.1111/j.1600-6143.2009.02973.x.
11. *De Pinho RA*. The age of cancer. *Nature*. 2000; 408: 248–254. doi: 10.1038/35041694.
12. *Higgins RS, Brown RN, Chang PP et al*. A multi-institutional study of malignancies after heart transplantation and a comparison with the general United States population. *J Heart Lung Transplant*. 2014; 33: 478–485. doi: 10.1016/j.healun.2014.01.862.
13. *Crespo-Leiro MG, Alonso-Pulpón L, Vázquez de Prada JA et al*. Malignancy after heart transplantation: incidence, prognosis and risk factors. *Am J Transplant*. 2008; 8: 1031–1039. doi: 10.1111/j.1600-6143.2008.02196.x.
14. *Molina BD, Leiro MGC, Pulpón LA et al*. Incidence and risk factors for nonmelanoma skin cancer after heart transplantation. *Transplant Proc*. 2010; 42: 3001–3005. doi: 10.1016/j.transproceed.2010.08.003.
15. *Brewer JD, Colegio OR, Phillips PK et al.* Incidence of and risk factors for skin cancer after heart transplant. *JAMA Dermatol.* 2009; 145: 1391–1416. doi: 10.1001/archdermatol.2009.276.
16. *Dorak MT, Karpuzoglu E.* Gender differences in cancer susceptibility: an inadequately addressed issue. *Front Genet*. 2012; 3: 268. *Siegel R, Naishadham D, Jemal A*. Cancer statistics, 2012. *Cancer*. 2012; 62: 10–29. doi: 10.3322/caac.20138.
17. *Pennell LM, Galligan CL, Fish EN*. Sex affects immunity. *J Autoimmun*. 2012; 38: J282–291. doi: 10.1016/j.jaut.2011.11.013.
18. *Cramer DW, Finn OJ*. Epidemiologic perspective on immune-surveillance in cancer. *Curr Opin Immunol*. 2011; 23: 265–271. doi: 10.1016/j.coi.2011.01.002.
19. *Alam M, Brown RN, Silber DH et al*. Increased incidence and mortality associated with skin cancers after cardiac transplant. *Am J Transplant*. 2011; 11: 1488–1497. doi: 10.1111/j.1600-6143.2011.03598.x.
20. *Jäämaa-Holmberg S, Salmela B, Lemström K, Pukkala E, Lommi J*. Cancer incidence and mortality after heart transplantation – A population-based national cohort study. *Acta Oncologica*. 2019; 58: 6, 859–863. doi: 10.1080/0284186X.2019.1580385.
21. *Acuna SA, Fernandes KA, Daly C et al*. Cancer mortality among recipients of solid-organ transplantation in Ontario, Canada. *JAMA Oncol*. 2016; 2: 463–469. doi: 10.1001/jamaoncol.2015.5137.
22. *Na R, Grulich AE, Meagher NS et al*. *De novo* cancer-related death in Australian liver and cardiothoracic transplant recipients. *Am J Trans*. 2013; 13: 1296–1304. doi: 10.1111/ajt.12192.
23. *Öhman J, Rexius H, Mjörnstedt L et al.* Oral and lip cancer in solid organ transplant patients – A cohort study from a Swedish Transplant Centre. *Oral Oncol*. 2015; 51: 146–150. doi: 10.1016/j.oraloncology.2014.11.007.
24. *Rodriguez Cetina Biefer H, Sündermann SH, Emmert MY et al*. Surviving 20 years after heart transplantation: a success story. *Ann Thorac Surg*. 2014; 97: 499–504. doi: 10.1016/j.athoracsur.2013.08.040.
25. *Gillison ML, Chaturvedi AK, Anderson WF et al*. Epidemiology of human papillomavirus-positive head and neck squamous cell carcinoma. *J Clin Oncol*. 2015; 33: 3235–3242. doi: 10.1200/JCO.2015.61.6995.
26. *Sherston SN, Carroll RP, Harden PN et al*. Predictors of cancer risk in the long-term solid-organ transplant recipient. *Transplantation*. 2014; 97: 605–611. doi: 10.1097/01.TP.0000436907.56425.5c.
27. *Tufaro AP, Azoury SC, Crompton JG et al*. Rising incidence and aggressive nature of cutaneous malignancies after transplantation: An update on epidemiology, risk factors, management and surveillance. *Surg Oncol*. 2015; 24: 345–352. doi: 10.1016/j.suronc.2015.09.007.
28. *Kumarasinghe G, Lavee O, Parker A et al*. Post-transplant lymphoproliferative disease in heart and lung transplantation: Defining risk and prognostic factors. *J Heart Lung Trans*. 2015; 34: 1406–1414. doi: 10.1016/j.healun.2015.05.021.
29. *Potena L, Zuckermann A, Barberini F, Aliabadi-Zuckermann A*. Complications of Cardiac Transplantation. *Curr Cardiol Rep*. 2018; 20 (9): 73. doi: 10.1007/s11886-018-1018-3.
30. *Engels EA, Pfeiffer RM, Fraumeni JF et al*. Spectrum of cancer risk among US solid organ transplant recipients. *JAMA*. 2011; 306: 1891–1901. doi: 10.1001/jama.2011.1592.
31. *Yamani MH, Taylor DO, Czerr J et al*. Thymoglobulin induction and steroid avoidance in cardiac transplantation: results of a prospective, randomized, controlled study. *Clin Transplant*. 2008; 22: 76–81.
32. *Cantarovich M, Giannetti N, Barkun J, Cecere R*. Antithymocyte globulin induction allows a prolonged

delay in the initiation of cyclosporine in heart transplant patients with postoperative renal dysfunction. *Transplantation*. 2004; 78: 779–81. doi: 10.1097/01.tp.0000130179.18176.3d.
33. *Rosenberg PB, Vriesendorp AE, Drazner MH et al*. Induction therapy with basiliximab allows delayed initiation of cyclosporine and preserves renal function after cardiac transplantation. *J Heart Lung Transplant*. 2005; 24: 1327–1331. doi: 10.1016/j.healun.2004.08.003.
34. *Costanzo MR, Dipchand A, Starling R et al*. International Society of Heart and Lung Transplantation guidelines. The International Society of Heart and Lung Transplantation guidelines for the care of heart transplant recipients. *J Heart Lung Transplant.* 2010; 29: 914–956. doi: 10.1016/j.healun.2010.05.034.
35. *Penninga L, Møller CH, Gustafsson F, Gluud C, Steinbrüchel DA*. Immunosuppressive T-cell antibody induction for heart transplant recipients. *Cochrane Database Syst Rev*. 2013; 12 (12): CD008842. doi: 10.1002/14651858.CD008842.pub2.
36. *Söderlund C, Rådegran G*. Immunosuppressive therapies after heart transplantation – The balance between under- and over-immunosuppression. *Transplantation Reviews*. 2015; 29 (3): 181–189. doi: 10.1016/j.trre.2015.02.005.
37. *Lindenfeld J, Miller GG, Shakar SF et al*. Drug therapy in the heart transplant recipient: part II: immunosuppressive drugs. *Circulation*. 2004; 110: 3858–3865. doi: 10.1161/01.CIR.0000150332.42276.69.
38. *Ensor CR, Doligalski CT*. Proliferation signal inhibitor toxicities after thoracic transplantation. *Expert Opin Drug Metab Toxicol*. 2013; 9: 63–77. doi: 10.1517/17425255.2012.726219.
39. *Yanik E, Gustafson S, Kasiske B et al*. Sirolimus use and cancer incidence among US kidney transplant recipients. *Am J Transplant*. 2015; 15: 129–136. doi: 10.1111/ajt.12969.
40. *Gurk-Turner C, Manitpisitkul W, Cooper M*. A comprehensive review of everolimus clinical reports: a new mammalian target of rapamycin inhibitor. *Transplantation*. 2012; 94: 659–668. doi: 10.1097/TP.0b013e31825b411c.
41. *Motzer RJ, Escudier B, Oudard S et al*. Efficacy of everolimus in advanced renal cell carcinoma: a double-blind, randomised, placebo-controlled phase III trial. *Lancet*. 2008; 372: 449–456. doi: 10.1016/S0140-6736(08)61039-9.
42. *Hoogendijk-van den Akker JM, Harden PN, Hoitsma AJ et al*. Two-year randomized controlled prospective trial converting treatment of stable renal transplant recipients with cutaneous invasive squamous cell carcinomas to sirolimus. *J Clin Oncol*. 2013; 31: 1317–1323. doi: 10.1200/JCO.2012.45.6376.
43. *Schena FP, Pascoe MD, Alberu J et al*. Conversion from calcineurin inhibitors to sirolimus maintenance therapy in renal allograft recipients: 24-month efficacy and safety results from the CONVERT trial. *Transplantation*. 2009; 87: 233–242. doi: 10.1097/TP.0b013e3181927a41.
44. *Wang SS, Chou NK, Chi NH et al*. Clinical experience of tacrolimus with everolimus in heart transplantation. *Transplant Proc*. 2012; 44: 907–909. doi: 10.1016/j.transproceed.2012.01.094.
45. *Penn I*. Tumors after renal and cardiac transplantation. *Hematol Oncol Clin North Am*. 1993; 7 (2): 431–445.
46. *Bavinck JN, De Boer A, Vermeer BJ et al*. Sunlight, keratotic skin lesions and skin cancer in renal transplant recipients. *Br J Dermatol*. 1993; 129 (3): 242–249. doi: 10.1111/j.1365-2133.1993.tb11841.x.
47. *Chen PL, Chang HH, Chen IM et al*. Malignancy after heart transplantation. *J Chin Med Assoc*. 2009; 72 (11): 588–593. doi: 10.1016/S1726-4901(09)70434-4.
48. *Espana A, Martinez-Gonzalez MA, Garcia-Granero M, Sanchez-Carpintero I, Rabago G, Herreros J*. A prospective study of incident nonmelanoma skin cancer in heart transplant recipients. *J Invest Dermatol*. 2000; 115 (6): 1158–1160. doi: 10.1046/j.1523-1747.2000.0202a-3.x.
49. *Euvrard S, Kanitakis J, Pouteil-Noble C et al*. Comparative epidemiologic study of premalignant and malignant epithelial cutaneous lesions developing after kidney and heart transplantation. *J Am Acad Dermatol*. 1995; 33 (2): 222–229. doi: 10.1016/0190-9622(95)90239-2.
50. *Serraino D, Piselli P, Busnach G et al*. Risk of cancer following immunosuppression in organ transplant recipients and in HIV-positive individuals in southern Europe. *Eur J Cancer*. 2007; 43 (14): 2117–2123. doi: 10.1016/j.ejca.2007.07.015.
51. *McLelland J, Rees A, Williams G, Chu T*. The incidence of immunosuppression-related skin disease in long-term transplant patients. *Transplantation*. 1988; 46 (6): 871–874. doi: 10.1097/00007890-198812000-00016.
52. *Hartevelt MM, Bavinck JN, Kootte AM, Vermeer BJ, Vandenbroucke JP*. Incidence of skin cancer after renal transplantation in The Netherlands. *Transplantation*. 1990; 49 (3): 506–509. doi: 10.1097/00007890-199003000-00006.
53. *Caforio AL, Fortina AB, Piaserico S et al*. Skin cancer in heart transplant recipients: risk factor analysis and relevance of immunosuppressive therapy. *Circulation*. 2000; 102 (19): 222–227. doi: 10.1161/01.cir.102.suppl_3.iii-222.
54. *Rabinovics N, Mizrachi A, Hadar T et al*. Cancer of the head and neck region in solid organ transplant recipients. *Head Neck*. 2014; 36 (2): 181–186. doi: 10.1002/hed.23283.
55. *Lott DG, Manz R, Koch C, Lorenz RR*. Aggressive behavior of nonmelanotic skin cancers in solid organ transplant recipients. *Transplantation*. 2010; 90 (6): 683–687. doi: 10.1097/TP.0b013e3181ec7228.
56. *Rinaldi M, Pellegrini C, D'Armini AM et al*. Neoplastic disease after heart transplantation: single center experience. *Eur J Cardiothorac Surg*. 2001; 19 (5): 696–701. doi: 10.1016/s1010-7940(01)00674-1.
57. *Evans W, Venyo A*. De-novo malignancies post heart transplantation: a review of the literature on the mechanisms, types, and causes of the malignancies. *Webmed Central*. 2012; 3 (6): WMC003425. doi: 10.4254/wjh.v8.i12.533.
58. *Roussel JC, Baron O, Perigaud C et al*. Outcome of heart transplants 15 to 20 years ago: graft survival, post-transplant morbidity, and risk factors for mortality. *J Heart*

Lung Transplant. 2008; 27 (5): 486–493. doi: 10.1016/j.healun.2008.01.019.

59. *Opelz G, Dohler B*. Lymphomas after solid organ transplantation: a collaborative transplant study report. *Am J Transplant*. 2004; 4 (2): 222–230. doi: 10.1046/j.1600-6143.2003.00325.x.
60. *Swinnen LJ, Costanzo-Nordin MR, Fisher SG et al*. Increased incidence of lymphoproliferative disorder after immunosuppression with the monoclonal antibody OKT3 in cardiac-transplant recipients. *N Engl J Med*. 1990; 323 (25): 1723–1728. doi: 10.1056/NEJM199012203232502.
61. *O'Neill JO, Edwards LB, Taylor DO*. Mycophenolate mofetil and risk of developing malignancy after orthotopic heart transplantation: analysis of the transplant registry of the International Society for Heart and Lung Transplantation. *J Heart Lung Transplant*. 2006; 25 (10): 1186–1191. doi: 10.1016/j.healun.2006.06.010.
62. *LaCasce AS.* Post-transplant lymphoproliferative disorders. *Oncologist*. 2006; 11 (6): 674–680. doi: 10.1634/theoncologist.11-6-674.
63. *Parker A, Bowles K, Bradley JA et al*. Diagnosis of post-transplant lymphoproliferative disorder in solid organ transplant recipients – BCSH and BTS Guidelines. *Br J Haematol*. 2010; 149: 675–692. doi: 10.1111/j.1365-2141.2010.08161.x.
64. *Smets F, Sokal EM*. Epstein–Barr virus-related lymphoproliferation in children after liver transplant: role of immunity, diagnosis, and management. *Pediatr Transplant*. 2002; 6 (4): 280–287. doi: 10.1034/j.1399-3046.2002.02029.x.
65. *Kinch A, Sundström C, Baecklund E, Backlin C, Molin D, Enblad G*. Expression of PD-1, PD-L1, and PD-L2 in posttransplant lymphoproliferative disorder after solid organ transplantation. *Leukemia and Lymphoma*. 2019; 60 (2): 376–384. doi: 10.1080/10428194.2018.1480767.
66. *Mihalov ML, Gattuso P, Abraham K, Holmes EW, Reddy V*. Incidence of post-transplant malignancy among 674 solid-organ-transplant recipients at a single center. *Clin Transplant*. 1996; 10 (3): 248–255.
67. *Strecker T, Rosch J, Weyand M, Agaimy A*. Frequency and spectrum of metachronous malignancies in heart transplant recipients: a 11-year-experience at a German heart center. *Int J Clin Exp Pathol*. 2013; 6 (3): 411–420.
68. *Pham SM, Kormos RL, Landreneau RJ et al*. Solid tumors after heart transplantation: lethality of lung cancer. *Ann Thorac Surg*. 1995; 60 (6): 1623–1626. doi: 10.1016/0003-4975(95)00120-4.
69. *Lateef N, Abdul Basit K, Abbasi N, Kazmi SM, Ansari AB, Shah M*. Malignancies After Heart Transplant. *Exp Clin Transplant*. 2016 Feb; 14 (1): 12–16. doi: 10.6002/ect.2015.0214.

The article was submitted to the journal on 22.04.2021

DOI: 10.15825/1995-1191-2021-2-177-182

PROSPECTS FOR THE USE OF ARTIFICIAL NEURAL NETWORKS FOR PROBLEM SOLVING IN CLINICAL TRANSPLANTATION

R.M. Kurabekova[1], A.A. Belchenkov[1], O.P. Shevchenko[1, 2]

[1] Shumakov National Medical Research Center of Transplantology and Artificial Organs, Moscow, Russian Federation

[2] Sechenov University, Moscow, Russian Federation

Management of solid organ recipients requires a significant amount of research and observation throughout the recipient's life. This is associated with accumulation of large amounts of information that requires structuring and subsequent analysis. Information technologies such as machine learning, neural networks and other artificial intelligence tools make it possible to analyze the so-called 'big data'. Machine learning technologies are based on the concept of a machine that mimics human intelligence and and makes it possible to identify patterns that are inaccessible to traditional methods. There are still few examples of the use of artificial intelligence programs in transplantology. However, their number has increased markedly in recent years. A review of modern literature on the use of artificial intelligence systems in transplantology is presented.

Keywords: artificial intelligence in transplantation, machine learning, expert system, artificial neural network.

INTRODUCTION

Solid organ transplantation is one of the most high-tech and knowledge-intensive fields of modern medicine. Therapy for solid organ recipients requires a significant amount of research and observation, both before transplantation and after surgery, throughout the recipient's life. Routine follow-up of recipients include a wide range of imaging, clinical and laboratory methods, which necessitates analysis of large volumes of data [1].

The accumulated data on patients and various procedures are typically stored in specialized databases [2, 3], scientific registries [4] and in medical histories. As these data and procedures increase in volume, there is a natural need for tools that can be used to analyze the so-called "big data". In recent years, information technologies, such as machine learning, neural networks and other artificial intelligence tools, have been increasingly used in biomedical research, mainly in fields involving large volumes of complex data, such as genomics and bioinformatics [5]. The number of examples of AI applications in transplantology is small, but they have noticeably increased in number in recent years [6–10].

Although the terms '*artificial intelligence*', '*machine learning*' or '*artificial neural networks*' are widely used in the literature, the essence of these methods, their capabilities and weaknesses are not fully understood [11, 12].

The aim of this study is to review the current literature on application of artificial intelligence (AI) systems for solving problems in transplantology.

A review of foreign and Russian research publications in the publicly available databases of Pubmed, Russian Science Citation Index, CyberLeninck and Google Scholar for the past 5 years, using keywords ("artificial intelligence", "machine learning", "artificial neural networks", "transpl*") and their combinations, enabled us to find over 6000 papers, of which about 30 were related to transplantology.

TERMINOLOGY

Artificial intelligence (AI) is the general name for a number of computer technologies, such as expert systems, computer vision, robotics, machine learning, etc., that are based on the concept of a machine simulating human intelligence. The first expert systems began to be used as early as the 1970s, for example, to interpret electrocardiograms. More significant advances were made at the beginning of the 21st century in the field of image recognition [13].

The main features of AI are considered to be the ability to analyze data, applying different algorithms to achieve given goals, analyze and tune the performance of algorithms, and then apply them to new data, repeating and updating the previous process and data samples.

AI technology, like any other technology, uses a large number of terms and definitions that require specialized knowledge to understand. Below are simplified definitions of the most commonly used terms in this field.

Machine learning (ML) is a class of artificial intelligence methods and a class of computer programs that

Corresponding author: Olga Shevchenko. Address: 1, Shchukinskaya str., Moscow, 123182, Russian Federation. Phone: (499) 190-38-77. E-mail: transplant2009@mail.ru

can, by performing certain tasks, improve and increase problem-solving performance over time and as new data are introduced in the program.

Expert system is a subset of machine learning. It is built on the basis of decision-making rules. A computer model is trained (to solve specific problems, e.g., prediction) using statistical theories/methods or by identifying certain patterns/regularities in the data.

Deep learning (DL) is a set of machine learning methods based on learning representations, rather than specialized algorithms designed to solve specific problems. In practice, deep learning, also known as deep structured or hierarchical learning, uses a large number of hidden layers of nonlinear processing to extract features from data and transform data to different levels of abstraction (representations). Artificial neural networks are created using deep machine learning methods.

Artificial neural network (ANN) is a mathematical model, as well as computer software, built on the principle of organization and functioning of biological neural networks – networks of epy nerve cells of a living organism. ANN is a system of interconnected and interacting simple processors (artificial neurons). Each processor of such a network deals only with signals it periodically receives and signals it periodically sends to other processors. Neurons are organized into layers. The number of layers for each network is individual and depends on the applied problem being solved. Technically, neural networks are not programmed, but trained. Learning is a process of finding coefficients of connections between neurons.

Decision tree is a tree-like flowchart structure with internal nodes, branches and leaves. The internal nodes contain questions (e.g., does the patient have fever >39 °C), branches represent the answer (e.g., yes or no), and the leaves represent the final definition of data classes (e.g., sick or healthy).

Random forest is a machine learning algorithm consisting of a set of decision trees.

K-nearest neighbor is a machine learning algorithm for solving classification and regression problems based on similarity (e.g., proximity or distance) between available data and new data.

Naive Bayes is a machine learning algorithm that uses probabilistic classifiers based on Bayes' theorem that assumes no relationship between predictor variables.

K-means clustering – an algorithm that identifies similar characteristics of data in a set and divides them into subgroups.

Various types of learning models are used in machine learning, which are not described in this paper [14–16].

EVALUATION OF AI MODELS

When analyzing the results obtained with ANN-based models, it is important to understand how adequate they are, what the performance of the model is, and whether it has been adequately validated. Usually used for this purpose are performance characteristics that are similar to those used for evaluating traditional tests, calculated using ROC analysis: AUROC (area under the receiver operating characteristic), C-statistic (sensitivity and specificity), and metrics such as accuracy, positive predictive value, negative predictive value, and F1 scores [17].

AI-based models, like traditional statistical models, must be validated in a different patient population, at a different center, or under different conditions. Model performance may change with new data, e.g., a different CT image resolution obtained with a different scanner, a different electronic medical record system, etc. Therefore, it is important to pay attention to whether the model has been externally validated.

AI IN TRANSPLANTOLOGY

Risk prediction plays an important role in clinical trials in transplantology. Most risk assessment models are based on regression analysis, which allows us to determine the nature of the relationship between predictors and outcomes [18]. However, such models have many disadvantages: they only allow estimating a limited number of predictors that are assumed not to change throughout the life of the participants. Besides, these methods do not allow for analysis of nonlinear relationships, often require data conversion into binary form, and do not allow for analysis of large datasets. Deep machine learning methods provide ways of overcoming these shortcomings [19, 20].

Much of the work on the use of AI in transplantology is devoted to solving survival and rejection problems, mainly in kidney or liver recipients [21–29]. Other important tasks to be solved by machine learning methods are selection of compatible donor/recipient pairs [7, 30], prediction of graft dysfunction [31–33], and selection of optimal immunosuppression regime [8, 34, 35].

Tapak et al. used machine learning algorithms to predict primary graft dysfunction as an important criterion for liver transplantation [36]. Machine learning was used to select 15 main donor, recipient and graft characteristics affecting the development of graft dysfunction within 30 days after transplantation. Based on the 15 donor and recipient parameters determined before transplantation, algorithms were developed to predict graft dysfunction with a mean AUROC of 0.835 – using ANN.

Several machine learning algorithms, including a neural network, were tested in Miller et al. using data from the United Network of Organ Sharing (UNOS) database from 1987 to 2014 [37]. The authors evaluated the 1-year survival of heart transplant recipients and compared the results with a standard statistical model based on logistic regression. They used 80% of the data as a training sample and 20% for validation. C statistic

evaluation of the models showed that the neural network had characteristics (AUROC = 0.66) similar to those of logistic regression (AUROC = 0.65). The authors concluded that the machine learning algorithms, derived from the original dataset they used, were not superior to traditional methods. However, they suggested that AI could outperform traditional statistical methods if augmented with new data from e-medical records.

In Reeve et al. [38], AI was used to assess the prognosis of renal transplant rejection. Clinically confirmed biopsy results were used to verify the diagnosis of T cell-mediated and antibody-mediated rejection. AI-based algorithms showed a higher level of accuracy compared to the accuracy obtained by physicians (92% for T cell-mediated rejection and 94% for antibody-mediated rejection).

Bertsimas et al. developed an optimized mortality prediction model (OPOM) for predicting the 3-month waitlist mortality in liver recipients [39]. The work used a large data set including 1,618,966 observations and various machine learning methods, including neural network and logistic regression. In liver transplantation, when the OPOM model was used for donor organ allocation, there were 41,796 fewer recipient deaths per year compared with the traditional MELD system: the AUROC for OPOM was higher than that for MELD: 0.859 and 0.841, respectively. The authors showed that the OPOM model is also suitable for patients with hepatocellular carcinoma, but the model requires external validation: there are plans for the model to be tested on a new group of patients.

I. Scheffner et al. derived a survival prediction model for kidney recipients [40]. A retrospective cohort of kidney recipients who underwent biopsy after transplantation according to the protocol was divided into data sets for training and validation. The model demonstrated good performance using data before kidney transplantation, as well as data 3 and 12 months after the surgery. Apart from previously established age, cardiovascular disease, diabetes and graft function, the effectiveness of graft rejection therapy and urinary tract infections were found to be important predictors of patient survival.

ADVANTAGES AND DISADVANTAGES OF AI

Machine learning methods are versatile tools that can be widely applied to a variety of problems in transplantology. However, like any other analytical method, machine learning has its strengths and weaknesses. The strengths of machine learning include the ability to detect patterns and trends that cannot be detected using the classical statistical methods, and the ability to process multidimensional and diverse data. An important feature of machine learning technology is the ability to improve the accuracy and efficiency of predictions as experience and data volume increase.

A weakness of machine learning is the difficulty in interpreting results, which in some cases may not make biological sense and have no practical application. In addition, large amounts of data are needed to ensure the accuracy of the results when training an algorithm or model. As with conventional diagnostic or predictive models, the quality of inferences drawn from AI algorithms depends on the characteristics of the dataset used to train the model. As with conventional methods, it is important to consider the inclusion and exclusion criteria of the study. For example, a model to predict liver transplant survival based on donor/recipient pair compatibility may be inaccurate for recipients with hepatocellular carcinoma if the input dataset did not include enough of such patients.

CONCLUSION

Machine learning algorithms can be valuable tools for supporting a decision-making process on donor organ allocation, level of risk of post-transplant complications, or selection of an immunosuppressive therapy regimen, which is particularly relevant in settings, where suboptimal donor organ use can worsen waitlist or post-transplant mortality. The use of artificial intelligence can help to gain new insights from "old" data and make a significant contribution to improving transplant outcomes and survival rates in solid organ recipients.

The authors declare no conflict of interest.

REFERENCES

1. *Gautier SV.* Transplantologiya XXI veka: vysokiye tekhnologii v meditsine i innovatsii v biomeditsinskoy nauke. *Vestnik transplantologii i iskusstvennykh organov*. 2017; 19 (3): 10–32. doi: 10.15825/1995-1191-2017-3-10-32.
2. *Shevchenko OP, Kurabekova RM, Shevchenko AO, Olefirenko GA, Makarova LV, Muminov II et al.* Biomarkery u recipientov serdtsa. *Svidetel'stvo o gosudarstvennoi registracii bazy dannykh № 2015620209*. 06.02.2015.
3. *Kurabekova RM, Shevchenko OP, Tsirulnikova OM, Olefirenko GA, Gichkun OE, Tsirulnikova IE et al*. Biomarkery u detey – recipientov pecheni. *Svidetel'stvo o gosudarstvennoi registracii bazy dannykh № 2015620210*. 06.02.2015.
4. *Gautier S, Starodubov V, Gabbasova L, Khomyakov S, Kucheryavyy A, Minina M.* Natsional'nyy transplantatsionnyy registr: sostoyaniye i perspektivy razvitiya. *Vestnik transplantologii i iskusstvennykh organov*. 2020; 22 (S): 5–7.
5. *Ho DSW, Schierding W, Wake M, Saffery R, O'Sullivan J.* Machine learning SNP based prediction for precision medicine. *Frontiers in genetics.* 2019; 10: 267.
6. *Niel O, Bastard P*. Artificial intelligence improves estimation of tacrolimus area under the concentration over time curve in renal transplant recipients. *Transpl Int.* 2018; 31 (8): 940–941. doi: 10.1111/tri.13271.

7. *Ayllón MD, Ciria R, Cruz-Ramírez M, Pérez-Ortiz M, Gómez I, Valente R et al*. Validation of artificial neural networks as a methodology for donor-recipient matching for liver transplantation. *Liver Transpl.* 2018; 24 (2): 192–203. doi: 10.1002/lt.24870.
8. *Naushad SM, Kutala VK*. Artificial neural network and bioavailability of the immunosuppression drug. *Curr Opin Organ Transplant.* 2020; 25 (4): 435–441. doi: 10.1097/MOT.0000000000000770.
9. *Ferrarese A, Sartori G, Orrù G, Frigo AC, Pelizzaro F, Burra P et al*. Machine learning in liver transplantation: a tool for some unsolved questions? *Transpl Int.* 2021; 34 (3): 398–411. doi: 10.1111/tri.13818.
10. *Sapir-Pichhadze R, Kaplan B*. Seeing the Forest for the Trees: Random Forest Models for Predicting Survival in Kidney Transplant Recipients. *Transplantation.* 2020; 104 (5): 905–906. doi: 10.1097/TP.0000000000002923.
11. *Park SH, Mazumder NR, Mehrotra S, Ho B, Kaplan B, Ladner DP*. Artificial Intelligence-related Literature in Transplantation: A Practical Guide. *Transplantation.* 2021; 105 (4): 704–708. doi: 10.1097/TP.0000000000003304.
12. *Edwards AS, Kaplan B, Jie T*. A Primer on Machine Learning. *Transplantation.* 2021; 105 (4): 699–703. doi: 10.1097/TP.0000000000003316.
13. *Yu KH, Beam AL, Kohane IS*. Artificial intelligence in healthcare. *Nat Biomed Eng.* 2018; 2 (10): 719–731. doi: 10.1038/s41551-018-0305-z.
14. *Hackeling G*. Mastering Machine Learning with scikit-learn: Packt Publishing Ltd; 2017. [1788298497].
15. *Rashidi HH, Tran NK, Betts EV, Howell LP, Green R*. Artificial Intelligence and Machine Learning in Pathology: The Present Landscape of Supervised Methods. *Acad Pathol.* 2019; 6 (2374289519873088): Jan-Dec. doi: 10.1177/2374289519873088.
16. *Liu Y, Chen PC, Krause J, Peng L*. How to Read Articles That Use Machine Learning: Users' Guides to the Medical Literature. *Jama.* 2019; 322 (18): 1806–1816. doi: 10.1001/jama.2019.16489.
17. *Tharwat A*. Classification assessment methods. *Applied Computing and Informatics.* 2020.
18. *Harrell FE*: Resampling, validating, describing, and simplifying the model. In: *Regression modeling strategies.* Springer; 2001: 87–103.
19. *Strobl C, Malley J, Tutz G*. An introduction to recursive partitioning: rationale, application, and characteristics of classification and regression trees, bagging, and random forests. *Psychological methods.* 2009; 14 (4): 323.
20. *Breiman L*. Random forests. *Machine learning.* 2001; 45 (1): 5–32.
21. *Hummel AD, Maciel RF, Rodrigues RG, Pisa IT*. Application of artificial neural networks in renal transplantation: classification of nephrotoxicity and acute cellular rejection episodes. *Transplant Proc.* 2010; 42 (2): 471–472. doi: 10.1016/j.transproceed.2010.01.051.
22. *Aubert O, Higgins S, Bouatou Y, Yoo D, Raynaud M, Viglietti D et al*. Archetype Analysis Identifies Distinct Profiles in Renal Transplant Recipients with Transplant Glomerulopathy Associated with Allograft Survival. *J Am Soc Nephrol.* 2019; 30 (4): 625–639. doi: 10.1681/ASN.2018070777.
23. *Zhou L, Tang L, Song AT, Cibrik DM, Song PX*. A LASSO Method to Identify Protein Signature Predicting Post-transplant Renal Graft Survival. *Stat Biosci.* 2017; 9 (2): 431–452. doi: 10.1007/s12561-016-9170-z.
24. *Yoo KD, Noh J, Lee H, Kim DK, Lim CS, Kim YH et al*. A Machine Learning Approach Using Survival Statistics to Predict Graft Survival in Kidney Transplant Recipients: A Multicenter Cohort Study. *Sci Rep.* 2017; 7 (1): 017-08008. doi: 10.1038/s41598-8.
25. *Bhat V, Tazari M, Watt KD, Bhat M*. New-Onset Diabetes and Preexisting Diabetes Are Associated With Comparable Reduction in Long-Term Survival After Liver Transplant: A Machine Learning Approach. *Mayo Clin Proc.* 2018; 93 (12): 1794–1802. doi: 10.1016/j.mayocp.
26. *Doyle HR, Dvorchik I, Mitchell S, Marino IR, Ebert FH, McMichael J et al*. Predicting outcomes after liver transplantation. A connectionist approach. *Ann Surg.* 1994; 219 (4): 408–415. doi: 10.1097/00000658-199404000-00012.
27. *Hughes VF, Melvin DG, Niranjan M, Alexander GA, Trull AK*. Clinical validation of an artificial neural network trained to identify acute allograft rejection in liver transplant recipients. *Liver Transpl.* 2001; 7 (6): 496–503. doi: 10.1053/jlts.2001.24642.
28. *Hoot N, Aronsky D*. Using Bayesian networks to predict survival of liver transplant patients. *AMIA Annu Symp Proc.* 2005: 345–349.
29. *Cruz-Ramírez M, Hervás-Martínez C, Fernández JC, Briceño J, de la Mata M*. Predicting patient survival after liver transplantation using evolutionary multi-objective artificial neural networks. *Artif Intell Med.* 2013; 58 (1): 37–49. doi: 10.1016/j.artmed.2013.02.004.
30. *Briceño J, Ayllón MD, Ciria R*. Machine-learning algorithms for predicting results in liver transplantation: the problem of donor-recipient matching. *Curr Opin Organ Transplant.* 2020; 25 (4): 406–411. doi: 10.1097/MOT.0000000000000781.
31. *Lau L, Kankanige Y, Rubinstein B, Jones R, Christophi C, Muralidharan V et al*. Machine-Learning Algorithms Predict Graft Failure After Liver Transplantation. *Transplantation.* 2017; 101 (4): e125–e132. doi: 10.1097/TP.0000000000001600.
32. *Dorado-Moreno M, Pérez-Ortiz M, Gutiérrez PA, Ciria R, Briceño J, Hervás-Martínez C*. Dynamically weighted evolutionary ordinal neural network for solving an imbalanced liver transplantation problem. *Artif Intell Med.* 2017; 77: 1–11. doi: 10.1016/j.artmed.2017.02.004.
33. *Haydon GH, Hiltunen Y, Lucey MR, Collett D, Gunson B, Murphy N et al*. Self-organizing maps can determine outcome and match recipients and donors at orthotopic liver transplantation. *Transplantation.* 2005; 79 (2): 213–218. doi: 10.1097/01.tp.0000146193.02231.e2.
34. *Tang J, Liu R, Zhang YL, Liu MZ, Hu YF, Shao MJ et al*. Application of Machine-Learning Models to Predict Tacrolimus Stable Dose in Renal Transplant Recipients. *Sci Rep.* 2017; 7 (42192). doi: 10.1038/srep42192.

35. *Thishya K, Vattam KK, Naushad SM, Raju SB, Kutala VK*. Artificial neural network model for predicting the bioavailability of tacrolimus in patients with renal transplantation. *PLoS One.* 2018; 13 (4). doi: 10.1371/journal.pone.0191921.
36. *Tapak L, Hamidi O, Amini P, Poorolajal J*. Prediction of Kidney Graft Rejection Using Artificial Neural Network. *Healthc Inform Res.* 2017; 23 (4): 277–284. doi: 10.4258/hir.2017.23.4.277.
37. *Miller PE, Pawar S, Vaccaro B, McCullough M, Rao P, Ghosh R et al*. Predictive Abilities of Machine Learning Techniques May Be Limited by Dataset Characteristics: Insights From the UNOS Database. *J Card Fail.* 2019; 25 (6): 479–483. doi: 10.1016/j.cardfail.2019.01.018.
38. *Reeve J, Böhmig GA, Eskandary F, Einecke G, Gupta G, Madill-Thomsen K et al*. Generating automated kidney transplant biopsy reports combining molecular measurements with ensembles of machine learning classifiers. *Am J Transplant.* 2019; 19 (10): 2719–2731. doi: 10.1111/ajt.15351.
39. *Bertsimas D, Kung J, Trichakis N, Wang Y, Hirose R, Vagefi PA*. Development and validation of an optimized prediction of mortality for candidates awaiting liver transplantation. *Am J Transplant.* 2019; 19 (4): 1109–1118. doi: 10.1111/ajt.15172.
40. *Scheffner I, Gietzelt M, Abeling T, Marschollek M, Gwinner W*. Patient Survival After Kidney Transplantation: Important Role of Graft-sustaining Factors as Determined by Predictive Modeling Using Random Survival Forest Analysis. *Transplantation.* 2020; 104 (5): 1095–1107. doi: 10.1097/TP.0000000000002922.

The article was submitted to the journal on 8.05.2021

INSTRUCTIONS TO AUTHORS

Articles should contain original information that has not been previously published and is not considered for publication in other editions. Fee for publication of manuscripts will not be charged.

Textual material should be presented in A4 format (1 copy, 1,5 pt spaced, font type Times New Roman, size 12 pt), as well as in Microsoft Word file of the identical content on electronic media (CD, attached to an e-mail file).

Structure of the article

The Title page should include:

– Initials (first name and patronymic) of the authors of the article should be specified before their respective last names.
– Full official name of the institution, city and country.
– If authors from different institutions participated in writing of the manuscript, it is necessary to correlate those with the names of the authors by adding a digital index uppercase after last name, and right before the name of the institution.

Information about the authors

For each author fully specify the last and the first name, patronymic and position in the relevant department/institution.

For correspondence

Fully specify the last and the first name, patronymic of the author, who will be holding correspondence, address (including postal code), telephone, fax number, e-mail.

Abstract

Each article must be accompanied by an abstract. The amount of text for the abstract of the original article should be of no more than 300 words, for a literature review, clinical observation – no more than 200 words. The abstract must fully comply with the content of the work. The abstract should not use abbreviations without prior expansion.

Abstract of ***the original article*** should contain the following sections: ***Objective***, ***Materials and methods***, ***Results***, ***Conclusion***. The abstract should present the most important results of the research.

Do not write: "*A comparative analysis of the sensitivity and specificity was conducted …*"

Should write: "*The sensitivity was ... % and ...%, p = , specificity, respectively ...% and ...%, p =* ".

Keywords

At the end of the abstract keywords must be given. To select the keywords a thesaurus of U.S. National Library of Medicine should be used – Medical Subject Headings (MeSH) at http://www.ncbi.nlm.nih.gov/mesh.

Conflict of interest

The author should inform the editor about the factual or potential conflict of interest have included the information about such conflict into the respective section of an article.

If there is no conflict of interest, the author should say so in the form like the following: "Author declares unawareness of the conflict of interest".

This information is supposed to be placed before the article text.

Text of article

Original article should include the following sections:

- Introduction
- Materials and methods
- Results
- Discussion
- Conclusion
- References

Review article should include an analysis of the literature with the presentation of modern sources (mainly in the last 5 years).

Clinical observation should be well illustrated (to reflect the essence of the problem) and include discussion with the use of literature data.

References in the text are indicated by number in square brackets: [1], [2, 5], [14–18] and ***in the references section are presented in order of their appearance in the text.*** All values given in the article should be expressed or duplicated in **SI** units.

References

The author is solely responsible for the accuracy of the data included in the references section of the article. References to unpublished papers or papers in print works are not allowed.

References are presented on a separate page.

The names of journals can be contracted in accordance with an embodiment of reduction adopted by the specific journal.

If the article quoted has DOI (a digital object identifier) or/and PMID (Pub Med identifier) they must be specified after the description of the article. To compile descriptions in References section NLM bibliographic reference citation standard is used – U.S. National Lib-

rary of Medicine (http://www.nlm.nih.gov/bsd/uniform_requirements.html). If the number of authors does not exceed 6, the bibliographic description includes all the authors. If the number of authors is more, only the first six authors should be indicated and then add et al.

Requirements for tables and figures

Tables should be placed into the text; they should have numbered heading and clearly labeled graphs, convenient and simple to read. Table's data must comply with the numbers in the text, but should not duplicate the information therein. Table references in the text are required.

Illustrations and drawings should be submitted in electronic format (JPEG or TIFF format with a resolution of at least 300 dpi and no smaller than 6 × 9 cm), in a volume of close to 1 MB. Drawings must include all copyright symbols – arrows, numbers, signs, etc. Figure captions should be submitted in a separate file with the extension *.doc. First, the name is given, then all arithmetic and alphabetical symbols (lettering) are explained.

Articles should be addressed to the Editor at:
Russian Journal of Transplantology and Artificial Organs
V.I. Shumakov National Medical Research Center of Transplantology and Artificial Organs
1, Shchukinskaya ul., Moscow 123182, Russian Federation
E-mail: **vestniktranspl@gmail.com**

Издание зарегистрировано в Госкомпечати РФ, № 018616 от 23.03.99 г.

Подписано к печати 29.06.21.

Тираж 1000 экз.

ООО «Издательство «Триада».
ИД № 06059 от 16.10.01 г.
170034, г. Тверь, пр. Чайковского, 9, оф. 514,
тел./факс: (4822) 42-90-22, 35-41-30
E-mail: triadatver@yandex.ru
http://www.triada.tver.ru

Отпечатано в ООО «Тверская фабрика печати».
170006, г. Тверь, Беляковский пер., 46.

Заказ 6359